UNIVERSITY OF CALIFORNIA
RIVERSIDE

Heterotrimeric G-Protein Signaling Regulates Cellulose Degradation in *Neurospora crassa*

A Dissertation submitted in partial satisfaction
of the requirements for the degree of

Doctor of Philosophy

in

Biochemistry and Molecular Biology

by

Logan Alexander Collier

December 2021

Dissertation Committee:
Dr. Katherine A. Borkovich, Chairperson
Dr. Charles Russell Hille
Dr. Caroline Roper

The Dissertation of Logan Alexander Collier is approved:

Committee Chairperson

University of California, Riverside

Acknowledgements

It seems impossible to properly thank all those who assisted in my academic journey. I am so grateful to all the people that have shared their insight and invested their time into my life. I hope that I can help others in a fraction of the way that everyone mentioned here has aided me in earning my doctorate.

I want to begin by thanking my elementary school teachers Mrs. Burgess and Mrs. Rosander who first saw my capabilities when I was young. They encouraged me to achieve what I thought was impossible even as a child. In high school, Coach Heckathorn taught me that your desire combined with your discipline will always equal your destiny. Coach Turner constantly pushed me to shave tenths of a second off my times. My AP Biology teacher Mr. Henderson who first introduced me to the wonders present within the cells of every organism on this planet. The most important lesson they all taught me was perseverance.

During my undergraduate education, my professors at Biola took the time to mentor me outside of the classroom. I remember countless talks in Dr. Dana Johnson's office where he would listen to my problems. These meetings would end with a prayer, and I always felt comforted afterward. Dr. Jason Tresser saw my determination early on and was key in helping me find the right career path. Jason (who insists I call him by his first name) has been vital in helping me move forward even as I take the next steps in my career. Dr. Matt Cruzen showed me that laughter is the best medicine, and that even if you have a doctorate you shouldn't take yourself too seriously. These mentors at Biola equipped me in

mind and character to impact the world for the Lord Jesus Christ, accomplishing the University mission statement.

While I have been at UC Riverside, I have had numerous professors who have offered their insight as well. I started as a rotation student in Dr. Jeff Perry's lab. The guidance he and Dr. Taylor Dennis, one of his students, directed me to find where I would fit in at UCR. Dr. Carolyn Rasmussen helped me to realize what it would take to endure graduate school. This was invaluable in my second year. Dr. Russ Hille and Dr. Caroline Roper served on my advancement and dissertation committees, providing much appreciated insight. Teaching Dynamic Genome with Dr. Matt Collin and Dr. Christine Pham showed me how satisfying this career path could be. Numerous meetings with Dr. Jason Stajich were necessary for understanding my bioinformatics datasets. I owe my knowledge of these techniques to him. Last, but certainly far from the least, I want to thank Julio Sosa for finding the answers to my frenzied questions whenever I called on him for help.

During my graduate career, I was able to attend the Fungal Genetics conference twice. It was at these meetings that I met Dr. N. Louise Glass and her former lab members Dr. Lori Huberman and Dr. Vincent Wu. Dr. Glass and her team at UC Berkeley gave critical advice on how to correctly culture *N. crassa* on cellulose medium. They gifted our lab several mutant strains and were very responsive to my questions regarding their protocols I adapted for our use. Their willingness to collaborate pushed me closer towards the goal.

Former Borkovich lab members were also supportive in achieving my doctorate. Dr. Patrick Schacht opened his home to me from the beginning of my graduate studies. He and Dr. Ilva Cabrera helped me in applying for teaching positions following graduate school. Dr. Arit Ghosh taught me basic methods in *N. crassa* while I was first starting, which was needed for my success.

Current lab members Dr. Alex Carrillo, Anthony Silva, and Yagna Oza provided helpful input regarding experimental design and discussion of my results. Their efforts helped create a friendly and collaborative culture in our lab. I have greatly valued the support I have received from each of them. My undergraduate mentee Abel Vargas was incredibly helpful as he became an expert at performing diagnostic PCRs. Dr. Derreck Carter-House and Sara Dorhmi were also great friends I could count on when experiments didn't quite pan out, despite not being members of our lab.

I especially want to thank my mentor, Dr. Kathy Borkovich. I am indebted to her for my success. She invested so much of her time and resources into my education over these past six years. Like a sculptor envisioning an elegant statue in the marble, I feel that she always saw in me what I could not see in myself at times. Her encouragement and assistance shaped me into the scientist I have become.

The support of my family and friends made this accomplishment possible. In many ways, this is their achievement as well. My friend Anna Plett helped me to endure numerous difficulties I faced before advancement to candidacy. Her

parent's house was a refuge of coffee, games, and good food during hard times. The combined experience in higher education of her brother Tim, her sister and brother-in-law Lydia and Brett, and her parents Steve and Jeanile was immeasurable help for me as a first-generation college student.

While at UC Riverside, I started attending Magnolia Church, and have had the opportunity to serve with several wonderful people. Mike Lovato has encouraged me and prayed for me many times. Partnering with him, Brett Vowell, and Dan Taylor to help lead MagCollege ministry helped me to remember the things that matter most to me while in grad school. Additionally, working in the children's ministry alongside Joni Lum, Joan Malcom, and Nicole Lovato was very refreshing. Seeing the smiles on all the kids faces as we played games with them and taught them about God's word was what I needed at the end of each week to carry on. I am immensely grateful for the way that all of these people included me in their church family.

My friends Hannah and Ryan Dea, Jimmy and Tiffany Dawson, Nate Landino, Scott Brutton, Trevan Meador, Emma Swanson, Alyssa and Jazmine Garcia, and my brother Nathan Collier assisted in my task of earning a doctorate during a global pandemic by providing an escape. When I needed to take a break, they were there to hear me. They also opened their homes and provided me with games and food. My sister Erika Melendez and her husband Jesse allowed me to vent my frustrations to them. She was so incredibly supportive through all of this.

My father Allen Collier and his wife Jodie have been beacons of encouragement this whole time. I looked forward to the phone calls I would have with them while they were driving across the country. I was exceedingly grateful when my mother Carla Jones would come to clean my house. Her hospitality was essential for my success. Her husband John always asked me pertinent questions regarding my work. Finally, my grandmother Virginia Louise would listen when I would explain my projects and kept notes to tell her friends about what I was doing. I miss her every single day, and I know that she and my grandfather Roy Collier are proud of the man I have become.

Thank you all for praying for me, for spurring me along, for buying me a meal, for playing a game with me, for advising me, and for believing I could make it to the end of this race. Your impact on my life will not be forgotten.

Dedication

Without the peace and comfort of my Lord and my God I would never have accomplished this. I dedicate this testament of my life's work and the remaining work to come to His Glorious Name. May He be praised for ever and ever, Amen.

When Peace, like a river, attendeth my way,

When sorrows like sea billows roll,

Whatever my lot,

Thou hast taught me to say

'It is well, it is well with my soul'

ABSTRACT OF THE DISSERTATION

Heterotrimeric G-Protein Signaling Regulates Cellulose Degradation in *Neurospora crassa*

by

Logan Alexander Collier

Doctor of Philosophy, Graduate Program in Biochemistry and Molecular Biology
University of California, Riverside, December 2021
Dr. Katherine A. Borkovich, Chairperson

Filamentous fungi such as *Neurospora crassa* use G protein coupled receptors (GPCRs) and associated heterotrimeric G proteins to respond to sensory cues from the environment. A fundamental challenge in G protein signaling is to identify the specific subunits of the heterotrimer (Gα, Gβ, Gγ) that interact in cases where multiple versions of subunits are present. Relevant to downstream signaling by heterotrimeric G proteins, fungi differentially regulate secreted enzymes for catabolism of cellulose, but the connection between cellulose metabolism and any signal transduction pathway is lacking in *N. crassa*. The primary objectives of this thesis are to 1. Determine genetic relationships between the putative Gβ subunit CPC-2 and the three Gα protein subunits in *N. crassa*, 2. Investigate the extent of G protein involvement in the cellulose response in *N. crassa*, and 3. Determine the role of *N. crassa* G proteins on the global transcriptional response to cellulose as a carbon source.

In Chapter 2, we characterized the relationships between the Gβ subunit CPC-2 and the other known G protein subunits in *N. crassa* on minimal medium containing sucrose. We illustrated that CPC-2 is cytoplasmic. We also

demonstrated that *cpc-2* is epistatic to *gna-2* with regards to basal hyphae growth rate and aerial hyphae height. Strains lacking both Gβ subunits possessed more severe defects for all phenotypic traits except for production of macroconidia, supporting a synergistic relationship between GNB-1 and CPC-2 in *N*. *crassa*.

In Chapter 3, I examined the relationship that G protein signaling has with cellulose metabolism. Loss of the Gα subunits *gna-1* and *gna-3,* the Gβ subunits *gnb-1* and *cpc-2,* the Gγ *gng-1,* or adenylyl cyclase (*cr-1*) resulted in loss of detectable cellulase activity. The expression patterns for five cellulase genes revealed that Δ*gna-1,* Δ*gnb-1*, and Δ*gna-3* mutants produce less cellulase mRNA than wild type, consistent with transcriptional regulation. Δ*cpc-2* and Δ*cr-1* mutants had wild-type levels of the cellulase transcripts. These results suggest that CPC-2 and CR-1 affect cellulase production in a post-transcriptional manner. Moreover, cAMP addition only partially corrected cellulase activity defects in Δ*gna-1* and Δ*gnb-1* mutants, indicating that GNA-1 and GNB-1 target cAMP-independent pathways to control cellulase activity.

In Chapter 4, I analyzed the transcriptomes and exoproteomes from cellulose grown cultures of the mutants for the Gα subunits *gna-1* and *gna-3*, as well as the adenylate cyclase *cr-1* via RNAseq and LC/MS-MS protein identification. 20 of the 22 highly expressed cellulases found in wild type cultures were transcriptionally downregulated in Δ*gna-1* mutants, and 6 of these 20 were also down-regulated in Δ*gna-3* mutants. Δ*cr-1* mutants were not transcriptionally

downregulated for any cellulase enzymes. Our transcriptional data suggests that *gna-1* and *gna-3* control the response to cellulose in *N. crassa*, while *cr-1* affects cellulases in a post-transcriptional manner.

Table of Contents

List of Figures

Chapter 1

Chapter 2

Chapter 3

Chapter 4

Appendix A

List of Tables

Chapter 1: Introduction

Neurospora crassa as a model eukaryote

Neurospora crassa is a multicellular filamentous fungus in the division Pezizomycotina under the phylum Ascomycota (1). Several genera in this division contain numerous plant pathogens. Despite this, the *Neurospora* species are all saprophytic, relying on decaying plant matter found in the environment for carbon metabolism (2, 3). *N. crassa* was discovered as a contaminant in French bakeries in the 1800s, and over the past hundred years has been used in countless studies as a model organism (4). There are several key features of this hardy bread mold that make it ideal for scientific research. *N. crassa* possesses numerous genes homologous to those in higher eukaryotes (2). Additionally, it exists most often in a haploid state, meaning that only one allele of each gene is present in the genome, allowing for simplified genetic modification (4). Discovery of the human *Ku70*/*Ku80* homologs (*mus-51* and *mus-52*, respectively), which control non-homologous end joining, was a major breakthrough in this system. Deletion of either of these genes results in strains that exhibit nearly 100% homologous recombination, facilitating precise mutation of genes of interest (5). Additionally, under laboratory conditions, *N. crassa* progresses through its asexual cycle in several days, and through the sexual cycle over the course of three weeks, meaning that experimentation can proceed quickly relative to other

model organisms (6). This also allows for quick generation of strains with multiple mutations via sexual crossing of strains of interest.

The features of *N. crassa* were used effectively in the last century to usher in major advancements in genetics and biochemistry. Perhaps most notably, Drs. George W. Beadle and Edward L. Tatum developed their “one gene one enzyme” theory using *N. crassa*, winning the Nobel Prize in Physiology or Medicine in 1958. (7). More recently, the genome of *N. crassa* was sequenced in 2003, revealing a 43 Mb genome with approximately 10,000 protein coding genes across seven chromosomes (8). Using readily available genetic techniques, the *Neurospora* scientific community developed gene deletion mutants for nearly every protein coding gene found in the genome. Many of these mutants are readily available at the Fungal Genetics Stock Center, and succinct protocols on how to produce mutants in genes of interest that may not be in the collection are easy to access and simple to use (9).

The life cycle of *N. crassa*

N. crassa is a multicellular eukaryote that is capable of reproducing both sexually and asexually. It is heterothallic, meaning that it is self-sterile, and is known to form over 28 different tissue types (10). *N. crassa* primarily exists in a vegetative state as tube-like structures known as hyphae that extend across a substrate (11). Growth occurs by polar extension, branching, and fusion of the hyphae (12). When neighboring hyphae interact, they fuse with each other,

forming a network known as the mycelium (4, 13). This polarized growth program is necessary for *N. crassa* to effectively colonize decaying plant matter in the environment (14). In pathogenic fungi, polarized growth is required to infiltrate the tissues of host organisms as well, and defects in polarized growth affect their virulence (15). In *N. crassa*, cells within the hyphae are designated by incomplete cell walls known as septa, and pores within the septa allow direct cytoplasmic contact and free flow of organelles (including nuclei) from cell to cell (16, 17). This can result in strains that are heterokaryotic, containing cells that contain multiple, genetically distinct nuclei.

Asexual sporulation occurs because of certain environmental stressors, such as changes in temperature or exposure to oxygen (18). This causes aerial hyphae to grow perpendicular to the substrate. These specialized aerial hyphae form chains of distinct spores (macroconidia) at their tips (19). Once macroconidia are dispersed and can detect nutrients outside of the cell, they germinate into basal hyphae and form a new mycelial mat. Sporulation from vegetative basal hyphae has also been observed under certain stress conditions. These microconidia are considerably smaller than macroconidia (1 μm in diameter), and are mononucleate as well, allowing for isolation of homokaryotic strains effectively without need of a sexual cross (20).

The sexual cycle in *N. crassa* involves the fusion of cells from the two mating types, *mat a* and *mat A* (21). When vegetative hyphae are starved for nitrogen, they form the protoperithecium, the female reproductive structure. Both

mating types are capable of forming protoperithecia, but require asexual spores of the opposite mating type to proceed through the sexual cycle (22). Pheromones from the male spore induce growth of a specialized hypha from the protoperithecia called the trichogyne (23). Upon fusion with the male spore, two rounds of meiosis will proceed as the fruiting body (the perithecium) forms. This results in an ascus containing eight ascospores, which are the homokaryotic progeny from meiosis (24). Ascospores are then ejected from the perithecium into the environment, and are activated via sufficient heating (25); once activated, the ascospores will germinate and exhibit vegetative basal hyphae growth as described above.

Past studies have taken advantage of the fact that *N. crassa* extends at a rate of 5 mm/hour on agar containing minimal medium (26). The rapid polarized growth of *N. crassa* across a substrate allows the organism to colonize decaying plant matter for carbon metabolism in nature (27). However, in laboratory studies using insoluble plant material for carbon metabolism, the insoluble material will settle at the bottom of the culture tube, resulting in growth conditions that more closely resemble carbon starvation (3). To address this, growth of the mycelium can take place in shaken liquid culture, resulting in full access to the insoluble carbon source, and its degradation into soluble sugars over the course of several days. Additionally, most strains will only form vegetative hyphae in submerged culture rather than conidia and other cell types, aiding in uniform analysis of the organism (28).

Cellulose Degradation in Filamentous Fungi

Plants use carbon fixation to generate glucose and other carbon compounds from carbon dioxide in the air. This glucose is incorporated into a complex cell wall that consists of several polysaccharides and branching organic compounds. While this source of glucose is readily abundant in nature, it requires specialized enzymes to break its β-1,4-linkages. The most abundant polymer found in the plant cell wall is cellulose, which is a chain of β-1,4-linked glucose monomers (14). This material is considered a waste byproduct of agriculture, but can be used for production of alternative fuel sources (29). Filamentous fungi have developed strategies to liberate glucose oligomers, the disaccharide cellobiose, and the monomer glucose from this material to use as a carbon source (30).

In *T. reesei* and in the genus *Aspergillus*, cellobiose can induce the production of cellulolytic enzymes, while in *N. crassa,* gene deletion of all three β-glucosidases is needed for cellulase induction by cellobiose (31), indicating that partial cellulose degradation is necessary before full induction can occur. When fungi can sense glucose and/or other carbon compounds that can be degraded to glucose readily, the transcription factor CRE-1 induces carbon catabolite repression (CCR), a process that represses transcription of genes for utilization of alternative carbon sources (30, 32). In *N. crassa* and *A. nidulans*, CRE-1 is localized to the nucleus when either fungus is grown in the presence of a rich carbon source (33, 34) . However, in the absence of a rich carbon source, CRE-1

is no longer localized to the nucleus, allowing other transcriptional regulators to activate cellulase transcription. *N. crassa Δcre-1* mutant strains also show an increase in cellulase mRNA when grown in media containing avicel (35). These findings illustrate the importance of this regulator in control of carbon metabolism.

While CRE-1 inhibits the expression of cellular components necessary for metabolism of alternative carbon sources, the cellulose degradation regulators (CLRs) are more specific to cellulose (36). Unlike some other filamentous fungi in which hemicellulose and cellulose degradation are driven by the same transcription factors, this process is uncoupled from hemicellulose degradation in *N. crassa* (30). CLR-1 is a transcription factor that induces expression of several cellulolytic genes, as well as a second transcription factor, *clr-2*. In the absence of cellulose, CLR-3, a protein of unknown function, inhibits CLR-1 (37). In the presence of cellulose, CLR-3 no longer represses CLR-1, allowing transcription of *clr-2* (38). CLR-2 then will drive the transcription of mRNAs for enzymes in the plant cell wall degradation network (PCWDN) that are specific to cellulose (39). The full response to cellulose seems to be governed mainly by CLR-2, as constitutive activation of *clr-2* leads to transcriptional activation of the cellulose regulon on a noninducing carbon source, while activation of *clr-1* does not have the same effect (36). Another transcription factor, CLR-4, has recently been characterized and was found to bind the promoters of *clr-1* in *N. crassa* and *xyr-1* and *clr-2* in *Myceliophthora thermophila*, perhaps orchestrating the whole process of cellulose detection in these fungi (40).

The carbohydrate-active enzymes (CAZymes) in the network for the metabolism of cellulose are referred to as cellulases and consist of several major classes (14). The activities of the five major cellulase classes are described below, and are illustrated in Figure 1.1. Cellobiohydrolases cleave β-1,4-linkages from the reducing ends of cellulose chains, producing cellobiose (39). Endoglucanases cleave β-1,4-linkages within the cellulose chain to produce more reducing ends for cellobiohydrolases to act upon (41). Cellobiose dehydrogensases oxidize free cellodextrins, such as cellobiose. The oxidized cellodextrins can then be used as an electron donors by polysaccharide monooxygenases to cleave β-1,4-linkages internally, releasing more reducing ends as well (42). β-glucosidases cleave cellobiose molecules to produce two glucose molecules (31). This cocktail of enzymes converts the recalcitrant cellulose into glucose for carbon metabolism by the fungus.

Heterotrimeric G protein Signaling in *N. crassa*

Numerous studies indicate that filamentous fungi use G protein coupled receptors (GPCRs) and their associated heterotrimeric guanine nucleotide binding proteins, or G proteins, to interrogate their surroundings much like other eukaryotic organisms (43, 44). GPCRs are characterized by their seven transmembrane helices and act as guanine nucleotide exchange factors (GEFs) for the Gα they activate (45). G proteins consist of α, β, and γ subunits (46-48). The Gα subunit binds to guanine nucleotides, and is in an active conformation

when bound to guanine triphosphate (GTP), and an inactive conformation when bound to guanine diphosphate (GDP) (49). This conformational change allows the Gα to disassociate with the GPCR and the Gβγ dimer (50). Both components will then signal downstream effectors, which includes adenylate cyclase, an enzyme that produces cyclic AMP as a second messenger (51, 52). This results in the activation of Protein Kinase A (PKA) which is known to have many downstream targets (53).

The Gβ and Gγ subunits are unable to unable to be dissociated from each other, and have a wide variety of downstream targets (50). The Gβ subunit contains seven tryptophan-aspartate (WD) repeats, similar to a wide array of diverse proteins with varied activites (54). In humans, there are 6 Gβ isoforms, and 12 Gγ isoforms known, but each fungal species appears to have one of each (55).

A homolog of the Receptor for Activated C Kinase, another WD repeat containing protein, has been identified as a Gβ homolog in several systems, including some fungal species (56). RACK-1 homologs are known to be multifunctional. While RACK-1 homologs have been found to interact directly with Gα subunits in several filamentous fungi, they are primarily known for their involvement in derepression of amino acid biosynthesis during starvation conditions in a process referred to as cross pathway control (57-59). Additionally, RACK-1 homologs may serve as chaperones for ribosomal proteins during translation (60).

While there are four major families of Gα subunits with multiple members in humans (G_i, G_s, G_q and $G_{12/13}$), there are only three known Gα subunits in *N. crassa*, which are GNA-1, GNA-2, and GNA-3 (61). GNA-1 and GNA-3 are well documented to be responsible for a variety of distinct functions in *N. crassa*, while GNA-2 plays a compensatory role for the other two (43, 44). Double mutants lacking *gna-1* and *gna-3* have stunted extension of aerial and basal hyphae, and precociously form macroconidia. These effects are heightened upon deletion of *gna-2* as well, indicating that all three Ga genes are needed for normal functioning in this organism (62). *N. crassa* has been demonstrated to contain one Gβ subunit, GNB-1, and one Gγ subunit, GNG-1 (55). GNB-1 and GNG-1 form a complex and GNB-1 is required for stability of GNA-1 and GNA-2 when *N. crassa* is grown on VM sucrose medium (55).

G Protein Involvement in Cellulose Metabolism

GPCRs allow fungi to interrogate their surroundings and respond to stimuli, causing them to regulate metabolism and development, as well as virulence in pathogenic species (44). Our understanding of these receptors is crucial to combatting fungal disease in both plants and animals. This will also aid in developing efficient ways to utilize the plentiful source of glucose present in the environment. In *N. crassa*, the GPCR GPR-4 was found to be homologous to known carbon sensory GPCRs in yeasts, and GPR-4 is required for levels of intracellular cAMP to rise after addition of glucose, indicative of glucose sensing

by this GPCR (63). A survey of all the known GPCRs in *N. crassa* indicated that several mutants for the class XIV Pth11-like GPCRs, a family of receptors specific to the division Pezizomycotina, had defects when grown on cellulose containing medium. Additionally, a majority of these GPCRs were more highly expressed when wild type *N. crassa* was grown on cellulose medium rather than sucrose (64, 65). Pth11 is a GPCR that is required for sensing the plant cell wall and the formation of the invasive pathogenic structure (appressorium) in the rice blast pathogen, *Magnaporthe oryzae* (66). Additionally, two *Fusarium graminearum* Pth11 like GPCRs have been found to interact with Gα subunits during heterologous expression in yeast (67). In *T. reesei,* the class XIII GPCR CSG1 is required for basal levels of cellulase activity in response to either cellulose or lactose (both are inducers of the cellulose response in this system) (68). These studies exemplify the importance of specific GPCRs to detection of cellulose as a carbon source.

Gα proteins are also tied to carbon metabolism. The N-terminus of the GPCR GPR-4 physically interacted with all three *N. crassa* Gα proteins in a yeast two hybrid assay, with the strongest interaction occurring with GNA-1. Experiments involving genetic epistasis also confirmed that GNA-1 is in a linear pathway downstream of GPR-4 (63). A study of the metabolome of wild type *N. crassa* and Δ*gna-3* mutants demonstrated that Δ*gna-3* mutants are unable to sense carbon sources in the environment (69). More specifically, cellulose metabolism is regulated by G protein subunits in several fungal species. Strains

containing overexpressed versions of *gna-3* express cellulases more highly in light during exposure to cellulose in *T reesei* (70). On a related note, in *M. oryzae* the GPCR Pth11 physically interacts with MagA (the *M. oryzae* homolog to GNA-3) and adenylate cyclase in late endosomes (71).

Adenylate cyclase is a known downstream target of G protein signaling and also affects carbon metabolism. In *N. crassa*, GNA-3 affects the protein levels of the adenylate cyclase CR-1 (52). GNA-1 is known to stimulate cAMP production via activation of CR-1 (51). Work in *N. crassa* and *Myceliopththora thermophila* revealed that strains overexpressing *cr-1* exhibited an increase in cellulase mRNA levels, including the mRNAs for the two major cellobiohydrolases *cbh-1* and *cbh-2* (NCU07340 and NCU09680) suggesting that cAMP-dependent signaling relays the cellulose signal to the nucleus(40).

Hypothesis and Objectives

All components of the heterotrimeric G protein in *N.* crassa are required for proper carbon sensing. Additionally, the RACK-1 homolog has been proposed in other systems as a Gβ subunit, and is known to be involved in regulation of amino acid metabolism in *N. crassa*. The recent work involving Pth11-like GPCRs suggests that G protein signaling is necessary for the proper detection of cellulose as a carbon source. Therefore, the hypothesis of this thesis is that multiple G protein subunits, including the potential Gβ subunit CPC-2, are required to detect cellulose. Based on the known involvement of cAMP signaling in carbon sensing in *N. crassa* and other fungi, it is proposed that G protein subunits then relay this message to the nucleus via cAMP dependent signal transduction, inducing a transcriptional response to cellulose. The main goal of this thesis is to determine whether signal transduction through G protein signaling affects cellulase transcription.

Objective 1: Determine genetic relationships between CPC-2 and the other G protein subunits

While CPC-2 is homologous to other Gβ subunits, no one has explored a possible function for CPC-2 in G protein signaling in *N*. *crassa*. Additionally, it is known that GNB-1 is needed for stability of GNA-1 and GNA-2 on sucrose-containing medium (72). Phylogenetic analysis of *cpc-2* will indicate its degree of similarity to *gnb-1.* Genetic analysis will provide evidence for or against a role as

an alternative Gβ subunit. Strains carrying single and double mutant combinations of *cpc-2* and G protein subunits or the *cpc-2* mutation and constitutively activated Gα genes are present in our laboratory. Using these strains, we will be able to determine the epistatic relationships between each gene and determine whether these subunits act together in a linear path. Production of a polyclonal antibody to CPC-2 will allow us to determine whether the other G protein subunits affect the levels of CPC-2 in the same manner as GNB-1. Antibodies to each G protein subunit are already available in our laboratory and will be used to show if CPC-2 alters the levels of the different G protein subunits. This will establish any relationships present between CPC-2 and the other G protein subunits. Relationships between the other subunits have been described previously and will be used as a baseline for the remainder of this work.

Objective 2: Investigate the extent of G protein involvement in the cellulose response

Previous work showing Pth11-like GPCR genes influence growth of *N. crassa* on cellulose prompted investigation into the role that heterotrimeric G protein signaling plays in cellulose sensing and degradation in *N. crassa*. A comprehensive genetic analysis using gene deletion mutants for all known G protein subunits and adenylyl cyclase, as well as strains expressing constitutively active versions of the Gα subunits will demonstrate if the G protein subunits are

indeed involved in cellulose degradation. This will be conducted using measurements of enzyme activity and mRNA levels for secreted cellulases in these strains. Additionally, western blot analysis will be used to explore possible effects of the various mutations on G protein levels.

Objective 3: Determine role of G proteins on the global transcriptional response to cellulose as a carbon source

Several studies have illustrated that disruption of different components of the cellulose signaling pathway interrupts global cellulase transcription. This information has been used to construct regulons controlled by particular transcription factors, as well as networks of genes affected when wild type is grown on a specific carbon source. Analysis of the total transcriptome from cellulose grown cultures of the mutants for the Gα subunits *gna-1* and *gna-3*, as well as the adenylate cyclase *cr-1*, will show whether these genes control cellulase transcription. Following a similar approach to the previous work, we should be able to construct a network of cellulolytic genes that are affected by cAMP signaling through the G protein subunits GNA-1 and GNA-3. Additionally, we may be able to identify other pathways that are affected by this process during growth on cellulose.

Figures

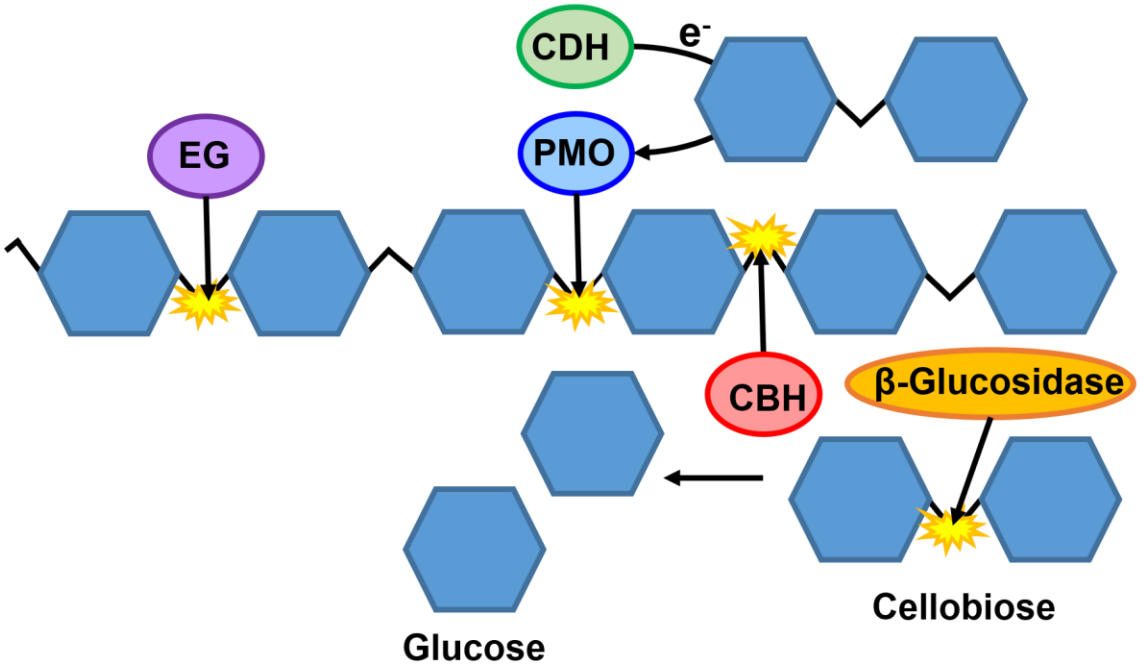

Figure 1.1 Activities of the five major cellulase classes in filamentous fungi. Filamentous fungi secrete a cocktail of enzymes to completely degrade cellulose into its dimer cellobiose, and then further into its monomer, glucose. Cellobiohydrolases (CBH), endoglucanases (EG), and β-glucosidases directly break β-1.4-linkages in cellulose, yielding cellobiose, glucose oligomers, and glucose, respectively. Cellobiose dehydrogenases (CDH) oxidize cellodextrins, allowing polysaccharide monooxygenases (PMO) to break β-1.4-linkages internally, yielding glucose oligomers.

References

1. Ruger-Herreros C, Corrochano LM. 2020. Conidiation in Neurospora crassa: vegetative reproduction by a model fungus. Int Microbiol 23:97-105.

2. Borkovich KA, Alex LA, Yarden O, Freitag M, Turner GE, Read ND, Seiler S, Bell-Pedersen D, Paietta J, Plesofsky N, Plamann M, Goodrich-Tanrikulu M, Schulte U, Mannhaupt G, Nargang FE, Radford A, Selitrennikoff C, Galagan JE, Dunlap JC, Loros JJ, Catcheside D, Inoue H, Aramayo R, Polymenis M, Selker EU, Sachs MS, Marzluf GA, Paulsen I, Davis R, Ebbole DJ, Zelter A, Kalkman ER, O'Rourke R, Bowring F, Yeadon J, Ishii C, Suzuki K, Sakai W, Pratt R. 2004. Lessons from the genome sequence of *Neurospora crassa*: tracing the path from genomic blueprint to multicellular organism. Microbiol Mol Biol Rev 68:1-108.

3. Tian C, Beeson WT, Iavarone AT, Sun J, Marletta MA, Cate JH, Glass NL. 2009. Systems analysis of plant cell wall degradation by the model filamentous fungus *Neurospora crassa*. Proc Natl Acad Sci U S A 106:22157-62.

4. Davis RH. 2000. Neurospora : contributions of a model organism. Oxford University Press, New York.

5. Ninomiya Y, Suzuki K, Ishii C, Inoue H. 2004. Highly efficient gene replacements in Neurospora strains deficient for nonhomologous end-joining. Proc Natl Acad Sci U S A 101:12248-53.

6. Davis RH, Perkins DD. 2002. Timeline: Neurospora: a model of model microbes. Nat Rev Genet 3:397-403.

7. Beadle GW, Tatum EL. 1941. Genetic Control of Biochemical Reactions in Neurospora. Proc Natl Acad Sci U S A 27:499-506.

8. Galagan JE, Calvo SE, Borkovich KA, Selker EU, Read ND, Jaffe D, FitzHugh W, Ma LJ, Smirnov S, Purcell S, Rehman B, Elkins T, Engels R, Wang S, Nielsen CB, Butler J, Endrizzi M, Qui D, Ianakiev P, Bell-Pedersen D, Nelson MA, Werner-Washburne M, Selitrennikoff CP, Kinsey JA, Braun EL, Zelter A, Schulte U, Kothe GO, Jedd G, Mewes W, Staben C, Marcotte E, Greenberg D, Roy A, Foley K, Naylor J, Stange-Thomann N, Barrett R, Gnerre S, Kamal M, Kamvysselis M, Mauceli E, Bielke C, Rudd S, Frishman D, Krystofova S, Rasmussen C, Metzenberg RL, Perkins DD, Kroken S, et al. 2003. The genome sequence of the filamentous fungus *Neurospora crassa*. Nature 422:859-68.

9. Colot HV, Park G, Turner GE, Ringelberg C, Crew CM, Litvinkova L, Weiss RL, Borkovich KA, Dunlap JC. 2006. A high-throughput gene knockout procedure for Neurospora reveals functions for multiple transcription factors. Proc Natl Acad Sci U S A 103:10352-7.

10. Bistis GN, Perkins DD, Read ND. 2003. Different cell types in *Neurospora crassa*. Fungal Genet Newsl 50:17-19.

11. Davis RH, deSerres FJ. 1970. Genetic and microbiological research techniques for *Neurospora crassa*. Methods Enzymol 71A:79-143.

12. Glass NL, Rasmussen C, Roca MG, Read ND. 2004. Hyphal homing, fusion and mycelial interconnectedness. Trends Microbiol 12:135-41.

13. Riquelme M, Yarden O, Bartnicki-Garcia S, Bowman B, Castro-Longoria E, Free SJ, Fleissner A, Freitag M, Lew RR, Mourino-Perez R, Plamann M, Rasmussen C, Richthammer C, Roberson RW, Sanchez-Leon E, Seiler S, Watters MK. 2011. Architecture and development of the Neurospora crassa hypha -- a model cell for polarized growth. Fungal Biol 115:446-74.

14. Glass NL, Schmoll M, Cate JH, Coradetti S. 2013. Plant Cell Wall Deconstruction by Ascomycete Fungi. Annu Rev Microbiol doi:10.1146/annurev-micro-092611-150044.

15. Castillo-Lluva S, Alvarez-Tabares I, Weber I, Steinberg G, Perez-Martin J. 2007. Sustained cell polarity and virulence in the phytopathogenic fungus Ustilago maydis depends on an essential cyclin-dependent kinase from the Cdk5/Pho85 family. J Cell Sci 120:1584-95.

16. Hickey PC, Jacobson D, Read ND, Glass NL. 2002. Live-cell imaging of vegetative hyphal fusion in Neurospora crassa. Fungal Genet Biol 37:109-19.

17. Harris SD. 2001. Septum formation in Aspergillus nidulans. Curr Opin Microbiol 4:736-9.

18. Hansberg W, de Groot H, Sies H. 1993. Reactive oxygen species associated with cell differentiation in *Neurospora crassa*. Free Radic Biol Med 14:287-93.

19. Springer ML. 1993. Genetic control of fungal differentiation: the three sporulation pathways of *Neurospora crassa*. Bioessays 15:365-74.

20. Ebbole DJ, Sachs MS. 1990. A rapid and simple method for isolation of *Neurospora crassa* homokaryons using microconidia. Fungal Genet Newsl 37:17-18.

21. Metzenberg RL, Glass NL. 1990. Mating type and mating strategies in Neurospora. Bioessays 12:53-9.

22. Raju NB. 1992. Genetic control of the sexual cycle in *Neurospora*. Mycol Res 96:241-262.

23. Bistis GN. 1981. Chemotropic Interactions between Trichogynes and Conidia of Opposite Mating-Type in *Neurospora crassa*. Mycologia 73:959-975.

24. Raju NB. 1980. Meiosis and ascospore genesis in Neurospora. Eur J Cell Biol 23:208-23.

25. Raju NB, Leslie JF. 1992. Cytology of recessive sexual-phase mutants from wild strains of Neurospora crassa. Genome 35:815-26.

26. Perkins DD, Davis RH. 2000. Neurospora at the millennium. Fungal Genet Biol 31:153-67.

27. Glass NL, Schmoll M, Cate JH, Coradetti S. 2013. Plant cell wall deconstruction by ascomycete fungi. Annu Rev Microbiol 67:477-98.

28. Cortat M, Turian G. 1974. Conidiation of *Neurospora crassa* in submerged culture without mycelial phase. Arch Mikrobiol 95:305-9.

29. Rubin EM. 2008. Genomics of cellulosic biofuels. Nature 454:841-5.

30. Huberman LB, Liu J, Qin L, Glass NL. 2016. Regulation of the lignocellulolytic response in filamentous fungi. Fungal Biol Rev 30:101-111.

31. Znameroski EA, Coradetti ST, Roche CM, Tsai JC, Iavarone AT, Cate JH, Glass NL. 2012. Induction of lignocellulose-degrading enzymes in *Neurospora crassa* by cellodextrins. Proc Nat Acad Sci USA 109:6012-7.

32. Vinuselvi P, Kim MK, Lee SK, Ghim CM. 2012. Rewiring carbon catabolite repression for microbial cell factory. BMB Rep 45:59-70.

33. Brown NA, de Gouvea PF, Krohn NG, Savoldi M, Goldman GH. 2013. Functional characterisation of the non-essential protein kinases and phosphatases regulating Aspergillus nidulans hydrolytic enzyme production. Biotechnol Biofuels 6:91.

34. Cupertino FB, Virgilio S, Freitas FZ, Candido Tde S, Bertolini MC. 2015. Regulation of glycogen metabolism by the CRE-1, RCO-1 and RCM-1 proteins in Neurospora crassa. The role of CRE-1 as the central transcriptional regulator. Fungal Genet Biol 77:82-94.

35. Sun J, Glass NL. 2011. Identification of the CRE-1 cellulolytic regulon in *Neurospora crassa*. PLoS One 6:e25654.

36. Coradetti ST, Xiong Y, Glass NL. 2013. Analysis of a conserved cellulase transcriptional regulator reveals inducer-independent production of cellulolytic enzymes in Neurospora crassa. Microbiologyopen 2:595-609.

37. Huberman LB, Coradetti ST, Glass NL. 2017. Network of nutrient-sensing pathways and a conserved kinase cascade integrate osmolarity and carbon sensing in *Neurospora crassa*. Proc Natl Acad Sci U S A 114:E8665-E8674.

38. Coradetti ST, Craig JP, Xiong Y, Shock T, Tian C, Glass NL. 2012. Conserved and essential transcription factors for cellulase gene expression in ascomycete fungi. Proc Natl Acad Sci U S A 109:7397-402.

39. Samal A, Craig JP, Coradetti ST, Benz JP, Eddy JA, Price ND, Glass NL. 2017. Network reconstruction and systems analysis of plant cell wall deconstruction by *Neurospora crassa*. Biotechnol Biofuels 10:225.

40. Liu Q, Li J, Gao R, Li J, Ma G, Tian C. 2019. CLR-4, a novel conserved transcription factor for cellulase gene expression in ascomycete fungi. Mol Microbiol 111:373-394.

41. Sun J, Phillips CM, Anderson CT, Beeson WT, Marletta MA, Glass NL. 2011. Expression and characterization of the Neurospora crassa endoglucanase GH5-1. Protein Expr Purif 75:147-54.

42. Phillips CM, Beeson WT, Cate JH, Marletta MA. 2011. Cellobiose dehydrogenase and a copper-dependent polysaccharide monooxygenase potentiate cellulose degradation by *Neurospora crassa*. ACS Chem Biol 6:1399-1406.

43. Li L, Wright SJ, Krystofova S, Park G, Borkovich KA. 2007. Heterotrimeric G protein signaling in filamentous fungi. Annu Rev Microbiol 61:423-52.

44. Brown NA, Schrevens S, van Dijck P, Goldman GH. 2018. Fungal G-protein-coupled receptors: mediators of pathogenesis and targets for disease control. Nat Microbiol 3:402-414.

45. Shukla AK, Singh G, Ghosh E. 2014. Emerging structural insights into biased GPCR signaling. Trends Biochem Sci 39:594-602.

46. Bock A, Kostenis E, Trankle C, Lohse MJ, Mohr K. 2014. Pilot the pulse: controlling the multiplicity of receptor dynamics. Trends Pharmacol Sci 35:630-638.

47. Chini B, Parenti M, Poyner DR, Wheatley M. 2013. G-protein-coupled receptors: from structural insights to functional mechanisms. Biochem Soc Trans 41:135-6.

48. Tesmer JJ. 2010. The quest to understand heterotrimeric G protein signaling. Nat Struct Mol Biol 17:650-2.

49. Lambright DG, Noel JP, Hamm HE, Sigler PB. 1994. Structural determinants for activation of the alpha-subunit of a heterotrimeric G protein. Nature 369:621-8.

50. Hamm HE. 1998. The many faces of G protein signaling. J Biol Chem 273:669-72.

51. Ivey FD, Yang Q, Borkovich KA. 1999. Positive regulation of adenylyl cyclase activity by a galphai homolog in Neurospora crassa. Fungal Genet Biol 26:48-61.

52. Kays AM, Rowley PS, Baasiri RA, Borkovich KA. 2000. Regulation of conidiation and adenylyl cyclase levels by the Galpha protein GNA-3 in *Neurospora crassa*. Mol Cell Biol 20:7693-705.

53. Horta MAC, Thieme N, Gao Y, Burnum-Johnson KE, Nicora CD, Gritsenko MA, Lipton MS, Mohanraj K, de Assis LJ, Lin L, Tian C, Braus GH, Borkovich KA, Schmoll M, Larrondo LF, Samal A, Goldman GH, Benz JP. 2019. Broad Substrate-Specific Phosphorylation Events Are Associated With the Initial Stage of Plant Cell Wall Recognition in Neurospora crassa. Front Microbiol 10:2317.

54. Clapham DE, Neer EJ. 1997. G protein beta gamma subunits. Annu Rev Pharmacol Toxicol 37:167-203.

55. Krystofova S, Borkovich KA. 2005. The heterotrimeric G-protein subunits GNG-1 and GNB-1 form a Gbetagamma dimer required for normal female fertility, asexual development, and Galpha protein levels in *Neurospora crassa*. Eukaryot Cell 4:365-78.

56. Ron D, Chen CH, Caldwell J, Jamieson L, Orr E, Mochly-Rosen D. 1994. Cloning of an intracellular receptor for protein kinase C: a homolog of the beta subunit of G proteins. Proc Natl Acad Sci U S A 91:839-43.

57. Yin Z, Zhang X, Wang J, Yang L, Feng W, Chen C, Gao C, Zhang H, Zheng X, Wang P, Zhang Z. 2018. MoMip11, a MoRgs7-interacting protein, functions as a scaffolding protein to regulate cAMP signaling and pathogenicity in the rice blast fungus Magnaporthe oryzae. Environ Microbiol 20:3168-3185.

58. Palmer DA, Thompson JK, Li L, Prat A, Wang P. 2006. Gib2, a novel Gbeta-like/RACK1 homolog, functions as a Gbeta subunit in cAMP signaling and is essential in Cryptococcus neoformans. J Biol Chem 281:32596-605.

59. Kruger D, Koch J, Barthelmess IB. 1990. cpc-2, a new locus involved in general control of amino acid synthetic enzymes in Neurospora crassa. Curr Genet 18:211-5.

60. Adams DR, Ron D, Kiely PA. 2011. RACK1, A multifaceted scaffolding protein: Structure and function. Cell Commun Signal 9:22.

61. Neves SR, Ram PT, Iyengar R. 2002. G protein pathways. Science 296:1636-9.

62. Kays AM, Borkovich KA. 2004. Severe impairment of growth and differentiation in a *Neurospora crassa* mutant lacking all heterotrimeric Galpha proteins. Genetics 166:1229-40.

63. Li L, Borkovich KA. 2006. GPR-4 is a predicted G-protein-coupled receptor required for carbon source-dependent asexual growth and development in *Neurospora crassa*. Eukaryot Cell 5:1287-300.

64. Cabrera IE, Pacentine IV, Lim A, Guerrero N, Krystofova S, Li L, Michkov AV, Servin JA, Ahrendt SR, Carrillo AJ, Davidson LM, Barsoum AH, Cao J, Castillo R, Chen WC, Dinkchian A, Kim S, Kitada SM, Lai TH, Mach A, Malekyan C, Moua TR, Torres CR, Yamamoto A, Borkovich KA. 2015. Global analysis of predicted G Protein-Coupled Receptor genes in the filamentous fungus, *Neurospora crassa*. G3 (Bethesda) 5:2729-43.

65. Kulkarni RD, Thon MR, Pan H, Dean RA. 2005. Novel G-protein-coupled receptor-like proteins in the plant pathogenic fungus *Magnaporthe grisea*. Genome Biol 6:R24.

66. DeZwaan TM, Carroll AM, Valent B, Sweigard JA. 1999. *Magnaporthe grisea* Pth11p is a novel plasma membrane protein that mediates appressorium differentiation in response to inductive substrate cues. Plant Cell 11:2013-30.

67. Dilks T, Halsey K, De Vos RP, Hammond-Kosack KE, Brown NA. 2019. Non-canonical fungal G-protein coupled receptors promote *Fusarium* head blight on wheat. PLoS Pathog 15:e1007666.

68. Stappler E, Dattenbock C, Tisch D, Schmoll M. 2017. Analysis of Light- and Carbon-Specific Transcriptomes Implicates a Class of G-Protein-Coupled Receptors in Cellulose Sensing. mSphere 2.

69. Kim JD, Kaiser K, Larive CK, Borkovich KA. 2011. Use of 1H nuclear magnetic resonance to measure intracellular metabolite levels during growth and asexual sporulation in Neurospora crassa. Eukaryot Cell 10:820-31.

70. Schmoll M, Schuster A, Silva Rdo N, Kubicek CP. 2009. The G-alpha protein GNA3 of Hypocrea jecorina (Anamorph Trichoderma reesei) regulates cellulase gene expression in the presence of light. Eukaryot Cell 8:410-20.

71. Ramanujam R, Calvert ME, Selvaraj P, Naqvi NI. 2013. The late endosomal HOPS complex anchors active G-protein signaling essential for pathogenesis in *Magnaporthe oryzae*. PLoS Pathog 9:e1003527.

72. Yang Q, Poole SI, Borkovich KA. 2002. A G-protein beta subunit required for sexual and vegetative development and maintenance of normal G alpha protein levels in *Neurospora crassa*. Eukaryot Cell 1:378-90.

Chapter 2: Genetic relationships between the RACK1 homolog cpc-2 and heterotrimeric G protein subunit genes in *Neurospora crassa*

Amruta Garud*, Alexander Carrillo*, Logan Collier*, Arit Ghosh*, James D. Kim, Berenise Lopez-Lopez, Shouqiang Ouyang and Katherine A. Borkovich

*These authors contributed equally to this work.

Contributions to this Chapter

This chapter was published in PLOS One (Garud A, Carrillo AJ, Collier LA, Ghosh A, Kim JD, Lopez-Lopez B, Ouyang S, Borkovich KA. 2019. Genetic relationships between the RACK1 homolog *cpc-2* and heterotrimeric G protein subunit genes in *Neurospora crassa*. PLoS One 14:e0223334). I contributed to this work by constructing the C2G3*#1–8, C2G3#1–6, and C2B1#2-1-1 mutants. I also verified the correct genotype for many of the strains (see Supporting Information). I developed the macroconidia quantification assay and helped develop the CPC-2 polyclonal antibody. I performed the experiments required for Figures 3-6. I performed the ANOVA and Multiple Comparisons test present in the Supporting Information, and the experiments for Supporting Figures 1 and 2.

Abstract

Receptor for Activated C Kinase-1 (RACK1) is a multifunctional eukaryotic scaffolding protein with a seven WD repeat structure. Among their many cellular roles, RACK1 homologs have been shown to serve as alternative Gβ subunits during heterotrimeric G protein signaling in many systems. We investigated genetic interactions between the RACK1 homolog *cpc-2*, the previously characterized Gβ subunit *gnb-1* and other G protein signaling components in the multicellular filamentous fungus *Neurospora crassa*. Results from cell fractionation studies and from fluorescent microscopy of a strain expressing a CPC-2-GFP fusion protein revealed that CPC-2 is a cytoplasmic protein. Genetic epistasis experiments between *cpc-2*, the three Gα genes (*gna-1*, *gna-2* and *gna-3*) and *gnb-1* demonstrated that *cpc-2* is epistatic to *gna-2* with regards to basal hyphae growth rate and aerial hyphae height, while deletion of *cpc-2* mitigates the increased macroconidiation on solid medium observed in Δ*gnb-1* mutants. Δ*cpc-2* mutants inappropriately produce conidiophores during growth in submerged culture and mutational activation of *gna-3* alleviates this defect. Δ*cpc-2* mutants are female-sterile and fertility could not be restored by mutational activation of any of the three Gα genes. With the exception of macroconidiation on solid medium, double mutants lacking *cpc-2* and *gnb-1* exhibited more severe defects for all phenotypic traits, supporting a largely synergistic relationship between GNB-1 and CPC-2 in *N. crassa*.

Introduction

Heterotrimeric G protein signaling cascades consist of seven-helix transmembrane G Protein Coupled Receptors (GPCRs) and the three G protein subunits—Gα, Gβ and Gγ (1-3). In the inactive state, the Gαβγ heterotrimer is associated with the GPCR. Ligand stimulation causes exchange of GDP for GTP on the Gα, leading to dissociation of Gα-GTP from the Gβγ heterodimer. The Gα-GTP and the Gβγ dimer can then regulate downstream effectors, leading to changes in cellular physiology (3). The Gα-GTP has native GTPase activity that causes release of the inorganic phosphate from the GTP. The Gα-GDP then reassociates with the Gβ subunit and GPCR, leading to signal termination and completion of the cycle.

Neurospora crassa is a multicellular ascomycete fungus that has emerged as a model system to study G protein signaling, and comparisons with *N*. *crassa* have driven discoveries in pathogenic fungi and higher eukaryotes (4, 5). In *N*. *crassa*, there are 43 predicted GPCRs, three Gα subunits (GNA-1, GNA-2 and GNA-3), one characterized Gβ subunit (GNB-1) and one Gγ subunit (GNG-1) (6, 7). Major processes such as hyphal growth, macroconidiation, conidial germination, mating, nutrient sensing and temperature and oxidative stress resistance are regulated by G protein signaling pathways in *N*. *crassa* (7-13).

Receptor for Activated C Kinase-1 (RACK1) is a major scaffolding protein in many eukaryotic systems. Similar to G protein β subunits, RACK1 has a seven

WD repeat structure, and is one of the best-studied proteins in the WD-repeat family (14). Initially identified as a protein that binds to the active conformation of protein kinase C (PKC) βII, RACK1 is now known to be multifunctional (14, 15). For example, RACK1 allows cross talk between the PKC and Mitogen Activated Kinase (MAP) pathways by acting as a scaffold for the Jun N-terminal Kinase (JNK) upon stimulation, leading to PKC-mediated phosphorylation and activation of JNK (16). It has been observed that RACK1 binds to the Gβγ dimer in HEK293 cells and also regulates a subset of its functions, including promoting its dislocation from the cytosol to the membrane (17). Additionally, RACK1 is known to associate with the 40S subunit of the ribosome, near the mRNA exit channel (18). Due to its conformation when bound to the ribosome, RACK1 is believed to serve as an adaptor, bringing together proteins at the ribosome during translation [reviewed in (14)].

Homologs of RACK1 have been implicated as alternative Gβ subunits in the fungal kingdom, through direct interaction with Gα subunits (19, 20). In *Saccharomyces cerevisiae*, Asc1p functions as a Guanine nucleotide Dissociation Inhibitor (GDI) for the Gα Gpa2, and is involved in regulating glucose responsiveness through its binding to adenylyl cyclase (Cyr1) (19). *gib2*, an essential gene in *Crytpococcus neoformans*, encodes a protein that binds to the Gα Gpa1 and two Gγ subunits, Gpg1 and Gpg2. It also associates with Smg1, a downstream target of cAMP signaling, and to the protein kinase C homolog Pkc1 (20). In *Magnaporthe oryzae*, the RACK1 ortholog MoMip11

interacts with the Gα protein MoMagA and the Regulator of G protein Signaling (RGS) protein MoRgs7 to regulate pathogenicity (21, 22).

Additional RACK1 orthologs have been shown to regulate various aspects of growth and development in several fungal systems, but without demonstration of a physical interaction with heterotrimeric Gα proteins. *S*. *pombe* Cpc2 plays a role in cell cycle regulation and stress responses through ribosomal association and translational control of the stress response transcriptional factor Atf1 (23). RACK1 orthologs from *Aspergillus nidulans* and *Aspergillus fumigatus* have been demonstrated to regulate sexual differentiation and asexual growth and development, respectively (24, 25). In *Ustilago maydis*, Rak1 is essential for the transcription of *rop*1, which is a direct positive regulator of the pheromone response factor (*prf1*), making it essential for mating (26). Strains lacking RAK1 also have attenuated filamentation and virulence, and abnormal cell morphology (26).

The *N*. *crassa* RACK1 homolog CPC-2 was the first reported RACK1 protein in fungi, initially identified as a component of the general amino acid regulation network (27). In *N*. *crassa*, starvation for a single amino acid leads to an overall derepression of all amino acid biosynthetic genes at the level of transcription (28). Loss of the *cpc-2* gene blocks derepression of amino acid biosynthetic genes during amino acid limiting conditions (27). Under non-starved conditions, loss of the *cpc-2* gene decreases growth by 50% (29). During the sexual cycle, the Δ*cpc-2* mutant lacks protoperithecia, and is female-sterile (29).

Other components of this cross pathway control network are *cpc-1*, homologous to *GCN4* (30), and *cpc-3*, the *N*. *crassa* equivalent of *GCN2* (31). Analysis of Δ*cpc-2* Δ*cpc-3* and Δ*cpc-2* Δ*cpc-1* double mutants showed that they possessed Δ*cpc-2* phenotypes, such as reduced growth and female sterility. These findings suggested that *cpc-2* has broader functions operating outside of amino acid control (31).

To-date, no one has explored a possible function for CPC-2 in G protein signaling in *N*. *crassa*. In this study, we use strains carrying single and double gene deletions or expressing constitutively activated Gα alleles to analyze genetic epistasis between components of the G protein pathway and the *cpc-2* gene. We produce a polyclonal antibody against CPC-2 and use western analysis to determine protein levels in the mutants lacking the other G protein subunits. Our results reveal that *N*. *crassa* mutants lacking both predicted Gβ subunits are viable, but possess major defects in growth and development. We also provide evidence for G protein dependent and independent functions for CPC-2 in *N*. *crassa*.

Materials and methods

Strains and Media

N. *crassa* strains were either obtained from the Fungal Genetics Stock Center (FGSC; Kansas State University, Manhattan, KS) (32) or created during this work (Table 2.1). Strains that are not deposited in the FGSC collection are available upon request. Strains were cultured in Vogel's minimal medium (VM) (33) to propagate vegetative hyphae or asexual spores (macroconidia; conidia). Synthetic Crossing Medium (SCM) plates containing 1% agar were used to induce development of female sexual reproductive structures (34). Sorbose-containing medium (FGS) was used to facilitate colony formation on plates (35). Media was supplemented with 100 µg/ml of histidine, 10 µg/ml pantothenate, 200 µg/ml hygromycin (Calbiochem, San Diego, CA), 200 µg/ml nourseothricin (Werner BioAgents, Germany) or 400 µg/ml phosphinothricin (purified from Finale, Farnam Companies, Inc., Phoenix, AZ), where indicated. Conidia were propagated in VM agar flasks as described previously (35). Liquid cultures were brought to a concentration of $1x10^6$ conidia/ml and incubated with shaking at 200 RPM at 30°C for 16 hr. *Escherichia coli* strain DH5α was used to maintain all plasmids.

Phylogenetic Analysis

Protein sequences orthologous to *N*. *crassa* CPC-2 (NCU05810) and GNB-1 (NCU00440) from 18 fungal species chosen to represent a diversity of fungi (36) were obtained from the FungiDB database (fungidb.org) (37). Sequences for the Gβ and RACK1 proteins from the plant *Arabidopsis thaliana* were retrieved from the National Center for Biotechnology Information (NCBI). The “One-Click Workflow” tool at NGPhylogeny.fr (38) was implemented for the phylogenetic analysis. This pipeline uses FASTA files to generate a multiple alignment using MAFFT (**M**ultiple **A**lignment using **F**ast **F**ourier Transform) (39). Alignments were inspected and proteins from the 18 species resulted in good alignments for both the Gβ and RACK1. The MAFFT alignments were curated using BMGE (**B**lock **M**apping and **G**athering with **E**ntropy) (40) and FastME (Fast **M**inimum **E**volution) (41) was used to produce the tree file. FastME uses distance algorithms to infer phylogenies. The final trees were drawn using tools at the Interactive Tree of Life (iTOL; itol.embl.de) (42). Species and gene accession numbers are in the legend to Figure 2.1.

N. crassa strain construction

The Δ*cpc-2*::*hph*^{R} knockout mutant was deposited at the FGSC as a heterokaryon (FGSC13695). Homokaryotic mutants were obtained from the heterokaryon after a sexual cross to wild type strain 74-OR23-1VA and plating ascospores on medium containing hygromycin. Progeny were checked using

diagnostic PCR (43) with *cpc-2* (Primer 1 or Primer 2) and *hph* (Primer 13 or Primer 14) primers (Table 2.2; Figure 2.S1), and then spot-tested on phosphinothricin to check for the presence of the *mus-51* mutation, which is marked with *bar* (44, 45).

Double mutants Δ*cpc-2*, Δ*gna-1*; Δ*cpc-2*, Δ*gna-2* and Δ*cpc-2*, Δ*gna-3* were made using genetic crosses between single mutants (35) (Table 2.1). In cases where both single mutants in the cross were female-sterile (Δ*cpc-2* and Δ*gna-1*), the strain used as the female was a heterokaryon with the a^{m1} helper strain (46). The presence of the mutations in the progeny was verified by diagnostic PCR using pairs of gene-specific and *hph* cassette-specific primers (Primers 1–14 in Table 2.2; Figure 2.S1).

Repeated attempts to generate a Δ*cpc-2* Δ*gnb-1* double mutant through a sexual cross were unsuccessful. Therefore, the double mutant was created by electroporation of the Δcpc2#6 strain using a knockout cassette for *gnb-1*, marked with nourseothricin resistance (nat^R) (47). The Δ*gnb-1* knockout cassette was created using yeast recombinational cloning in vector pRS426 (48), with methods previously described (49). Primers used to amplify fragments for the construct are listed in Table 2.2. Primer pairs 15–16 and 17–18 were used to amplify the 1 kb 5’ and 3’ flanks of *gnb-1*, respectively, from genomic DNA. Primers 19 and 20 were used to amplify the nourseothricin resistance marker from plasmid pD-NAT-1 (47). The three purified PCR products plus pRS426 digested with *Xho*I and *Eco*RI were transformed into yeast strain FY834 (50).

Transformants were selected on FGS plates containing nourseothricin and then checked for the presence of the Δ*gnb-1*::*nat*^{R} mutation using diagnostic PCR with gene-specific primers (Primers 21 and 22; Table 2.2). Positive strains were then purified to homokaryons using serial streaking of macroconidia (43) and checked again using diagnostic PCR (Figure 2.S1).

Vectors containing predicted GTPase-deficient, constitutively activating mutations *gna-1*^{Q204L} (pSVK51), *gna-2*^{Q205L} (pSVK52), and *gna-3*^{Q208L} (pSVK53) were previously made using site-directed mutagenesis (51). Electroporation of *N*. *crassa* with 1–2 µg of pSVK51, pSVK52 or pSVK53 was as previously described (52), using the Δcpc2his3A strain as the recipient, with selection on FGS plates without histidine. Genomic DNA was extracted from transformants and subjected to Southern analysis for *gna-1*, *gna-2* and *gna-3* as described (51). Transformants determined to have a single integration event of the transforming DNA at the *his-3* locus were purified to homokaryons using microconidiation (53) or serial streaking of macroconidia (43) on FGS plates lacking histidine. Genomic DNA was extracted from these strains and analyzed using diagnostic PCR (Figure 2.S1) to confirm genotypes.

A vector was produced to allow expression of a GFP-tagged version of *cpc-2* in *trans* to the wild-type copy. The vector backbone (pRS426PVG) (54) was assembled in plasmid pRS426 using yeast recombinational cloning (49). The fragments included a region 1kb 5’ of the *pan-2* ORF, the *ccg-1* promoter amplified from pMF272 (55), a multiple cloning sequence, a 5xGlycine linker, a

V5-tag, GFP sequence amplified from pMF272 (55), the *bar* gene, amplified from vector pTJK1 (56) and a 1 kb fragment 3' of the *pan-2* ORF (54). All fragments were amplified using Phusion High-Fidelity DNA Polymerase (New England Biolabs, Ipswich, MA). The *pan-2* flanking sequences allow targeting to, and deletion of, the *pan-2* ORF, resulting in pantothenate auxotrophy. The final expression construct for CPC-2 was produced by insertion of the *cpc-2* ORF (amplified using Primers 27 and 28; Table 2.2) into vector pRS426PVG (linearized using *Pac*I) using yeast recombinational cloning (49). Vector pRS426PVG-CPC2 was transformed using electroporation into *N*. *crassa* strain 51-IV-4 (Table 2.1) (54). Transformants were selected on medium containing phosphinothricin and pantothenate (54) and screened for the presence of the inserted DNA at the *pan-2* locus using PCR. Positive strains were crossed to wild-type strain 74-OR23-1VA, and ascospores were plated on medium containing phosphinothricin and pantothenate. Progeny were screened for panthothenate auxotrophy by spot-testing and for the presence of the integrated DNA using diagnostic PCR (Figure 2.S1). Strain CPC-2-GFP-9-10 was selected for further study (Table 2.1).

A *cpc-2* complemented strain was obtained by crossing the transformants expressing GFP-tagged *cpc-2* described above to Δ*cpc-2* mutant strain Δcpc2#11 (Table 2.1). Ascospores were plated on FGS plates containing hygromycin and pantothenate to select strains carrying the Δ*cpc-2* mutation. Progeny were spot-tested on medium containing phosphinothricin and

panthothenate, followed by diagnostic PCR (Figure 2.S1), to determine those that also carried the *cpc-2* GFP trans gene construct at the *pan-2* locus. Positive strains were tested for the presence of the CPC-2 GFP fusion protein using western analysis with CPC-2 antiserum as described below. Strain CPC-2-GFP-13.2 was selected for further analysis (Table 2.1).

Purification of a CPC-2 fusion protein for production of a polyclonal antiserum in rabbits

CPC-2 was expressed as an in-frame, N-terminal Maltose Binding Protein (MBP) fusion protein in *E*. *coli* and then purified and used as an antigen for antibody generation in rabbits. The *cpc-2* ORF was cloned as an *EcoR*I-*Pst*I fragment in *E*. *coli* vector pMAL-c2X (New England Biolabs). The MBP-CPC-2 fusion protein was expressed in *E*. *coli* strain K12 ER2508 (New England Biolabs) with induction using 300 µM IPTG (isopropyl β-D-1-thiogalactopyranoside; Sigma) and the fusion protein purified using an amylose resin according to the manufacturer's recommendations. A polyclonal antiserum specific for the MBP-CPC-2 protein was raised in rabbits by Cocalico Biologicals, Inc. (Stevens, PA, USA).

Western analysis to confirm genotypes and check protein levels in mutants

Western analysis was used to check strains for expression of CPC-2 and the G protein subunits GNA-1, GNA-2, GNA-3 and GNB-1. For confirming genotypes, submerged cultures were grown, frozen in liquid nitrogen and then pulverized in 2-ml tubes with metal beads using a TissueLyser (Qiagen Retsch GbmH, Hannover, Germany) as previously described (43). Subsequently, 500–800 µl of extraction buffer (10mM TrisCl pH 7.5, 0.5 mM EDTA, 0.1% Fungal Protease Inhibitor Cocktail (FPIC), 1 mM PMSF and 1mM DTT) was added to the tube, the solution was mixed and then centrifuged at 5000 x g for 10 min at 4°C. Protein concentration was determined using the Bradford Protein Reagent Concentrate (Bio-Rad, Hercules, CA). Approximately 50 µg of supernatant protein (whole cell extract) was loaded onto a 10% SDS-PAGE gel and then transferred to a nitrocellulose membrane (GE Water and Process Technologies) (57). For checking G protein levels in the Δ*cpc-2* mutant, cultures were grown and the protein fraction enriched in plasma membranes was isolated as previously described (12). For determining CPC-2 protein amount in the G protein mutants, whole cell extracts were isolated as previously described (12). The protein concentration in the preparations was determined using the Bradford Protein Reagent Concentrate. Aliquots containing equal amounts of protein were subjected to SDS-PAGE, and a western blot was prepared as described above for confirming genotypes of G protein subunit mutants.

Western blot membranes were reacted with the CPC-2 antibody at a dilution of 1:1000 or antiserum raised against GNA-1, GNA-2, GNA-3 or GNB-1 at dilutions of 1:2000 (51, 52, 58, 59). Blots were then incubated with a goat anti-rabbit antibody horseradish peroxidase conjugate (Bio-Rad; 1:10,000 dilution). Chemiluminescent detection was performed as previously described (57) using the Super Signal West Pico Plus kit (Thermo Fisher, Rockford, IL). Western blots presented in figures are representative of three biological replicates.

Phenotypic analysis

Quantitative assays for aerial hyphae height and growth rates of basal hyphae and qualitative analysis of female fertility were performed as described previously (5, 60). Twelve biological replicates were obtained for aerial hyphae height and four were used for basal hyphae growth rate calculations. Investigation of hyphal morphology and conidiation in submerged cultures and conidial germination on solid medium were conducted as described previously (51, 61) and the results shown are representative of 2–3 biological replicates. Because the Δ*cpc-2 gna-3*^{Q208L} strain KAB3210 does not produce appreciable macroconidia, 200 microliters of packed aerial hyphae were used to inoculate submerged cultures for this strain. For quantifying macroconidia, strains were inoculated in 13x100mm glass slant tubes containing 3 ml of VM agar medium and incubated for 4 days in the dark at 30°C and 3 days in light at room temperature. Macroconidia were collected from tubes by adding 2 ml water,

mixing vigorously using a vortex mixer and filtering through Handiwipes into a 15 ml conical tube using a small funnel. This step was repeated twice, once using a wooden stick to dislodge residual macroconidia from the glass tube prior to vortexing and filtering. Macroconidia were pelleted by centrifugation and the water aspirated. Water was added to an appropriate volume and the absorbance read at 600nm using a spectrophotometer. The readings for different strains were all normalized to the same volume (1 ml) to yield a macroconidial concentration expressed as OD600/ml. Eight biological replicates were obtained.

GraphPad Prism 6.0 (GraphPad Software Inc., La Jolla, CA) was used to analyze quantitative traits (hyphal growth rate, aerial hyphae height and conidia abundance). Grubb's Q test was utilized to detect and eliminate outliers and then the Ordinary One-Way ANOVA test was used for detecting statistical significance. The p-value cutoff was set to 0.05, confidence intervals were 95% and pair-wise comparisons were made. Graphs were created using Microsoft Excel (Microsoft, Redmond, WA).

CPC-2 localization experiments

Two approaches were undertaken to determine the intracellular localization of the CPC-2 protein: cell fractionation studies using centrifugation with a wild-type strain and live-cell microscopic imaging of a strain that produces GFP-tagged CPC-2. Cell fractionation of a whole cell extract of strain 74-OR23-IVA (Table 2.1) was performed as described (51). Fractions containing whole cell

extract, cytosol, and the particulate fraction (membranous organelles and large macromolecular structures) were isolated. The volumes of the cytosol and particulate fractions were adjusted to the same total volume as the original whole cell extract to allow comparison. The protein concentration of the whole cell extract was determined using the Bradford Protein Reagent Concentrate (Bio-Rad). Aliquots containing a volume identical to that containing 50 µg of protein from the whole cell extract were subjected to SDS-PAGE and gels were blotted onto nitrocellulose membranes. Antibody to arginase/AGA (cytosolic marker) (62) was used at a dilution of 1:10,000 and the plasma membrane ATPase/PMA-1 (plasma membrane marker; gift from Kenneth Allen and Clifford Slayman) (63) was used at a dilution of 1:3000. Westerns shown in figures are representative of four biological replicates.

Fluorescence microscopy of the CPC-2-GFP-9-10 strain was conducted essentially as described (61). The germinating conidia were visualized using differential interference microscopy on an Olympus IX71 inverted microscope (Olympus America) with a 60X oil immersion objective. For visualization of GFP fluorescence, the GFP laser was used for excitation at 400 nm. Images were captured using a QIClickTM digital CCD camera (QImaging Surrey, British Columbia, Canada).

Results

N. crassa CPC-2 is homologous to predicted RACK1 proteins from other fungi

N. *crassa* CPC-2 is 316 amino acids in length and was previously reported to have 70% percent identity with RACK1 proteins (29). *N*. *crassa* CPC-2 and GNB-1 each possess seven WD-40 repeats and share 39% similarity and 24% identity at the protein level. In order to investigate the relationships between CPC-2, GNB-1 and RACK1 and Gβ subunit proteins from other fungi, we subjected orthologous sequences from 18 fungal species to multiple sequence alignment and tree rendering (See Materials and methods for details). Gβ and RACK1 orthologs from the plant *Arabidopsis thaliana* were included as outgroups for the analysis. The fungal species include representatives from the Ascomycota (nine species), Basidiomycota (four species), Chytridiomycota (two species) and Mucoromycota (three species) (36). Two of the species from the Mucoromycotina possessed multiple orthologs of both GNB-1 and CPC-2, and all proteins were included in our analysis.

The results for the Gβ group showed that the proteins from *N*. *crassa* and the other Ascomycete filamentous fungi (*Sordaria macrospora*, *Fusarium graminearum*, *Botrytis cinerea*, *Magnaporthe oryzae* and *Aspergillus nidulans*) cluster together and are more closely related to proteins from Basidiomycetes (*Ustilago maydis*, *Cryptococcus neoformans*, *Sporisorium reilianum* and *Puccinia*

graminis f. sp. tritici), Chytridiomycetes (*Batrachochytrium dendrobatidis* and *Spizellomyces punctatus*) and Mucoromycetes (*Phycomyces blakesleeanus* and *Mucor circinelloides f. lusitanicus*) than to the three Ascomycete yeasts (*Saccharomyces cerevisiae*, *Candida albicans* and *Schizosaccharomyces pombe*) (Figure 2.1A). These relationships are in keeping with our previous observations that a heterotrimeric Gα subunit from *N. crassa* (GNA-3) is more closely related to proteins from filamentous Ascomycetes and Basidiomycetes than to those from *S. cerevisiae* or *S. pombe* (13). We also noted that each of the GNB-1 orthologs from *M. circinelloides f. lusitanicus* cluster with 1–2 orthologs from *P. blakesleeanus*, consistent with an ancient duplication event in an ancestor of these two species and later divergence (Figure 2.1A). Evidence supporting genome duplication in these species has been previously published (64).

In contrast to the Gβ orthologs, the RACK1 proteins distribute into two major clades, with one corresponding to all of the Ascomycetes (including *N. crassa*) and the other containing the Basdiomycetes, Mucoromycetes and Chytridiomycetes (Figure 2.1B). In the case of the two Mucoromycete species, the RACK1 proteins from each species have the other protein from the same species are their closest neighbor on the tree (Figure 2.1B). This suggests a more recent gene duplication event for the RACK1 orthologs that occurred after divergence of these two species.

CPC-2 is a cytoplasmic protein

We utilized two independent methods to assess subcellular localization of CPC-2. First, differential centrifugation was performed on protein extracts from wild type and the fractions subjected to western analysis using antibodies to marker proteins and CPC-2. Since there was no antibody for CPC-2 available prior to our study, we first expressed and purified an MBP-CPC-2 fusion protein from *E*. *coli* and used the protein to produce polyclonal antisera in rabbits (see Materials and methods for details). Tests of the serum showed that it recognized a protein of the predicted molecular mass of CPC-2 (~35 kDa) in whole cell extracts from wild type.

For the differential centrifugation approach, we generated whole cell extracts, and samples enriched for cytosol and the particulate fraction (membranous organelles and large macromolecular assemblies). Western analysis was performed using antibodies directed against arginase/AGA (cytosolic marker) (62)and the plasma membrane ATPase/PMA-1 (plasma membrane marker) (63), with the results showing good separation of the fractions (Figure 2.2A). Some contamination of the cytosolic fraction with plasma membranes (but not vice-versa) is evident from the presence of trace amounts of PMA-1 in the cytosol and the absence of the AGA from the particulate fraction. Western analysis using the CPC-2 antibody demonstrated that the great majority of CPC-2 was localized to the cytoplasm, with a small amount in the particulate fraction.

As an alternative method, we implemented fluorescence microscopy to determine the subcellular localization of CPC-2 in a strain expressing a GFP-tagged version of the protein (Figure 2.2B). The CPC-2-GFP signal was localized in the cytoplasm and excluded from the nucleus (as represented by DAPI staining) in both macroconidia and 6 h germlings (Figure 2.2B). Thus, both subcellular fractionation and live-cell imaging approaches support a cytoplasmic localization for CPC-2 in *N*. *crassa*.

Creation of mutants lacking cpc-2 and G protein subunit genes and analysis of G protein levels in Δcpc-2 strains

We have previously demonstrated that components of the G protein signaling pathway are crucial for hyphal growth and asexual and sexual development of *N*. *crassa* (8, 9, 11, 57, 65, 66). In order to explore a possible role for *cpc-2* as a heterotrimeric Gβ gene in *N*. *crassa*, we created strains that could be used for genetic epistasis analysis. We previously employed a similar approach for analysis of genetic relationships between the Gβ *gnb-1* and the three Gα subunit genes (51). We first purified Δ*cpc-2* homokaryotic knockout mutants from a transformant created during the Neurospora Genome Project (49, 67) (see Materials and methods). We constructed complemented strains carrying the Δ*cpc-2* mutation and a *pan-2* targeted, GFP-tagged version of the *cpc-2*$^{+}$ gene *in trans* (see Materials and methods and Table 2.1). The complemented strains exhibited significant complementation of several phenotypes, including

hyphal growth rate (Figure 2.S2) and partial complementation of aerial hyphae height (Figure 2.S2). We used sexual crosses or transformation to generate deletion mutants lacking *cpc-2* alone or in combination with mutations in the three Gα genes or the Gβ, *gnb-1*. We also constructed Δ*cpc-2* strains expressing GTPase-deficient, constitutively activated Gα alleles (*gna-1*^{Q204L}, *gna-2*^{Q205L} or *gna-3*^{Q208L}; see Materials and methods and Table 2.1).

We have previously shown that, depending on the growth conditions, loss of the Gβ subunit *gnb-1* leads to lower levels of one or all three Gα proteins in *N*. *crassa* (51, 57, 59). The exact mechanism underlying this regulation is unknown, but appears to be post-transcriptional, as Gα mRNA levels are normal in Δ*gnb-1* mutants (57, 59). Therefore, prior to initiating genetic epistasis experiments with *cpc-2*, we utilized western blot analysis with protein-specific antisera to check levels of G protein subunits in the Δ*cpc-2* mutant (Figure 2.3). The results demonstrate that in contrast to *gnb-1*, loss of *cpc-2* does not greatly influence levels of the three Gα proteins or GNB-1 (Figure 2.3; compare wild type and Δ*cpc-2* lanes). However, Gα protein levels are still reduced when *gnb-1* is mutated in the Δ*cpc-2* background (Figure 2.3). We also consistently noted an increased level of GNA-3 in the Δ*cpc-2* Δ*gnb-1* double mutant vs. the Δ*gnb-1* single mutant, suggesting that loss of *cpc-2* partially reverses the effect of the Δ*gnb-1* mutation. The observation that the Δ*cpc-2* single mutant has normal levels of G protein subunits greatly streamlines interpretation of genetic epistasis experiments using *cpc-2*.

We next wanted to determine whether loss of any of the G protein subunits affects CPC-2 protein levels. Because CPC-2 is a cytoplasmic protein (Figure 2.2), we used protein from whole cell extracts for western analysis using the CPC-2 antiserum (Figure 2.3). The results demonstrated that CPC-2 protein levels were relatively normal in the G protein single mutants (Figure 2.3). Thus, similar to the situation with GNB-1 levels in the Δ*cpc-2* strain, CPC-2 levels are not affected by loss of *gnb-1*; the two predicted Gβ proteins are independent of one another in this regard. Our findings suggest that if CPC-2 does operate as a Gβ subunit, it does not share all functions with GNB-1 in *N. crassa*.

cpc-2 is epistatic to gna-2 during regulation of basal hyphal growth rate

N. crassa grows by elongation, branching and fusion of hyphae, eventually forming a network structure called the mycelium (rev. in (68)). From this mycelium, aerial hyphae grow upward and spore-forming structures (macroconidiophores) are elaborated from their tips. Formation of cross-walls and constriction of macroconidiophores leads to formation of the mature multinucleated asexual spores, macroconidia. Macroconidia are disseminated in nature by wind currents, enabling the fungus to colonize new areas. When in the presence of water and suitable nutrients, macroconidia germinate to form a hyphal tube, which then begins the growth program described above (68).

We began our genetic epistasis analysis by investigating the set of mutants for defects in basal hyphae extension rate, using macroconidia to inoculate race tubes (see Materials and methods). The results from genetic epistasis analysis were interpreted as reported previously (51): If the phenotype of the Δ*cpc-2*, ΔGα double mutant resembles the phenotype of the ΔGα mutant, and if the mutationally activated Gα allele bypasses the phenotype of Δ*cpc-2*, then the Gα gene is epistatic to (implied downstream) to *cpc-2*. If the opposite is true, then *cpc-2* is epistatic to the Gα gene. If contradicting results are seen, this is interpreted as the two genes being partially or completely independent in regulation of the phenotype being assessed.

All of the single gene mutants had a basal hyphal growth rate phenotype (Figure 2.4, Table 2.S1). In Δ*cpc-2* mutants, the growth rate was 61% of wild type (Figure 2.4). The findings from ANOVA of the characterized strains revealed several relationships (Table 2.S1). First, *cpc-2* may operate downstream of *gna-2*. Both mutants are significantly different than wild type, the double mutant grows slower than Δ*gna*-2, but slightly faster than Δ*cpc-2*, and mutational activation of *gna-2* (*gna-2*^{Q205L} allele) does not lead to an increase in growth rate in the Δ*cpc-2* background. Second, the Δ*gna-1* and Δ*cpc-2* knockout mutations are synergistic with regards to reduction in growth rate, and mutational activation of *gna-1* does not rescue the Δ*cpc-2* phenotype; in fact, the growth rate is further reduced in the Δ*cpc-2 gna-1*^{Q204L} strain. The same relationships hold between *gna-3* and *cpc-2*. These results suggest that *cpc-2* regulates growth rate

using a different pathway than *gna-1* or *gna-3*. Finally, Δ*cpc-2* and Δ*gnb-1* are also synergistic, with the double mutant having a significantly slower growth rate than either single mutant (Figure 2.4). This suggests that these two Gβ-like genes have some independent functions during regulation of hyphal growth in *N. crassa*.

We have previously demonstrated that strains lacking either of the G protein subunit genes *gna-1* and *gna-3*, but not *gna-2* or *gnb-1*, have a defect in germination of macroconidia, an essential step prior to hyphal growth and formation of a colony (61). Therefore, we explored this phenotype in Δ*cpc-2* mutants, using wild type as a control (Figure 2.S3). Similar to Δ*gnb-1* mutants, strains lacking *cpc-2* are normal with respect to germination of macroconidia (Figure 2.S3). Thus, overall colony size of Δ*cpc-2* mutants is compromised by slower extension of basal hyphae, and not by a defect in germination of macroconidia.

cpc-2 is epistatic to _gna-2_ with regards to aerial hyphae height and Δ_cpc-2_ mitigates the increased macroconidia production of Δ_gnb-1_ mutants on solid medium

We next explored epistatic relationships between *cpc-2* and the other genes for two quantitative traits relevant to macroconidiation: aerial hyphae height and macroconidia abundance. Similar to the case for basal hyphae growth rate, all of the single gene deletion mutants had an aerial hyphae height defect

(Figure 2.5A, Table 2.S1). For Δ*cpc-2*, aerial hyphae heights were 69% of wild type (Figure 2.5A).

ANOVA of the strain set produced results similar to those noted for basal hyphae, above (Table 2.S1). The aerial hyphae height of the Δ*cpc-2* and Δ*cpc-2* Δ*gna-2* double mutants is significantly less than that of the Δ*gna-2* single mutant and the Δ*cpc-2 gna-2*^{Q205L} strain is similar to the Δ*cpc-2* single mutant (Figure 2.5A). This result is consistent with *cpc-2* functioning downstream of *gna-2* to control aerial hyphae height. In contrast, *gna-1* and *cpc-2* appear to be independent; the double mutant has shorter aerial hyphae than either single mutant and introduction of *gna-1*^{Q204L} does not rescue the aerial hyphae defect of Δ*cpc-2* (Figure 2.5A). Δ*gna-3* mutants are shorter than Δ*cpc-2* and the double mutant is similar to Δ*gna-3* (Figure 2.5A). However, the finding that aerial hyphae height is not rescued by the *gna-3*^{Q208L} allele in the Δ*cpc-2* background (Table 2.S1) supports independent regulation by these two subunits. Δ*cpc-2* and Δ*gnb-1* mutants have similar aerial hyphae height and the double mutant is shorter (Figure 2.5A; Table 2.S1). As observed for regulation of basal hyphal growth, this finding supports independent signaling by *cpc-2* and *gnb-1* during control of aerial hyphae height in *N*. *crassa*.

Quantitative analysis of macroconidia production in agar slants did not reveal a phenotype for Δ*cpc-2* mutants (Figure 2.5B, Table 2.S1). In fact, of the single mutants analyzed, only Δ*gnb-1* possessed a phenotype (greater conidia production; Figure 2.5B) and the phenotype of the Δ*cpc-2* Δ*gnb-1* double mutant

was similar to that of Δ*cpc-2* (like wild type). This suggests that loss of *cpc-2* mitigates the overproduction of conidia observed in the Δ*gnb-1* mutant, and that *cpc-2* is epistatic to *gnb-1*. For the Gα subunit double mutants, Δ*cpc-2* Δ*gna-3* produces fewer conidia than either single mutant and differentiation of macroconidia is nearly halted in the Δ*cpc-2 gna-3*^{Q208L} strain (Figure 2.5B). These results support independence of *cpc-2* and *gna-3* during regulation of macroconidiation. A similar situation exists for *gna-2*, as the Δ*cpc-2* Δ*gna-2* double mutant and the Δ*cpc-2 gna-2*^{Q205L} strain produce fewer conidia than either single mutant (Figure 2.5B). With *gna-1*, the double mutant is similar to the single mutants, but the Δ*cpc-2 gna-1*^{Q204L} mutant produces less macroconidia, consistent with independence (Figure 2.5B). The results from analysis of strains carrying the three mutationally activated Gα alleles suggest that all three Gα proteins inhibit macroconidiation when locked in the GTP-bound form.

cpc-2 mutants produce macroconidia in submerged cultures

Wild-type *N*. *crassa* strains do not differentiate macroconidia while growing in shaken submerged culture unless subjected to heat shock, nitrogen or carbon starvation (69-73). We have previously demonstrated that loss of the G protein subunits *gna-3*, *gnb-1* and *gng-1* leads to macroconidiation in submerged culture under all conditions (13, 57, 59), while Δ*gna-1* mutants only form macroconidia at high inoculation cell density (≥3x10^6/ml) in liquid culture (74).

Based on the precedent that the Gβ gene *gnb-1* is a negative regulator of macroconidiation in submerged cultures, we analyzed our group of strains for phenotypes at a low inoculation density ($1x10^6$/ml). Similar to previous findings, wild type and Δ*gna-2* mutants do not produce macroconidiophores in submerged culture, while single mutants lacking *gna-3*, *gnb-1* and *gng-1* all produce abundant macroconidiophores (Figure 2.6). Rare macroconidiophores could also be observed in the Δ*gna-1* strain. We also noted that Δ*cpc-2* knockout mutants produce macroconidiophores in submerged culture (Figure 2.6).

Double mutants Δ*cpc-2* Δ*gna-1*, Δ*cpc-2* Δ*gna-2*, Δ*cpc-2* Δ*gna-3* and Δ*cpc-2* Δ*gnb-1* all produce conidia in submerged culture. In all four cases, loss of *cpc-2* either leads to submerged conidiation or intensifies the conidiation phenotype of the G protein subunit mutants and the *Δgna-3* Δ*cpc-2* double mutant cultures are mostly conidia (Figure 2.6). Interestingly, introduction of mutationally activated *gna-3* corrects the submerged conidiation phenotype of Δ*cpc-2*, while the corresponding activated alleles of *gna-1* or *gna-2* do not (Figure 2.6). This result suggests that GNA-3 may operate downstream of CPC-2, but also has a CPC-2 independent function in controlling submerged conidiation.

Constitutive activation of Gα subunits does not restore female fertility to the Δ*cpc-2* mutant

N. *crassa* is a heterothallic organism, meaning that a given strain has one of two different mating type genes present at a single genomic locus (idiomorphs; *mat A* or *mat a*) (75, 76). Upon nitrogen limitation, *N*. *crassa* forms protoperithecia (the female reproductive structures) (68, 77). In the presence of a male cell (usually conidia) of the opposite mating type, pheromone detection results in chemotropic growth of specialized hyphae called trichogynes from the protoperithecium. The fruiting body, or perithecium, is then formed and contains asci, each with eight haploid spores (ascospores). Upon maturation, ascospores are ejected from the tips (beaks) of perithecia, in the direction of light. Under laboratory conditions, protoperithecial development can be induced using Synthetic Crossing Medium (SCM), and progeny are obtained from sexual crosses approximately 2–3 weeks post-fertilization (68, 77).

Our previous work showed that the mutationally activated *gna-1*^{Q204L}, *gna-2* ^{Q205L} and *gna-3*^{Q208L} alleles were not able to restore fertility to the Δ*gnb-1* mutant. In fact, introduction of *gna-3*^{Q208L} resulted in complete inhibition of protoperithecial development, a phenotype that was more severe than that of the Δ*gnb-1* mutant (51). Δ*gnb-1* ΔGα double mutant strains resemble the Δ*gnb-1* mutant, in that they form protoperithecia, but no perithecia after fertilization (51).

Muller et al. (29) previously reported that *cpc-2* point mutants do not produce protoperithecia and are thus female-sterile. In contrast, our results with the Δ*cpc-2* knockout mutant indicate some protoperithecia are present, as the cultures produce rare perithecia after fertilization that are mostly submerged in the agar (Figure 2.7). This phenotype is distinct from that of Δ*gna-2* and Δ*gna-3* strains that produce perithecia similar to wild type and from Δ*gna-1* and Δ*gnb-1* mutants that do not form perithecia after fertilization (Figure 2.7).

Inspection of double mutants revealed that Δ*cpc-2* Δ*gna-1* strains do not produce visible protoperithecia, perithecia or ascospores (Figure 2.7), a more severe phenotype than either single mutant. In contrast, Δ*cpc-2* Δ*gna-2* mutants resemble Δ*cpc-2* single mutants. Δ*cpc-2* Δ*gna-3* strains exhibit a variable phenotype, with either small, submerged perithecia or no visible perithecia (Figure 2.7), and no ascospores. Mutational activation of either *gna-1* or *gna-3* in the Δ*cpc-2* background leads to no visible protoperithecia, perithecia or ascospores, while activation of *gna-2* results in the Δ*cpc-2* phenotype (Figure 2.7). These results are consistent with synergy between *cpc-2* and *gna-1* and *gna-3*. The phenotype of Δ*cpc-2 gna-3*^{Q208L} and Δ*gnb-1 gna-3*^{Q208L} strains are similar (51), suggesting a common mode of action for *gna-3*^{Q208L} and/or interaction between GNA-3 and the two candidate Gβ proteins. In contrast, the different results observed after introduction of *gna-1*^{Q204L} into the two mutants hints at a different role for CPC-2 vs. GNB-1 during regulation of female fertility.

As noted previously, the Δ*gnb-1* strain forms small, aberrant protoperithecia, but no perithecia, upon fertilization (57) (Figure 2.7). In contrast, similar to Δ*gnb-1* single mutants, Δ*cpc-2* Δ*gnb-1* double mutants do not produce perithecia (Figure 2.7). This result suggests that *gnb-1* is epistatic to *cpc-2* during sexual development.

Discussion

The *N. crassa cpc-2* gene is not essential and the encoded protein is similar to other RACK1 homologs in fungi. Genetic epistasis between *cpc-2* and components of the G protein pathway was performed using double deletion mutants and strains containing Gα activated alleles (see model in Figure 2.8). The results revealed genetic relationships between *cpc-2* and *gna-2* during growth of basal and aerial hyphae, *cpc-2* and *gna-3* during growth in submerged cultures and *cpc-2* and *gnb-1* in regulation of sexual development. In the cases of basal and aerial hyphae growth, the epistatic relationships suggest that CPC-2 operates downstream of the Gα protein, implying a tethering function for the Gα in regulation of CPC-2. However, the GNA-3 Gα acts downstream of CPC-2 during submerged culture conidiation, suggesting that the RACK1 protein is holding GNA-3 inactive. CPC-2 appears to operate upstream of the Gβ GNB-1 during sexual development and to act in an antagonistic function during production of macroconidia in agar cultures.

Our investigation of epistasis between the three Gα genes and *gnb-1* and *cpc-2* revealed some interesting parallels. As mentioned above, the results from the current study suggest that *gna-3* is at least partially epistatic to *cpc-2* during control of appropriate conidiation in submerged cultures. This is similar to the earlier relationship observed for *gnb-1* and *gna-3* for this same phenotype, with *gna-3* epistatic to *gnb-1* (51). The other two Gα subunits are independent of both *cpc-2* (this study) and *gnb-1* (51) during the regulation of this trait. This

indicates that *cpc-2*, like *gnb-1*, is a negative regulator of conidiation in submerged culture, and that only activation of *gna-3* offers a genetic bypass mechanism to restore normal hyphal growth. Our previous results from epistasis studies of aerial hyphae height demonstrated that *gnb-1* is epistatic to both *gna-2* and *gna-3* and independent of *gna-1* (51). Together with the current study, the findings are consistent with a model in which the Gβ gene lies downstream of the Gα gene(s) and that *gna-1* is independent of both *gnb-1* and *cpc-2* during aerial hyphae elongation. However, any conclusions based on Δ*cpc-2* Δ*gnb-1* double mutants need to be tempered, as loss of *gnb-1* leads to decreased levels of the three Gα proteins in all genetic backgrounds tested.

It is intriguing that the Δ*cpc-2* Δ*gnb-1* double mutants have higher levels of GNA-3 protein than Δ*gnb-1* single mutants (but still less than in wild type; Figure 2.3A). This finding suggests that loss of *cpc-2* partially mitigates the effects of the Δ*gnb-1* mutation. In a canonical model for G protein signaling, GNB-1 would function as a GDI for GNA-3 and loss of GNB-1 might lead to misfolding and/or proteolysis of GNA-3. Mutation of *cpc-2* partially counteracts this effect, suggesting that CPC-2 participates in the pathway leading to decreased levels of GNA-3 protein. Furthermore, the finding that Gα single mutants have slower basal hyphae growth rates than wild type and that loss of *gnb-1* leads to lower levels of Gα proteins supports a possible tethering function for GNB-1 during hyphal growth. Loss of one Gα protein could free more GNB-1 to bind the other Gα subunits, potentially inhibiting them from serving as positive regulators of

basal hyphae growth rate. Along these lines, it has been demonstrated in *S*. *cerevisiae* that levels of the Gα protein Gpa1p are regulated by ubiquitin-mediated proteolysis, and it has been proposed that this is a mechanism used to modulate levels of the active, free Gβγ dimer during mating (78, 79).

Analysis of the sexual cycle demonstrated that the Δ*cpc-2* forms rare protoperithecia and perithecia and is therefore female sterile. In contrast, mutants lacking other components of the cross pathway control network (*cpc-1* and *cpc-3*) have normal sexual cycles (30, 31). This indicates that the sexual cycle defect of Δ*cpc-2* mutants is not solely due to a defect in the response to amino acid limitation. However, there is a possibility that the two processes may be linked. It has been reported in *A*. *nidulans* that amino acid limitation arrests sexual development (24). Furthermore, loss of the RACK1/*cpc-2* homolog *cpcB* or overexpression of the *cpc-1* homolog *cpcA* also block sexual development, supporting a link between the sexual cycle program and the network that regulates amino acid biosynthesis (24).

Attempts to detect an interaction between CPC-2 and other G protein subunits in *N*. *crassa* using the yeast two-hybrid assay were unsuccessful. Presumably due to the large number of binding partners, the difficulty in solubilizing peripheral membrane proteins such as Gα subunits, and protein folding concerns with heterologously expressed proteins, we were also unable to achieve co-immunoprecipitation between CPC-2 and GNB-1 or any of the three Gα proteins using cell extracts or proteins expressed and purified from *E*. *coli*. A

similar result has been reported for the RACK1 homolog RAK1 in *U*. *maydis* (26). Knowledge of the interactions between RACK1 and G protein subunits is important for full understanding of the biology of G protein signaling. Therefore, experiments such as these and others that investigate the detailed mechanistic wiring that connects CPC-2 to heterotrimeric G protein signaling will be the focus of future work.

Acknowledgements

We thank Kenneth Allen and Clifford Slayman for the gift of PMA-1 antibody and Jason Stajich for advice on phylogenetic analysis. We acknowledge the Fungal Genetics Stock Center for supplying strains. We thank Gloria Turner and members of the Borkovich laboratory for many helpful discussions.

Funding Statement

Funding for this study was provided by NIH grants GM086565 and GM068087 (to KAB) and University of California Agriculture and Natural Resources Agricultural Experiment Station mission funding (to KAB). The funders had no role in study design, data collection and analysis, decision to publish, or preparation of the manuscript.

Data Availability

All relevant data are within the manuscript and its Supporting Information files.

Figures

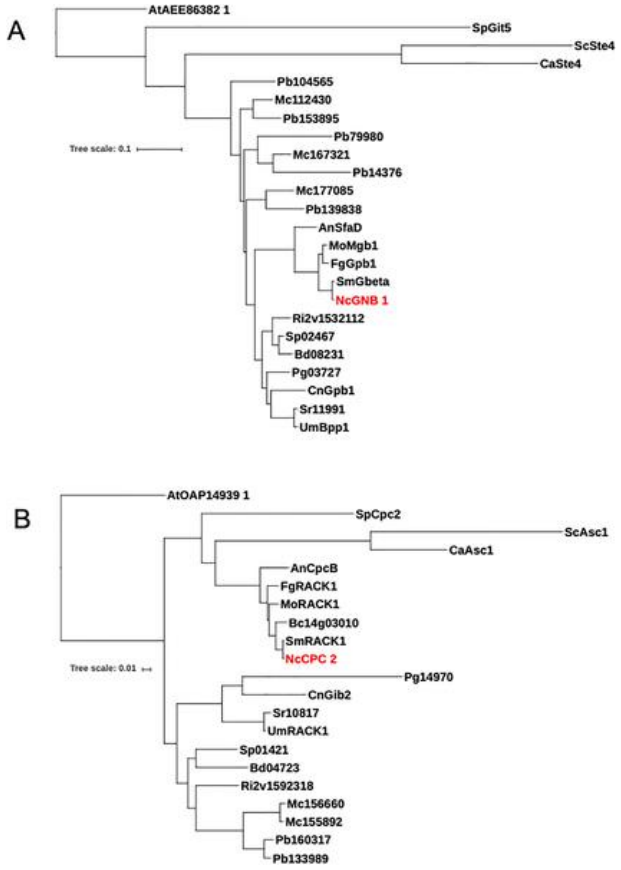

Figure 2.1. Phylogenetic analysis of Gβ and RACK1 proteins from 10 fungal species. Amino acid sequences were obtained from FungiDB or NCBI and phylogenetic analysis conducted using the "One-Click Workflow" tool at NGPhylogeny.fr. The final trees were drawn using tools at itol.embl.de (see Materials and methods for details). A. Gβ proteins. Organisms and protein names/accession numbers for the Gβ orthologs are *Neurospora crassa* NcGNB-1/NCU00440; *Sordaria macrospora* SmGbeta/SMAC01876*; Fusarium graminearum* GzGPB1/FGRAMPH101G14499; *Magnaporthe oryzae* MoMgb1/MGG05201; *Aspergillus nidulans* AnSfaD/AN0081; *Ustilago maydis* UmBpp1/UMAG00703; *Cryptococcus neoformans* CnGpb1/CNAG01262; *Candida albicans* CaSte4/C204210WA; *Schizosaccharomyces pombe* SpGit5/SPBC32H8.07 and *Saccharomyces cerevisiae* ScSte4/YOR212W; *Batrachochytrium dendrobatidis*/BDEG_08231; *Botrytis cinerea*/Bcin08g01420; *Puccinia graminis f. sp. tritici*/PGTG_03727; *Sporisorium reilianum*/sr11991; *Spizellomyces punctatus*/SPPG_02467; *Phycomyces blakesleeanus*/PHYBL_104565; *Phycomyces blakesleeanus*/PHYBL_139838; *Phycomyces blakesleeanus*/PHYBL_14376; *Phycomyces blakesleeanus*/PHYBL_153895; *Phycomyces blakesleeanus*/PHYBL_79980; *Mucor circinelloides f. lusitanicus*/QYA_112430; *Mucor circinelloides f. lusitanicus*/QYA_167321; *Mucor circinelloides f. lusitanicus*/QYA_177085; *Rhizophagus irregularis*/GLOIN_2v1532112; *Arabidopsis thaliana*/AEE86382.1 B. RACK1 proteins. Organisms and protein names or accession numbers for the RACK1 orthologs are *Neurospora crassa* NcCPC-2/NCU05810; *Sordaria macrospora* SmRACK1/SMAC07639; *Fusarium graminearum* FgRACK1/FGRAMPH101G06721; *Magnaporthe oryzae* MoRACK1/MGG04719; *Aspergillus nidulans* AnCpcB/AN4163; *Ustilago maydis* UmRACK1/UMAG10146; *Cryptococcus neoformans* CnGib2/CNAG05465; *Candida albicans* CaAsc1/C701250WA; *Schizosaccharomyces pombe* SpCpc2/SPAC6B12.15; *Saccharomyces cerevisiae* ScAsc1/YMR116C; *Batrachochytrium dendrobatidis*/BDEG_04723; Botrytis cinerea/Bcin14g03010; *Sporisorium reilianum*/sr10817; Puccinia graminis f. sp. tritici/PGTG_14970; *Phycomyces blakesleeanus*/PHYBL_133989; *Phycomyces blakesleeanus*/PHYBL_160317; *Mucor circinelloides f. lusitanicus*/QYA_155892; *Mucor circinelloides f. lusitanicus*/QYA_156660; *Rhizophagus irregularis*/GLOIN_2v1592318; *Arabidopsis thaliana*/AT OAP14939.1.

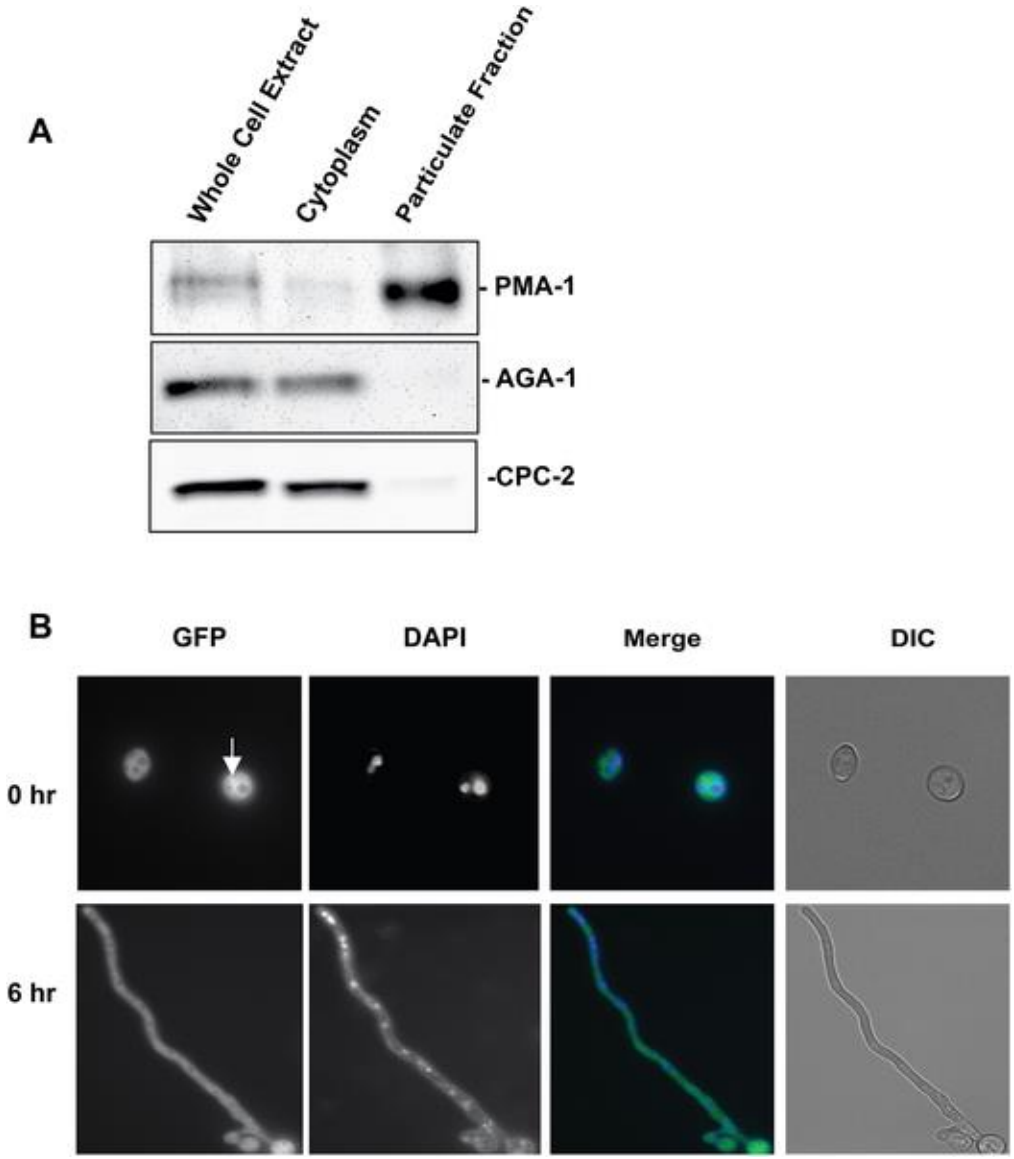

Figure 2.2. Subcellular localization of CPC-2. A. Fractionation of CPC-2 during differential centrifugation of cell extracts. Cytosolic and particulate fractions were isolated from a cell extract of wild-type strain 74-OR23-1VA as described in the Materials and methods. Samples corresponding to the same volume of original cell extract were subjected to SDS-PAGE and western analysis using CPC-2, arginase (AGA; cytosol), and plasma membrane ATPase (PMA-1; plasma membrane) antibodies. The results shown are representative of four biological replicates. B. Localization of GFP-tagged CPC-2 protein in vivo. An aliquot containing 8 x 106 macroconidia from the CPC-2-GFP-9-10 strain was inoculated on VM agarose plates and incubated at 30°C for 0 h and 6 h. Images for the GFP channel were obtained via fluorescence microscopy and also stained with DAPI to visualize the nucleus (see Materials and methods for details). Images for GFP and DAPI were merged using ImageJ (National Institutes of Health, Bethesda, MD). Differential interference contrast (DIC) images were taken to show overall morphology of macroconidia and hyphae. Scale bar = 10 microns.

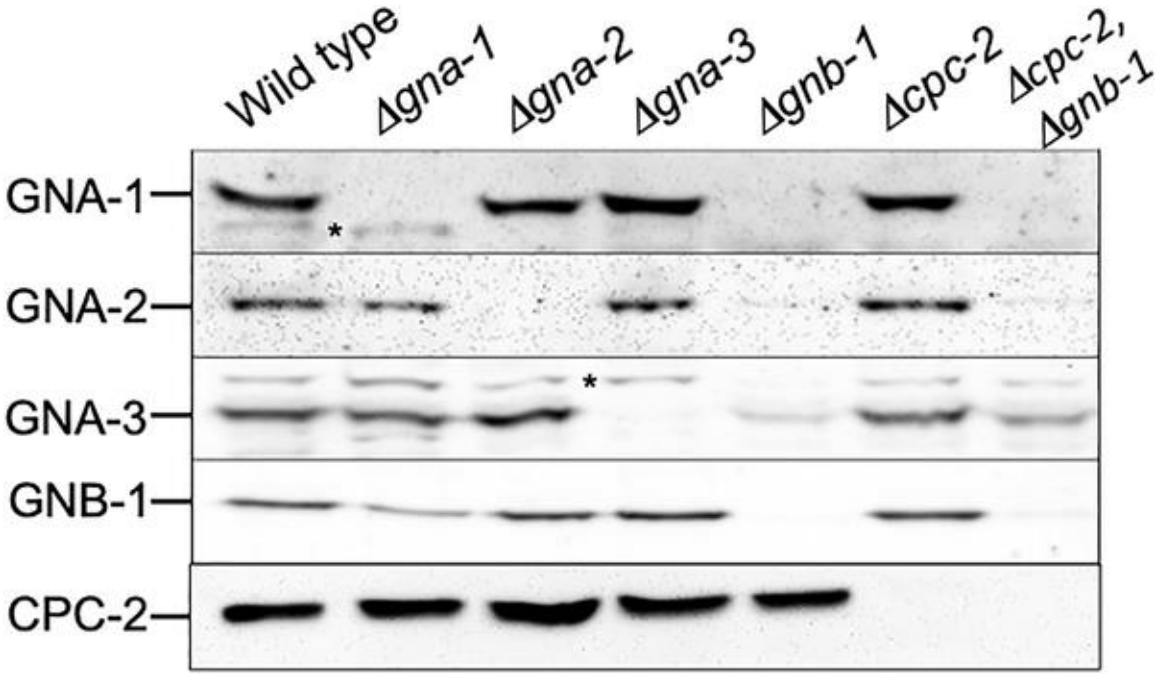

Figure 2.3. Levels of CPC-2 and other G protein subunits in different strain backgrounds. For detection of GNA-1, GNA-2, GNA-3 and GNB-1, differential centrifugation was used to isolate the particulate fraction from whole cell protein extracts of the indicated strains. Samples were subjected to SDS-PAGE and western blots prepared. Blots were reacted with antiserum for GNA-1, GNA-2, GNA-3 or GNB-1. For detection of CPC-2, protein from whole cell extracts was used to prepare western blots. Blots were reacted with polyclonal antiserum raised against a MBP-CPC-2 fusion protein purified from E. coli. The results shown are representative of three biological replicates. The migration position of each protein is shown along the right side of the panel.

A

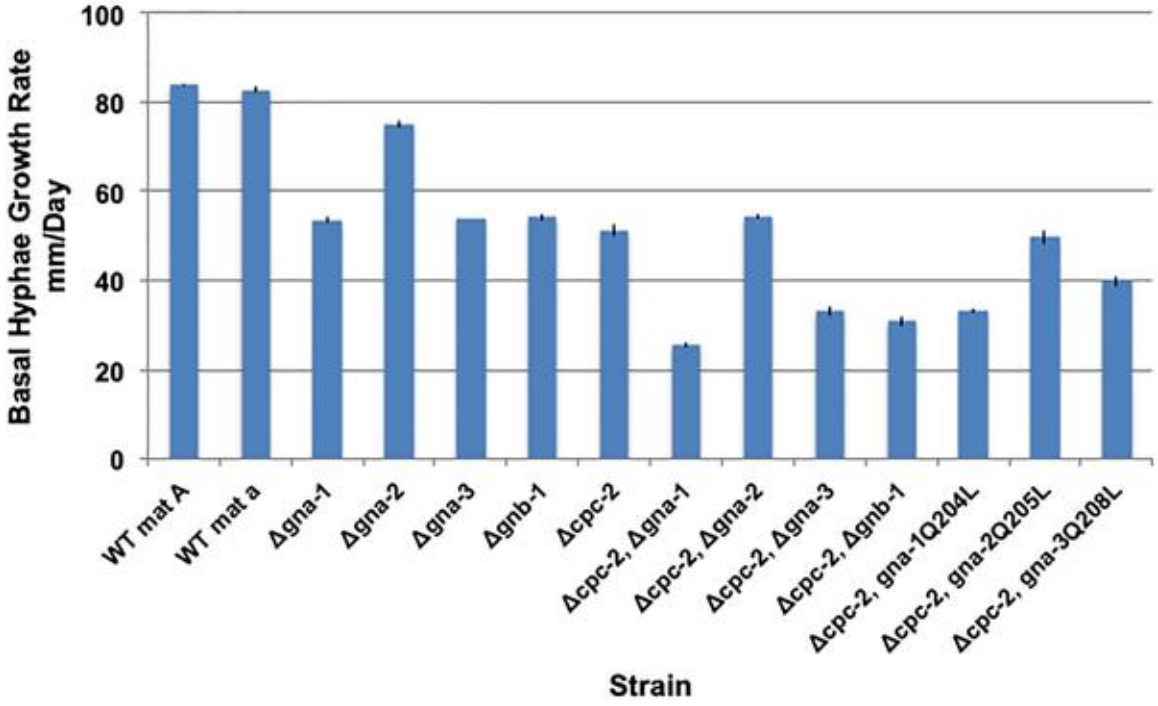

Figure 2.4. Growth rate of basal hyphae. VM agar race tubes were inoculated with the indicated genotypes, incubated at 25°C and marked at various times as previously described [65]. Linear growth rates were determined with values (expressed as mm/day) taken from four biological replicates. Strains used were 74-OR23-1VA, ORS-SL6a, 3B10, Δgna2-2476, 3lc2, 42-8-3, Δcpc2#11, C2B1#2-1-1, C2G1#39, C2G2#37, C2G3#1–6, C2G1*#44, C2G2*#4 and C2G3*#1–8 (See Table 1 for genotypes). Error was calculated as the standard error of the mean. ANOVA was performed to identify strains that were significantly different from one another (Table 2.S1).

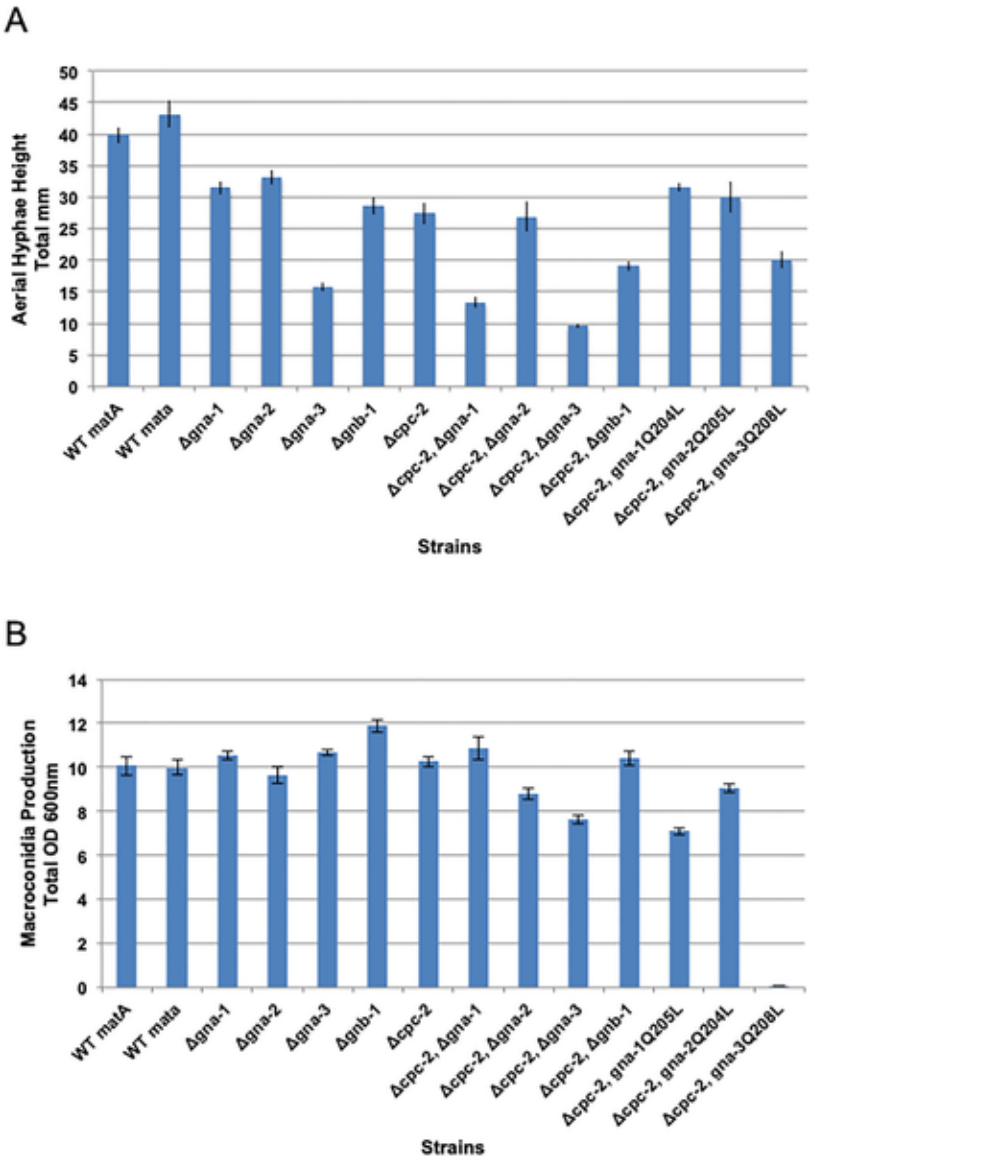

Figure 2.5. Quantative phenotypes during asexual development. Strains, error calculations and ANOVA were as in Fig 4. A. Aerial hyphae height. Culture tubes containing liquid VM medium were inoculated with the indicated strains and incubated statically in the dark for three days at room temperature. The distance grown by the aerial hyphae above the medium interface was then measured. Values (mm) were taken from 12 biological replicates. B. Macroconidia production. Macroconidia from the indicated strains were propagated by growth in VM agar culture tubes in the dark at 30°C for four days followed by three days in light at room temperature. Macroconidia were harvested from the cultures and quantitated as described in the Materials and methods. Values represent eight biological replicates.

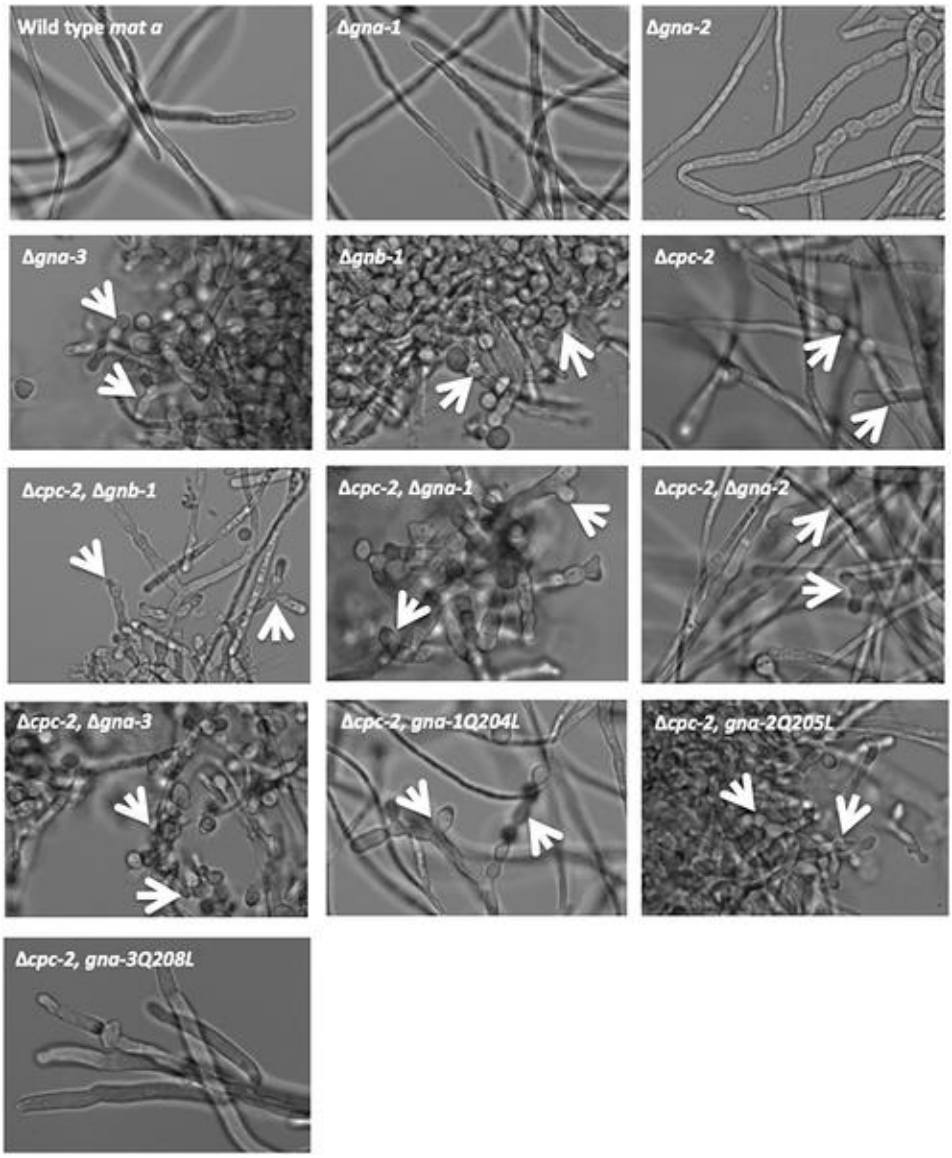

Figure 2.6. Morphology in submerged culture. Macroconidia isolated from the strains used in Fig 4 were inoculated at a concentration of 1x106 macroconidia/ml and cultured in VM liquid medium for 16 h with shaking at 200 rpm in the dark at 30°C. In the case of strain C2G3*#1–8 (Δcpc-2 gna-3Q208L), a small volume of aerial hyphae was used to inoculate cultures, as this strain does not produce a significant amount of macroconidia. A sample of each culture was imaged at 40x magnification using DIC (see Materials and methods). Examples of conidiophores and/or free macroconidia are indicated by the white arrows.

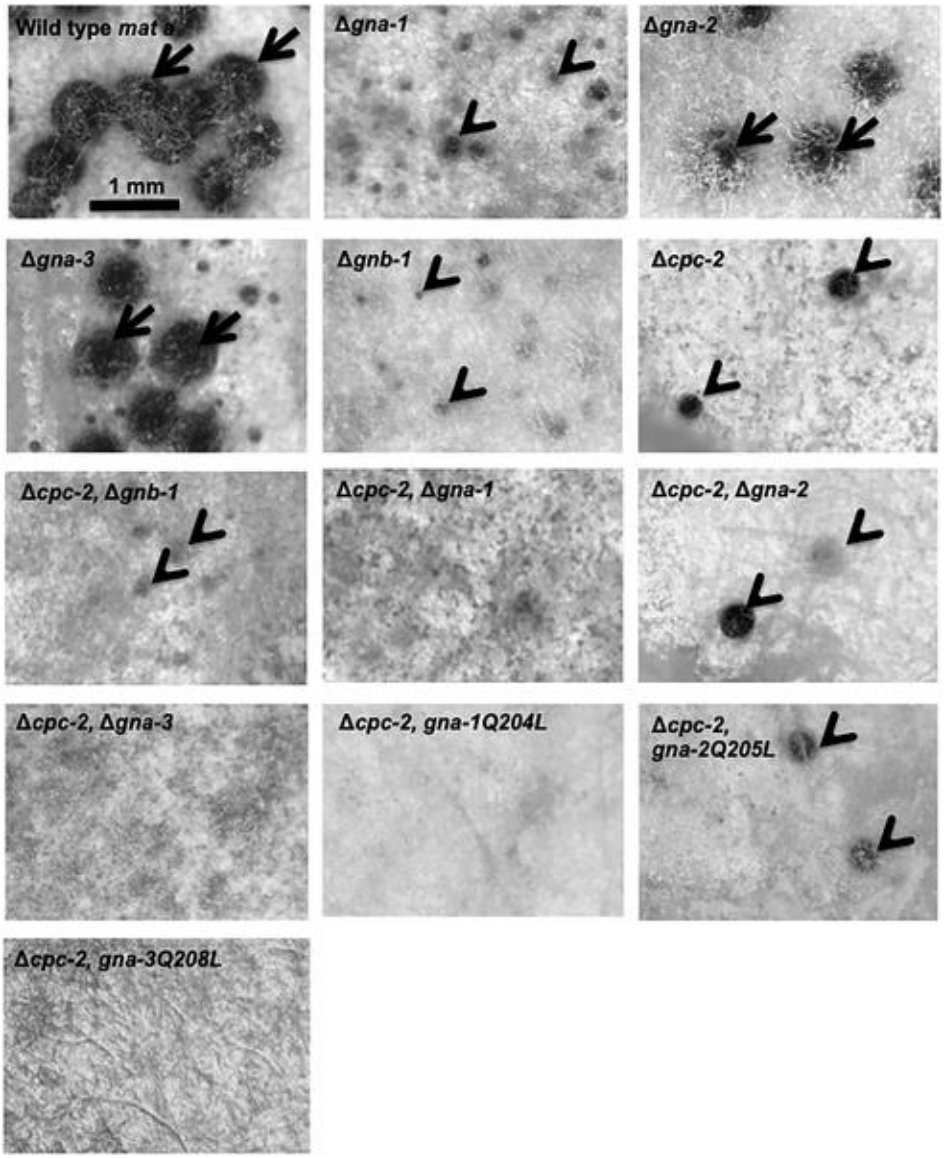

Figure 2.7. Phenotypes during the sexual cycle. Strains were ORS-SL6a, 3B10, Δgna2-2476, 3lc2, 42-8-3, Δcpc2#11, C2B1#2-1-1, C2G1#39, C2G2#37, C2G3#1–6, C2G1*#44, C2G2*#4 and C2G3*#1–8 (See Table 1 for genotypes). Macroconidia or hyphae from strains were inoculated onto SCM plates and incubated in constant light at room temperature for 7 days. At that time, half of each plate was inoculated with either macroconidia (males) of opposite mating type or water (control). Males were from wild-type strains 74-OR23-1VA (mat A) or ORS-SL6a (mat a). Incubation was continued under the same conditions for an additional 7 days. The fertilized side of each plate was then photographed using a Leica S8APO stereomicroscope with a DFC280 camera (Leica Microsystems, Buffalo Grove, IL USA). Examples of protoperithecia or submerged, aberrant perithecia are indicated by the black arrowheads, while mature perithecia are shown by the black arrows.

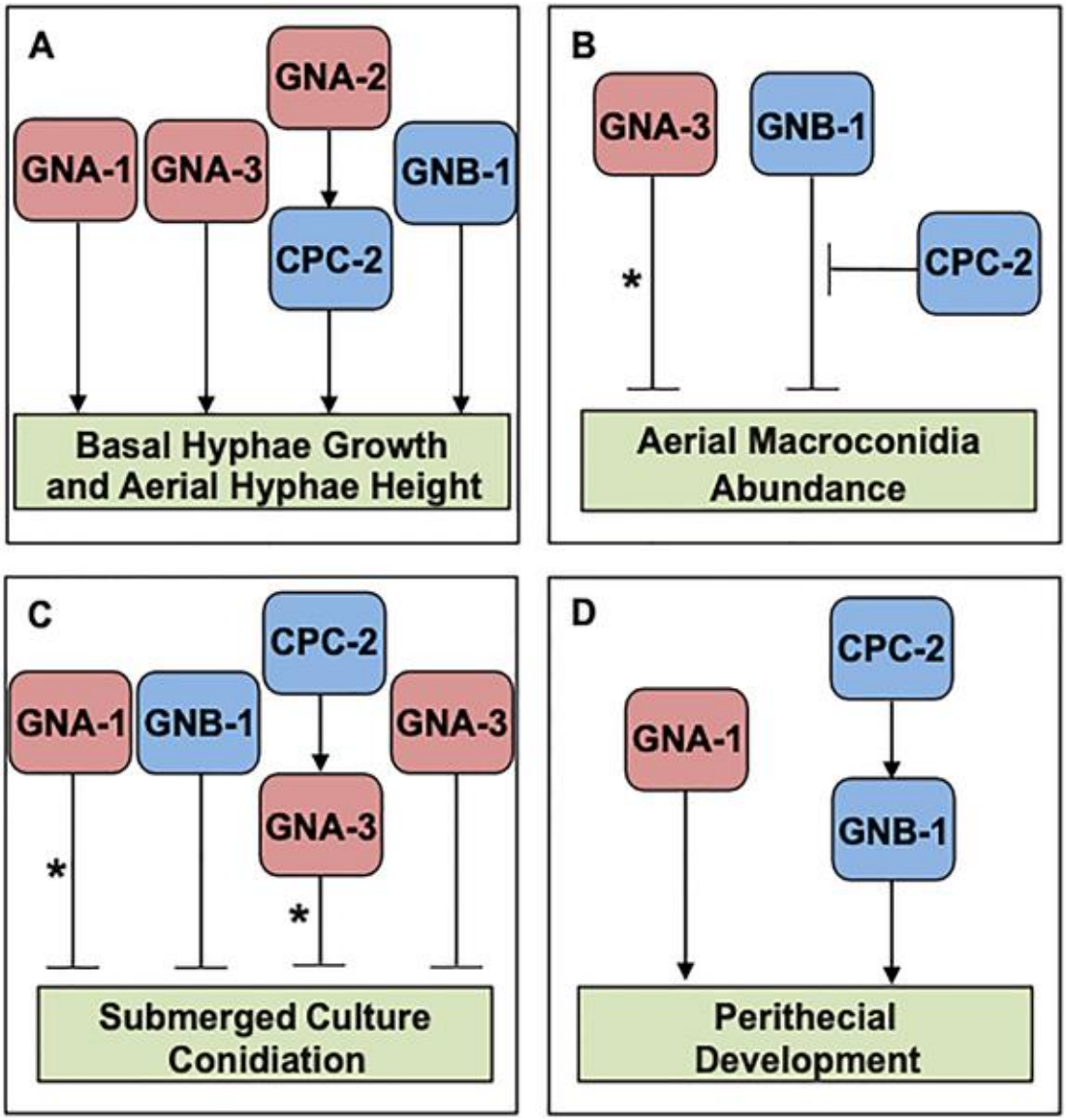

Figure 2.8. Models for interactions between CPC-2 and G protein subunits in N. crassa.
The three Gα proteins are colored red, while the two predicted Gβ proteins are blue in the various panels. A. Basal hyphae growth and aerial hyphae height. GNA-2 operates upstream of CPC-2 to positively modulate basal hyphae growth rate and aerial hyphae height. GNA-1, GNA-3 and GNB-1 act independently of CPC-2 to regulate this trait. B. Aerial macroconidia abundance. GNB-1 is a negative regulator of macroconidia abundance in agar cultures and loss of cpc-2 suppresses this effect. The asterisk indicates that GNA-3 only influences macroconidiation when mutationally activated. C. Submerged culture conidiation. CPC-2, GNA-1, GNA-3 and GNB-1 are negative regulators of conidiation in liquid submerged cultures. The asterisk on the GNA-1 arrow denotes the cell density dependence of the GNA-1 effect. The asterisk on the GNA-3 arrow indicates that GNA-3 may function with CPC-2 or independently, as Δgna-3 Δcpc-2 mutants have a more severe phenotype than the single mutants, but mutational activation of gna-3 corrects the phenotype of the Δcpc-2 mutant. D. Perithecial development. GNB-1 functions downstream of CPC-2 to regulate perithecial development. The action of GNA-1 to control perithecial development is independent of CPC-2.

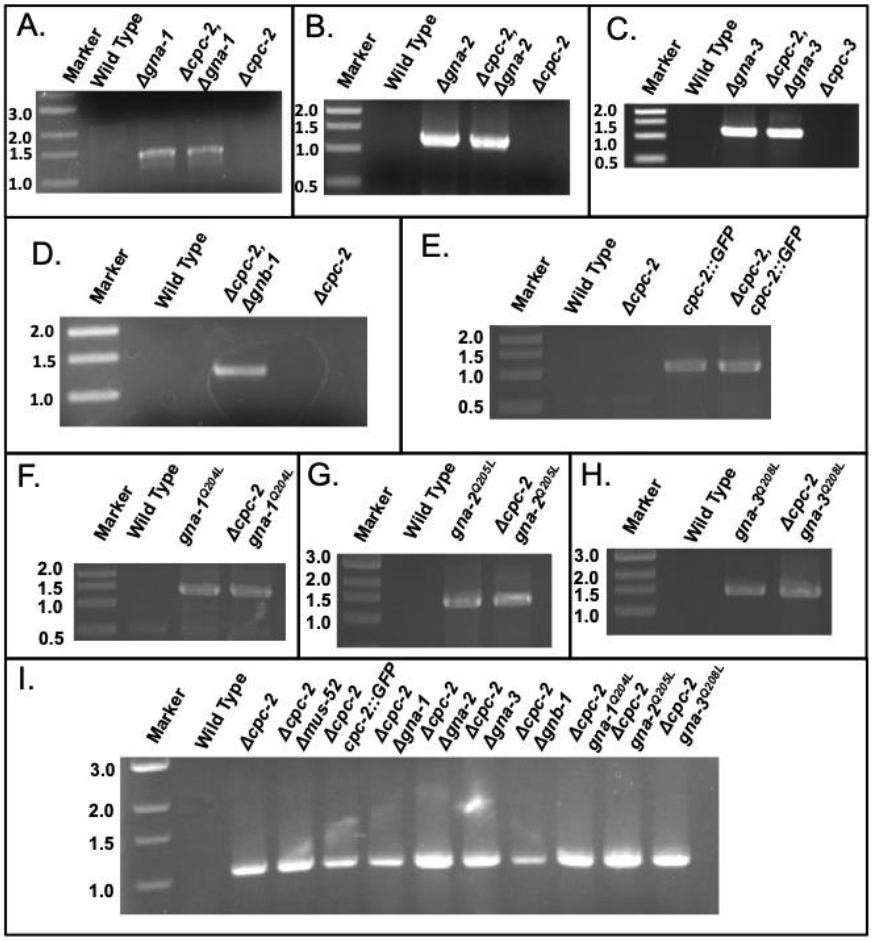

Figure 2.S1. Strain genotyping using PCR. Strains created in this study were checked for proper integration of the DNA construct at the correct locus via diagnostic Polymerase Chain Reactions (PCRs). Genomic DNA was isolated from the indicated genotypes and used in PCRs with the indicated primers. After electrophoresis, agarose gels were stained using ethidium bromide and imaged. The strains used were 74-OR23-1VA (Wild Type), 3B10 (Δgna-1), Δgna2-2477 (Δgna-2), 31c2 (Δgna-3), 42-8-3 (Δgnb-1), Δcpc2#11 (Δcpc-2), Δcpc2#6 (Δcpc-2 Δmus-52), C2G1*#44 (Δcpc-2 gna-1Q204L), C2G2*#4 (Δcpc-2 gna-2Q205L), C2G3*#1–8 (Δcpc-2 gna-3Q208L), C2G1#39 (Δcpc-2 Δgna-1), C2G2#37 (Δcpc-2 Δgna-2), C2G3#1–6 (Δcpc-2 Δgna-3), C2B1#2-1-1 (Δcpc-2 Δgnb-1), CPC-2-GFP-9-10 (cpc-2::GFP), and CPC-2-GFP-13.2 (Δcpc-2 cpc-2::GFP). A. Δgna-1. Primers #4 and #14 were used to amplify a 1.45 kb band corresponding to the Δgna-1 deletion from the indicated strains. B. Δgna-2. Primers #7 and #14 were used to amplify a 1.3 kb band corresponding to the Δgna-2 deletion from the indicated strains. C. Δgna-3. Primers #9 and #13 were used to amplify a 1 kb band corresponding to the Δgna-3 deletion from the indicated strains. D. Δgnb-1. Primers #21 and #22 were used to amplify a 1.3 kb band corresponding to the Δgnb-1 deletion from the indicated strains. E. ccg-1 promoter-cpc-2 ORF region. Primers #23 and #29 were used to amplify a 1.0 kb band corresponding to the ccg-1 promoter-cpc-2 ORF region from the indicated strains. F. ccg-1 promoter-gna-1 ORF region. Primers #23 and #24 were used to amplify a 1.3 kb band corresponding to the ccg-1 promoter-gna-1 ORF region from indicated strains. G. ccg-1 promoter-gna-2 ORF region. Primers #23 and #25 were used to amplify a 1.4 kb band corresponding to the ccg-1 promoter-gna-2 ORF region from indicated strains. H. ccg-1 promoter-gna-3 ORF region. Primers #23 and #26 were used to amplify a 1.5 kb band corresponding to the ccg-1 promoter-gna-3 ORF region from indicated strains. I. Δcpc-2. Primers #1 and #14 were used to amplify a 1.1 kb band corresponding to the Δcpc-2 deletion from the indicated strains.

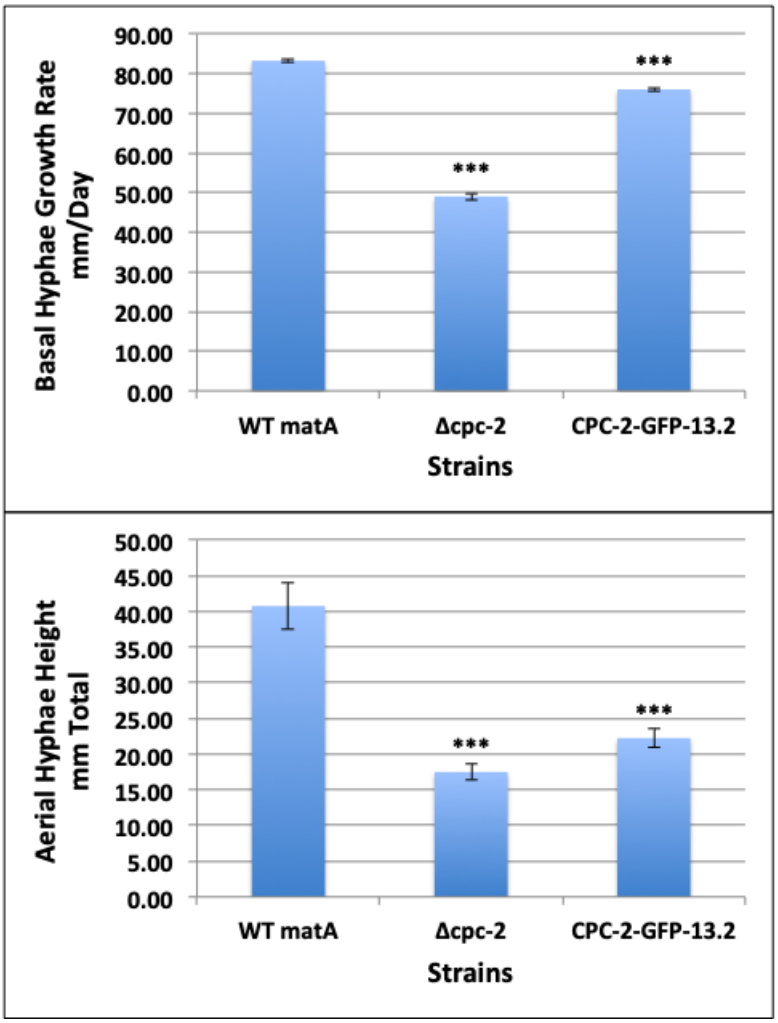

Figure 2.S2. Analysis of growth rate and asexual development in a complemented strain. Δcpc-2 complemented strain CPC-2-GFP-13.2 was compared to wild type (WT matA) and Δcpc-2 strain Δcpc2#11 with respect to growth rate of basal hyphae (top; four replicates) and aerial hyphae height (bottom; 12 replicates) on VM medium supplemented with 10 µg/ml pantothenate. Error is indicated as the standard error of the mean. *** p value <0.001 relative to wild type.

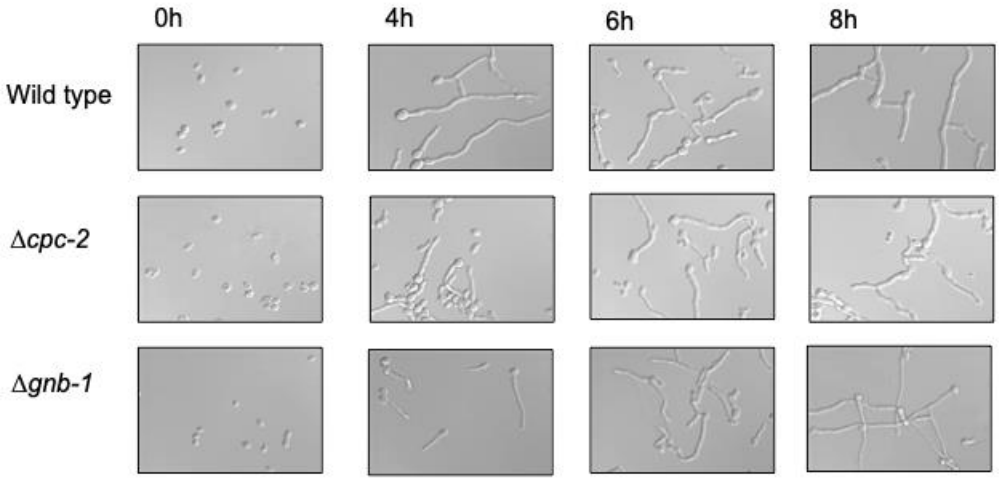

Figure 2.S3. Germination of macroconidia. Macroconidia were harvested as described in [59]. An aliquot containing 8×106 macroconidia was spread on a VM agar plate (100mm plate containing 10 ml agar medium) and spore germination monitored microscopically at 30°C over the indicated times. DIC (differential interference contrast) micrograph images were obtained using an Olympus IX71 microscope with a QIClick digital CCD camera and analyzed using Metamorph software. Strains used were wild type, Δcpc-2 and Δgnb-1.

Tables

Table 2.1. *N. crassa* strains used in this study

Strain name	Relevant genotype	Comments	Source or Reference
74-OR23-1VA	Wild type, *mat A*		FGSC[a] 2489
ORS-SL6a	Wild type, *mat a*		FGSC4200
74A-OR23-1A	Wild type, *mat A*		FGSC987
a^{m1}	*cyh-1, ad3B,* a^{m1}		FGSC4564
Y234M723	*his-3, mat A*		FGSC6103
his-3a#14	*his-3, mat a*		(50)
3B10	Δ*gna-1::hph*$^+$, *mat a*		(73)
Δgna2-2477	Δ*gna-2::hph*$^+$, *mat a*		FGSC12377
Δgna2-2476	Δ*gna-2::hph*$^+$, *mat A*		FGSC12376
3lc2	Δ*gna-3::hph*$^+$, *mat A*		(13)
42-8-3	Δ*gnb-1::hph*$^+$, *mat A*		(53)
Δcpc2Het	Δ*cpc-2::hph*$^+$, Δ*mus-51::bar*$^+$, *mat a* (heterokaryon)		FGSC
Δcpc2#1	Δ*cpc-2::hph*$^+$, Δ*mus-51::bar*$^+$, *mat a*	Progeny from cross of Δcpc2Het to 74-OR23-1VA	This Study
Δcpc2#6	Δ*cpc-2::hph*$^+$, Δ*mus-51::bar*$^+$, *mat a*	Progeny from cross of Δcpc2Het to 74-OR23-1VA	This Study
Δcpc2#11	Δ*cpc-2::hph*$^+$, *mat A*	Progeny from cross of Δcpc2Het to 74-OR23-1VA	This Study
Δcpc2his3A	Δ*cpc-2::hph*$^+$, *his-3, mat A*	Progeny from cross of Δcpc2Het to Y234M723	This Study
cpc2+$a^{m\,1}$	Δ*cpc-2::hph*$^+$, *his-3, mat A +* $a^{m\,1}$*, cyh-1, ad3B, mat A* (heterokaryon)	Heterokaryon of Δcpc2his3A and a^{m1}	This Study
C2G1*#44	Δ*cpc-2::hph*$^+$, *his-3*$^+$*::gna-1*^{Q204L}, *mat A*	Δcpc2his3A purified transformant	This Study
C2G2*#4	Δ*cpc-2::hph*$^+$, *his-3*$^+$*::gna-2*^{Q205L}, *mat A*	Δcpc2his3A purified transformant	This Study
C2G3*#1-8	Δ*cpc-2::hph*$^+$, *his-3*$^+$*::gna-3*^{Q208L}, *mat A*	Δcpc2his3A purified transformant	This Study
C2G1#39	Δ*cpc-2::hph*$^+$, Δ*gna-1::hph*$^+$, *mat a*	Progeny from cross of cpc2+$a^{m\,1}$ to 3b10	This Study
C2G2#37	Δ*cpc-2::hph*$^+$, Δ*gna-2::hph*$^+$, *mat a*	Progeny from cross of cpc2+$a^{m\,1}$ to Δgna2-2477	This Study
C2G3#1-6	Δ*gna-3::hph*$^+$, Δ*cpc-2::hph*$^+$, *mat A*	Progeny from cross of 31c2 to Δcpc2#6	This Study
C2B1#2-1-1	Δ*gnb-1::nat*$^+$, Δ*cpc-2::hph*$^+$, *mus-51::bar*$^+$, *mat a*	Δcpc2#6 purified transformant	This Study
51-4	Δ*rid*::*nat*$^+$, Δ*mus-51*::*nat*$^+$, *mat a*		This Study
CPC-2-GFP-9	Δ*pan-2*::p*ccg-1*::*cpc-2*-V5-GFP::*bar*$^+$, *mat a*	51-4-1 transformant	This Study
CPC-2-GFP-9-10	Δ*pan-2*::p*ccg-1*::*cpc-2*-V5-GFP::*bar*$^+$, *mat a*	Progeny of CPC-2-GFP-9 crossed to 74-OR23-1VA	This Study
pccg-1_GFP	Δ*pan-2*::p*ccg-1*::V5-GFP::*bar*$^+$, *mat a*	Empty vector control for CPC-2-GFP-9-10	(47)
CPC-2-GFP-13	Δ*pan-2*::p*ccg-1*::*cpc-2*-V5-GFP::*bar*$^+$, *mat a*	51-4-1 transformant	This Study
CPC-2-GFP-13.2	Δ*cpc-2::hph*$^+$, Δ*pan-2*::p*ccg-1*::*cpc-2*-V5-GFP::*bar*$^+$, *mat a*	Progeny of CPC-2-GFP-13 crossed to 74-OR23-1VA	This Study

[a]FGSC: Fungal Genetics Stock Center, Kansas State University, Manhattan, KS (32)

Table 2.2. Oligonucleotides used in this study

	Primer Name	Sequence 5' to 3'
1	CPC2FORDIAG	AGCAGGGCCGGGTGGAGATT
2	CPC2REVDIAG	CGAAGGTCCCACCCTAACAGCC
3	GNA1FORDIAG-1	CTTGGAGAGTGCGTGGTGGG
4	GNA1FORDIAG-2	GTCGGGTGGGCGATGGATCAA
5	GNA1REVDIAG	GTGTCGGGTGCTTTCTGCCA
6	GNA2FORDIAG-1	GCCCTGGGCACTACCGAAACG
7	GNA2FORDIAG-2	GGGCCAGAAATGGAACCTACC
8	GNA2REVDIAG	TTCCGGCCGAGTGAAACGCT
9	GNA3FORDIAG	GCGGCCTGCCCTAGCAATTCA
10	GNA3REVDIAG	GGAGTAGCGAGGTGTATGAGTGGT
11	GNB1FORDIAG	GTGCCTTCGGCCAGGCTTGT
12	GNB1REVDIAG	TTGGTTACGTATGCTGAGCAAGGG
13	HPHREV	TGCTCCTTCAATATCATCTTCTGTC
14	HPHFOR	TGTGTAGAAGTACTCGCCGATAGTG
15	GNB1NAT5'FLANK-FWD	GTAACGCCAGGGTTTTCCCAGTCACGACGGTTCCATCGGGGGTGCGGTGC
16	GNB1NAT5'FLANK-REV	CTACATGAGCATGCCCTGCCCCTGATCGCTTCTGCGAGTGGGCGGGCGGC
17	GNB1NAT3'FLANK-FWD	CTCCTTCAATATCATCTTCTGTCGAGCTCTCGCTTGTATGCATCAGGTCT
18	GNB1NAT3'FLANK-REV	GCGGATAACAATTTCACACAGGAAACAGCAAGGGCACTGGCCCACTGGAC
19	PTRPC5'GNB1	AGACCTGATGCATACAAGCGAGAGCTCGACAGAAGATGATATTGAAGGAG
20	NAT3'GNB1	GCCGCCCGCCCACTCGCAGAAGCGATCAGGGGCAGGGCATGCTCATGTAG
21	GNB1NAT-REV-DIAG	TCACGTAGACCTGATGCATA
22	NAT 5' REV DIAG	CAAAAAGTGCTCCTTCAATA
23	pCCG1 FWD	CCATCATCAGCCAACAAAGC
24	GNA1ORF REV	GGGAATTCTCAAATCAAACCGCAG
25	GNA2ORF REV	GGGAATTCCTACAGGATAAGTTGT
26	GNA3ORF REV	GGGAATTCTCATAGAATACCGGAG
27	F-C2	CCACTTTCACAACCCCTCACATCAACCAAAATGGCTGAGCAACTCATCCTCAAG
28	R-C2-V5G	GTTAGGGATAGGCTTTCCGCCGCCTCCGCCAGCGCGGGACATGACACCCCAGGC
29	P-CPC-2-REV	TATGCTAGTTATGCGGCCGCTGCAGTTAAGCGCGGGACATGACACCCCAG

Table 2.S1. Multiple Comparisons test for different phenotypes.

Multiple Comparisons for Aerial Hyphae						
Uncorrected Fisher's LSD	**Mean Diff.**	**95% CI of diff.**	**Significant?**	**Summary**	**Individual P Value**	
WT A vs. WT a	-3.333	-7.400 to 0.7329	No	ns	0.1074	A-B
WT A vs. gna-1	8.333	4.267 to 12.40	Yes	****	< 0.0001	A-C
WT A vs. gna-2	6.667	2.600 to 10.73	Yes	**	0.0015	A-D
WT A vs. gna-3	24	19.93 to 28.07	Yes	****	< 0.0001	A-E
WT A vs. gnb-1	11.25	7.184 to 15.32	Yes	****	< 0.0001	A-F
WT A vs. cpc-2	12.42	8.350 to 16.48	Yes	****	< 0.0001	A-G
WT A vs. cpc-2 gna-1	26.5	22.43 to 30.57	Yes	****	< 0.0001	A-H
WT A vs. cpc-2 gna-2	12.92	8.850 to 16.98	Yes	****	< 0.0001	A-I
WT A vs. cpc-2 gna-3	30.25	26.18 to 34.32	Yes	****	< 0.0001	A-J
WT A vs. cpc-2 gnb-1	20.75	16.68 to 24.82	Yes	****	< 0.0001	A-K
WT A vs. cpc-2 gna-1*	8.25	4.184 to 12.32	Yes	****	< 0.0001	A-L
WT A vs. cpc-2 gna-2*	9.833	5.767 to 13.90	Yes	****	< 0.0001	A-M
WT A vs. cpc-2 gna-3*	19.75	15.68 to 23.82	Yes	****	< 0.0001	A-N
WT a vs. gna-1	11.67	7.600 to 15.73	Yes	****	< 0.0001	B-C
WT a vs. gna-2	10	5.934 to 14.07	Yes	****	< 0.0001	B-D
WT a vs. gna-3	27.33	23.27 to 31.40	Yes	****	< 0.0001	B-E
WT a vs. gnb-1	14.58	10.52 to 18.65	Yes	****	< 0.0001	B-F
WT a vs. cpc-2	15.75	11.68 to 19.82	Yes	****	< 0.0001	B-G
WT a vs. cpc-2 gna-1	29.83	25.77 to 33.90	Yes	****	< 0.0001	B-H
WT a vs. cpc-2 gna-2	16.25	12.18 to 20.32	Yes	****	< 0.0001	B-I
WT a vs. cpc-2 gna-3	33.58	29.52 to 37.65	Yes	****	< 0.0001	B-J
WT a vs. cpc-2 gnb-1	24.08	20.02 to 28.15	Yes	****	< 0.0001	B-K
WT a vs. cpc-2 gna-1*	11.58	7.517 to 15.65	Yes	****	< 0.0001	B-L
WT a vs. cpc-2 gna-2*	13.17	9.100 to 17.23	Yes	****	< 0.0001	B-M
WT a vs. cpc-2 gna-3*	23.08	19.02 to 27.15	Yes	****	< 0.0001	B-N
gna-1 vs. gna-2	-1.667	-5.733 to 2.400	No	ns	0.4194	C-D
gna-1 vs. gna-3	15.67	11.60 to 19.73	Yes	****	< 0.0001	C-E
gna-1 vs. gnb-1	2.917	-1.150 to 6.983	No	ns	0.1585	C-F
gna-1 vs. cpc-2	4.083	0.01712 to 8.150	Yes	*	0.0491	C-G
gna-1 vs. cpc-2 gna-1	18.17	14.10 to 22.23	Yes	****	< 0.0001	C-H
gna-1 vs. cpc-2 gna-2	4.583	0.5171 to 8.650	Yes	*	0.0274	C-I
gna-1 vs. cpc-2 gna-3	21.92	17.85 to 25.98	Yes	****	< 0.0001	C-J
gna-1 vs. cpc-2 gnb-1	12.42	8.350 to 16.48	Yes	****	< 0.0001	C-K
gna-1 vs. cpc-2 gna-1*	-0.08333	-4.150 to 3.983	No	ns	0.9678	C-L
gna-1 vs. cpc-2 gna-2*	1.5	-2.566 to 5.566	No	ns	0.4673	C-M
gna-1 vs. cpc-2 gna-3*	11.42	7.350 to 15.48	Yes	****	< 0.0001	C-N
gna-2 vs. gna-3	17.33	13.27 to 21.40	Yes	****	< 0.0001	D-E
gna-2 vs. gnb-1	4.583	0.5171 to 8.650	Yes	*	0.0274	D-F
gna-2 vs. cpc-2	5.75	1.684 to 9.816	Yes	**	0.0059	D-G
gna-2 vs. cpc-2 gna-1	19.83	15.77 to 23.90	Yes	****	< 0.0001	D-H
gna-2 vs. cpc-2 gna-2	6.25	2.184 to 10.32	Yes	**	0.0028	D-I
gna-2 vs. cpc-2 gna-3	23.58	19.52 to 27.65	Yes	****	< 0.0001	D-J
gna-2 vs. cpc-2 gnb-1	14.08	10.02 to 18.15	Yes	****	< 0.0001	D-K
gna-2 vs. cpc-2 gna-1*	1.583	-2.483 to 5.650	No	ns	0.4429	D-L
gna-2 vs. cpc-2 gna-2*	3.167	-0.8995 to 7.233	No	ns	0.126	D-M
gna-2 vs. cpc-2 gna-3*	13.08	9.017 to 17.15	Yes	****	< 0.0001	D-N
gna-3 vs. gnb-1	-12.75	-16.82 to -8.684	Yes	****	< 0.0001	E-F
gna-3 vs. cpc-2	-11.58	-15.65 to -7.517	Yes	****	< 0.0001	E-G
gna-3 vs. cpc-2 gna-1	2.5	-1.566 to 6.566	No	ns	0.2264	E-H

gna-3 vs. cpc-2 gna-2	-11.08	-15.15 to -7.017	Yes	****	< 0.0001	E-I
gna-3 vs. cpc-2 gna-3	6.25	2.184 to 10.32	Yes	**	0.0028	E-J
gna-3 vs. cpc-2 gnb-1	-3.25	-7.316 to 0.8162	No	ns	0.1164	E-K
gna-3 vs. cpc-2 gna-1*	-15.75	-19.82 to -11.68	Yes	****	< 0.0001	E-L
gna-3 vs. cpc-2 gna-2*	-14.17	-18.23 to -10.10	Yes	****	< 0.0001	E-M
gna-3 vs. cpc-2 gna-3*	-4.25	-8.316 to -0.1838	Yes	*	0.0406	E-N
gnb-1 vs. cpc-2	1.167	-2.900 to 5.233	No	ns	0.5717	F-G
gnb-1 vs. cpc-2 gna-1	15.25	11.18 to 19.32	Yes	****	< 0.0001	F-H
gnb-1 vs. cpc-2 gna-2	1.667	-2.400 to 5.733	No	ns	0.4194	F-I
gnb-1 vs. cpc-2 gna-3	19	14.93 to 23.07	Yes	****	< 0.0001	F-J
gnb-1 vs. cpc-2 gnb-1	9.5	5.434 to 13.57	Yes	****	< 0.0001	F-K
gnb-1 vs. cpc-2 gna-1*	-3	-7.066 to 1.066	No	ns	0.147	F-L
gnb-1 vs. cpc-2 gna-2*	-1.417	-5.483 to 2.650	No	ns	0.4923	F-M
gnb-1 vs. cpc-2 gna-3*	8.5	4.434 to 12.57	Yes	****	< 0.0001	F-N
cpc-2 vs. cpc-2 gna-1	14.08	10.02 to 18.15	Yes	****	< 0.0001	G-H
cpc-2 vs. cpc-2 gna-2	0.5	-3.566 to 4.566	No	ns	0.8084	G-I
cpc-2 vs. cpc-2 gna-3	17.83	13.77 to 21.90	Yes	****	< 0.0001	G-J
cpc-2 vs. cpc-2 gnb-1	8.333	4.267 to 12.40	Yes	****	< 0.0001	G-K
cpc-2 vs. cpc-2 gna-1*	-4.167	-8.233 to -0.1005	Yes	*	0.0447	G-L
cpc-2 vs. cpc-2 gna-2*	-2.583	-6.650 to 1.483	No	ns	0.2114	G-M
cpc-2 vs. cpc-2 gna-3*	7.333	3.267 to 11.40	Yes	***	0.0005	G-N
cpc-2 gna-1 vs. cpc-2 gna-2	-13.58	-17.65 to -9.517	Yes	****	< 0.0001	H-I
cpc-2 gna-1 vs. cpc-2 gna-3	3.75	-0.3162 to 7.816	No	ns	0.0704	H-J
cpc-2 gna-1 vs. cpc-2 gnb-1	-5.75	-9.816 to -1.684	Yes	**	0.0059	H-K
cpc-2 gna-1 vs. cpc-2 gna-1*	-18.25	-22.32 to -14.18	Yes	****	< 0.0001	H-L
cpc-2 gna-1 vs. cpc-2 gna-2*	-16.67	-20.73 to -12.60	Yes	****	< 0.0001	H-M
cpc-2 gna-1 vs. cpc-2 gna-3*	-6.75	-10.82 to -2.684	Yes	**	0.0013	H-N
cpc-2 gna-2 vs. cpc-2 gna-3	17.33	13.27 to 21.40	Yes	****	< 0.0001	I-J
cpc-2 gna-2 vs. cpc-2 gnb-1	7.833	3.767 to 11.90	Yes	***	0.0002	I-K
cpc-2 gna-2 vs. cpc-2 gna-1*	-4.667	-8.733 to -0.6005	Yes	*	0.0248	I-L
cpc-2 gna-2 vs. cpc-2 gna-2*	-3.083	-7.150 to 0.9829	No	ns	0.1362	I-M
cpc-2 gna-2 vs. cpc-2 gna-3*	6.833	2.767 to 10.90	Yes	**	0.0011	I-N
cpc-2 gna-3 vs. cpc-2 gnb-1	-9.5	-13.57 to -5.434	Yes	****	< 0.0001	J-K
cpc-2 gna-3 vs. cpc-2 gna-1*	-22	-26.07 to -17.93	Yes	****	< 0.0001	J-L
cpc-2 gna-3 vs. cpc-2 gna-2*	-20.42	-24.48 to -16.35	Yes	****	< 0.0001	J-M
cpc-2 gna-3 vs. cpc-2 gna-3*	-10.5	-14.57 to -6.434	Yes	****	< 0.0001	J-N
cpc-2 gnb-1 vs. cpc-2 gna-1*	-12.5	-16.57 to -8.434	Yes	****	< 0.0001	K-L
cpc-2 gnb-1 vs. cpc-2 gna-2*	-10.92	-14.98 to -6.850	Yes	****	< 0.0001	K-M
cpc-2 gnb-1 vs. cpc-2 gna-3*	-1	-5.066 to 3.066	No	ns	0.6278	K-N
cpc-2 gna-1* vs. cpc-2 gna-2*	1.583	-2.483 to 5.650	No	ns	0.4429	L-M
cpc-2 gna-1* vs. cpc-2 gna-3*	11.5	7.434 to 15.57	Yes	****	< 0.0001	L-N
cpc-2 gna-2* vs. cpc-2 gna-3*	9.917	5.850 to 13.98	Yes	****	< 0.0001	M-N

Multiple Comparisons for Basal Hyphae						
Uncorrected Fisher's LSD	**Mean Diff.**	**95% CI of diff.**	**Significant?**	**Summary**	**Individual P Value**	
WT mat A vs. WT mat a	0.966	-1.672 to 3.604	No	ns	0.4636	A-B
WT mat A vs. gna-1	30.29	27.65 to 32.93	Yes	****	< 0.0001	A-C
WT mat A vs. gna-2	8.655	6.017 to 11.29	Yes	****	< 0.0001	A-D
WT mat A vs. gna-3	29.91	27.06 to 32.76	Yes	****	< 0.0001	A-E
WT mat A vs. gnb-1	29.66	27.03 to 32.30	Yes	****	< 0.0001	A-F
WT mat A vs. cpc-2	32.53	29.89 to 35.17	Yes	****	< 0.0001	A-G
WT mat A vs. cpc-2 gna-1	58.25	55.61 to 60.89	Yes	****	< 0.0001	A-H
WT mat A vs. cpc-2 gna-2	29.58	26.73 to 32.43	Yes	****	< 0.0001	A-I
WT mat A vs. cpc-2 gna-3	50.7	48.06 to 53.33	Yes	****	< 0.0001	A-J
WT mat A vs. cpc-2 gnb-1	52.92	50.28 to 55.56	Yes	****	< 0.0001	A-K
WT mat A vs. cpc-2 gna-1*	50.63	48.00 to 53.27	Yes	****	< 0.0001	A-L
WT mat A vs. cpc-2 gna-2*	34.16	31.52 to 36.80	Yes	****	< 0.0001	A-M
WT mat A vs. cpc-2 gna-3*	44.01	41.38 to 46.65	Yes	****	< 0.0001	A-N
WT mat a vs. gna-1	29.33	26.69 to 31.96	Yes	****	< 0.0001	B-C
WT mat a vs. gna-2	7.689	5.051 to 10.33	Yes	****	< 0.0001	B-D
WT mat a vs. gna-3	28.95	26.10 to 31.80	Yes	****	< 0.0001	B-E
WT mat a vs. gnb-1	28.7	26.06 to 31.34	Yes	****	< 0.0001	B-F
WT mat a vs. cpc-2	31.56	28.92 to 34.20	Yes	****	< 0.0001	B-G
WT mat a vs. cpc-2 gna-1	57.29	54.65 to 59.92	Yes	****	< 0.0001	B-H
WT mat a vs. cpc-2 gna-2	28.62	25.77 to 31.46	Yes	****	< 0.0001	B-I
WT mat a vs. cpc-2 gna-3	49.73	47.09 to 52.37	Yes	****	< 0.0001	B-J
WT mat a vs. cpc-2 gnb-1	51.95	49.31 to 54.59	Yes	****	< 0.0001	B-K
WT mat a vs. cpc-2 gna-1*	49.67	47.03 to 52.31	Yes	****	< 0.0001	B-L
WT mat a vs. cpc-2 gna-2*	33.19	30.55 to 35.83	Yes	****	< 0.0001	B-M
WT mat a vs. cpc-2 gna-3*	43.05	40.41 to 45.69	Yes	****	< 0.0001	B-N
gna-1 vs. gna-2	-21.64	-24.27 to -19.00	Yes	****	< 0.0001	C-D
gna-1 vs. gna-3	-0.3775	-3.227 to 2.472	No	ns	0.7903	C-E
gna-1 vs. gnb-1	-0.6266	-3.265 to 2.012	No	ns	0.6339	C-F
gna-1 vs. cpc-2	2.236	-0.4023 to 4.875	No	ns	0.0945	C-G
gna-1 vs. cpc-2 gna-1	27.96	25.32 to 30.60	Yes	****	< 0.0001	C-H
gna-1 vs. cpc-2 gna-2	-0.71	-3.560 to 2.140	No	ns	0.6174	C-I
gna-1 vs. cpc-2 gna-3	20.4	17.77 to 23.04	Yes	****	< 0.0001	C-J
gna-1 vs. cpc-2 gnb-1	22.63	19.99 to 25.27	Yes	****	< 0.0001	C-K
gna-1 vs. cpc-2 gna-1*	20.34	17.71 to 22.98	Yes	****	< 0.0001	C-L
gna-1 vs. cpc-2 gna-2*	3.868	1.230 to 6.507	Yes	**	0.0051	C-M
gna-1 vs. cpc-2 gna-3*	13.72	11.08 to 16.36	Yes	****	< 0.0001	C-N
gna-2 vs. gna-3	21.26	18.41 to 24.11	Yes	****	< 0.0001	D-E
gna-2 vs. gnb-1	21.01	18.37 to 23.65	Yes	****	< 0.0001	D-F
gna-2 vs. cpc-2	23.87	21.23 to 26.51	Yes	****	< 0.0001	D-G
gna-2 vs. cpc-2 gna-1	49.6	46.96 to 52.24	Yes	****	< 0.0001	D-H
gna-2 vs. cpc-2 gna-2	20.93	18.08 to 23.78	Yes	****	< 0.0001	D-I
gna-2 vs. cpc-2 gna-3	42.04	39.40 to 44.68	Yes	****	< 0.0001	D-J
gna-2 vs. cpc-2 gnb-1	44.26	41.62 to 46.90	Yes	****	< 0.0001	D-K
gna-2 vs. cpc-2 gna-1*	41.98	39.34 to 44.62	Yes	****	< 0.0001	D-L
gna-2 vs. cpc-2 gna-2*	25.5	22.87 to 28.14	Yes	****	< 0.0001	D-M
gna-2 vs. cpc-2 gna-3*	35.36	32.72 to 38.00	Yes	****	< 0.0001	D-N
gna-3 vs. gnb-1	-0.2491	-3.099 to 2.601	No	ns	0.8607	E-F
gna-3 vs. cpc-2	2.614	-0.2362 to 5.464	No	ns	0.0712	E-G
gna-3 vs. cpc-2 gna-1	28.34	25.49 to 31.19	Yes	****	< 0.0001	E-H
gna-3 vs. cpc-2 gna-2	-0.3325	-3.379 to 2.714	No	ns	0.8266	E-I

gna-3 vs. cpc-2 gna-3	20.78	17.93 to 23.63	Yes	****	< 0.0001	E-J
gna-3 vs. cpc-2 gnb-1	23	20.15 to 25.85	Yes	****	< 0.0001	E-K
gna-3 vs. cpc-2 gna-1*	20.72	17.87 to 23.57	Yes	****	< 0.0001	E-L
gna-3 vs. cpc-2 gna-2*	4.246	1.396 to 7.096	Yes	**	0.0045	E-M
gna-3 vs. cpc-2 gna-3*	14.1	11.25 to 16.95	Yes	****	< 0.0001	E-N
gnb-1 vs. cpc-2	2.863	0.2243 to 5.501	Yes	*	0.0342	F-G
gnb-1 vs. cpc-2 gna-1	28.59	25.95 to 31.23	Yes	****	< 0.0001	F-H
gnb-1 vs. cpc-2 gna-2	-0.08342	-2.933 to 2.766	No	ns	0.9531	F-I
gnb-1 vs. cpc-2 gna-3	21.03	18.39 to 23.67	Yes	****	< 0.0001	F-J
gnb-1 vs. cpc-2 gnb-1	23.25	20.62 to 25.89	Yes	****	< 0.0001	F-K
gnb-1 vs. cpc-2 gna-1*	20.97	18.33 to 23.61	Yes	****	< 0.0001	F-L
gnb-1 vs. cpc-2 gna-2*	4.495	1.856 to 7.133	Yes	**	0.0014	F-M
gnb-1 vs. cpc-2 gna-3*	14.35	11.71 to 16.99	Yes	****	< 0.0001	F-N
cpc-2 vs. cpc-2 gna-1	25.73	23.09 to 28.36	Yes	****	< 0.0001	G-H
cpc-2 vs. cpc-2 gna-2	-2.946	-5.796 to -0.09632	Yes	*	0.0431	G-I
cpc-2 vs. cpc-2 gna-3	18.17	15.53 to 20.81	Yes	****	< 0.0001	G-J
cpc-2 vs. cpc-2 gnb-1	20.39	17.75 to 23.03	Yes	****	< 0.0001	G-K
cpc-2 vs. cpc-2 gna-1*	18.11	15.47 to 20.75	Yes	****	< 0.0001	G-L
cpc-2 vs. cpc-2 gna-2*	1.632	-1.006 to 4.270	No	ns	0.2185	G-M
cpc-2 vs. cpc-2 gna-3*	11.49	8.848 to 14.12	Yes	****	< 0.0001	G-N
cpc-2 gna-1 vs. cpc-2 gna-2	-28.67	-31.52 to -25.82	Yes	****	< 0.0001	H-I
cpc-2 gna-1 vs. cpc-2 gna-3	-7.556	-10.19 to -4.918	Yes	****	< 0.0001	H-J
cpc-2 gna-1 vs. cpc-2 gnb-1	-5.334	-7.972 to -2.696	Yes	***	0.0002	H-K
cpc-2 gna-1 vs. cpc-2 gna-1*	-7.618	-10.26 to -4.979	Yes	****	< 0.0001	H-L
cpc-2 gna-1 vs. cpc-2 gna-2*	-24.09	-26.73 to -21.45	Yes	****	< 0.0001	H-M
cpc-2 gna-1 vs. cpc-2 gna-3*	-14.24	-16.88 to -11.60	Yes	****	< 0.0001	H-N
cpc-2 gna-2 vs. cpc-2 gna-3	21.11	18.26 to 23.96	Yes	****	< 0.0001	I-J
cpc-2 gna-2 vs. cpc-2 gnb-1	23.34	20.49 to 26.19	Yes	****	< 0.0001	I-K
cpc-2 gna-2 vs. cpc-2 gna-1*	21.05	18.20 to 23.90	Yes	****	< 0.0001	I-L
cpc-2 gna-2 vs. cpc-2 gna-2*	4.578	1.728 to 7.428	Yes	**	0.0024	I-M
cpc-2 gna-2 vs. cpc-2 gna-3*	14.43	11.58 to 17.28	Yes	****	< 0.0001	I-N
cpc-2 gna-3 vs. cpc-2 gnb-1	2.222	-0.4161 to 4.861	No	ns	0.0964	J-K
cpc-2 gna-3 vs. cpc-2 gna-1*	-0.0612	-2.700 to 2.577	No	ns	0.9628	J-L
cpc-2 gna-3 vs. cpc-2 gna-2*	-16.54	-19.18 to -13.90	Yes	****	< 0.0001	J-M
cpc-2 gna-3 vs. cpc-2 gna-3*	-6.682	-9.321 to -4.044	Yes	****	< 0.0001	J-N
cpc-2 gnb-1 vs. cpc-2 gna-1*	-2.284	-4.922 to 0.3549	No	ns	0.0879	K-L
cpc-2 gnb-1 vs. cpc-2 gna-2*	-18.76	-21.40 to -16.12	Yes	****	< 0.0001	K-M
cpc-2 gnb-1 vs. cpc-2 gna-3*	-8.905	-11.54 to -6.266	Yes	****	< 0.0001	K-N
cpc-2 gna-1* vs. cpc-2 gna-2*	-16.48	-19.11 to -13.84	Yes	****	< 0.0001	L-M
cpc-2 gna-1* vs. cpc-2 gna-3*	-6.621	-9.259 to -3.983	Yes	****	< 0.0001	L-N
cpc-2 gna-2* vs. cpc-2 gna-3*	9.854	7.216 to 12.49	Yes	****	< 0.0001	M-N

Multiple Comparisons for Conidiation						
Uncorrected Fisher's LSD	**Mean Diff.**	**95% CI of diff.**	**Significant?**	**Summary**	**Individual P Value**	
WT A vs. WT a	0.07125	-0.7421 to 0.8846	No	ns	0.8623	A-B
WT A vs. gna-1	-0.4856	-1.299 to 0.3277	No	ns	0.2389	A-C
WT A vs. gna-2	0.4069	-0.4065 to 1.220	No	ns	0.3233	A-D
WT A vs. gna-3	-0.6233	-1.465 to 0.2186	No	ns	0.145	A-E
WT A vs. gnb-1	-1.824	-2.638 to -1.011	Yes	****	< 0.0001	A-F
WT A vs. cpc-2	-0.1894	-1.003 to 0.6240	No	ns	0.645	A-G
WT A vs. cpc-2 gnb-1	-0.3506	-1.164 to 0.4627	No	ns	0.3943	A-H
WT A vs. cpc-2 gna-1	-0.7894	-1.603 to 0.02399	No	ns	0.057	A-I
WT A vs. cpc-2 gna-2	1.269	0.4560 to 2.083	Yes	**	0.0026	A-J
WT A vs. cpc-2 gna-3	2.432	1.619 to 3.245	Yes	****	< 0.0001	A-K
WT A vs. cpc-2 gna-1*	2.978	2.164 to 3.791	Yes	****	< 0.0001	A-L
WT A vs. cpc-2 gna-2*	1.013	0.1991 to 1.826	Yes	*	0.0152	A-M
WT A vs. cpc-2 gna-3*	9.994	9.181 to 10.81	Yes	****	< 0.0001	A-N
WT a vs. gna-1	-0.5569	-1.370 to 0.2565	No	ns	0.1773	B-C
WT a vs. gna-2	0.3356	-0.4777 to 1.149	No	ns	0.4148	B-D
WT a vs. gna-3	-0.6946	-1.536 to 0.1474	No	ns	0.1048	B-E
WT a vs. gnb-1	-1.896	-2.709 to -1.082	Yes	****	< 0.0001	B-F
WT a vs. cpc-2	-0.2606	-1.074 to 0.5527	No	ns	0.5263	B-G
WT a vs. cpc-2 gnb-1	-0.4219	-1.235 to 0.3915	No	ns	0.3058	B-H
WT a vs. cpc-2 gna-1	-0.8606	-1.674 to -0.04726	Yes	*	0.0383	B-I
WT a vs. cpc-2 gna-2	1.198	0.3848 to 2.011	Yes	**	0.0043	B-J
WT a vs. cpc-2 gna-3	2.361	1.547 to 3.174	Yes	****	< 0.0001	B-K
WT a vs. cpc-2 gna-1*	2.906	2.093 to 3.720	Yes	****	< 0.0001	B-L
WT a vs. cpc-2 gna-2*	0.9413	0.1279 to 1.755	Yes	*	0.0238	B-M
WT a vs. cpc-2 gna-3*	9.923	9.109 to 10.74	Yes	****	< 0.0001	B-N
gna-1 vs. gna-2	0.8925	0.07913 to 1.706	Yes	*	0.0318	C-D
gna-1 vs. gna-3	-0.1377	-0.9796 to 0.7042	No	ns	0.7462	C-E
gna-1 vs. gnb-1	-1.339	-2.152 to -0.5254	Yes	**	0.0015	C-F
gna-1 vs. cpc-2	0.2963	-0.5171 to 1.110	No	ns	0.4715	C-G
gna-1 vs. cpc-2 gnb-1	0.135	-0.6784 to 0.9484	No	ns	0.7425	C-H
gna-1 vs. cpc-2 gna-1	-0.3037	-1.117 to 0.5096	No	ns	0.4604	C-I
gna-1 vs. cpc-2 gna-2	1.755	0.9416 to 2.568	Yes	****	< 0.0001	C-J
gna-1 vs. cpc-2 gna-3	2.918	2.104 to 3.731	Yes	****	< 0.0001	C-K
gna-1 vs. cpc-2 gna-1*	3.463	2.650 to 4.276	Yes	****	< 0.0001	C-L
gna-1 vs. cpc-2 gna-2*	1.498	0.6848 to 2.311	Yes	***	0.0004	C-M
gna-1 vs. cpc-2 gna-3*	10.48	9.666 to 11.29	Yes	****	< 0.0001	C-N
gna-2 vs. gna-3	-1.03	-1.872 to -0.1883	Yes	*	0.017	D-E
gna-2 vs. gnb-1	-2.231	-3.045 to -1.418	Yes	****	< 0.0001	D-F
gna-2 vs. cpc-2	-0.5962	-1.410 to 0.2171	No	ns	0.1489	D-G
gna-2 vs. cpc-2 gnb-1	-0.7575	-1.571 to 0.05587	No	ns	0.0676	D-H
gna-2 vs. cpc-2 gna-1	-1.196	-2.010 to -0.3829	Yes	**	0.0044	D-I
gna-2 vs. cpc-2 gna-2	0.8625	0.04913 to 1.676	Yes	*	0.0379	D-J
gna-2 vs. cpc-2 gna-3	2.025	1.212 to 2.838	Yes	****	< 0.0001	D-K
gna-2 vs. cpc-2 gna-1*	2.571	1.757 to 3.384	Yes	****	< 0.0001	D-L
gna-2 vs. cpc-2 gna-2*	0.6056	-0.2077 to 1.419	No	ns	0.1427	D-M
gna-2 vs. cpc-2 gna-3*	9.587	8.774 to 10.40	Yes	****	< 0.0001	D-N
gna-3 vs. gnb-1	-1.201	-2.043 to -0.3592	Yes	**	0.0056	E-F
gna-3 vs. cpc-2	0.4339	-0.4080 to 1.276	No	ns	0.3089	E-G
gna-3 vs. cpc-2 gnb-1	0.2727	-0.5692 to 1.115	No	ns	0.5219	E-H
gna-3 vs. cpc-2 gna-1	-0.1661	-1.008 to 0.6758	No	ns	0.6963	E-I
gna-3 vs. cpc-2 gna-2	1.893	1.051 to 2.735	Yes	****	< 0.0001	E-J

gna-3 vs. cpc-2 gna-3	3.055	2.213 to 3.897	Yes	****	< 0.0001	E-K
gna-3 vs. cpc-2 gna-1*	3.601	2.759 to 4.443	Yes	****	< 0.0001	E-L
gna-3 vs. cpc-2 gna-2*	1.636	0.7939 to 2.478	Yes	***	0.0002	E-M
gna-3 vs. cpc-2 gna-3*	10.62	9.775 to 11.46	Yes	****	< 0.0001	E-N
gnb-1 vs. cpc-2	1.635	0.8216 to 2.448	Yes	***	0.0001	F-G
gnb-1 vs. cpc-2 gnb-1	1.474	0.6604 to 2.287	Yes	***	0.0005	F-H
gnb-1 vs. cpc-2 gna-1	1.035	0.2216 to 1.848	Yes	*	0.0132	F-I
gnb-1 vs. cpc-2 gna-2	3.094	2.280 to 3.907	Yes	****	< 0.0001	F-J
gnb-1 vs. cpc-2 gna-3	4.256	3.443 to 5.070	Yes	****	< 0.0001	F-K
gnb-1 vs. cpc-2 gna-1*	4.802	3.989 to 5.615	Yes	****	< 0.0001	F-L
gnb-1 vs. cpc-2 gna-2*	2.837	2.024 to 3.650	Yes	****	< 0.0001	F-M
gnb-1 vs. cpc-2 gna-3*	11.82	11.00 to 12.63	Yes	****	< 0.0001	F-N
cpc-2 vs. cpc-2 gnb-1	-0.1613	-0.9746 to 0.6521	No	ns	0.6948	G-H
cpc-2 vs. cpc-2 gna-1	-0.6	-1.413 to 0.2134	No	ns	0.1464	G-I
cpc-2 vs. cpc-2 gna-2	1.459	0.6454 to 2.272	Yes	***	0.0006	G-J
cpc-2 vs. cpc-2 gna-3	2.621	1.808 to 3.435	Yes	****	< 0.0001	G-K
cpc-2 vs. cpc-2 gna-1*	3.167	2.354 to 3.980	Yes	****	< 0.0001	G-L
cpc-2 vs. cpc-2 gna-2*	1.202	0.3885 to 2.015	Yes	**	0.0042	G-M
cpc-2 vs. cpc-2 gna-3*	10.18	9.370 to 11.00	Yes	****	< 0.0001	G-N
cpc-2 gnb-1 vs. cpc-2 gna-1	-0.4388	-1.252 to 0.3746	No	ns	0.287	H-I
cpc-2 gnb-1 vs. cpc-2 gna-2	1.62	0.8066 to 2.433	Yes	***	0.0001	H-J
cpc-2 gnb-1 vs. cpc-2 gna-3	2.783	1.969 to 3.596	Yes	****	< 0.0001	H-K
cpc-2 gnb-1 vs. cpc-2 gna-1*	3.328	2.515 to 4.141	Yes	****	< 0.0001	H-L
cpc-2 gnb-1 vs. cpc-2 gna-2*	1.363	0.5498 to 2.176	Yes	**	0.0012	H-M
cpc-2 gnb-1 vs. cpc-2 gna-3*	10.34	9.531 to 11.16	Yes	****	< 0.0001	H-N
cpc-2 gna-1 vs. cpc-2 gna-2	2.059	1.245 to 2.872	Yes	****	< 0.0001	I-J
cpc-2 gna-1 vs. cpc-2 gna-3	3.221	2.408 to 4.035	Yes	****	< 0.0001	I-K
cpc-2 gna-1 vs. cpc-2 gna-1*	3.767	2.954 to 4.580	Yes	****	< 0.0001	I-L
cpc-2 gna-1 vs. cpc-2 gna-2*	1.802	0.9885 to 2.615	Yes	****	< 0.0001	I-M
cpc-2 gna-1 vs. cpc-2 gna-3*	10.78	9.970 to 11.60	Yes	****	< 0.0001	I-N
cpc-2 gna-2 vs. cpc-2 gna-3	1.163	0.3491 to 1.976	Yes	**	0.0056	J-K
cpc-2 gna-2 vs. cpc-2 gna-1*	1.708	0.8948 to 2.521	Yes	****	< 0.0001	J-L
cpc-2 gna-2 vs. cpc-2 gna-2*	-0.2569	-1.070 to 0.5565	No	ns	0.5323	J-M
cpc-2 gna-2 vs. cpc-2 gna-3*	8.725	7.911 to 9.538	Yes	****	< 0.0001	J-N
cpc-2 gna-3 vs. cpc-2 gna-1*	0.5456	-0.2677 to 1.359	No	ns	0.1862	K-L
cpc-2 gna-3 vs. cpc-2 gna-2*	-1.419	-2.233 to -0.6060	Yes	***	0.0008	K-M
cpc-2 gna-3 vs. cpc-2 gna-3*	7.562	6.749 to 8.375	Yes	****	< 0.0001	K-N
cpc-2 gna-1* vs. cpc-2 gna-2*	-1.965	-2.778 to -1.152	Yes	****	< 0.0001	L-M
cpc-2 gna-1* vs. cpc-2 gna-3*	7.016	6.203 to 7.830	Yes	****	< 0.0001	L-N
cpc-2 gna-2* vs. cpc-2 gna-3*	8.981	8.168 to 9.795	Yes	****	< 0.0001	M-N

References

1. Bock A, Kostenis E, Trankle C, Lohse MJ, Mohr K. 2014. Pilot the pulse: controlling the multiplicity of receptor dynamics. Trends Pharmacol Sci 35:630-638.

2. Chini B, Parenti M, Poyner DR, Wheatley M. 2013. G-protein-coupled receptors: from structural insights to functional mechanisms. Biochem Soc Trans 41:135-6.

3. Tesmer JJ. 2010. The quest to understand heterotrimeric G protein signaling. Nat Struct Mol Biol 17:650-2.

4. Selker EU. 2011. Neurospora. Curr Biol 21:R139-40.

5. Borkovich KA, Alex LA, Yarden O, Freitag M, Turner GE, Read ND, Seiler S, Bell-Pedersen D, Paietta J, Plesofsky N, Plamann M, Goodrich-Tanrikulu M, Schulte U, Mannhaupt G, Nargang FE, Radford A, Selitrennikoff C, Galagan JE, Dunlap JC, Loros JJ, Catcheside D, Inoue H, Aramayo R, Polymenis M, Selker EU, Sachs MS, Marzluf GA, Paulsen I, Davis R, Ebbole DJ, Zelter A, Kalkman ER, O'Rourke R, Bowring F, Yeadon J, Ishii C, Suzuki K, Sakai W, Pratt R. 2004. Lessons from the genome sequence of *Neurospora crassa*: tracing the path from genomic blueprint to multicellular organism. Microbiol Mol Biol Rev 68:1-108.

6. Cabrera IE, Pacentine IV, Lim A, Guerrero N, Krystofova S, Li L, Michkov AV, Servin JA, Ahrendt SR, Carrillo AJ, Davidson LM, Barsoum AH, Cao J, Castillo R, Chen WC, Dinkchian A, Kim S, Kitada SM, Lai TH, Mach A, Malekyan C, Moua TR, Torres CR, Yamamoto A, Borkovich KA. 2015. Global analysis of predicted G Protein-Coupled Receptor genes in the filamentous fungus, *Neurospora crassa*. G3 (Bethesda) 5:2729-43.

7. Li L, Wright SJ, Krystofova S, Park G, Borkovich KA. 2007. Heterotrimeric G protein signaling in filamentous fungi. Annu Rev Microbiol 61:423-52.

8. Wright SJ, Inchausti R, Eaton CJ, Krystofova S, Borkovich KA. 2011. RIC8 is a guanine-nucleotide exchange factor for Galpha subunits that regulates growth and development in *Neurospora crassa*. Genetics 189:1-12.

9. Li L, Borkovich KA. 2006. GPR-4 is a predicted G-protein-coupled receptor required for carbon source-dependent asexual growth and development in Neurospora crassa. Eukaryot Cell 5:1287-300.

10. Kim H, Wright SJ, Park G, Ouyang S, Krystofova S, Borkovich KA. 2012. Roles for receptors, pheromones, G proteins, and mating type genes during sexual reproduction in Neurospora crassa. Genetics 190:1389-404.

11. Krystofova S, Borkovich KA. 2006. The predicted G-protein-coupled receptor GPR-1 is required for female sexual development in the multicellular fungus *Neurospora crassa*. Eukaryot Cell 5:1503-16.

12. Turner GE, Borkovich KA. 1993. Identification of a G protein alpha subunit from *Neurospora crassa* that is a member of the G_i family. J Biol Chem 268:14805-11.

13. Kays AM, Rowley PS, Baasiri RA, Borkovich KA. 2000. Regulation of conidiation and adenylyl cyclase levels by the Galpha protein GNA-3 in Neurospora crassa. Mol Cell Biol 20:7693-705.

14. Adams DR, Ron D, Kiely PA. 2011. RACK1, A multifaceted scaffolding protein: Structure and function. Cell Commun Signal 9:22.

15. Ron D, Chen CH, Caldwell J, Jamieson L, Orr E, Mochly-Rosen D. 1994. Cloning of an intracellular receptor for protein kinase C: a homolog of the beta subunit of G proteins. Proc Natl Acad Sci U S A 91:839-43.

16. Lopez-Bergami P, Habelhah H, Bhoumik A, Zhang W, Wang LH, Ronai Z. 2005. RACK1 mediates activation of JNK by protein kinase C [corrected]. Mol Cell 19:309-20.

17. Chen S, Dell EJ, Lin F, Sai J, Hamm HE. 2004. RACK1 regulates specific functions of Gbetagamma. J Biol Chem 279:17861-8.

18. Sengupta J, Nilsson J, Gursky R, Spahn CM, Nissen P, Frank J. 2004. Identification of the versatile scaffold protein RACK1 on the eukaryotic ribosome by cryo-EM. Nat Struct Mol Biol 11:957-62.

19. Zeller CE, Parnell SC, Dohlman HG. 2007. The RACK1 ortholog Asc1 functions as a G-protein beta subunit coupled to glucose responsiveness in yeast. J Biol Chem 282:25168-76.

20. Palmer DA, Thompson JK, Li L, Prat A, Wang P. 2006. Gib2, a novel Gbeta-like/RACK1 homolog, functions as a Gbeta subunit in cAMP signaling and is essential in Cryptococcus neoformans. J Biol Chem 281:32596-605.

21. Li G, Zhang X, Tian H, Choi YE, Tao WA, Xu JR. 2017. MST50 is involved in multiple MAP kinase signaling pathways in Magnaporthe oryzae. Environ Microbiol 19:1959-1974.

22. Yin Z, Zhang X, Wang J, Yang L, Feng W, Chen C, Gao C, Zhang H, Zheng X, Wang P, Zhang Z. 2018. MoMip11, a MoRgs7-interacting protein, functions as a scaffolding protein to regulate cAMP signaling and pathogenicity in the rice blast fungus Magnaporthe oryzae. Environ Microbiol 20:3168-3185.

23. Nunez A, Franco A, Madrid M, Soto T, Vicente J, Gacto M, Cansado J. 2009. Role for RACK1 orthologue Cpc2 in the modulation of stress response in fission yeast. Mol Biol Cell 20:3996-4009.

24. Hoffmann B, Wanke C, Lapaglia SK, Braus GH. 2000. c-Jun and RACK1 homologues regulate a control point for sexual development in Aspergillus nidulans. Mol Microbiol 37:28-41.

25. Cai ZD, Chai YF, Zhang CY, Qiao WR, Sang H, Lu L. 2015. The Gbeta-like protein CpcB is required for hyphal growth, conidiophore morphology and pathogenicity in Aspergillus fumigatus. Fungal Genet Biol 81:120-31.

26. Wang L, Berndt P, Xia X, Kahnt J, Kahmann R. 2011. A seven-WD40 protein related to human RACK1 regulates mating and virulence in Ustilago maydis. Mol Microbiol 81:1484-98.

27. Kruger D, Koch J, Barthelmess IB. 1990. cpc-2, a new locus involved in general control of amino acid synthetic enzymes in Neurospora crassa. Curr Genet 18:211-5.

28. Barthelmess IB, Kolanus J. 1990. The range of amino acids whose limitation activates general amino-acid control in Neurospora crassa. Genet Res 55:7-12.

29. Muller F, Kruger D, Sattlegger E, Hoffmann B, Ballario P, Kanaan M, Barthelmess IB. 1995. The cpc-2 gene of Neurospora crassa encodes a protein entirely composed of WD-repeat segments that is involved in general amino acid control and female fertility. Mol Gen Genet 248:162-73.

30. Paluh JL, Orbach MJ, Legerton TL, Yanofsky C. 1988. The cross-pathway control gene of Neurospora crassa, cpc-1, encodes a protein similar to GCN4 of yeast and the DNA-binding domain of the oncogene v-jun-encoded protein. Proc Natl Acad Sci U S A 85:3728-32.

31. Sattlegger E, Hinnebusch AG, Barthelmess IB. 1998. cpc-3, the Neurospora crassa homologue of yeast GCN2, encodes a polypeptide with juxtaposed eIF2alpha kinase and histidyl-tRNA synthetase-related domains required for general amino acid control. J Biol Chem 273:20404-16.

32. McCluskey K, Wiest A, Plamann M. 2010. The Fungal Genetics Stock Center: a repository for 50 years of fungal genetics research. J Biosci 35:119-26.

33. Vogel HJ. 1964. Distribution of lysine pathways among fungi: Evolutionary implications. Am Nat 98:435-446.

34. Westergaard M, Mitchell HK. 1947. Neurospora V. A synthetic medium favoring sexual reproduction. Amer J Bot 34:573-577.

35. Davis RH, deSerres FJ. 1970. Genetic and microbiological research techniques for *Neurospora crassa*. Methods Enzymol 71A:79-143.

36. Spatafora JW, Aime MC, Grigoriev IV, Martin F, Stajich JE, Blackwell M. 2017. The Fungal Tree of Life: from Molecular Systematics to Genome-Scale Phylogenies. Microbiol Spectr 5.

37. Stajich JE, Harris T, Brunk BP, Brestelli J, Fischer S, Harb OS, Kissinger JC, Li W, Nayak V, Pinney DF, Stoeckert CJ, Jr., Roos DS. 2012. FungiDB: an integrated functional genomics database for fungi. Nucleic Acids Res 40:D675-81.

38. Lemoine F, Correia D, Lefort V, Doppelt-Azeroual O, Mareuil F, Cohen-Boulakia S, Gascuel O. 2019. NGPhylogeny.fr: new generation phylogenetic services for non-specialists. Nucleic Acids Res 47:W260-W265.

39. Katoh K, Standley DM. 2013. MAFFT multiple sequence alignment software version 7: improvements in performance and usability. Mol Biol Evol 30:772-80.

40. Criscuolo A, Gribaldo S. 2010. BMGE (Block Mapping and Gathering with Entropy): a new software for selection of phylogenetic informative regions from multiple sequence alignments. BMC Evol Biol 10:210.

41. Lefort V, Desper R, Gascuel O. 2015. FastME 2.0: A Comprehensive, Accurate, and Fast Distance-Based Phylogeny Inference Program. Mol Biol Evol 32:2798-800.

42. Letunic I, Bork P. 2019. Interactive Tree Of Life (iTOL) v4: recent updates and new developments. Nucleic Acids Res 47:W256-W259.

43. Ghosh A, Servin JA, Park G, Borkovich KA. 2014. Global analysis of serine/threonine and tyrosine protein phosphatase catalytic subunit genes in *Neurospora crassa* reveals interplay between phosphatases and the p38 mitogen-activated protein kinase. G3 (Bethesda) 4:349-65.

44. Avalos J, Geever RF, Case ME. 1989. Bialaphos resistance as a dominant selectable marker in Neurospora crassa. Curr Genet 16:369-72.

45. Pall M. 1993. The use of Ignite (basta; glufosinate; phosphinothricin) to select transformants of *bar*-containing plasmids in *Neurospora crassa*. Fungal Genet Newsl 40:57.

46. Perkins D. 1985. Advantages of using the inactive-mating-type a^{m1} strain as a helper component in heterokaryons. Neurospora Newslett 31:41-42.

47. Kuck U, Hoff B. 2006. Application of the nourseothricin acetyltransferase gene (*nat1*) as dominant marker for the transformation of filamentous fungi. Fungal Genet Newsl 53:9-11.

48. Christianson TW, Sikorski RS, Dante M, Shero JH, Hieter P. 1992. Multifunctional yeast high-copy-number shuttle vectors. Gene 110:119-22.

49. Colot HV, Park G, Turner GE, Ringelberg C, Crew CM, Litvinkova L, Weiss RL, Borkovich KA, Dunlap JC. 2006. A high-throughput gene knockout procedure for Neurospora reveals functions for multiple transcription factors. Proc Natl Acad Sci U S A 103:10352-7.

50. Winston F, Dollard C, Ricupero-Hovasse SL. 1995. Construction of a set of convenient Saccharomyces cerevisiae strains that are isogenic to S288C. Yeast 11:53-5.

51. Won S, Michkov AV, Krystofova S, Garud AV, Borkovich KA. 2012. Genetic and physical interactions between Galpha subunits and components of the Gbetagamma dimer of heterotrimeric G proteins in *Neurospora crassa*. Eukaryot Cell 11:1239-48.

52. Ivey FD, Hodge PN, Turner GE, Borkovich KA. 1996. The Galphai homologue *gna-1* controls multiple differentiation pathways in *Neurospora crassa*. Mol Biol Cell 7:1283-97.

53. Ebbole DJ, Sachs MS. 1990. A rapid and simple method for isolation of *Neurospora crassa* homokaryons using microconidia. Fungal Genet Newsl 37:17-18.

54. Ouyang S, Beecher CN, Wang K, Larive CK, Borkovich KA. 2015. Metabolic impacts of using nitrogen and copper-regulated promoters to regulate gene expression in *Neurospora crassa*. G3 (Bethesda) 5:1899-908.

55. Freitag M, Hickey PC, Raju NB, Selker EU, Read ND. 2004. GFP as a tool to analyze the organization, dynamics and function of nuclei and microtubules in *Neurospora crassa*. Fungal Genet Biol 41:897-910.

56. Park G, Servin JA, Turner GE, Altamirano L, Colot HV, Collopy P, Litvinkova L, Li L, Jones CA, Diala FG, Dunlap JC, Borkovich KA. 2011. Global analysis of serine-threonine protein kinase genes in *Neurospora crassa*. Eukaryot Cell 10:1553-64.

57. Krystofova S, Borkovich KA. 2005. The heterotrimeric G-protein subunits GNG-1 and GNB-1 form a Gbetagamma dimer required for normal female fertility, asexual development, and galpha protein levels in Neurospora crassa. Eukaryot Cell 4:365-78.

58. Baasiri RA, Lu X, Rowley PS, Turner GE, Borkovich KA. 1997. Overlapping functions for two G protein alpha subunits in *Neurospora crassa*. Genetics 147:137-45.

59. Yang Q, Poole SI, Borkovich KA. 2002. A G-protein beta subunit required for sexual and vegetative development and maintenance of normal G alpha protein levels in *Neurospora crassa*. Eukaryot Cell 1:378-90.

60. Turner GE. 2011. Phenotypic analysis of *Neurospora crassa* gene deletion strains. Methods Mol Biol 722:191-8.

61. Eaton CJ, Cabrera IE, Servin JA, Wright SJ, Cox MP, Borkovich KA. 2012. The guanine nucleotide exchange factor RIC8 regulates conidial germination through Galpha proteins in *Neurospora crassa*. PLoS One 7:e48026.

62. Borkovich KA, Weiss RL. 1987. Purification and characterization of arginase from *Neurospora crassa*. J Biol Chem 262:7081-6.

63. Hager KM, Mandala SM, Davenport JW, Speicher DW, Benz EJ, Jr., Slayman CW. 1986. Amino acid sequence of the plasma membrane ATPase of Neurospora crassa: deduction from genomic and cDNA sequences. Proc Natl Acad Sci U S A 83:7693-7.

64. Corrochano LM, Kuo A, Marcet-Houben M, Polaino S, Salamov A, Villalobos-Escobedo JM, Grimwood J, Alvarez MI, Avalos J, Bauer D, Benito EP, Benoit I, Burger G, Camino LP, Canovas D, Cerda-Olmedo E, Cheng JF, Dominguez A, Elias M, Eslava AP, Glaser F, Gutierrez G, Heitman J, Henrissat B, Iturriaga EA, Lang BF, Lavin JL, Lee SC, Li W, Lindquist E, Lopez-Garcia S, Luque EM, Marcos AT, Martin J, McCluskey K, Medina HR, Miralles-Duran A, Miyazaki A, Munoz-Torres E, Oguiza JA, Ohm RA, Olmedo M, Orejas M, Ortiz-Castellanos L, Pisabarro AG, Rodriguez-Romero J, Ruiz-Herrera J, Ruiz-Vazquez R, Sanz C, Schackwitz W, et al. 2016. Expansion of Signal Transduction Pathways in Fungi by Extensive Genome Duplication. Curr Biol 26:1577-1584.

65. Kim H, Borkovich KA. 2004. A pheromone receptor gene, *pre-1*, is essential for mating type-specific directional growth and fusion of trichogynes and female fertility in *Neurospora crassa*. Mol Microbiol 52:1781-98.

66. Kays AM, Borkovich KA. 2004. Severe impairment of growth and differentiation in a *Neurospora crassa* mutant lacking all heterotrimeric Galpha proteins. Genetics 166:1229-40.

67. Park G, Colot HV, Collopy PD, Krystofova S, Crew C, Ringelberg C, Litvinkova L, Altamirano L, Li L, Curilla S, Wang W, Gorrochotegui-Escalante N, Dunlap JC, Borkovich KA. 2011. High-throughput production of gene replacement mutants in *Neurospora crassa*. Methods Mol Biol 722:179-89.

68. Springer ML. 1993. Genetic control of fungal differentiation: the three sporulation pathways of *Neurospora crassa*. Bioessays 15:365-74.

69. Cortat M, Turian G. 1974. Conidiation of *Neurospora crassa* in submerged culture without mycelial phase. Arch Mikrobiol 95:305-9.

70. That TC, Turian G. 1978. Ultrastructural study of microcyclic macroconidiation in *Neurospora crassa*. Arch Microbiol 116:279-88.

71. Plesofsky-Vig N, Light D, Brambl R. 1983. Paedogenetic Conidiation in *Neurospora crassa*. Exp Mycol 7:283-286.

72. Guignard R, Grange F, Turian G. 1984. Microcycle Conidiation Induced by Partial Nitrogen Deprivation in *Neurospora crassa*. Canadian Journal of Microbiology 30:1210-1215.

73. Madi L, McBride SA, Bailey LA, Ebbole DJ. 1997. *rco-3*, a gene involved in glucose transport and conidiation in *Neurospora crassa*. Genetics 146:499-508.

74. Ivey FD, Kays AM, Borkovich KA. 2002. Shared and independent roles for a Galpha(i) protein and adenylyl cyclase in regulating development and stress responses in *Neurospora crassa*. Eukaryot Cell 1:634-42.

75. Metzenberg RL, Glass NL. 1990. Mating type and mating strategies in Neurospora. Bioessays 12:53-9.

76. Randall TA, Metzenberg RL. 1995. Species-specific and mating type-specific DNA regions adjacent to mating type idiomorphs in the genus Neurospora. Genetics 141:119-36.

77. Raju NB. 2009. Neurospora as a model fungus for studies in cytogenetics and sexual biology at Stanford. J Biosci 34:139-59.

78. Xu BE, Kurjan J. 1997. Evidence that mating by the *Saccharomyces cerevisiae gpa1Val50* mutant occurs through the default mating pathway and a suggestion of a role for ubiquitin-mediated proteolysis. Mol Biol Cell 8:1649-64.

79. Schauber C, Chen L, Tongaonkar P, Vega I, Madura K. 1998. Sequence elements that contribute to the degradation of yeast G alpha. Genes Cells 3:307-19.

Chapter 3: Heterotrimeric G-Protein Signaling is Required for Cellulose Degradation in *Neurospora crassa*

Logan Collier, Arit Ghosh and Katherine A. Borkovich

Contributions to this Chapter

This chapter was published in MBio (Collier LA, Ghosh A, Borkovich KA. 2020. Heterotrimeric G-Protein Signaling Is Required for Cellulose Degradation in Neurospora crassa. mBio 11:6). I performed the experiments for this work and wrote the manuscript as well. Katherine Borkovich and Arit Ghosh discussed experimental design and instructed me on how to perform the experiments in this work. Katherine also extensively edited the manuscript for this chapter into the current version.

Abstract

The filamentous fungus *Neurospora crassa* decomposes lignocellulosic biomass to generate soluble sugars as carbon sources. In this study, we investigated a role for heterotrimeric G-protein signaling in cellulose degradation. Loss of the Gα subunits *gna-1* and *gna-3,* the Gβ subunits *gnb-1* and *cpc-2,* the Gγ *gng-1,* or the downstream effector adenylyl cyclase (*cr-1*) resulted in loss of detectable cellulase activity. This defect was also observed in strains expressing a constitutively active version of *gna-3* (*gna-3*^{Q208L}). We found that GNA-1 levels are greatly reduced in Δ*gna-3,* Δ*gnb-1,* and Δ*gng-1* strains, likely contributing to

cellulase defects in these genetic backgrounds. The observation that *gna-3*^{Q208L} Δ*gnb-1* strains exhibit cellulase activity, despite greatly reduced levels of GNA-1 protein, is consistent with positive control of cellulase production by GNA-3 that is manifested in the absence of *gnb-1*. Expression patterns for five cellulase genes showed that Δ*gna-1,* Δ*gnb-1*, and Δ*gna-3* mutants produce less cellulase mRNA than wild type, consistent with transcriptional regulation. Δ*cpc-2* mutants had wild-type levels of cellulase transcripts, suggesting post-transcriptional control. In contrast, results for Δ*cr-1* mutants support both transcriptional and post-transcriptional control of cellulase activity by cAMP signaling. Cellulase activity defects in Δ*gna-3* mutants were fully remediated by cAMP supplementation, consistent with GNA-3 operating upstream of cAMP signaling. In contrast, cAMP addition only partially corrected cellulase activity defects in Δ*gna-1* and Δ*gnb-1* mutants, suggesting participation of GNA-1 and GNB-1 in additional cAMP-independent pathways that control cellulase activity.

Importance

Filamentous fungi are critical for recycling of plant litter in the biosphere by degrading lignocellulosic biomass into simpler compounds for metabolism. Both saprophytic and pathogenic fungi utilize plant cell wall degrading enzymes to liberate carbon for metabolism. Several studies have demonstrated a role for cellulase enzymes during infection of economically relevant crops by fungal pathogens. Especially in the third world, severe plant disease means loss of entire crops, sometimes leading to starvation. In this study, we demonstrate that G-protein signaling is a key component of cellulase production. Therefore, understanding the role of G-protein signaling in regulation of the unique metabolism of cellulose by these organisms can inform innovations in strain engineering of industrially relevant species for biofuel production and in combatting food shortages caused by plant pathogens.

Introduction

The cell walls of all plants are primarily composed of lignocellulosic biomass, making it the most abundant biological composite produced on earth (1). In agricultural processes, this material is considered a waste byproduct, but it is commonly used as feedstock for production of alternative fuel sources (2, 3). Secreted enzymes from filamentous fungi are used to degrade lignocellulose polymers. Optimizing fungal platforms for greater enzyme production is a major bottleneck to cost-efficient biofuels (4). Additionally, numerous fungal species are plant pathogens that decimate crops (5) and several studies have demonstrated a role for cellulase enzymes during infection (rev. in (6)). Understanding the pathways of carbon sensing in these organisms will have significant implications in the optimization of agricultural methods and fuel production.

Fungi differentially regulate enzymes for catabolism of specific carbon polymers. For example, in *Neurospora crassa* and *Aspergillus nidulans,* cellulose-specific regulons have been well characterized (7). Studies in *Trichoderma reesei,* several *Aspergillus* species, and *N. crassa* indicate that cellobiose, a break-down product of cellulose, is the inducer of cellulolytic genes (8), demonstrating that some cellulose deconstruction is required prior to full cellulase induction. In many fungal species, glucose sensing activates the transcription factor CRE-1, preventing induction of cellulolytic genes in a process called carbon catabolite repression (CCR) (2, 7, 9). Derepression of CRE-1

allows expression of the transcription factor CLR-1, leading to transcription of CLR-2, which activates transcription of most cellulolytic genes (7, 10, 11).

Genes that are induced via disruption of the CCR response and the presence of cellobiose are part of the plant cell wall degradation network (12). In this network, carbohydrate-active enzymes (CAZymes) that degrade cellulose are termed cellulases. These can be categorized into several classes, including cellobiohydrolases, endoglucanases, β-glucosidases, polysaccharide monooxygenases, and cellobiose dehydrogenases, each of which play a specific role in cleaving β-1,4-linkages present in cellulose (rev. in (1)).

Filamentous fungi use heterotrimeric G-proteins and membrane-associated G-protein coupled receptors (GPCRs) to sense and respond to their environment (13, 14). G-proteins consist of α, β, and γ subunits, with the βγ subunits tightly associated (15-17). G-protein signaling begins with GPCR activation by a ligand, causing the GPCR to facilitate exchange of GDP for GTP on the Gα subunit. This causes dissociation of the Gα from the βγ dimer, allowing both to signal downstream effectors. *N. crassa* uses G-proteins to regulate basal hyphae growth, sexual development, asexual sporulation, and stress responses (13, 18-23). *N. crassa* possesses three Gα proteins (GNA-1, GNA-2, and GNA-3) (24), two Gβ proteins (GNB-1 and CPC-2) (25), and a Gγ that associates with GNB-1 (GNG-1) (26). *N. crassa* also has two Protein Kinase A (PKA) catalytic subunits (27, 28) that are predicted downstream targets of cAMP produced by the adenylyl cyclase CR-1 (29). Previous studies have shown that CR-1 is an

effector of G-protein signaling in *N. crassa*, with GNA-1 regulating GTP-stimulated CR-1 enzyme activity (30), and GNA-3 controlling CR-1 protein levels (21).

The three *N. crassa* Gα subunits are required for carbon sensing (22, 31), but have not been implicated in cellulose degradation. In *T. reesei*, constitutive activation of the *gna-3* homolog results in cellulase expression in constant light (32), while deletion of the homologous *gna-1* gene leads to increased cellulase expression in darkness (33). In *A. nidulans*, deletion of *pkaA* results in an inability to localize CreA to the nucleus, causing mis-regulation of CCR and induction of hydrolytic enzymes on glucose medium (11). Recent work in *N. crassa* and *Myceliopththora thermophila* showed that the CLR-4 transcription factor binds to the promoter region of *cr-1* in both fungi. Loss of *clr-4* resulted in down-regulation of *cr-1* and cellulase genes and strains overexpressing the *cr-1* open reading frame exhibited a 3-20 fold increase in cellulase mRNA levels (34), implicating cAMP signaling in regulation of cellulase gene expression.

In a recent study, we analyzed phenotypes for mutants lacking 21 of the known Pth11-like GPCRs in *N. crassa.* Three mutants exhibited growth phenotypes when cultured on medium containing Avicel (crystalline cellulose) (35). Pth11 is required for pathogenicity on rice (*Oryza sativa*) by *Magnaporthe oryzae* (36). This GPCR physically interacts with MagA (a Gα homologous to GNA-3) and adenylyl cyclase during early stages of pathogenesis (37). A recent investigation showed that two *Fusarium graminearum* Pth11-like proteins

required for virulence against wheat interact with Gα proteins when expressed in yeast (38). These findings support interaction between Pth11-like GPCRs and heterotrimeric G-proteins in filamentous fungi.

Our previous work showing Pth11-like GPCRs influence growth of *N. crassa* on Avicel prompted investigation into the role that G-proteins play in cellulose sensing and degradation in *N. crassa*. In this study, we embarked on a systematic analysis of cellulose phenotypes for all known G-protein subunits and adenylyl cyclase. For this work, we utilized deletion mutants for all six G-protein subunits (24, 25, 39) and strains expressing constitutively activated, GTPase-deficient versions of each Gα subunit gene (40) (*gna-1*^{Q204L}*, gna-2*^{Q205L}*, gna-3*^{Q208L}; Table 3.S1). Our results provide evidence for transcriptional, post-transcriptional and cAMP-dependent and independent control of cellulase enzymes via G-protein signaling in *N. crassa.*

Materials and methods

Media and strains.

The strains used in this study are indicated in Table 3.S1, and strain construction is described in the Supplemental Methods. Strains were cultured on Vogel's Minimal Medium [VM, (41)], with the exception that the indicated carbon source replaced sucrose. All carbon sources were used at a final concentration of 2% (weight/volume). Alternative carbon sources were crystalline cellulose (Avicel-PH101, 50 µm particle; Sigma-Aldrich, St. Louis, MO), glucose (MP Biomedicals, Santa Ana, CA) or no carbon source. Where indicated, cAMP (Sigma Aldrich, #A6885) was added at a final concentration of 3 mM to medium after autoclaving. Macroconidia (conidia) or packed hyphae used for inoculation of cultures were obtained as described (25).

Isolation of culture supernatants, cellulase and protein assays and western analysis.

Cultures were inoculated with conidia at a final concentration of 1 x 10^6 cells/mL in 25 mL VM-Glucose and grown for 16 h at 25˚C in constant light with shaking at 200 rpm. Cell pads were harvested via centrifugation at 5000 rpm at 20˚C for 5 min, and the supernatant was removed (Avanti J26XP, JS-5.3 Rotor, Beckman Coulter). Cell pads were resuspended in 25 mL VM with no carbon source and centrifuged again. This wash step was repeated once. The cell pads

were then resuspended in 25 mL VM-Avicel and transferred to a new sterile flask. The cultures were incubated at 25˚C for three days in constant light with shaking at 200 rpm. The cultures were then centrifuged at 5000 rpm at 20˚C for 5 min, and the supernatant was separated from the cell pad. Cells were removed from culture supernatants by passage through a 0.45 µm filter and the filtrate was used for assay of protein concentration and cellulase activity. For SDS-PAGE, one mL of supernatant sample was concentrated to 200 µL (Amicon Ultra 4 Centrifugal Filter Unit, MilliporeSigma, Burlington, MA) and 20 µL was loaded on a 10% SDS PAGE gel. Gels were stained with GelCode Blue (Thermo Fisher Scientific).

A coupled enzyme assay was used (42) to quantify the ability of the culture supernatants to convert cellulose into glucose. Units are expressed as nmol of glucose produced/µL of supernatant. Protein concentration was determined for the supernatant samples using the Pierce Bicinchoninic Acid (BCA) Protein Assay (Thermo Fisher Scientific, Chino, CA) with BSA as the standard. The cellulase activity and protein concentration in the supernatants was normalized to the amount of protein in the cell pad. Extraction of cell pad protein is described in the Supplemental Methods.

Cell disruption and isolation of whole cell extracts and the membrane particulate fraction for western analysis is described in the Supplemental Methods. Equal amounts of protein were electrophoresed using 10% SDS-PAGE gels and blotted to nitrocellulose as previously described (26). Primary antibodies (25, 39, 40, 43, 44) were used at a 1:1000 dilution. Incubation with secondary antibody and chemiluminescent detection was as previously described (26).

Total RNA isolation and quantitative reverse-transcriptase-PCR (qRT-PCR).

Cultures were grown in VM Glucose for 12 h at 25°C in constant light with shaking at 200 rpm and washed with VM No Carbon as described above. After washing, cell pads were transferred to VM Avicel and incubated at 25°C for 4 h in constant light with shaking at 200 rpm. Methods for cell collection, mRNA extraction, production of cDNA and qRT-PCR are described in the Supplemental Methods. Three biological replicates, each with three technical replicates were tested for each strain, for a total of nine determinations/gene transcript. The primers used for qRT-PCR are listed in Table 3.S2.

Results

Alteration of growth, cellulase activity and supernatant protein concentration in mutants cultured on Avicel.

We began our analysis of roles for G-proteins in cellulose degradation by growing strains in shaken liquid cultures containing Avicel using a previously described approach (42). This method relies on the observation that intact Avicel is insoluble and will sediment at the bottom of cultures after centrifugation. After three days wild type, Δ*gna-1*, and Δ*gna-2* strains appeared to have degraded the Avicel (Figure 3.S1). In contrast, cultures of Δ*gna-3,* Δ*gnb-1,* Δ*gng-1* and Δ*cpc-2*, mutants contained residual Avicel, suggesting that these G-protein subunits are required to degrade cellulose into soluble cellodextrins in *N. crassa*.

Mutants for both of the known PKA catalytic subunits in *N. crassa* were tested in preliminary experiments, with Δ*pkac-1* mutants containing residual Avicel during growth and Δ*pkac-2* mutants resembling wild type. These observations were supported by preliminary measurements of cellulase activity in cell-free supernatants from these two mutants. These results suggested that while PKAC-1 may be more important with regards to cellulase activity, there is some redundancy between the two catalytic subunits. We attempted to create a double mutant lacking both PKA catalytic subunit genes (28), but were unsuccessful. Therefore, we utilized the Δ*cr-1* mutant, which lacks intracellular cAMP (29, 41), to approximate loss of cAMP signaling in our study. The results

showed that Δ*cr-1* mutant cultures contained residual Avicel, implicating adenylyl cyclase and cAMP signaling in degradation of cellulose.

The most likely explanation for the reduced tissue formation observed in most of the mutants is reduced accumulation of cellulase enzymes. To address this possibility, we measured cellulase activity and protein concentration in cell-free supernatants from the strains. To help mitigate the mass accumulation issues observed after direct inoculation into VM-Avicel described above, we pre-grew cultures in VM-Glucose for 16 h and then transferred to VM-Avicel or to VM-Glucose for three days. We then collected cell-free supernatants for the assays and extracted and quantified the cell biomass protein in the cell pads. The cellulase activity and protein concentration in the supernatant samples were normalized to cell biomass protein, to account for possible growth defects due to the gene deletion.

We assessed cellulase activity in the cell-free supernatant samples using an *in vitro* coupled enzyme assay that detects glucose levels after incubation of samples with Avicel (42). Δ*gna-1,* Δ*gna-3,* Δ*gnb-1,* Δ*gng-1*, Δ*cpc-2,* Δ*cr-1*, and *gna-3*^{Q208L} strains had no detectable cellulase activity (Figure 3.1). The lack of cellulase activity in Δ*gna-1* culture supernatants contrasts with the ability of the mutant to degrade Avicel (Figure 3.S1). This may result from degradation of Avicel into smaller cellodextrins, but not completely to glucose. This result shows that loss of five of the six G-protein subunits or adenylyl cyclase has a profound effect on cellulase activity. The observation that loss or activation of *gna-3* results

in a similar phenotype is reminiscent of the relationship between the Gpa1p Gα and the Ste4p Gβ in *Saccharomyces cerevisiae* (45-47). By analogy, this suggests a regulatory circuit involving tethering between GNA-3 and the Gβγ dimer in *N. crassa*.

Protein measurements demonstrated that only three of the strains with undetectable cellulase activity had reduced extracellular protein relative to wild type after growth on Avicel: Δ*gna-3,* Δ*cr-1*, and *gna-3*^{Q208L} (Figure 3.1). Furthermore, the reduction in extracellular protein for these three strains (maximum ~55%) does not explain the loss of detectable cellulase activity. In contrast to the strains with severe cellulase defects, we observed that Δ*gna-2* and *gna-2*^{Q205L} strains had higher and lower levels, respectively, of extracellular protein on Avicel (Figure 3.1). The opposing results obtained for loss vs. activation of *gna-2* implicate GNA-2 as a negative regulator of supernatant protein accumulation on VM-Avicel.

To determine whether the protein accumulation defects observed in some strains on Avicel extended to growth on glucose, we compared results for these two carbon sources (Figure 3.S2). No strain had lower protein accumulation on glucose than wild type, and levels were actually elevated in Δ*cpc-2* mutants. Δ*gna-3,* Δ*gnb-1,* Δ*gng-1,* Δ*cpc-2,* Δ*cr-1,* and *gna-3*^{Q208L} strains accumulated less protein on VM-Avicel than on VM-Glucose. *gna-1*^{Q204L} strains had a slight increase in protein accumulation on Avicel relative to glucose.

To address the possibility that impaired glucose transport contributes to the mass accumulation defects of some mutants on Avicel, we performed the glucose detection assay with culture supernatants from glucose-grown cultures. None of the strains in this study had detectable glucose remaining in their supernatants after three days of growth on VM-Glucose, suggesting that either they have normal glucose transport or that three days is adequate for uptake of all glucose in the medium.

Previous work has demonstrated different protein banding patterns after subjecting cell-free supernatants of mutants impaired in cellulase production to SDS-PAGE (42, 48). To explore this possibility with our set of strains, we subjected equal volumes of the concentrated VM-Avicel supernatant samples to SDS-PAGE analysis (Figure 3.S3A). Several prominent bands were observed in wild type samples, with the most intense appearing at 70 kDa, the migration position of several cellulase enzymes (42). This band was excised from gels containing wild type samples and subjected to LC/MS (48). Among the identified proteins, cellobiohydrolase CBH-1 (NCU07340) was present in the largest amount (41% of the total; Figure 3.S3B), followed by the β-glucosidase GH3-4 (NCU04952; 13%) and the non-cell wall-anchored protein NCW-1 (NCU05137; 12%).

Inspection of the stained SDS-PAGE gels showed that levels of the 70kDa band were lowest in Δ*gna-1,* Δ*gna-3,* Δ*gnb-1* and *gna-3*^{Q208L} strains (Figure 3.S3A), consistent with loss of cellulase activity (Figure 3.1). Although Δ*gng-1*,

Δ*cpc-2* and Δ*cr-1* strains still produce a prominent band at 70 kDa (Figure 3.S3A), these strains lack detectable cellulase activity, suggesting that the cellulases are nonfunctional.

Overall, our results demonstrate that of the three Gα subunits, GNA-2 does not greatly influence cellulase activity. GNA-1 is required for activity, but constitutive activation does not lead to higher levels. Loss or activation of *gna-3* leads to reduced cellulase activity, suggesting a mechanism involving a tethering relationship between GNA-3 and the Gβγ dimer.

Levels of the Gα GNA-1 are reduced in Δ*gna-3,* Δ*gnb-1*, and Δ*gng-1* mutants.

The above results show that most of the G-protein subunits are required for *N. crassa* to efficiently degrade cellulose into glucose. We have shown previously that loss of the Gβγ dimer affects levels of Gα proteins and that mutation of *gna-1* or *gng-1* results in lower GNB-1 levels during growth on VM-Sucrose (24, 26). To investigate whether this is also the case for VM-Avicel, we isolated membrane fractions from VM-Avicel grown cell pads and used western blotting to determine levels of the different G-protein subunits. Since CPC-2 is cytoplasmic in *N. crassa* (25), whole cell extracts were used to determine protein levels in the various strains.

The results from western blot analysis demonstrate that as observed for sucrose, deletion of *gnb-1* or *gng-1* results in greatly reduced amounts of GNA-1 and GNA-2, and a slight decrease in GNA-3 levels during growth on Avicel (Figure 3.2). Additionally, levels of GNA-1 were significantly reduced in Δ*gna-3* mutants. GNB-1 was not detectable in Δ*gng-1* mutants and was diminished in Δ*gna-3* strains. CPC-2 does not appear to be affected by the other G-proteins, since levels were similar in all strains. Since GNA-1 and GNA-3 appear to positively regulate cellulase activity in *N. crassa,* reduced amounts of these Gα proteins may explain loss of cellulase activity in many strains (Figure 3.1). Taken together, the results show that *gna-3*, *gnb-1* and *gng-1* are most important for maintaining protein levels of the other subunits during Avicel growth.

Constitutive activation of GNA-1 or GNA-3 completely or partially overrides the effects of the Δ*gnb-1* mutation.

The observation that Δ*gnb-1* mutants lack detectable cellulase activity is consistent with *gnb-1* as a positive regulator. However, the negative influence of the Δ*gnb-1* mutation on Gα protein levels (Figure 3.2) suggested a more complex interaction. Furthermore, the absence of cellulase activity in the Δ*gna-3* and *gna-3*^{Q208L} strains supports negative regulation by *gnb-1*. We therefore investigated whether any of the three constitutively active Gα alleles could override the defects of the Δ*gnb-1* mutation. We examined cellulase activity and extracellular

protein levels in the strains, as well as the banding pattern of supernatant proteins during SDS-PAGE analysis (Figure 3.3A,B).

The Δ*gnb-1 gna-1*^{Q204L} strain resembled the *gna-1*^{Q204L} and wild type strains with regards to cellulase activity (Figure 3.3A). Additionally, the concentration and SDS-PAGE banding pattern of the extracellular proteins was similar to wild type. These results are consistent with a scenario in which *gna-1* is epistatic to *gnb-1* (Figure 3.3A,B).

Cellulase activity was not detected in the Δ*gnb-1* or Δ*gnb-1 gna-2*^{Q205L}strains, while the *gna-2*^{Q205L}strain was normal (Figure 3.3A). Although levels of extracellular protein were normal in the Δ*gnb-1 gna-2*^{Q205L}strain (Figure 3.3A), the SDS-PAGE protein banding pattern resembled Δ*gnb-1* (Figure 3.3B). The inability of the *gna-2*^{Q205L} allele to increase cellulase activity in the Δ*gnb-1* background supports GNB-1 operating downstream of GNA-2 (Figure 3.3A,B).

In contrast to the non-detectable levels in the Δ*gnb-1* and *gna-3*^{Q208L} strains, cellulase activity in the Δ*gnb-1 gna-3*^{Q208L} strain was significantly greater than in wild type (Figure 3.3A). Likewise, extracellular protein levels were higher than wild type (Figure 3.3A). The SDS-PAGE protein banding pattern resembled wild type, but was less intense (Figure 3.3B). These results suggest a positive role for GNA-3 in regulating cellulase activity that is normally masked by a negative regulatory activity for GNB-1.

To investigate the epistatic relationships further, we performed western analysis for GNA-1, GNA-2 and GNA-3 in this group of strains (Figure 3.3C). We found that the only strain with detectable levels of GNA-1 was Δ*gnb-1 gna-1*^{Q204L} (Figure 3.3C). The low levels of GNA-1 in the Δ*gnb-1 gna-2*^{Q205L} strain correlate with lack of activity in this background. GNA-3 appears to be the only Gα present in the Δ*gnb-1 gna-3*^{Q208L} strain (Figure 3.3C). This last observation, coupled with the high cellulase activity in the Δ*gnb-1 gna-3*^{Q208L} strain, further supports a model in which the positive action of GNA-3 on cellulase activity is impaired when GNB-1 is present.

Cellulase mRNA levels are reduced in Δ*gna-1,* Δ*gna-3* and Δ*gnb-1* mutants.

We next asked whether the defects observed in the single gene deletion mutants resulted from reduced cellulase gene expression. We assessed mRNA levels at 4 h after transfer to Avicel, to reflect early fluctuations in CCR and cellulase mRNA induction. We selected five well-characterized cellulase genes that are among the most highly expressed in wild type *N. crassa* (8) and encode the most abundant proteins in the cellulose secretome (48) for Quantitative Reverse-Transcriptase PCR (RT-qPCR). Three of the five genes also encode proteins that were constituents of the prominent 70 kDa band in wild type protein samples after SDS-PAGE (Figure 3.S3). *cbh-1* (NCU07340) and *gh6-2* (NCU09680) encode exo-β-1,4-glucanases, while *gh5-1* (NCU00762) corresponds to an endo-β-1,4-glucanase (12). *gh3-4* (NCU04952) encodes the

only β-glucosidase in the *N. crassa* genome with a predicted secretion signal (8). *cdh-1* (NCU00206) is the most highly expressed cellobiose dehydrogenase in *N. crassa* and its deletion results in a 37%-49% reduction in cellulase activity (49).

The results from qRT-PCR analysis demonstrated that relative to wild type, Δ*gna-1,* Δ*gna-3* and Δ*gnb-1* mutants expressed lower levels of mRNA for all five genes (Fig. 4). Δ*gna-1* strains exhibited an eight-fold decrease in *cbh-1* transcripts, a more than 10-fold difference in *gh6-2* and *gh5-1*, a four-fold decrease in *cdh-1*, and a seven-fold decrease in *gh3-4*. Δ*gna-3* strains had a three-fold reduction of mRNA for *cbh-1* and *gh6-2*, and a two-fold decrease in *gh5-1*, *cdh-1,* and *gh3-4*. Δ*gnb-1* strains had a three-fold decrease in *cbh-1* mRNA levels and a five-fold decrease in both *gh6-2* and *gh5-1*. In addition, this strain had no detectable message for *cdh-1* or *gh3-4* (Fig. 4 D, E). Δ*cr-1* mutants had a two-fold decrease in expression of *cbh-1*, but normal levels of *gh6-2*, *gh5-1*, *cdh-1*, and *gh3-4*. This implies that transcription of these four genes may be influenced by a non-cAMP-related target of G-protein signaling, since their mRNA levels are also reduced in Δ*gna-1,* Δ*gna-3,* and Δ*gnb-1* mutants. Δ*gna-2* and Δ*cpc-2* mutants had wild type levels of mRNA for most genes, with the exception of *cdh-1* and *gh3-4* that were expressed at levels 3-5 fold higher in Δ*cpc-2* mutants.

The findings from qRT-PCR analysis further support a positive regulatory role for GNA-1 and GNA-3 in control of cellulase activity. The low levels of mRNA for the five genes observed in Δ*gna-3* and Δ*gnb-1* mutants may be influenced by

the apparent absence of GNA-1 protein in both strains (Figure 3.2). *cpc-2* and *cr-1* appear to have posttranscriptional effects on expression of cellulase genes, since the corresponding mutants lack cellulase activity (Figure 3.1). Since the proteins appear to be made in these mutant backgrounds (Figure 3.1, 3.S3), these may affect posttranslational modification required for the cellulase enzymes to be functional(50, 51). It should be noted that since the time point selected for our study was early during cellulase induction, it is possible that levels of these mRNAs may be higher at later times after transfer to Avicel.

cAMP supplementation results in full rescue of Δ*gna-3* mutants and partial remediation of Δ*gna-1* and Δ*gnb-1* strains.

Δ*gna-1,* Δ*gna-3*, Δ*gnb-1* and Δ*cr-1* mutants exhibit defects in cAMP signaling on VM-Sucrose (21, 26, 30, 52), and we have previously shown that the defects of Δ*cr-1* and Δ*gna-3* mutants are partially corrected by exogenous cAMP. We investigated whether this was the case on VM-Avicel by supplementing the most affected strains with cAMP: Δ*gna-1*, Δ*gna-3*, *gna-3*^{Q208L}*,* Δ*gnb-1*, Δ*cpc-2* and Δ*cr-1*. Exogenous cAMP should bypass the missing signaling components and directly activate PKA (29).

cAMP supplementation resulted in higher cellulase activity and extracellular protein levels in wild type, consistent with a positive role for cAMP signaling (Fig. 5A). cAMP led to at least partial remediation in the other six strains (Fig. 5A). Δ*cr-1* mutants had cellulase activity greater than wild type and

Δ*gna-3* mutants were restored to wild type levels. Although cAMP did not fully correct phenotypes in Δ*gna-1, gna-3*^{Q208L} and Δ*gnb-1* strains (73%, 17% and 53% of wild type, respectively; compare Figure 3.1 and Fig. 5A), no cellulase activity was detectable in these strains without exogenous cAMP (Figure 3.1). Furthermore, the partial complementation using cAMP observed in these three strains supports a cAMP-independent pathway that contributes to cellulase activity.

Addition of cAMP led to increased extracellular protein levels for Δ*gna-3,* Δ*cr-1,* and *gna-3*^{Q208L} strains, while a decrease was observed in Δ*gna-1* and Δ*gnb-1* mutants (See Figure 3.S4 for comparison of supernatant protein concentration +/- cAMP). SDS-PAGE analysis of supernatant samples demonstrated that cAMP supplementation restored many of the bands present in wild type to Δ*gna-1,* Δ*gna-3, gna-3*^{Q208L}*,* Δ*gnb-1* and Δ*cr-1* strains (compare Figure 3S3A to Figure 3.5B).

We next asked whether cAMP supplementation restored expression of the five cellulase genes analyzed in Fig. 4 in Δ*gna-1,* Δ*gna-3*, Δ*gnb-1*, and Δ*cr-1* strains. We again used a time point early after transfer to Avicel (4 h). Due to the increased cellulase activity observed in wild type after cAMP treatment, we utilized wild type without supplementation as the control. The results showed that Δ*gna-1* strains had increased levels for all five cellulase mRNAs, with those for *cdh-1* and *gh3-4* restored to that of unsupplemented wild type (compare Fig. 4 to Figure 3.6). Levels of four mRNAs resembled those of wild type in Δ*gna-3*

mutants, and *cbh-1* levels were increased over those in cultures without added cAMP (Figure 3.6). cAMP addition did not restore cellulase mRNA levels in Δ*gnb-1* mutants to those in wild type but did result in detectable amounts of *cdh-1* and *gh3-4* mRNAs (Figure 3.6). Transcript levels for Δ*cr-1* strains were similar to wild type for *cbh-1*, and levels of *cdh-1* and *gh3-4* were elevated (Figure 3.6).

Some hypotheses can be derived from these results (see below) that must be tempered by the difference in timing of the samples used for RT-qPCR analysis and measurement of cellulase activity. Since loss of *gna-3* also leads to greatly reduced levels of GNA-1 protein (Figure 3.2), effects due to loss of either Gα subunit cannot be easily resolved using a Δ*gna-3* mutant. Despite low levels of GNA-1, exogenous cAMP increased early cellulase transcription in the Δ*gna-3* mutant, consistent with cAMP acting downstream of both Gα subunits and bypassing the negative regulatory effect of GNB-1 on GNA-3. Loss of *gnb-1* also impacts early cellulase transcription, perhaps due to the effect that *gnb-1* has on GNA-1 and GNA-3 protein levels (Figure 3.2). Exogenous cAMP did not affect the Δ*gnb-1* mutant as much as either Gα single mutant, indicating that GNB-1 may also possess a positive regulatory role, independent of cAMP signaling. Finally, despite the posttranscriptional role adenylyl cyclase (*cr-1*) appears to play in regulating cellulase activity (compare Figure 3.1 and Fig. 4), exogenous cAMP increases cellulase transcription in the Δ*cr-1* mutant (Figure 3.6).

Discussion

We used a comprehensive approach to investigate the effect that every G-protein subunit has on cellulose metabolism in a filamentous fungus. We measured extracellular cellulase activity and protein concentration, levels of several cellulase mRNAs and amounts of each G-protein subunit in the strains. Our findings support a scenario in which *gna-1*, *gna-3, gnb-1* and *gng-1* regulate cellulase activity, partially due to their influence on cAMP signaling (see model in Figure 3.7). Our results show that GNA-1 and GNA-3 are the major positive regulators of cellulase transcription via cAMP signaling in *N. crassa*. Additionally, the phenotypes observed in some mutants can be explained by the combined effect of the mutation and reduced levels of other G-protein subunit(s). For example, *gnb-1* is required to maintain normal levels of GNA-1 and GNA-2 during growth on Avicel medium, and loss of *gna-3* also resulted in lower levels of GNA-1 protein. The positive effect of GNA-3 was not observed until GNA-3 was constitutively activated and *gnb-1* was absent, demonstrating that GNB-1 is a negative regulator of GNA-3. We suggest that there is a tethering relationship between the Gβγ dimer and GNA-3 that may inhibit signaling to downstream effectors.

Exogenous cAMP rescued phenotypes observed in Δ*cr-1* mutants, bypassing the loss of adenylyl cyclase and activating PKA. Δ*cr-1* mutants had decreased levels of mRNA for only one of the five cellulase genes analyzed, indicating that *cr-1* has a minimal effect on transcription four hours after transfer

to Avicel. This suggests that the CR-1 protein mainly regulates cellulase activity through a posttranscriptional mechanism, with the caveat that cellulase activity was measured using a later time point than the mRNA levels. The observation that cAMP addition results in partial rescue of cellulase phenotypes in Δ*gna-1* and Δ*gna-3* mutants supports a mechanism in which the GNA-1 and GNA-3 Gα proteins modulate cellulase transcription through adenylyl cyclase. However, early transcription is more impaired in Δ*gna-1,* Δ*gna-3,* and Δ*gnb-1* mutants than in the Δ*cr-1* mutant, and cAMP did not completely remediate Δ*gna-1* or Δ*gnb-1* phenotypes. These results suggest that G-proteins may also regulate cellulase transcription through additional pathways not related to cAMP signaling.

There are several possibilities for the alternative pathway(s) downstream of G-protein signaling that could regulate cellulase gene transcription. There is precedence for involvement of Mitogen Activated Protein Kinase (MAPK) cascades in cellulase regulation in fungi. For example, the osmosensing (OS) MAP kinase cascade in *N. crassa* suppresses cellulase expression during conditions when free carbohydrates are available (higher osmolarity) (10). Under low osmolarity (i.e. growth on an insoluble carbon source), this pathway leads to cellulase induction. Results from RNAseq analysis of *T. reesei* strains lacking the *tmk2* MAPK grown on sugarcane baggase revealed that genes involved in G-protein related processes are differentially regulated in this background. Among these are the *T. reesei* GNA-1 homolog, as well as three Pth11-like GPCRs and a RGS gene (53) directly tying G-protein signaling to this MAPK pathway.

Other studies in *T. reesei* implicate calcium signaling in cellulase gene expression. Addition of 50-100 mM Ca^{2+} to Avicel medium resulted in higher levels of cellulase activity and biomass production in the hyper-secreting Rut-C30 strain (54) and loss of the transcription factor *crz1*, a downstream target of the Ca^{2+}/Calmodulin pathway resulted in reduced cellulase activity and transcription of *cbh1*, *eg1*, and *xyr1*. *crz1* was found to bind to the promoter of *cbh1*, and its binding affinity increases with added calcium (54). The homologous components of the Ca^{2+}/Calmodulin pathway in *N. crassa* have been characterized (55, 56) and may also play a role in regulating cellulase expression.

Our work supports a post-transcriptional role for CPC-2 in control of cellulase activity in *N. crassa*. Cellulase mRNA levels in the Δ*cpc-2* mutant are either similar to or greater than those in wild type, but the Δ*cpc-2* mutant lacks detectable cellulase activity and does not respond to cAMP. We propose that CPC-2 may impact post translational modifications of cellulases required for activity, perhaps through translational control of the modifying proteins (50, 51). dditional experiments are necessary to determine the exact post-transcriptional effect of CPC-2 on cellulase production in *N. crassa.*

Previous work has determined the transcription factors responsible for cellulase induction (10, 34), the intracellular molecule that induces cellulolytic enzymes (57), and the adaptor proteins needed for efficient exit of cellulases from the ER to the Golgi in fungi (51). Our results contribute to this body of knowledge by providing a comprehensive analysis illustrating the importance of

G-protein signaling during upstream regulation of cellulose sensing and cellulase induction. Further study will be required to characterize the detailed molecular mechanism(s) underlying this relationship, as well as to determine whether the actions of various G-protein subunits influence cellulase mRNA transcription, stability or translation, or regulate post-translational modification or secretion of cellulases in filamentous fungi.

Acknowledgements

We thank Hyojeong Kim, Svetlana Krystofova, Susan Won, and Sara Wright for strain construction. We acknowledge the Fungal Genetics Stock Center (58) for supplying strains. We thank Olga Saquiche, Yesenia Rodezno, Fernando Olvera, and Briana Cabrera for technical assistance and other members of the Borkovich laboratory for many helpful discussions. We thank Lori Huberman, Vincent Wu, and N. Louise Glass for advice on protocols. We thank students in the 2017 *Experimental Microbiology* course at UC Riverside who performed preliminary experiments for this work. This work was partially supported by National Institute of General Medical Sciences grants GM068087 and GM086565 and National Institute of Food and Agriculture Hatch Project #CA-R-PPA-6980-H to K.A.B. We acknowledge funding from NIH S10 OD010669 for proteomics equipment.

Supplemental Methods

Strain construction.

Vectors containing predicted GTPase-deficient, constitutively activating mutations for *gna-1*^{Q204L}, *gna-2*^{Q205L}, and *gna-3*^{Q208L} (pQY21, pSVK52, and pSVK53, respectively) were previously made using site-directed mutagenesis (40, 59). Electroporation of *N. crassa* with 1-2 µg of pQY21, pSVK52 or pSVK53 was as previously described (43), using the FGSC6103 strain (Table 1) as the recipient, with selection on FGS plates without histidine. Genomic DNA was extracted from transformants and subjected to Southern analysis for *gna-1, gna-2* or *gna-3* as described (40). Transformants determined to have a single integration event of the transforming DNA at the *his-3* locus were purified to homokaryons by serial streaking of macroconidia (60) on FGS plates lacking histidine. Genomic DNA was extracted from these strains and analyzed using Southern analysis to confirm that they were homokaryons.

The Δ*cr-1::hph*^{R} knockout mutant was deposited at the FGSC as a heterokaryon (FGSC 11514). Homokaryotic mutants were obtained from the heterokaryon after a sexual cross to wild type strain 74-OR23-1VA and plating ascospores on medium containing hygromycin. Progeny were analyzed using diagnostic PCR (60) with *cr-1* and *hph* primers (Table 3.S2; primers designed as in (61)), and then spot-tested on phosphinothricin to check for the presence of the *mus-51* mutation, which is marked with *bar* (62, 63). All other strains were created as described.

Growth of strains after direct inoculation into avicel medium.

N. crassa strains were inoculated at a density of 1 x10^{6} conidia/mL in 25 mL of VM containing 2% Avicel (crystalline cellulose) as the carbon source and grown with shaking in constant light at 25°C for 4 days. Cultures were then centrifuged at 5000xg for 10 min and photographed.

Extraction of total protein from Avicel cell pads to normalize cellulase activity and supernatant protein level.

The cellulase activity and protein concentration in the supernatants was normalized to the amount of protein in the cell pad from the indicated strains. Cell pads were mixed with 10 ml Protein Extraction Buffer (1% SDS, 50 mM Tris pH 7.5, 5 mM EDTA) and 5 ml glass beads in a 50 ml conical tube and then heated at 60°C with intermittent vortexing over 12 h. The tubes were centrifuged and the

supernatant retained and frozen at -20C. This process was repeated 3-4 times. The total extract volume was recorded and the protein concentration determined as described above. The total mg of cell mass protein in each sample was used to normalize cellulase activity and supernatant protein measurements for that biological replicate.

Discovery proteomics of the 70 kDa region in SDS-PAGE gels of culture supernatants from wild type.

Three biological replicate samples from wild type were subjected to SDS-PAGE and the gels stained using GelCode Blue. The region of the gel containing the 70 kDa bands was excised and destained in 1 mL 50% acetonitrile-water containing 50 mM Triethylammonium bicarbonate (TEAB, Sigma Aldrich, St. Louis, MO) with shaking at 4°C for 16 h. The solution was then removed from the gel slices. Samples were reduced by the addition of 100 µL of 500 mM tris(2-carboxyethyl)phosphine (Thermo Scientific, Rockford, IL) and incubated at 37°C for 1 h. An aliquot containing 50 µL of 500 mM Iodoacetamide (Sigma Aldrich) and 50 µL 50% acetonitrile-water with 50 mM TEAB was subsequently added and samples were incubated in the dark at room temperature for 1 h. After the reducing buffer was removed, 200 µL of 50% acetonitrile-water with 50 mM TEAB was added, and samples were incubated at 4°C for one h with shaking to remove residual staining agent. The solution was discarded and gel pieces were incubated at room temperature with 1mL of ACN for 15 min. The ACN was

removed and the gel pieces were dried under nitrogen for 15 min. Gel pieces were reconstituted with the addition of 250 µL of water and 250 µL of 100 mM TEAB. Subsequently, 5 µL (1µg) of trypsin/lysC mix (Promega, Madison, WI) was added and samples were digested at 37°C overnight (~16 h).

An aliquot containing 10 µL of the above digest was injected for liquid chromatography on a Thermo nLC1200 in single-pump trapping mode with a Thermo PepMap RSLC C18 EASY-spray column (2 µm, 100 Å, 75 µm x 25 cm) and a Pepmap C18 trap column (3 µm, 100 Å, 75 µm x 20 mm). Solvents used were A: water with 0.1% formic acid and B: 80% acetonitrile with 0.1% formic acid. Samples were separated at 300 nL/min with a 260 min gradient ,starting at 3% B, increasing to 30% B from 1 to 230 min, then to 85% B at 240 min hold for 10 min, then back to 3% B in 10 min. Mass spectrometry data was acquired on a Thermo Orbitrap Fusion in data-dependent mode. A full scan was conducted using 60k resolution in the Orbitrap in positive mode. Precursors for MS^2 were filtered by monoisotopic peak determination for peptides, intensity threshold 5.0e3, charge state 2-7, and 60 sec dynamic exclusion after one analysis with a mass tolerance of 10 ppm. Collisionally induced dissociation spectra were collected in ion trap MS^2 at 35% energy and isolation window 1.6 m/z.

Results were searched individually in Proteome Discoverer 2.2 (Thermo Scientific) against the UniProt FASTA database for *Neurospora crassa* (accessed 2/12/2020). The precursor mass tolerance was set to 10 ppm and fragment mass tolerance to 0.6 Da. Fixed modifications were carbamidomethyl

(Cys +57.021 Da), 13C labelled carbamidomethyl (Cys +58.024 Da), and dynamic modifications included methionine oxidation (+15.995 Da) N-terminal acetylation (+42.011 Da). Results were filtered to a strict 1% false discovery rate. The peptide spectral matches (PSMs) for each protein were compared to the total PSMs to give the percentage of the total.

Preparation of protein extracts for western analysis.

Cultures were grown in VM-Glucose medium in constant light for 16 h with shaking at 200 rpm and washed with VM No Carbon as described in the Methods. After washing, cell pads were transferred to VM Avicel and incubated at 25°C for three days. Cell pads were pulverized in liquid nitrogen using a mortar and pestle. Four mL of extraction buffer (100 mM Tris, pH 7.5, 1 mM EDTA, 1mM PMSF, 1 mM DTT) was added to the pulverized tissue. The mixture was homogenized using a glass Dounce and the unbroken cells were pelleted by centrifugation at 5000 x g for 10 min at 4°C (Avanti J26XP, JS-5.3 Rotor, Beckman Coulter). An aliquot of the supernatant was reserved as the whole cell extract for western blotting using the CPC-2 antibody. The supernatant was then centrifuged at 46,000 x g (Avanti J26XP, JA-25.50 Rotor, Beckman Coulter) to pellet the particulate fraction as described (40). The pellet was resuspended in wash buffer (100 mM Tris, pH 7.5, 10% glycerol, 1mM PMSF, 1 mM DTT) and was considered the particulate fraction. Protein concentration was determined

using the BCA assay, and equal amounts of protein were loaded onto SDS-PAGE gels for western analysis, as described in the Methods.

Total RNA isolation and quantitative reverse-transcriptase-PCR (qRT-PCR).

Cell pads were collected using vacuum filtration, flash-frozen in liquid nitrogen and then ground using a chilled mortar and pestle with liquid nitrogen. Total RNA was extracted from ground samples using the TRIzol reagent (Thermo Fisher Scientific). Each sample was tested for purity and concentration using a Nanodrop spectrophotometer (Nanodrop 2000c, Thermo Fisher Scientific).

For qRT-PCR, total RNA was treated with RQ1 DNAse (Promega Corporation, Madison, WI) and cDNA was synthesized using the Maxima First Strand cDNA Synthesis Kit (Thermo Fisher Scientific). qPCR was performed using the Dynamo HS SYBR Green qPCR kit (Thermo Fisher Scientific) and the CFX Connect Real Time PCR Detection System (BioRad Laboratories, Inc.) according to the manufacturer's instructions. Actin (NCU04173) was used as a control. Primers are described in Table 3.S2. Primer sequences for actin, *cbh-1*, *gh6-2*, and *gh5-1* are identical to those in (8).

Figures

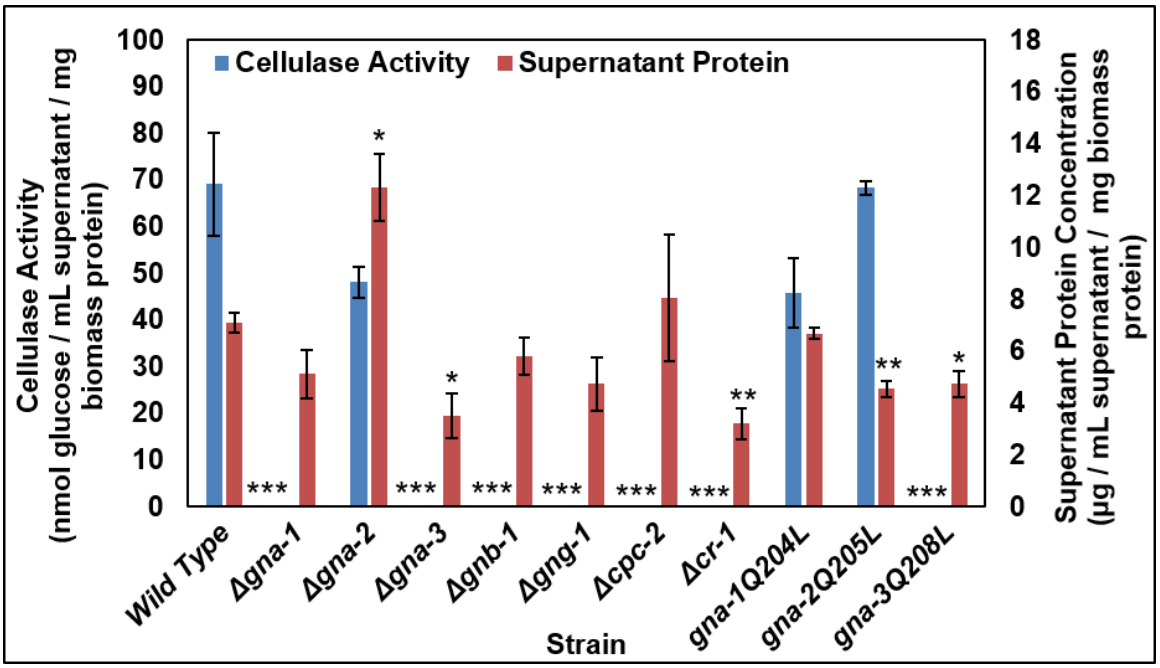

Figure 3.1. Cellulase activity and protein concentration in culture supernatants after growth in VM-Avicel. Cultures were grown overnight (16 h) on VM-Glucose and then washed twice in VM without a carbon source. The cultures were transferred to VM-Cellulose or to fresh VM-Glucose and grown for three days or overnight, respectively. A sample of the culture supernatant was withdrawn and passed through a 0.45 µm filter. Total protein was extracted from the cell pads of each culture as described in the Methods. All protein concentrations were determined using the BCA protein assay. Cellulase activity was assayed as described in (44) and activity is defined as nmol glucose/mL supernatant/mg biomass produced. A minimum of three replicates were used and errors are expressed as the standard error. Statistical significance relative to Wild type *mat a* was determined using a two-tailed Students T-Test and strains with protein levels or cellulase activity significantly different than wild type are indicated by an asterisk ($p < 0.05$ = *, $p < 0.01$ = **, $p < 0.001$ = ***).

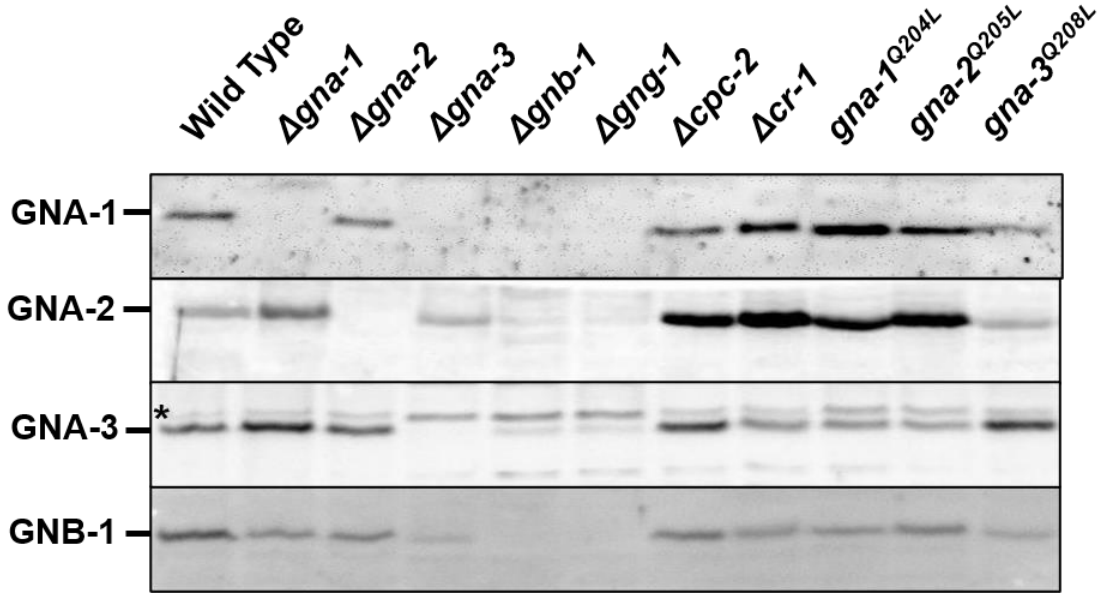

Figure 3.2. Levels of G-protein subunits in strains cultured on Avicel medium. Whole cell extracts were prepared from strains cultured on Avicel as described in the Methods. Differential centrifugation was used to isolate the particulate fraction, that was then utilized to check amounts of the membrane-associated Gα proteins and GNB-1. Since CPC-2 is cytoplasmic (25), whole cell extracts were used for determining CPC-2 levels. Samples containing equal amounts of protein were subjected to SDS-PAGE, and gels blotted to nitrocellulose. Blots were reacted with antiserum for GNA-1, GNA-2, GNA-3, GNB-1, or CPC-2 (see Methods). The results shown are representative of three biological replicates. The migration position of each protein is indicated along the left side of the figure. An asterisk indicates a background band that cross-reacts with GNA-3 antiserum.

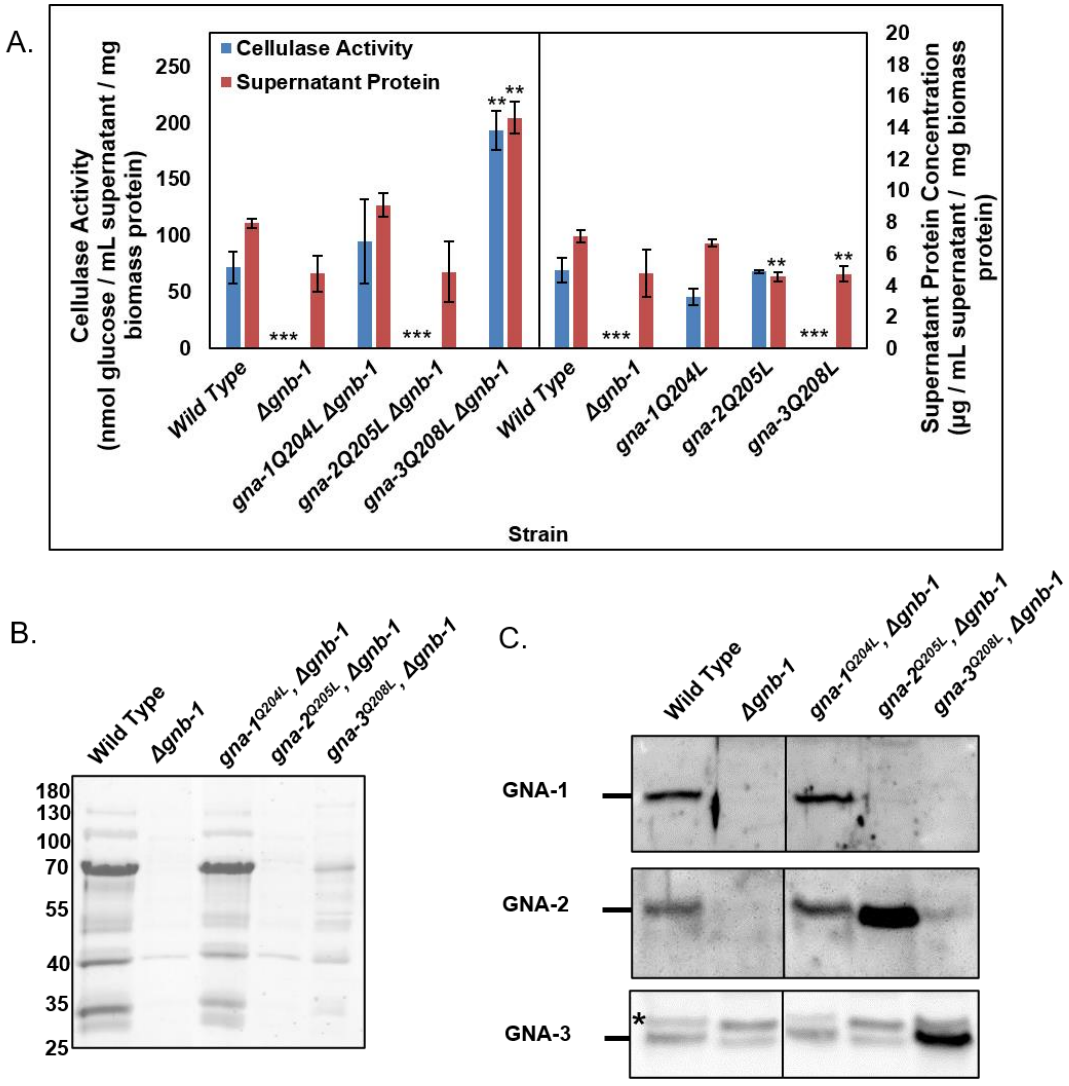

Figure 3.3. Analysis of strains containing activating Gα mutations in a *Δgnb-1* background. Cultures were grown as described in the legend to Figure 3.1. Both cell-free culture supernatants and cell pads were retained.

A. Cellulase activity and supernatant protein concentration. Assays were performed as described in the legend to Figure 3.1. Errors are expressed as the standard error. Statistical significance relative to Wild type *mat A* was determined using a two-tailed Students T-Test and strains with cellulase activity or supernatant protein concentration significantly different than wild type are indicated by an asterisk ($p < 0.05$ = *, $p < 0.01$ = **, $p < 0.001$ = ***). Values from *gna-1*^{Q204L}, *gna-2*^{Q205L}, and *gna-3*^{Q208L} were replotted from Figure 3.1 for comparison. The vertical line on the graph indicates that the two groups of strains were analyzed separately.

B. SDS PAGE analysis of supernatants. SDS-PAGE of supernatant protein from the indicated strains was performed as described in the legend to Figure 3.S3.

C. Levels of Gα subunits in strains containing constitutively active Gα mutations in a Δ*gnb-1* background. Differential centrifugation was used to isolate the particulate fraction from whole cell protein extracts. Samples were subjected to SDS-PAGE and gels blotted to nitrocellulose. Blots were reacted with antiserum for GNA-1, GNA-2 and GNA-3. The results shown are representative of three biological replicates. The migration position of each protein is shown along the right side of the panel.

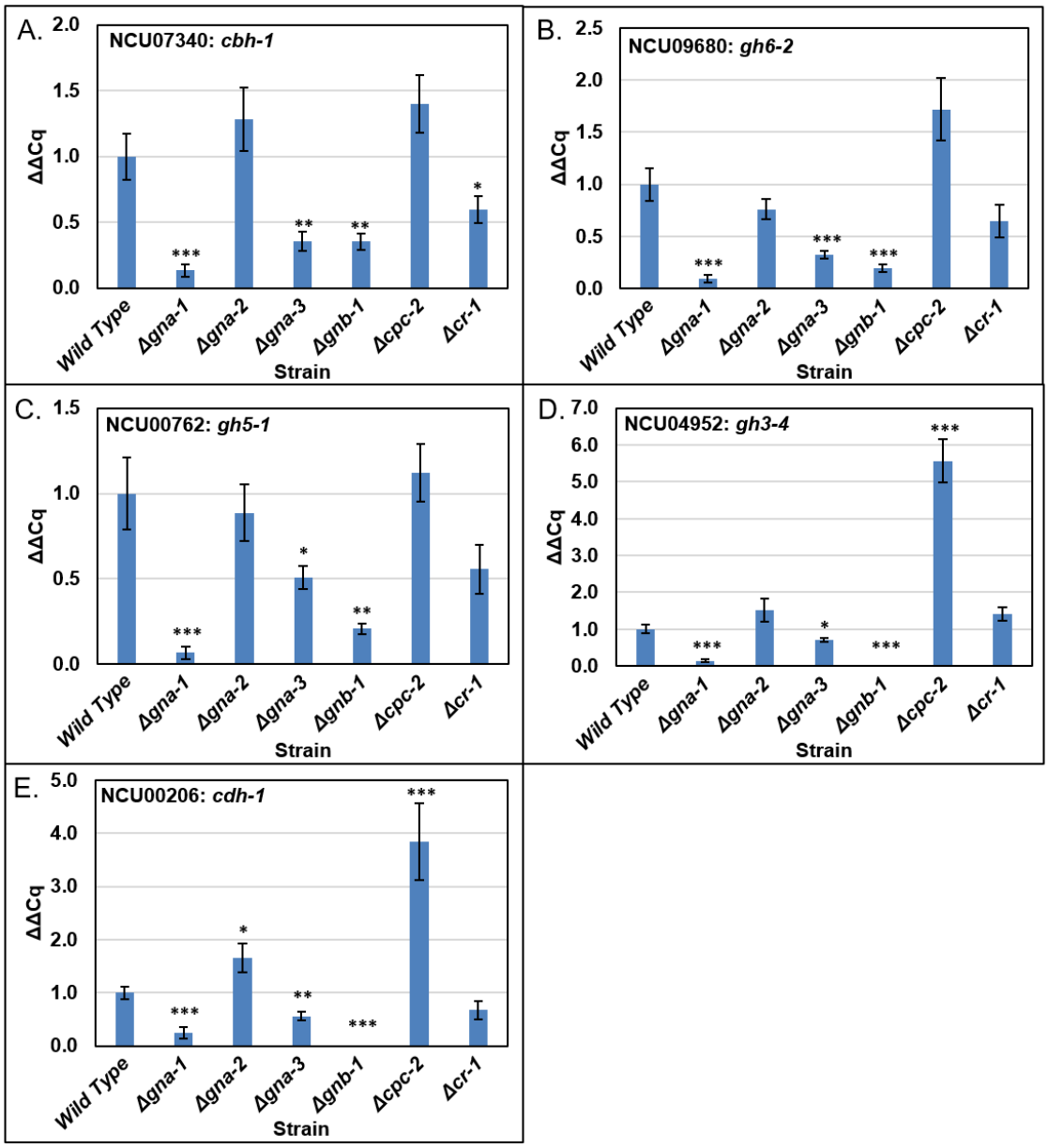

Figure 3.4 qRT-PCR to determine mRNA levels for major cellulases. Cultures were grown on VM-Glucose for 12 h and then transferred to VM-Avicel for 4 h. Total RNA isolated from the indicated strains was then converted to cDNA using reverse transcriptase. The cDNA was then used as a template in qPCR for *cbh-1*/NCU07340, *gh6-2*/NCU09680, *gh5-1*/NCU00762, *gh3-4*/NCU04952, *cdh-1*/NCU00206, and actin/NCU04173 (control). In all, three biological replicates were used, and three technical replicates were tested for each biological replicate. Values were normalized to actin and then to wild type. Errors are expressed as the standard error. Asterisks indicate a statistically significant difference relative to wild type ($p<0.05$ = *, $p<0.01$ = **, $p<0.001$ = ***).

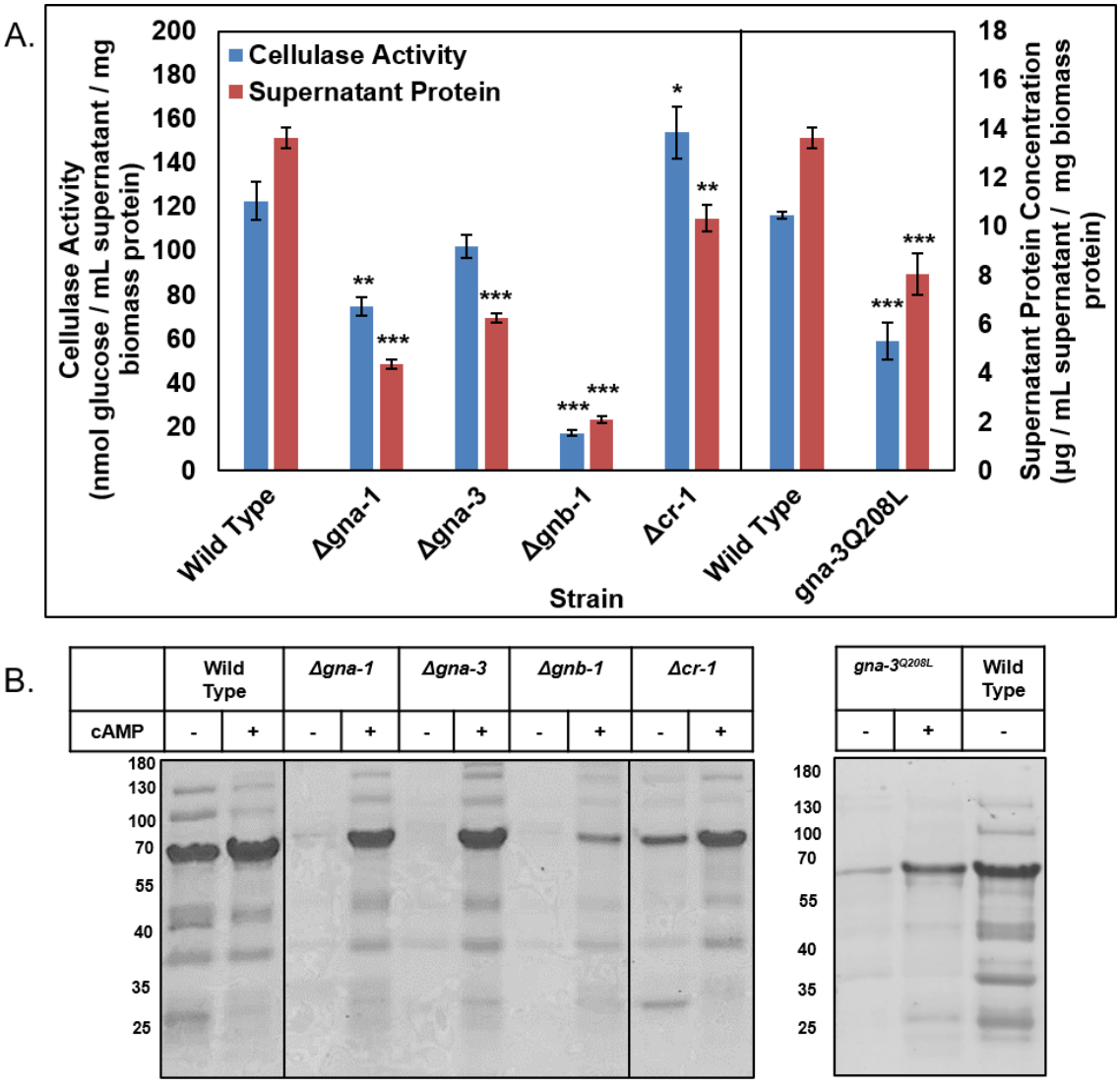

Figure 3.5. Analysis of strains with cAMP added to the medium. Cultures were grown as described in the legend to Figure 3.1, with the exception that cAMP was added to VM-Glucose and VM-Avicel at a concentration of 3 mM.

A. Cellulase activity and supernatant protein concentration. Assays for cellulase activity and supernatant protein concentration were performed as described in the legend to Figure 3.1. Errors are expressed as the standard error. Asterisks indicate a statistically significant difference relative to Wild type *mat A* with cAMP ($p<0.05$ = *, $p<0.01$ = **, $p<0.001$ = ***, ND = not detectable). The vertical line on the graph indicates that the two groups of strains were analyzed separately.

B. SDS PAGE analysis of supernatants. SDS-PAGE of supernatant protein from the indicated strains +/- added cAMP was performed as described in the legend to Figure 3.S3, with equal volumes of concentrated protein loaded on the gel.

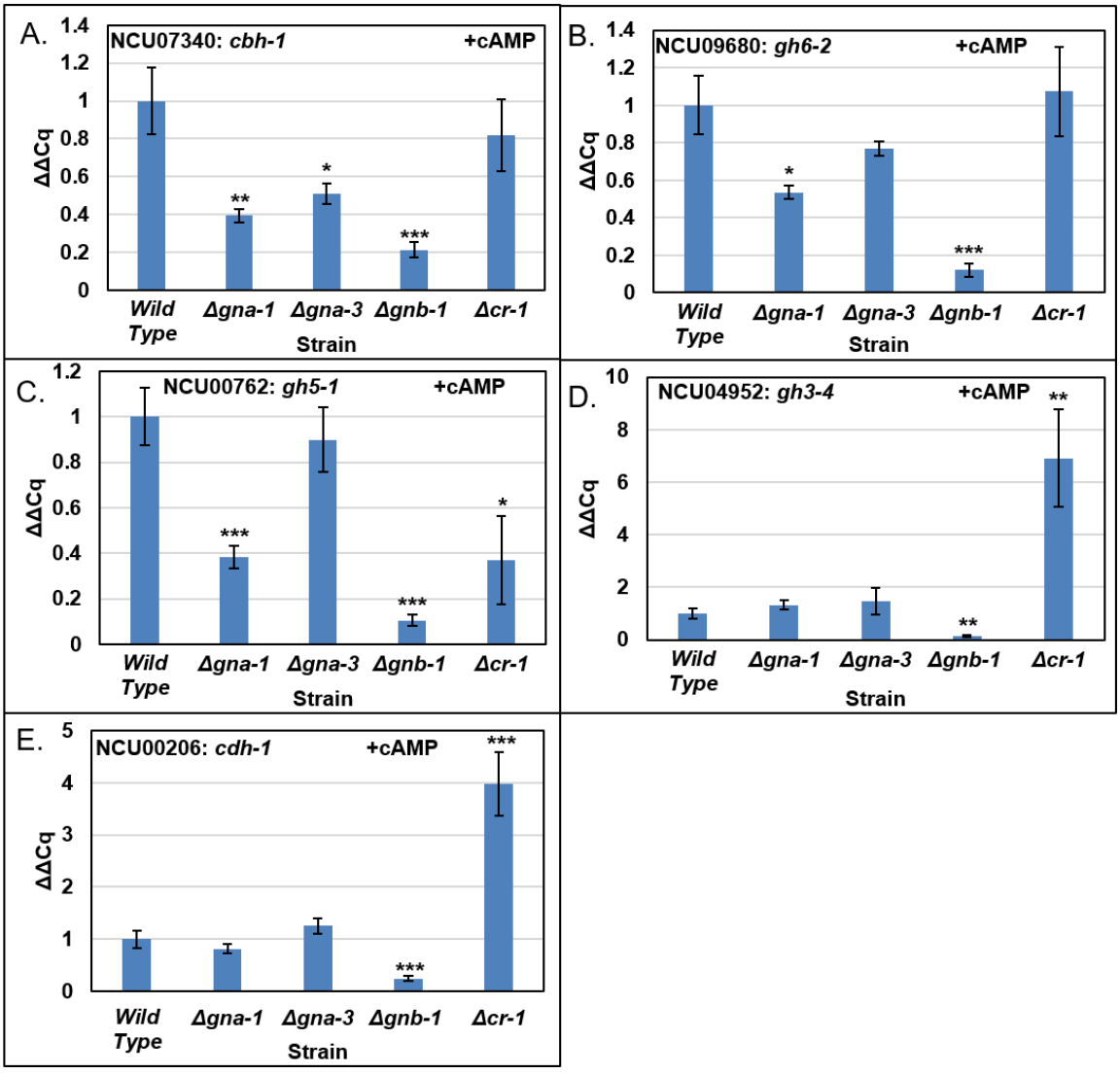

Figure 3.6. qRT-PCR to determine mRNA levels for major cellulases after growth in Avicel medium containing cAMP. Cultures were grown on VM-Glucose containing 3 mM cAMP for 12 h and then transferred to VM-Avicel containing 3 mM cAMP for 4 h. Total mRNA was isolated as described (Methods). qRT-PCR was carried out as described in the legend to Fig. 5, using RNA isolated from mutants cultured in the presence of cAMP and wild type without cAMP. Asterisks indicate a statistically significant difference relative to wild type ($p<0.05$ = *, $p<0.01$ = **, $p<0.001$ = ***).

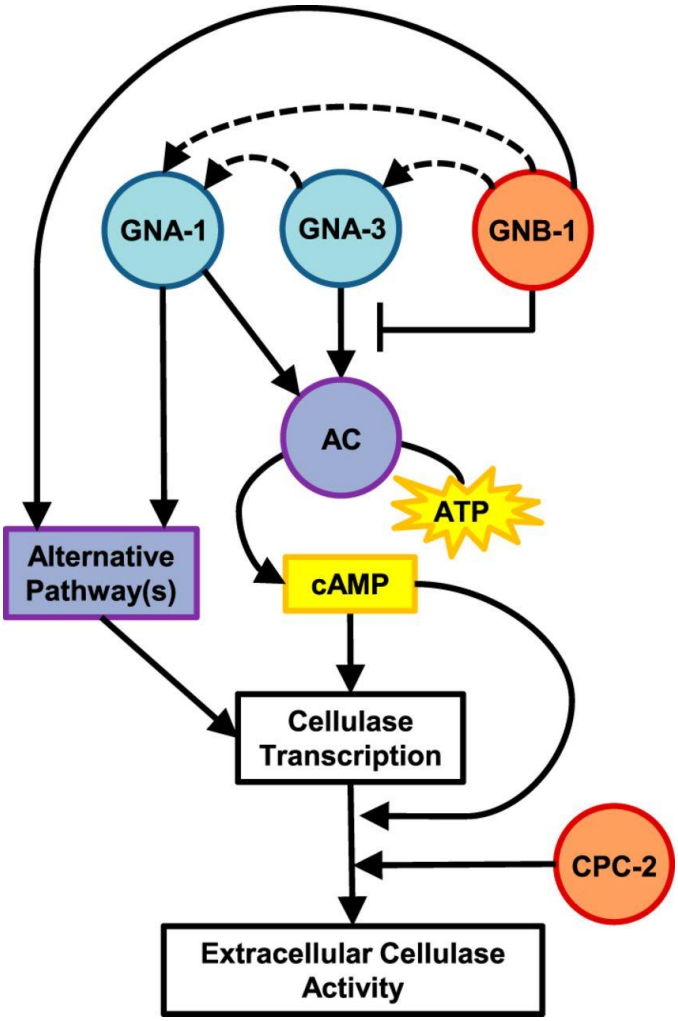

Figure 3.7. Model for regulation of cellulase activity by G-protein signaling. Gα proteins are shaded in blue, Gβ subunits in orange, effector pathways in purple and small molecules in yellow. Positive regulation is indicated by solid or dashed lines with arrowheads, while negative regulation is shown using a line that ends with a perpendicular line. Dashed arrows illustrate effects on protein levels. The Gα proteins GNA-1 and GNA-3 positively regulate cellulase activity via cAMP levels through adenylyl cyclase (AC/CR-1). G-protein signaling also controls cellulase transcription via an unknown effector pathway(s) that may correspond to one or more of the three MAPK cascades, Ca^{2+}/calmodulin signaling or another mode of signal transduction. GNA-3 and the Gβ subunit GNB-1 are required to maintain GNA-1 protein levels (indicated by the dashed arrows). Activated GNA-1 is able to overcome the negative regulation by GNB-1 on cellulase production, while the positive role of GNA-3 is only manifested in the absence of GNB-1. AC/CR-1 and the RACK1 Gβ homolog CPC-2 play post-transcriptional roles in regulation of cellulase activity/supernatant protein levels.

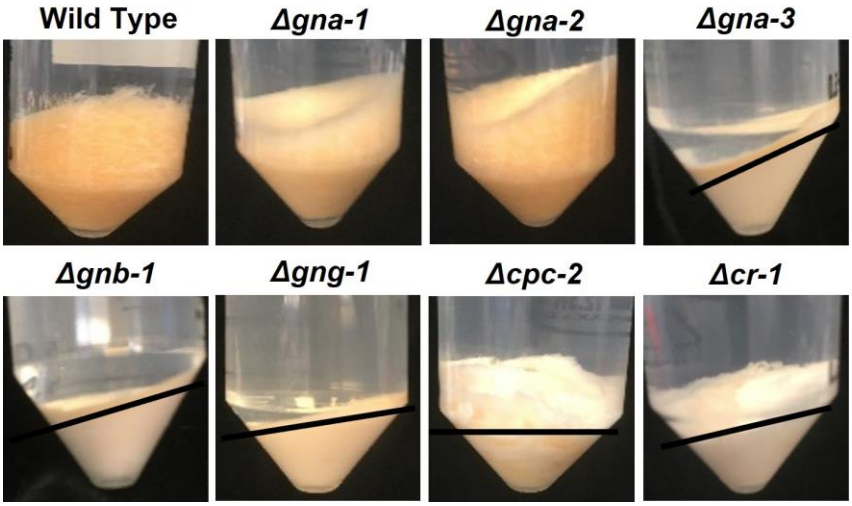

Figure 3.S1. Growth of strains on cellulose medium. *N. crassa* strains were grown at 25°C in constant light for 4 days in 25 mL of VM containing 2% Avicel (crystalline cellulose) as the carbon source. Cultures were then centrifuged at 5000xg for 10 minutes and photographed. Strains that did not completely degrade cellulose into soluble glucose or glucose oligomers still have Avicel (white powder) remaining in the bottom of the tube. The black line indicates the top of the Avicel pellet. There was no remaining Avicel pellet in cultures from wild type, *Δgna-1* or *Δgna-2* mutants.

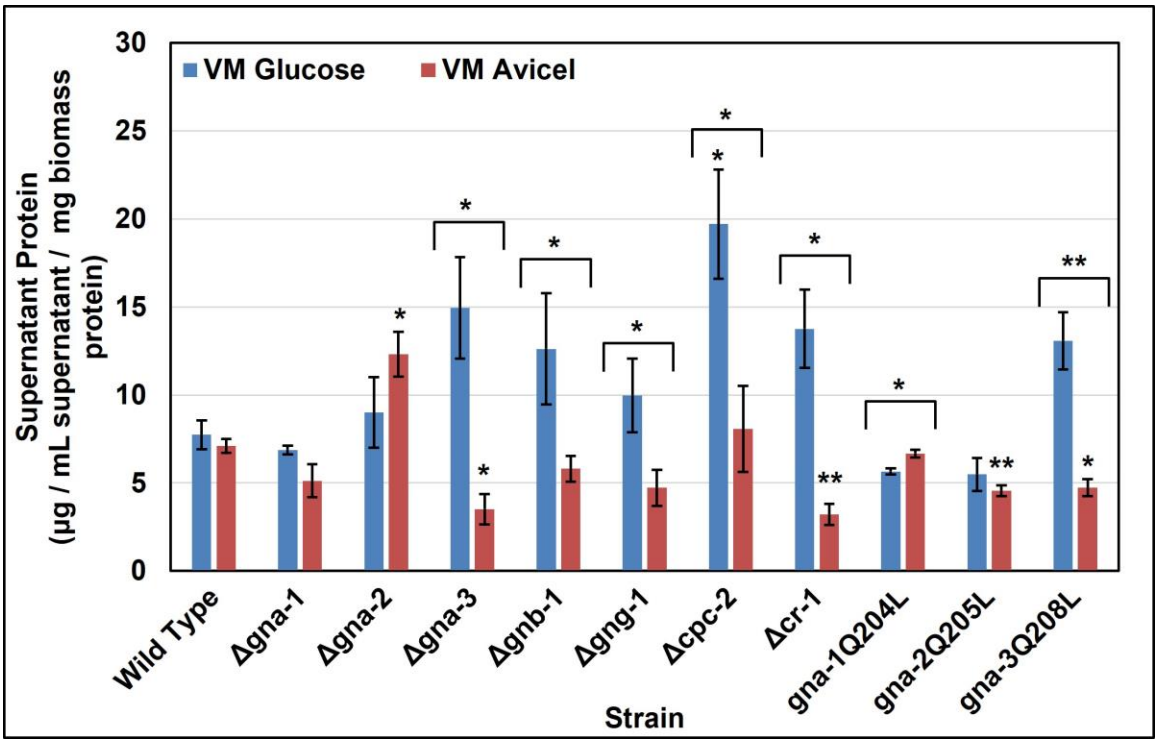

Figure 3.S2. Total protein in culture supernatants during growth in liquid culture. Cultures were grown overnight (16 hrs) on VM-Glucose, then were washed twice in VM without a carbon source. The cultures were transferred to VM-Cellulose for three days or to fresh VM-Glucose and grown overnight. A sample of the culture supernatant was withdrawn, filtered through a 0.45 µm filter and were assayed as described below. Total protein was extracted from the cell pads of each culture as described in the Methods. A minimum of three replicates were used and errors are expressed as the standard error. Statistical significance from wild type on the same carbon source was determined using a two tailed Students T-Test and strains with protein levels significantly different than wild type are indicated by an asterisk ($p < 0.05$ = *, $p < 0.01$ = **, $p < 0.001$ = ***) Strains with protein levels significantly different on the two carbon sources are indicated by the asterisk above the line. Protein concentration of the supernatant was quantified using the BCA protein assay.

A.

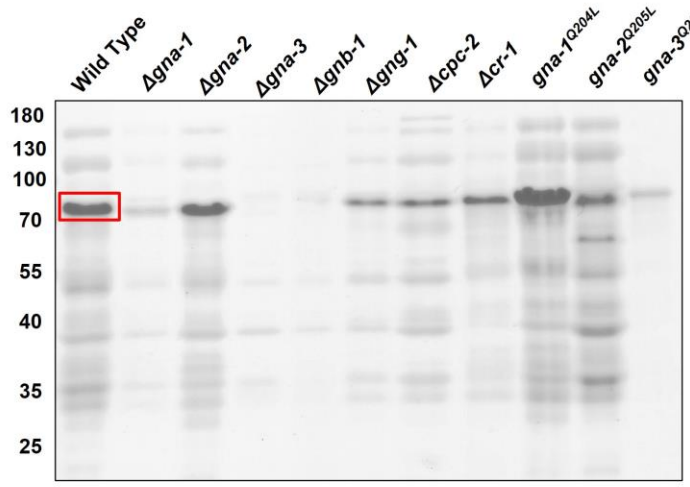

B.

Gene Name	NCU Number	% of total PSMs
cbh-1	NCU07340	41±2%
gh3-4	NCU04952	13±0%
ncw-1	NCU05137	12±2%
gh51-1	NCU02343	6±0%
gla-1	NCU01517	5±1%
inv	NCU04265	5±0%
cdh-1	NCU00206	4±1%
null	NCU09024	3±1%
scp	NCU00831	2±0%
mpr-17	NCU09228	2±0%
spr-9	NCU09992	2±0%
gh6-2	NCU09680	2±1%
gel-3	NCU08909	1±0%
gh74-1	NCU05955	1±0%

Figure S3. Content of the 70 kDa band present in culture supernatants

A. SDS-PAGE analysis of Avicel supernatants. One mL of cell-free culture supernatant obtained as indicated was concentrated as described in the Materials and Methods. A volume containing 20 µL was subjected to SDS-PAGE using a 10% resolving gel. The position of molecular weight markers is shown along the left side of the figure.

B. Discovery Proteomics of the band appearing at 70 kDa. Cell-free secreted protein samples were obtained from VM cellulose cultures as described in the legend to Figure 2A. 20 µg of protein was electrophoresed on a 10% gel and the prominent band at 70 kDa was excised as indicated by the red square in 3A. Proteins displayed in the table had at minimum 10 peptide spectral matches (PSMs) in all three biological replicates. The number of PSMs for each protein was divided by the total detected in each sample to give the percent of total PSMs.A minimum of three biological replicates were used. Errors are expressed as the standard error.

Tables

Table 3.S1. Strains used in this study

Strain	Relevant Genotype	Source
74-OR23-1A	Wild type, *mat A*	FGSC[1]
OR8-1a	Wild type, *mat a*	FGSC
6103	*his-3, mat A*	FGSC
3b10	Δ*gna-1*::*hph, mat a*	(30)
12378	Δ*gna-2*::*hph, mat A*	FGSC
31c2	Δ*gna-3*::*hph, mat A*	(21)
42-8-3	Δ*gnb-1*::*hph, mat A*	(39)
5-5-3	Δ*gng-1*::*hph, mat A*	(26)
Δ1gna-1*	Δ*gna-1*::*hph, gna-1*^{Q204L}::*his-3*$^{+}$, *mat A*	This study
G2-7	p*ccg-1*::*gna-2*^{Q205L}::*his-3*$^{+}$, *mat A*	This study
gna3Q208L	p*ccg-1*::*gna-3*^{Q208L}::*his-3*$^{+}$, *mat A*	This study
cpc-2-5	Δ*cpc-2*::*hph, mat A*	(25)
Δcr-1	Δ*cr-1*::*hph, mat a*	FGSC
G1-F	Δ*gnb-1*::*hph, his-3,* p*ccg-1*::*gna-1*^{Q204L}::*his-3*$^{+}$, *mat a*	(40)
G2-D	Δ*gnb-1*::*hph, his-3,* p*ccg-1*::*gna-2*^{Q205L}::*his-3*$^{+}$, *mat a*	
G3-C	Δ*gnb-1*::*hph, his-3,* p*ccg-1*::*gna-3*^{Q208L}::*his-3*$^{+}$, *mat a*	

1. FGSC = Fungal Genetics Stock Center (58)

Table 3.S2. Primers used in this study

Primer	Sequence (5'-3')	Amplicon Size
Δ*cr-1* 5' diagnostic	GGCCCTGGCAGTCAGGTTGC	1 kb
hph 5' diagnostic	GGGATTCATTGTTGACCTCCA	
Δ*cr-1* 3' diagnostic	TGTCGTCGTCGGTTGGTCGC	1 kb
hph 3' diagnostic	CGCCCCAGCACTCGTCCGAGG	
NCU00206 FWD qPCR	TGCTCATCGAGAAGGGTTTC	90 bp
NCU00206 REV qPCR	CGAAGCGAGTAAGGGATGTATT	
NCU00762 FWD qPCR	GAGTTCACATTCCCTGACA	72 bp
NCU00762 REV qPCR	CGAAGCCAACACGGAAGA	
NCU04952 FWD qPCR	GAAAGAGCTAGGCTTCAAAGGA	99 bp
NCU04952 REV qPCR	CCTGGCATCGTCATATCCATAC	
NCU07340 FWD qPCR	ATCTGGGAAGCGAACAAAG	113 bp
NCU07340 REV qPCR	TAGCGGTCGTCGGAATAG	
NCU09680 FWD qPCR	CCCATCACCACTACTACC	108 bp
NCU09680 REV qPCR	CCAGCCCTGAACACCAAG	
Actin FWD qPCR	TGATCTTACCGACTACCT	102 bp
Actin REV qPCR	CAGAGCTTCTCCTTGATG	

References

1. Glass NL, Schmoll M, Cate JH, Coradetti S. 2013. Plant cell wall deconstruction by ascomycete fungi. Annu Rev Microbiol 67:477-98.

2. Huberman LB, Liu J, Qin L, Glass NL. 2016. Regulation of the lignocellulolytic response in filamentous fungi. Fungal Biol Rev 30:101-111.

3. Rubin EM. 2008. Genomics of cellulosic biofuels. Nature 454:841-5.

4. Yenkie KM, Wu W, Clark RL, Pfleger BF, Root TW, Maravelias CT. 2016. A roadmap for the synthesis of separation networks for the recovery of bio-based chemicals: Matching biological and process feasibility. Biotechnol Adv 34:1362-1383.

5. Dean R, Van Kan JA, Pretorius ZA, Hammond-Kosack KE, Di Pietro A, Spanu PD, Rudd JJ, Dickman M, Kahmann R, Ellis J, Foster GD. 2012. The Top 10 fungal pathogens in molecular plant pathology. Mol Plant Pathol 13:414-30.

6. Kubicek CP, Starr TL, Glass NL. 2014. Plant cell wall degrading enzymes and thier secretion in plant pathogenic fungi. Annu Rev Phytopathol 52:(in press).

7. Coradetti ST, Xiong Y, Glass NL. 2013. Analysis of a conserved cellulase transcriptional regulator reveals inducer-independent production of cellulolytic enzymes in *Neurospora crassa*. Microbiologyopen 2:595-609.

8. Znameroski EA, Coradetti ST, Roche CM, Tsai JC, Iavarone AT, Cate JH, Glass NL. 2012. Induction of lignocellulose-degrading enzymes in *Neurospora crassa* by cellodextrins. Proc Nat Acad Sci USA 109:6012-7.

9. Sun J, Glass NL. 2011. Identification of the CRE-1 cellulolytic regulon in *Neurospora crassa*. PLoS One 6:e25654.

10. Huberman LB, Coradetti ST, Glass NL. 2017. Network of nutrient-sensing pathways and a conserved kinase cascade integrate osmolarity and carbon sensing in *Neurospora crassa*. Proc Natl Acad Sci U S A 114:E8665-E8674.

11. de Assis LJ, Ries LN, Savoldi M, Dos Reis TF, Brown NA, Goldman GH. 2015. *Aspergillus nidulans* protein kinase A plays an important role in cellulase production. Biotechnol Biofuels 8:213.

12. Samal A, Craig JP, Coradetti ST, Benz JP, Eddy JA, Price ND, Glass NL. 2017. Network reconstruction and systems analysis of plant cell wall deconstruction by *Neurospora crassa*. Biotechnol Biofuels 10:225.

13. Li L, Wright SJ, Krystofova S, Park G, Borkovich KA. 2007. Heterotrimeric G protein signaling in filamentous fungi. Annu Rev Microbiol 61:423-52.

14. Brown NA, Schrevens S, van Dijck P, Goldman GH. 2018. Fungal G-protein-coupled receptors: mediators of pathogenesis and targets for disease control. Nat Microbiol 3:402-414.

15. Bock A, Kostenis E, Trankle C, Lohse MJ, Mohr K. 2014. Pilot the pulse: controlling the multiplicity of receptor dynamics. Trends Pharmacol Sci 35:630-638.

16. Chini B, Parenti M, Poyner DR, Wheatley M. 2013. G-protein-coupled receptors: from structural insights to functional mechanisms. Biochem Soc Trans 41:135-6.

17. Tesmer JJ. 2010. The quest to understand heterotrimeric G protein signaling. Nat Struct Mol Biol 17:650-2.

18. Wright SJ, Inchausti R, Eaton CJ, Krystofova S, Borkovich KA. 2011. RIC8 is a guanine-nucleotide exchange factor for Galpha subunits that regulates growth and development in *Neurospora crassa*. Genetics 189:165-76.

19. Kim H, Wright SJ, Park G, Ouyang S, Krystofova S, Borkovich KA. 2012. Roles for receptors, pheromones, G proteins, and mating type genes during sexual reproduction in *Neurospora crassa*. Genetics 190:1389-404.

20. Krystofova S, Borkovich KA. 2006. The predicted G-protein-coupled receptor GPR-1 is required for female sexual development in the multicellular fungus *Neurospora crassa*. Eukaryot Cell 5:1503-16.

21. Kays AM, Rowley PS, Baasiri RA, Borkovich KA. 2000. Regulation of conidiation and adenylyl cyclase levels by the Galpha protein GNA-3 in *Neurospora crassa*. Mol Cell Biol 20:7693-705.

22. Li L, Borkovich KA. 2006. GPR-4 is a predicted G-protein-coupled receptor required for carbon source-dependent asexual growth and development in *Neurospora crassa*. Eukaryot Cell 5:1287-300.

23. Turner GE, Borkovich KA. 1993. Identification of a G protein alpha subunit from *Neurospora crassa* that is a member of the G_i family. J Biol Chem 268:14805-11.

24. Kays AM, Borkovich KA. 2004. Severe impairment of growth and differentiation in a *Neurospora crassa* mutant lacking all heterotrimeric G alpha proteins. Genetics 166:1229-40.

25. Garud A, Carrillo AJ, Collier LA, Ghosh A, Kim JD, Lopez-Lopez B, Ouyang S, Borkovich KA. 2019. Genetic relationships between the RACK1 homolog cpc-2 and heterotrimeric G protein subunit genes in Neurospora crassa. PLoS One 14:e0223334.

26. Krystofova S, Borkovich KA. 2005. The heterotrimeric G-protein subunits GNG-1 and GNB-1 form a Gbetagamma dimer required for normal female fertility, asexual development, and galpha protein levels in Neurospora crassa. Eukaryot Cell 4:365-78.

27. Park G, Servin JA, Turner GE, Altamirano L, Colot HV, Collopy P, Litvinkova L, Li L, Jones CA, Diala FG, Dunlap JC, Borkovich KA. 2011. Global analysis of serine-threonine protein kinase genes in *Neurospora crassa*. Eukaryotic cell 10:1553-64.

28. Banno S, Ochiai N, Noguchi R, Kimura M, Yamaguchi I, Kanzaki S, Murayama T, Fujimura M. 2005. A catalytic subunit of cyclic AMP-dependent protein kinase, PKAC-1, regulates asexual differentiation in *Neurospora crassa*. Genes Genet Syst 80:25-34.

29. Terenzi HF, Flawia MM, Tellez-Inon MT, Torres HN. 1976. Control of *Neurospora crassa* morphology by cyclic adenosine 3', 5'-monophosphate and dibutyryl cyclic adenosine 3', 5'-monophosphate. J Bacteriol 126:91-9.

30. Ivey FD, Yang Q, Borkovich KA. 1999. Positive regulation of adenylyl cyclase activity by a galphai homolog in Neurospora crassa. Fungal Genet Biol 26:48-61.

31. Kim JD, Kaiser K, Larive CK, Borkovich KA. 2011. Use of 1H nuclear magnetic resonance to measure intracellular metabolite levels during growth and asexual sporulation in *Neurospora crassa*. Eukaryot Cell 10:820-831.

32. Schmoll M, Schuster A, Silva Rdo N, Kubicek CP. 2009. The G-alpha protein GNA3 of *Hypocrea jecorina* (Anamorph *Trichoderma reesei*) regulates cellulase gene expression in the presence of light. Eukaryot Cell 8:410-20.

33. Seibel C, Gremel G, do Nascimento Silva R, Schuster A, Kubicek CP, Schmoll M. 2009. Light-dependent roles of the G-protein alpha subunit GNA1 of *Hypocrea jecorina* (anamorph *Trichoderma reesei*). BMC Biol 7:58.

34. Liu Q, Li J, Gao R, Li J, Ma G, Tian C. 2019. CLR-4, a novel conserved transcription factor for cellulase gene expression in ascomycete fungi. Mol Microbiol 111:373-394.

35. Cabrera IE, Pacentine IV, Lim A, Guerrero N, Krystofova S, Li L, Michkov AV, Servin JA, Ahrendt SR, Carrillo AJ, Davidson LM, Barsoum AH, Cao J, Castillo R, Chen WC, Dinkchian A, Kim S, Kitada SM, Lai TH, Mach A, Malekyan C, Moua TR, Torres CR, Yamamoto A, Borkovich KA. 2015. Global analysis of predicted G Protein-Coupled Receptor genes in the filamentous fungus, *Neurospora crassa*. G3 (Bethesda) 5:2729-43.

36. DeZwaan TM, Carroll AM, Valent B, Sweigard JA. 1999. *Magnaporthe grisea* Pth11p is a novel plasma membrane protein that mediates appressorium differentiation in response to inductive substrate cues. Plant Cell 11:2013-30.

37. Ramanujam R, Calvert ME, Selvaraj P, Naqvi NI. 2013. The late endosomal HOPS complex anchors active G-protein signaling essential for pathogenesis in *Magnaporthe oryzae*. PLoS Pathog 9:e1003527.

38. Dilks T, Halsey K, De Vos RP, Hammond-Kosack KE, Brown NA. 2019. Non-canonical fungal G-protein coupled receptors promote *Fusarium* head blight on wheat. PLoS Pathog 15:e1007666.

39. Yang Q, Poole SI, Borkovich KA. 2002. A G-protein beta subunit required for sexual and vegetative development and maintenance of normal G alpha protein levels in *Neurospora crassa*. Eukaryot Cell 1:378-90.

40. Won S, Michkov AV, Krystofova S, Garud AV, Borkovich KA. 2012. Genetic and physical interactions between Galpha subunits and components of the Gbetagamma dimer of heterotrimeric G proteins in *Neurospora crassa*. Eukaryot Cell 11:1239-48.

41. Vogel HJ. 1964. Distribution of lysine pathways among fungi: Evolutionary implications. Am Nat 98:435-446.

42. Tian C, Beeson WT, Iavarone AT, Sun J, Marletta MA, Cate JH, Glass NL. 2009. Systems analysis of plant cell wall degradation by the model filamentous fungus *Neurospora crassa*. Proc Natl Acad Sci U S A 106:22157-62.

43. Ivey FD, Hodge PN, Turner GE, Borkovich KA. 1996. The G alpha i homologue gna-1 controls multiple differentiation pathways in *Neurospora crassa*. Mol Biol Cell 7:1283-97.

44. Baasiri RA, Lu X, Rowley PS, Turner GE, Borkovich KA. 1997. Overlapping functions for two G protein alpha subunits in *Neurospora crassa*. Genetics 147:137-45.

45. Dietzel C, Kurjan J. 1987. The yeast SCG1 gene: a G alpha-like protein implicated in the a- and alpha-factor response pathway. Cell 50:1001-10.

46. Jahng KY, Ferguson J, Reed SI. 1988. Mutations in a gene encoding the alpha subunit of a *Saccharomyces cerevisiae* G protein indicate a role in mating pheromone signaling. Mol Cell Biol 8:2484-93.

47. Miyajima I, Nakafuku M, Nakayama N, Brenner C, Miyajima A, Kaibuchi K, Arai K, Kaziro Y, Matsumoto K. 1987. GPA1, a haploid-specific essential gene, encodes a yeast homolog of mammalian G protein which may be involved in mating factor signal transduction. Cell 50:1011-9.

48. Phillips CM, Iavarone AT, Marletta MA. 2011. Quantitative proteomic approach for cellulose degradation by *Neurospora crassa*. J Proteome Res 10:4177-85.

49. Phillips CM, Beeson WT, Cate JH, Marletta MA. 2011. Cellobiose dehydrogenase and a copper-dependent polysaccharide monooxygenase potentiate cellulose degradation by *Neurospora crassa*. ACS Chem Biol 6:1399-1406.

50. Wu VW, Dana CM, Iavarone AT, Clark DS, Glass NL. 2017. Identification of Glutaminyl Cyclase Genes Involved in Pyroglutamate Modification of Fungal Lignocellulolytic Enzymes. MBio 8.

51. Starr TL, Goncalves AP, Meshgin N, Glass NL. 2018. The major cellulases CBH-1 and CBH-2 of *Neurospora crassa* rely on distinct ER cargo adaptors for efficient ER-exit. Mol Microbiol 107:229-248.

52. Ivey FD, Kays AM, Borkovich KA. 2002. Shared and independent roles for a Galpha(i) protein and adenylyl cyclase in regulating development and stress responses in *Neurospora crassa*. Eukaryot Cell 1:634-42.

53. de Paula RG, Antonieto ACC, Carraro CB, Lopes DCB, Persinoti GF, Peres NTA, Martinez-Rossi NM, Silva-Rocha R, Silva RN. 2018. The Duality of the MAPK Signaling Pathway in the Control of Metabolic Processes and Cellulase Production in *Trichoderma reesei*. Sci Rep 8:14931.

54. Chen L, Zou G, Wang J, Wang J, Liu R, Jiang Y, Zhao G, Zhou Z. 2016. Characterization of the Ca(2+) -responsive signaling pathway in regulating the expression and secretion of cellulases in *Trichoderma reesei* Rut-C30. Mol Microbiol 100:560-75.

55. Gohain D, Tamuli R. 2019. Calcineurin responsive zinc-finger-1 binds to a unique promoter sequence to upregulate neuronal calcium sensor-1, whose interaction with MID-1 increases tolerance to calcium stress in *Neurospora crassa*. Mol Microbiol 111:1510-1528.

56. Tamuli R, Deka R, Borkovich KA. 2016. Calcineurin subunits A and B interact to regulate growth and asexual and sexual development in *Neurospora crassa*. PLoS One 11:e0151867.

57. Znameroski EA, Li X, Tsai JC, Galazka JM, Glass NL, Cate JH. 2014. Evidence for transceptor function of cellodextrin transporters in *Neurospora crassa*. J Biol Chem 289:2610-9.

58. McCluskey K, Wiest A, Plamann M. 2010. The Fungal Genetics Stock Center: a repository for 50 years of fungal genetics research. J Biosci 35:119-26.

59. Yang Q, Borkovich KA. 1999. Mutational activation of a Galphai causes uncontrolled proliferation of aerial hyphae and increased sensitivity to heat and oxidative stress in *Neurospora crassa*. Genetics 151:107-17.

60. Ghosh A, Servin JA, Park G, Borkovich KA. 2014. Global analysis of serine/threonine and tyrosine protein phosphatase catalytic subunit genes in *Neurospora crassa* reveals interplay between phosphatases and the p38 mitogen-activated protein kinase. G3 (Bethesda) 4:349-65.

61. Borkovich KA, Alex LA, Yarden O, Freitag M, Turner GE, Read ND, Seiler S, Bell-Pedersen D, Paietta J, Plesofsky N, Plamann M, Goodrich-Tanrikulu M, Schulte U, Mannhaupt G, Nargang FE, Radford A, Selitrennikoff C, Galagan JE, Dunlap JC, Loros JJ, Catcheside D, Inoue H, Aramayo R, Polymenis M, Selker EU, Sachs MS, Marzluf GA, Paulsen I, Davis R, Ebbole DJ, Zelter A, Kalkman ER, O'Rourke R, Bowring F, Yeadon J, Ishii C, Suzuki K, Sakai W, Pratt R. 2004. Lessons from the genome sequence of *Neurospora crassa*: tracing the path from genomic blueprint to multicellular organism. Microbiol Mol Biol Rev 68:1-108.

62. Avalos J, Geever RF, Case ME. 1989. Bialaphos resistance as a dominant selectable marker in Neurospora crassa. Curr Genet 16:369-72.

63. Pall M. 1993. The use of Ignite (basta; glufosinate; phosphinothricin) to select transformants of *bar*-containing plasmids in *Neurospora crassa*. Fungal Genet Newsl 40:57.

Chapter 4: Heterotrimeric G-Protein Signaling Regulates Transcription of Cellulase Enzyme Genes

Abstract

Transcriptional regulators of genes encoding plant cell wall degrading enzymes have been characterized in several species of filamentous fungi. Those involved in cellulose degradation are known, but the upstream signal transduction pathways have yet to be identified. We have previously demonstrated that two heterotrimeric G protein Gα genes (*gna-1* and *gna-3*) and adenylyl cyclase (*cr-1*) are required for cellulase activity in *Neurospora crassa*. In this study, we explored transcriptional regulation by these genes using RNAseq. We compared the transcriptomes of wild type on glucose medium to those grown on Avicel. We also analyzed the transcriptomes from cellulose-grown cultures of mutants lacking the Gα subunits *gna-1* and *gna-3*, as well as the adenylate cyclase *cr-1*, via RNAseq. A total of 22 highly expressed cellulases were detected in wild type cultures grown on cellulose. 20 of these were transcriptionally down-regulated in Δ*gna-1* mutants, and six of these were also down-regulated in Δ*gna-3* mutants. The shared group included the cellobiose dehydrogenase *cdh-1* and the xyloglucanase *cel74a*, genes required for full cellulase activity in *T. reesei*. The combined down-regulation of these two mRNAs alone may be enough to abolish cellulase activity in Δ*gna-1* and Δ*gna-3* mutants. None of the major cellulases are down-regulated in Δ*cr-1* mutants,

suggesting post-transcriptional regulation. All three mutants shared 10 transcriptionally down-regulated genes that are involved in metabolism of extracellular carbon sources. LC-MS/MS analysis of the exoproteome of these strains showed that despite transcriptional down-regulation of cellulase enzyme genes, all of the major cellulases present in wild type are still detectable in all three mutant backgrounds. Δ*gna-3* mutants possessed all of the cellulases present in wild type. Δ*gna-1* mutants lacked one enzyme detected in wild type, which was GH61-8 (NCU03000). The Δ*cr-1* secretome was missing one cellulase; GH7-4 (NCU05104), an exoglucanase. In addition, the proteomes of all three mutants lacked enzymes found in the wild type exoproteome and had secreted proteins that were not present in wild type. These results support a model in which GNA-1 and GNA-3 regulate cellulase enzyme transcription, while CR-1 regulates cellulases post-transcriptionally.

Introduction

Saprophytic and plant pathogenic fungi secrete a cocktail of enzymes to degrade the polymers of the plant cell wall to utilize as carbon sources (1). Fungal transcription factors required for degradation of the plant cell wall have been extensively studied (2-5). In most fungi, the homolog of the *Neurospora crassa* transcription factor CRE-1 regulates carbon catabolite repression (CCR), a response that suppresses utilization of alternative carbon sources in the presence of a rich carbon source (6). While CCR is typically thought of as a response to glucose specifically, in saprophytic species other breakdown products of complex polymers can also induce this process. In the absence of a rich carbon source, CRE-1 exits the nucleus, lifting CCR conditions. (7-9). Thus, *N. crassa* Δ*cre-1* mutant strains produce higher levels of mRNAs coding for cellulases (2).

In *Trichoderma reesei* and *Aspergillus niger,* metabolism of cellulose is controlled primarily by homologs of the transcription factor *xlr-1*, allowing cellulase expression to occur (10, 11). However, in species such as *Aspergillus nidulans* and *N. crassa*, cellulose degradation has been uncoupled from hemicellulose breakdown (12). In these fungi, the transcription factors *clr-1* and *clr-2* are required for effective breakdown of cellulose into β-1,4-linked glucose oligomers and finally into glucose, with CLR-1 activating transcription of *clr-2*, and CLR-2 driving transcription of numerous cellulase genes (Figure 4.1) (13). The protein of unknown function CLR-3 was identified as a negative regulator of

CLR-1, inhibiting its ability to activate transcription of *clr-2* as well (4). Recently, another transcription factor CLR-4 was characterized. CLR-4 binds to the promoter of *clr-1* as well as the promoter of the adenylate cyclase *cr-1* (14). While transcription factors involved in cellulose degradation have been extensively characterized, upstream effectors have not been clearly identified. It has been suggested that the cellodextrin transporters CDT-1 and CDT-2 also act as receptors for the cellulose signal, but the connection between any receptor and the transcription factors involved is lacking (15).

Fungi have evolved numerous ways to detect changes in their environment, relay that information to the nucleus, and enact transcriptional responses. G protein coupled receptors (GPCRs) comprise the largest known class of membrane-bound receptors in fungi, and use heterotrimeric G proteins to relay their signal (16). Heterotrimeric G proteins are activated when a guanine nucleotide exchange factor (GEF) such as a GPCR causes the Gα subunit to change conformation, releasing GDP and allowing GTP to bind (17). The Gα subunit then dissociates from their GPCR and the Gβγ dimer, and both the Gα and Gβγ may signal downstream effectors, such as adenylate cyclase or mitogen activated protein kinase (MAPK) cascades (18, 19).

Filamentous fungi possess a vast array of GPCRs to detect pheromones, light, and potential carbon sources present in the environment. For example, in *N. crassa,* GPR-4 and its associated Gα GNA-1 are required for growth on poor carbon sources such as glycerol (20). In this species, mutants lacking the *gna-3*

Gα gene do not exhibit great differences in their metabolomes when cultured on 1.5% (high) and 0.15% (low) sucrose. In contrast, the metabolic landscapes of wild type cultured under the same conditions are distinguishable from each other, suggesting that G protein signaling is required for cellular recognition of extracellular carbon (21). The GNA-1 and GNA-3 homologs of *T. reesei* are also known to affect cellulase production under a variety of conditions involving differences in light (22, 23). In *A. nidulans*, Protein Kinase A, a downstream target of G protein signaling, is necessary to localize the CRE-1 homolog to the nucleus (8). In *N. crassa*, strains that overexpress the adenylate cyclase gene *cr-1* exhibit increased levels of eight cellulase mRNAs, as well as higher expression of the transcription factors *clr-1*, *clr-2,* and *xlr-1*(14). Furthermore, the authors of this study noted that addition of cyclic AMP to cultures of the Δ*cr-1* mutant led to increased levels of these transcripts (14).

The work described in Chapter 3 demonstrated that mutants lacking the Gα subunits *gna-1* and *gna-3,* the Gβ subunits *gnb-1* and *cpc-2,* the Gγ *gng-1,* the adenylate cyclase *cr-1,* and strains with the *gna-3*^{Q208L} mutation (a constitutively active *gna-3* allele) have no detectable cellulase activity (24). Apart from the Gα GNA-2, this comprises all G protein subunits in *N. crassa*, as well as the known downstream target *cr-1* (25). Furthermore, we found that transcription of at least five key cellulase enzymes was impaired in Δ*gna-1*, Δ*gna-3*, and Δ*gnb-1* mutants, while expression of these same genes was either unaltered or slightly elevated in Δ*cpc-2* and Δ*cr-1* mutants. Our laboratory previously showed

that cAMP supplementation to the medium rescues phenotypes observed in Δ*gna-3* and Δ*cr-1* mutants during growth on sucrose (26). In Chapter 3, we used this approach to determine whether this was also the case on cellulose medium. We found that cAMP supplementation resulted in detectable activity in Δ*gna-1*, Δ*gna-3*, *gna-3*^{Q208L}, Δ*cr-1*, and Δ*gnb-1* mutants. Additionally, transcription of the five cellulases tested was also remediated in Δ*gna-1*, Δ*gna-3*, and Δ*gnb-1* strains. Since remediation was not complete in the Δ*gna-1* and Δ*gnb-1* mutants, we suggested that GNA-1 and GNB-1 may also regulate cellulase expression using a separate cAMP-independent pathway. In addition, the observation that expression of the cellulase genes in Δ*cr-1* and Δ*cpc-2* strains was normal or elevated suggests that these genes exert post-transcriptional control on cellulase gene transcription.

In this study, I explored the effects of G protein signaling on transcription of cellulase enzymes. I isolated RNA from mutants lacking the G protein subunits *gna-1*, *gna-3*, and the adenylate cyclase *cr-1*, after transfer to medium containing crystalline cellulose (Avicel). I performed RNAseq analysis on the transcriptomes for wild type and the mutants cultured on Avicel. Using RNAseq data for wild type cultured on glucose provided by Alexander Carrillo, I compared the transcriptomes of wild type grown on glucose and Avicel. Finally, I compared the transcriptomes of the G protein mutants to that of wild type *N. crassa* cultured on Avicel. I also used LC/MS to analyze the exoproteome in mutants cultured on cellulose, to determine whether the presence of cellulase enzymes was affected

in any of the mutant backgrounds. Collectively, I show that GNA-1 and GNA-3 are responsible for inducing the cellulolytic transcriptional response in *N. crassa*.

Materials and Methods

Strains and growth conditions

The strains used in this study are indicated in Table 4.1. Strains were cultured on Vogel's Minimal Medium [VM, (27)], with the exception that the indicated carbon source replaced sucrose. All carbon sources were used at a final concentration of 2% (weight/volume). Alternative carbon sources were crystalline cellulose (Avicel-PH101, 50 µm particle; Sigma-Aldrich, St. Louis, MO) or glucose (MP Biomedicals, Santa Ana, CA). Macroconidia (conidia) used for inoculation of cultures were obtained as described (28).

Total RNA isolation and analysis of RNAseq data

Cell pads were collected using vacuum filtration, flash-frozen in liquid nitrogen and then ground using a chilled mortar and pestle with liquid nitrogen. Total RNA was extracted from ground samples using the TRIzol reagent (Thermo Fisher Scientific). Each sample was tested for purity and concentration using a Nanodrop spectrophotometer (Nanodrop 2000c, Thermo Fisher Scientific). Aliquots containing 20 µg of total RNA were treated with RQ1 DNAse (Promega Corporation, Madison, WI) for 30 min at 37°C. RNA samples were then concentrated using the RNA Clean and Concentrator Kit (Zymo Research Corporation, Irvine, CA). Samples were quantified using an Agilent 2100 Bioanalyzer (Agilent, Santa Clara, CA) at the University of California, Riverside

Institute for Integrative Genome Biology and RNA Integrity Numbers (RIN) were assigned to each sample.

RNA samples were submitted to the University of California, Davis DNA Technologies and Expression Analysis Core Laboratory for Illumina library preparation and sequencing. Paired-end sequencing (2x150 bp) was performed using a NovaSeq 6000 with an S4 flow cell (Illumina, San Diego, CA). Raw reads were mapped against a generated index file using Kallisto version 0.46.1 (29) to generate raw counts and transcripts per million reads (TPMs). Differential expression analysis was performed on raw counts that were filtered to include only those genes which had counts greater than 10 using DEseq2 version 1.26.0 (30). DEseq2 uses the Wald test to determine p-values, and then adjusts them using the Benjamini-Hochberg method, resulting in more stringent p-values than a two-tailed Student's t-test. Genes with p-values greater than 0.05 were not considered differentially expressed, and only genes with a $\log_2$ fold difference greater than 2 or -2 (≥4-fold difference) were considered up-regulated or down-regulated in our study. Differentially expressed genes were then filtered to exclude genes with less than 10 transcripts per million. Functional Catalogue analysis of the mis-regulated genes in each mutant was performed using FungiFun 2 (31).

Exoproteome analysis of G protein mutants

Two biological replicates were used for each strain. Cultures were grown as previously described (24) to obtain supernatant protein from *N. crassa* VM Avicel cultures. The supernatants from these cultures were harvested and concentrated 10-fold (Pierce Protein Concentrators PES, 10K MWCO, Thermo Fisher Scientific), and the protein samples were prepared for LC/MS using the protocol from the S-Trap Mini Spin Column kit for trypsin digestion and peptide purification (Protifi, Farmingdale, NY). Peptides were then submitted to the University of California, Davis Proteomics Core Facility for protein identification via LC/MS-MS. Scaffold 4 was used to determine the exclusive spectra for each protein (i.e. spectra that only mapped to a specific protein). Any protein that had 10 or more exclusive spectra was considered to be present in a biological replicate, and proteins that were present in at least one biological replicate were included. Two experiments were performed, with the first using wild type and Δ*gna-1* mutant strains, and the second using wild type, Δ*gna-3,* and Δ*cr-1* strains. The predicted signal peptide tool and transmembrane domain count tool on FungiDB were used to determine which proteins contained a secretion signal and did not possess transmembrane domains, which would therefore qualify them as bonafide members of the exoproteome (32). Functional Catalogue analysis of these proteins was performed using FungiFun 2 (31).

Results

Identification of genes that are differentially regulated in wild type cultures grown on glucose vs. Avicel as a carbon source

We first wanted to compare wild type cultures grown on minimal medium containing 2% glucose as the carbon source to those cultured with 2% Avicel to determine differences in the transcriptome in these two media types. Cultures were grown on glucose medium for 12 hours, and were then transferred to either Avicel or glucose medium. After 4 hours, total RNA was isolated from these cultures and RNAseq was performed. We used Kallisto to generate the raw counts as well as the transcripts per million reads (TPMs). DEseq was used to determine the genes that were differentially expressed across various conditions and genotypes, and a p value less than 0.05 indicated a difference in the expression of the gene under the conditions compared. In this study, we considered genes with a $\log_2$ between 2 and -2 (≥4 fold difference) to be differentially expressed.

Previous work in *N. crassa* used a similar approach to determine which genes were most highly expressed when wild type *N. crassa* was grown in medium containing Avicel (5). This earlier study found that there is a two-stage induction of expression of plant cell wall degrading enzymes, with a 2-10 fold increase of occurring during the first hour following transfer to Avicel or no carbon conditions. After one hour, induction of cellulase genes expression increased several thousand-fold; this increase was not observed in cultures lacking a

carbon source. The authors of this study identified 333 genes that were differentially regulated in no carbon cultures vs. Avicel grown cultures. A total of 212 genes were up-regulated during growth under Avicel conditions and were defined as the “Avicel regulon”. While these genes are clearly important to cellulose degradation and are not indicative of a starvation response, they are not a direct comparison between Avicel and rich, CCR-inducing conditions, such as medium containing sucrose or glucose.

In our study, we compared the transcriptomes of wild type cultures grown on glucose vs. Avicel. This revealed a total of 1124 genes that were differentially expressed. From these, we identified 770 that were up-regulated, and 359 that were down-regulated. Of the 770 genes that were up-regulated, 155 encode predicted proteins with a secretion signal, and 153 of these are in common with the 212 genes of the Avicel regulon as previously defined (5). Additionally, of the 31 previously identified cellulase genes in *N. crassa*, 22 are more highly expressed in this group based on the criteria described above (Figure 4.2) (33). Four of the 31 genes were differentially expressed, but did not have TPMs >10 in wild type grown on Avicel. The other five cellulase enzyme genes were not differentially expressed compared to wild type on glucose.

The Functional Catalogue (FunCat) is a robust tool for assigning functions to large groups of genes present in omics datasets regardless of the organism, and is commonly used to determine what types of genes are represented (34). Additionally, FungiFun2 is a user-friendly resource that has been optimized to

search fungal databases specifically (31). We used FungiFun2 to determine category associations for those genes which were differentially expressed in wild type in Avicel relative to glucose. The top ten categories assigned to the up-regulated 770 genes include polysaccharide metabolism (62 genes), C-compound and carbohydrate transport (29 genes), sugar, glucoside, polyol and carboxylate metabolism (52 genes), degradation / modification of foreign (exogenous) polysaccharides (10 genes), and cellular import (40 genes) (Figure 4.3A). From this, it is clear that wild type is under carbon catabolite repression during growth in glucose and that genes required for degradation of complex polysaccharides are up-regulated in wild type during growth on Avicel medium.

Of the 359 genes down-regulated in Avicel medium, 29 were predicted to encode secreted proteins. Two of these 359 genes were members of the Avicel regulon, including a nitrite reductase (NCU04720) and a gene that encodes a hypothetical protein, (NCU04928). The top ten categories assigned to this group of genes include assimilation of ammonia/metabolism of the glutamate group (18 genes), biosynthesis of vitamins, cofactors, and prosthetic groups (24 genes, metabolism of the pyruvate family (alanine, isoleucine, leucine, valine) and D-alanine (13 genes), metabolism of the aspartate family (25 genes) and metabolism of the cysteine - aromatic group (28 genes) (Figure 4.3B). It appears that after the transfer from glucose to Avicel, wild type *N. crassa* down-regulates other metabolic pathways, particularly those involved in amino acid and nitrogen metabolism.

Identification of genes that are differentially regulated in Δ*gna-1* mutants

We next investigated the transcriptional effect of gene deletion of *gna-1*, *gna-3*, and *cr-1* during Avicel growth conditions. We have previously shown that these genes are required for effective cellulose degradation and variously implicated in transcription of a small group of cellulase genes (Chapter 3). We next wished to determine whether these genes were required more globally for expression of cellulases and other genes during growth on Avicel (24). Among the three mutants, Δ*gna-1* had the greatest expression differences relative to wild type, supporting the hypothesis that *gna-1* plays a significant role in transcriptional regulation of the cellulose response (24). Δ*gna-1* mutants had 699 genes that were differentially regulated relative to wild type during growth on Avicel. Of these, 348 genes were down-regulated and 351 were up-regulated in comparison to wild type in Avicel conditions. These 348 genes share 86 genes in common with the 212 genes present in the Avicel regulon, and 20 of the 22 highly expressed cellulases found in wild type *N. crassa* are significantly down-regulated in Δ*gna-1* mutants (Figures 4.4, 4.5, and 4.6). The two cellulases that are not down-regulated are NCU05057, an endoglucanase, and NCU08755, a cell wall bound β-glucosidase (35). Most of the other 18 genes are required for proper cellulose degradation. In many cases, missing even one of them results in loss of total cellulose conversion into glucose (36, 37). Despite the low levels of cellulase enzyme transcripts, the transcription factors *clr-1*, *clr-2*, and *clr-4* were

not differentially regulated according to our criteria in Δ*gna-1* mutants (See Figure 4.1 for a description of the roles of these transcription factors). However, the product of the *clr-3* gene, which is known to inhibit CLR-1 in the absence of cellulose, was differentially down-regulated in Δ*gna-1* mutants (4). Additionally, transcript levels were lower for *clr-1* and *clr-4* (3.64 -fold and 3.51-fold, $p < 0.05$), despite not meeting our thresholds. While the decrease in *clr-3* mRNA levels would suggest that Δ*gna-1* mutants should have increased cellulase enzyme levels, as well as increased levels of the *clr-2* transcript, this is not the case, possibly due to the lower levels of *clr-1*.

Functional Catalogue enrichment for the 348 down-regulated genes in the Δ*gna-1* mutant supported the finding that cellulose metabolism is impaired, as the top four categories were polysaccharide metabolism (40 genes), sugar, glucoside, polyol and carboxylate metabolism (32 genes), degradation / modification of foreign (exogenous) polysaccharides (8 genes), and extracellular polysaccharide degradation (7 genes) (Figure 4.7A). All of these categories were also enriched in the 770 up-regulated genes in wild type cultures cultured on medium containing Avicel.

Functional Catalogue analysis for the 351 up-regulated genes in the Δ*gna-1* mutant showed that some up-regulated genes do fall into the categories of sugar, glucoside, polyol and carboxylate metabolism (14 genes) and polysaccharide metabolism (19 genes), although the numbers of these genes are reduced compared to wild type (compare Figure 4.3A to Figure 4.7B). Other

enriched categories include metabolism of fatty acids (9 genes), secondary products derived from L-phenylalanine and L-tyrosine (5 genes) are up-regulated processes, indicating that metabolism is not solely focused on cellulose in this mutant.

Identification of genes that are differentially regulated in Δ*gna-3* mutants

Δ*gna-3* mutants had 309 genes differentially expressed relative to wild type, with 107 differentially down-regulated and 202 genes up-regulated in comparison to wild type. Only 24 of these 107 genes are in common with the 212 in the Avicel regulon, and only 3 of the 22 highly expressed cellulase enzymes were found to be transcriptionally down-regulated in Δ*gna-3* mutants according to our criteria (Figure 4.4, 4.5, and 4.6). However, the group of down-regulated genes includes the cellobiose dehydrogenase *cdh-1* (NCU00206). Gene deletion of this enzyme results in a reduction of cellulase activity between 37-49% of wild type (37). The other two enzymes that are down-regulated in Δ*gna-3* mutants are NCU02916, which encodes an endoglucanase, and NCU05955, which encodes the *N. crassa* homolog of *cel74a*, a xyloglucanase from *T. reesei.* In *T. reesei*, gene deletion of this enzyme results in an 8-fold reduction of glucose released from sugarcane baggase (38). This suggests that *cel74a* may assist in the function of β-glucosidases and cellobiohydrolases by increasing access to reducing ends in cellulose in a manner like endoglucanases and polysaccharide monooxygenases. The combined reductions in mRNA levels for NCU05955 and

NCU00206 could potentially be enough to explain the complete loss of cellulase activity observed in Δ*gna-3* mutants described in Chapter 3. Additionally, Δ*gna-3* mutants had normal levels of *clr-2* and *clr-4* transcripts, but lower levels for *clr-1* [albeit not reaching our cutoff levels (2.96-fold, $p < 0.05$)]. Furthermore, in contrast to Δ*gna-1* mutants, Δ*gna-3* strains did not have altered levels of *clr-3* mRNA. Since all three of the cellulose-related transcription factors are expressed at normal levels in Δ*gna-3* mutants, GNA-3 may be required for a post-transcriptional mechanism controlling cellulase expression.

FunCat analysis showed that the top 10 enriched categories in the 107 down-regulated genes in the Δ*gna-3* mutant included polysaccharide metabolism (11 genes), sugar, glucoside, polyol and carboxylate metabolism (7 genes), and extracellular polysaccharide degradation (2 genes) (Figure 4.8A). This is indicative of the incorrect response to cellulose we have previously observed in these mutants and may be a result of an inability to detect cellulose outside the cell. For the 202 up-regulated genes in the Δ*gna-3* mutant, the categories include fatty acid metabolism and metabolism of the pyruvate family (alanine, D-alanine, isoleucine, leucine, valine), indicating an improper metabolic response (Figure 4.8B). An intriguing observation was that the categories for heat shock response, alcohol fermentation, and drug/toxin transport were also enriched in this group, suggesting a stress response.

Identification of genes that are differentially regulated in Δ*cr-1* mutants

We observed that Δ*cr-1* mutants had 133 genes differentially expressed, with 38 down-regulated and 95 genes up-regulated in comparison to wild type. GNA-1 and GNA-3 are thought to act upstream of CR-1, but despite this, only 13 of the 212 genes of the Avicel regulon and none of the 22 cellulase genes were down-regulated in Δ*cr-1* mutants (Figures 4.4, 4.5, and 4.6) (26, 39). This is consistent with the observation in Chapter 3 that loss of *cr-1* does not have the same transcriptional effect as deletion of either Gα gene, despite the fact that Δ*cr-1* mutants do exhibit complete loss of cellulase activity (24). Additionally, Δ*cr-1* mutants did not exhibit mis-regulation of *clr-1, clr-2, clr-3,* or *clr-4.* These results suggest that Δ*cr-1* mutants are still able to receive the cellulose signal. They also support the hypothesis that, apart from its enzymatic conversion of ATP to cAMP, *cr-1* affects another post-transcriptional process of cellulose metabolism.

For the 38 down-regulated genes in Δ*cr-1* mutants, FunCat analysis showed enrichment in polysaccharide metabolism (6 genes), degradation / modification of foreign (exogenous) polysaccharides (2 genes), sugar, glucoside, polyol and carboxylate metabolism (4 genes) and C-2 compound and organic acid metabolism (2 genes) (Figure 4.9A). While enrichment in these categories does suggest some transcriptional down-regulation of cellulose metabolism in Δ*cr-1* mutants, it is not to the extent seen in the other two mutants. FunCat analysis of the 95 highly expressed genes resulted in only five categories. These

were tissue pattern formation (2 genes), homeostasis of anions (2 genes), phosphotransferase system (1 gene), fatty acid metabolism (3 genes), and gas and metabolite distribution (1 gene) (Figure 4.9B).

While our definition of differentially expressed genes ($p < 0.05$, ≥ 4-fold difference) does show major differences in the transcriptomes of these mutants relative to wild type and encompasses many of the cellulase genes, it is important to note that there is still transcriptional down-regulation of the 22 cellulases in both Δ*gna-3* and Δ*cr-1* mutants, as defined by a significant decrease in total TPMs present for the different members of the glycoside hydrolase families in all three mutants. For example, of the 22 highly expressed genes, the β-glucosidases NCU00130 and NCU08755 meet our p-value, but not our fold difference, threshold (3.76-fold and 2.08-fold, respectively) in Δ*gna-3* mutants. The low transcript levels for 2/3 *N. crassa* β-glucosidases may contribute to the lack of cellulase activity in the Δ*gna-3* mutant. Additionally, NCU07760, a polysaccharide monooxygenase is down-regulated in all three mutants (13.54-fold, 3.83-fold, and 3.36-fold in Δ*gna-1,* Δ*gna-3,* and Δ*cr-1* mutants respectively).

Comparison of the down-regulated genes across the mutant strains

Further, we examined the transcriptomes of the Δ*gna-1*, Δ*gna-3*, and Δ*cr-1* mutants to determine whether any genes are down-regulated in common across the mutants (Figure 4.10). We found that Δ*gna-1* and Δ*gna-3* mutants had the most shared genes, with 62 down-regulated in both of these genotypes (Table 4.2). FunCat enrichment of these 62 genes included degradation / modification of foreign (exogenous) polysaccharides (4 genes), polysaccharide metabolism (7 genes), extracellular aminosaccharide degradation (1 gene), sugar, glucoside, polyol and carboxylate metabolism (5 genes), defense related proteins (2 genes), mRNA synthesis (1 gene), and degradation / modification of foreign (exogenous) ester compounds (1 gene). Of the 22 cellulase enzymes highly expressed in wild type, *cdh-1, cel74a,* and *gh61-3* (NCU00206, NCU05955, and NCU02916) are both down-regulated in Δ*gna-1* and Δ*gna-3* strains.

Δ*gna-1* and Δ*cr-1* mutants had 10 genes in common that were down-regulated (Table 4.3). FunCat analysis for these 10 genes produced categories for regulation of amino acid metabolism (1 gene), pyridoxal phosphate binding (1 gene) and heat shock response (1 gene). Δ*gna-3* and Δ*cr-1* mutants only had two genes in common that were down-regulated, which code for NCU16615 (a hypothetical protein) and NCU16915 (pheromone *mfa-1,* the *mata* pheromone) (40). We also found that among all three mutants, 10 genes were commonly down-regulated (Table 4.4) and were enriched for polysaccharide metabolism (4

genes), extracellular ester compound degradation (2 genes), virulence/disease factors (2 genes) and degradation / modification of foreign polysaccharides (2 genes). These results suggest that the mutants are impaired in metabolism of complex extracellular carbon sources.

We also compared the mRNA levels of the transcriptional regulators *clr-1*, *clr-2, clr-3, clr-4,* and *cre-1* in the three mutant backgrounds to wild type (Figure 4.11). We found that *clr-2* and *cre-1* did not have different expression levels from wild type in any of the mutant backgrounds using the statistical test in the DESeq2 package. The transcriptional regulator *clr-3* was down-regulated in Δ*gna-1* mutants, suggesting that this strain should have higher levels of cellulases. Using the Student's t-test, we found that *clr-2* was significantly down-regulated in all three mutant backgrounds, albeit to a lesser degree in Δ*cr-1*. The levels of *clr-1* were significantly reduced in both Δ*gna-1* and Δ*gna-3* mutants as well, but did not meet our criteria for down-regulation (≥4-fold difference). This was also observed for *clr-4* in the Δ*gna-1* mutant relative to wild type.

Subtle fluctuations in the levels of transcription factors may have a greater effect than other genes. Lower levels of *clr-1* and *clr-2* may explain the loss of cellulase transcription in both Δ*gna-1* and Δ*gna-3* strains. As mentioned above, *clr-3* mRNA levels are down-regulated in the Δ*gna-1* background, suggesting that cellulase transcription should be higher in this background. However, the reduction of *clr-1* mRNA in this mutant may explain why this effect is not observed. Levels of all five of these genes were unaffected in Δ*cr-1* mutants,

supporting our previous findings that *cr-1* does not affect cellulases transcriptionally.

Analysis of the exoproteome of G protein and adenylate cyclase mutants

For filamentous fungi to metabolize extracellular polymers, they must secrete degradative enzymes to break down the polymers into smaller molecules. In the case of cellulose, the cellulase enzyme cocktail is capable of degrading cellulose to cellobiose and glucose. This allows entry of these smaller units into the cell via transporters. *N. crassa* possesses a dual affinity glucose transport system that has been well characterized (41). In high glucose conditions, the low affinity glucose transporter GLT-1 is the primary means of bringing glucose into the cell. However, under low glucose conditions, such as in Avicel, the high affinity glucose transporters (HGT-1 and HGT-2) are responsible for uptake of glucose. For transport of β-1,4 linked glucose oligomers (cellodextrins), the cellodextrin transporters (CDT-1 and CDT-2) primarily transport the disaccharide cellobiose across the plasma membrane. The *cdt-1* and *cdt-2* genes are functionally redundant and gene deletion mutants lacking both *cdt-1* and *cdt-2* are not able to induce cellulase transcription (15). All five of these transporters have been hypothesized to take part in the signal transduction mechanism of the cellulose response. The presence of these transporters implies that incomplete cellulose breakdown will still allow smaller cellodextrins to enter

the cell, and it has been hypothesized that these cellodextrins, particularly the glucose dimer cellobiose, activate the cellulose response (15)

In Chapter 3, we showed that the G protein mutants (with the exception of Δ*gna-2*) are not able to degrade Avicel completely to glucose (24). While supernatant protein levels in most of the mutants were at the same level as that in wild type, we suggested that the extracellular enzyme cocktail in these mutants is either not the same composition as wild type cultures, or that the proteins are not in the right abundance necessary for cellulose degradation to occur. Secretion is a necessary process for production of functional cellulase enzymes, as previous work has indicated that defects in the secretory machinery can disrupt cellulase transport (42). Additionally, many cellulases are modified post-translationally by glycosylation, which is necessary for them to bind to cellulose (43, 44). If these processes are perturbed, cellulases may be secreted outside the cell, but not be functional. This would result in an inability to degrade cellulose to glucose in these mutants.

In order to investigate the composition of the exoproteome of wild type and the three mutants, cultures were grown overnight in glucose medium, and then were transferred for three days to Avicel medium. The supernatants from these cultures were harvested and the protein samples were prepared for protein identification via LC/MS-MS. Scaffold 4 was used to determine the exclusive spectra for each protein (i.e. spectra that only mapped to a specific protein). Any protein that had 10 or more exclusive spectra was considered to be present in a

biological replicate, and proteins that were present in at least one biological replicate were included. Two experiments were performed, with the first using wild type and Δ*gna-1* mutant strains, and the second using wild type, Δ*gna-3,* and Δ*cr-1* strains. The predicted signal peptide tool and transmembrane domain count tool on FungiDB were used to determine which proteins contained a secretion signal and did not possess transmembrane domains, which would therefore qualify them as bonafide members of the exoproteome (32). FunCat analysis was again used to categorize the groups of genes found in this experiment (31).

In the first experiment, there were 109 proteins detected that were secreted and possessed no transmembrane domains in wild type. A total of 19 of the 31 cellulase enzymes were detected in this experiment, and of the 13 enzymes detected via quantitative proteomics, 9 were observed in our wild type exoproteome (45). FunCat analysis showed that the proteins present in wild type only were enriched for polysaccharide metabolism (6 genes), extracellular polysaccharide degradation (4 genes), and degradation / modification of exogenous (foreign) polysaccharides (3 genes).

In Δ*gna-1* mutants, there were 111 proteins found under the same conditions (Figure 4.12). Of the 31 *N. crassa* cellulases, 18 were detected in both wild type and Δ*gna-1* mutants. Wild type only had one cellulase enzyme detected that was not present in Δ*gna-1* mutants, which was GH61-8 (NCU03000), a polysaccharide monooxygenase. This protein was not detected previously via

quantitative proteomics, and there is no current evidence that losing this particular polysaccharide monooxygenase eliminates cellulase activity (45).

In the second experiment, 87 proteins were detected in wild type that had both a secretion signal and no transmembrane domains. Of the 31 cellulases, we detected 18 in wild type in the second experiment. Three of the cellulase enzymes found in wild type in the first experiment were not detected in the second experiment. These were GH61-8, GH61-6, and GH6-1 (NCU03000, NCU03328, and NCU03996). All of the nine cellulase enzymes that were previously detected by quantitative proteomics found in wild type in Experiment 1 were found in Experiment 2. Those proteins that were present in wild type only were enriched for polysaccharide metabolism (5 genes), sugar, glucoside, polyol and carboxylate metabolism (5 genes), and degradation / modification of foreign (exogenous) polysaccharides (2 genes).

In Δ*gna-3* and Δ*cr-1* mutants, 88 and 98 proteins were detected, respectively (Figure 4.11). Δ*gna-3* mutants possessed all of the 18 cellulases detected in wild type in this experiment. The Δ*cr-1* secretome was missing one cellulase; GH7-4 (NCU05104), an exoglucanase. This protein was not one of the major cellulase enzymes detected via quantitative proteomics (45).

Δ*gna-1* mutants lack 17 of the proteins found in wild type (Table 4.5). While these enzymes are not annotated as cellulases, they are required for polysaccharide metabolism, and may prevent Δ*gna-1* mutants from efficiently degrading cellulose. Δ*gna-3* mutants were missing 22 proteins present in the wild

type secretome (Table 4.6) and 16 proteins were present in wild type but missing from Δ*cr-1* mutants (Table 4.7). Proteins that were found in wild type but not in Δ*cr-1* mutants were enriched for polysaccharide metabolism (4 genes) and sugar, glucoside, polyol and carboxylate metabolism (3 genes). Δ*gna-1* mutants also possessed 19 proteins not present in wild type samples (Table 4.5). Δ*gna-3* mutants had 23 proteins that were not found in wild type (Table 4.6). Δ*cr-1* was also the most unique relative to wild type in the proteins secreted, containing 27 proteins not present in the wild type (Table 4.7). The results from the exoproteome analysis provided evidence for aberrant protein secretion in all three mutant backgrounds.

Discussion

To our knowledge, this is the first comprehensive look at the cellulose transcriptome and exoproteome of Gα protein and adenylate cyclase mutants in *N. crassa*. In this study, we support our previous observation that the G protein subunits GNA-1 and GNA-3 are required for a proper transcriptional response to extracellular cellulose. The results suggest that Δ*gna-1* and Δ*gna-3* mutants appear unable to detect cellulose and without intact G protein signaling, the organism is unable to effectively receive the cellulose signal, and therefore cannot respond successfully.

Previous studies outline the importance of the transcription factors CLR-1 and CLR-2 to cellulose degradation in *N. crassa* (5). Additionally, the transcription factor CLR-4 and the hypothetical protein CLR-3 are also critical to this process (4, 14). However, only *clr-3* was altered in the Δ*gna-1* mutant by our criteria (≥4-fold difference) in the mutants. However, when using the Student's t-test, we saw that *clr-2* is significantly down-regulated in all three mutant backgrounds. Additionally, *clr-1* mRNA is reduced in both Δ*gna-1* and Δ*gna-3* mutants, and *clr-4* mRNA is also reduced in Δ*gna-1.* The lower levels of these transcriptional regulators may explain why several cellulase genes are down-regulated in these genetic backgrounds. Of the numerous cellulase genes that are down-regulated in Δ*gna-1* and Δ*gna-3* mutants, we found that *cdh-1* and the homolog of *T. reesei cel74a* were significantly down-regulated (≤ 4-fold

difference). It is possible that while the abundance of the transcription factors is not altered, the signaling to them is severely hampered.

As in previous work, we also wanted to determine if the mRNA levels for any of the G protein subunits or their known downstream targets were affected. This includes *cr-1*, the two catalytic subunits of Protein Kinase A, *pkac-1* and *pkac-2*, as well as the regulatory subunit, *mcb*. We found that according to our criteria (≤ 4-fold difference), none of these genes were differentially regulated in the mutant backgrounds relative to wild type.

We found that detectable amounts of the cellulase enzymes were present in the exoproteomes of all three mutants (33). Since our method was not quantitative, it is possible that despite their presence, either the cellulase enzymes are at much lower levels than those in wild type, or their function is critically impaired. If these proteins are as abundant in the mutant samples as they are in wild type, then it is most likely that these cellulases are nonfunctional. However, due to the severe down-regulation of these cellulases observed in the transcriptional profiling data, it is perhaps reasonable to conclude that these proteins are most likely not as abundant in the mutant backgrounds.

Δ*gna-1* mutants exhibit transcriptional down-regulation of 20 of the 22 cellulase enzymes highly expressed in wild type under Avicel growth conditions. This result highlights the importance of GNA-1 not only as a carbon sensor, but also as a cellulose specific inducer of cellulase enzyme transcription (20). In *T. reesei*, the Group I Gα homologous to GNA-1 is a known positive regulator of

cellulase transcription (23). Additionally, recent work in *Chaetomium globosum* illustrated the importance of GNA-1 in this process, as a mutant containing a knocked down version of the *C. globosum* homolog of *gna-1* exhibited transcriptional down-regulation of several important cellulase enzymes (46).

In Δ*gna-3* mutants, we observed that three cellulase enzymes were transcriptionally down-regulated, and that two of the three β-glucosidases (NCU00130 and NCU08755) and a polysaccharide monooxygenase (NCU07760) were down-regulated, despite not meeting our threshold levels. Down-regulation of these six genes alone may be enough to impact cellulose degradation in the manner we observed in Chapter 3. It is also possible that GNA-3 is affecting cellulase production in both its regulation of transcription and in its effects on the activity of adenylate cyclase, as Δ*gna-3* mutants exhibit very poor growth when inoculated directly to Avicel-containing medium (24). The GNA-3 homolog is known to affect cellulase activity in *T. reesei*, (22). However, to our knowledge, the only evidence supporting transcriptional regulation of cellulase enzymes in filamentous fungi via a Group III Gα is from our previous work, showing that Δ*gna-3* mutants down-regulate five key cellulase mRNAs (24).

While CR-1 itself appears to not be a key transcriptional regulator, it is necessary for proper cellulase export and activity, as Δ*cr-1* mutants had the most distinct exoproteome from wild type, and lack the ability to convert cellulose completely into glucose (24). It is possible that CR-1 affects the activity or

stability of the components of the secretory pathway. Previous work indicates that without ERV-29 and other p24 cargo adaptors present in the endoplasmic reticulum, the major cellulases CBH-1 and CBH-2 cannot exit the cell (42). It is also possible that CR-1 is altering post-translational processing of celluloytic enzymes, causing cellulases to be secreted but inactive upon being released from the cell.

We also observed that all three mutant strains are impaired in their ability to respond to extracellular carbon sources, since all three mutants had significant groups of up-regulated genes that were not involved in cellulose metabolism. FunCat analysis of the up-regulated genes for all three mutants were enriched for fatty acid metabolism (9, 8, and 3 genes for Δ*gna-1,* Δ*gna-3,* and Δ*cr-1* mutants respectively). Additionally, both Δ*gna-1* and Δ*gna*-3 mutants were enriched for polysaccharide metabolism (19 genes and 14 genes respectively, 11 of which are in common). A closer look at these groups indicate that none of them are in common with the 212 of the Avicel regulon. Included in these two groups are two chitinases, an α-amylase, and an endo-1,3 (4)-β-glucanase. Additionally, Δ*gna-1,* Δ*gna-3,* and Δ*cr-1* mutants had 21, 41, and 8 genes in common with the genes that were transcriptionally down-regulated in wild type cultured on Avicel medium compared to glucose cultures. Only one gene was found in common among all three mutants: *chit-1* (NCU02184) which encodes a chitinase. Taken together, these results suggest that these mutants are incapable of sensing what carbon source is present in the medium.

From this work, we further illustrate that G protein signaling through the Gα subunits GNA-1 and GNA-3 controls cellulase transcription. We also show that CR-1 is an important regulator of proper cellulase secretion and suggest that CR-1 is involved in post-transcriptional processing of this class of enzymes. Without these three proteins, the cellulose signal is not able to activate transcription of the genes needed for metabolism of this complex carbohydrate.

Figures

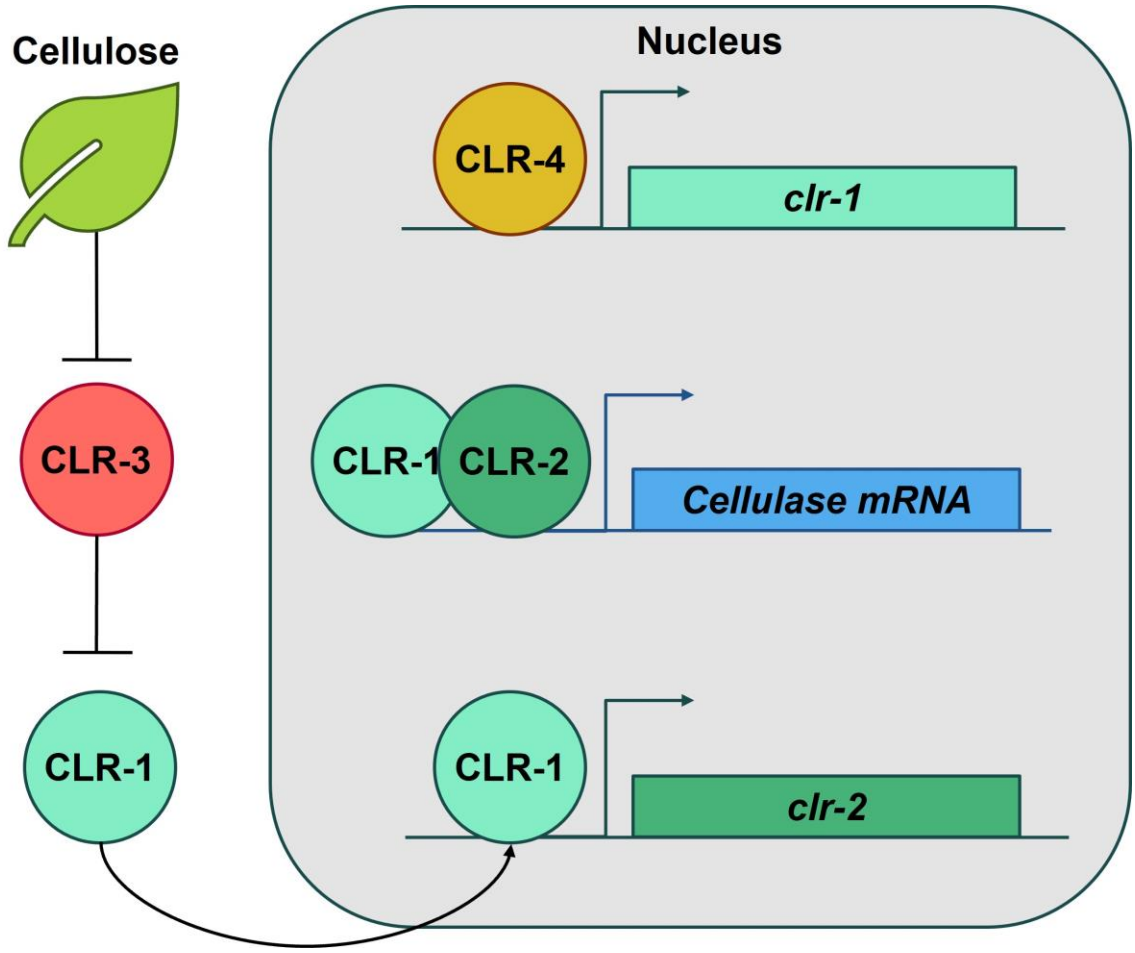

Figure 4.1. Relationships between the CLR transcriptional regulators in *N. crassa*. Cellulose detection relieves carbon catabolite repression via the transcription factors in the CLR pathway. Upon cellulose detection, the activity of CLR-3 is repressed, allowing CLR-1 to activate transcription of *clr-2* (4). Cellulase transcription is then driven primarily by CLR-2, but also partially by CLR-1 (5). CLR-4 binds to the promoter region of *clr-1* (14).

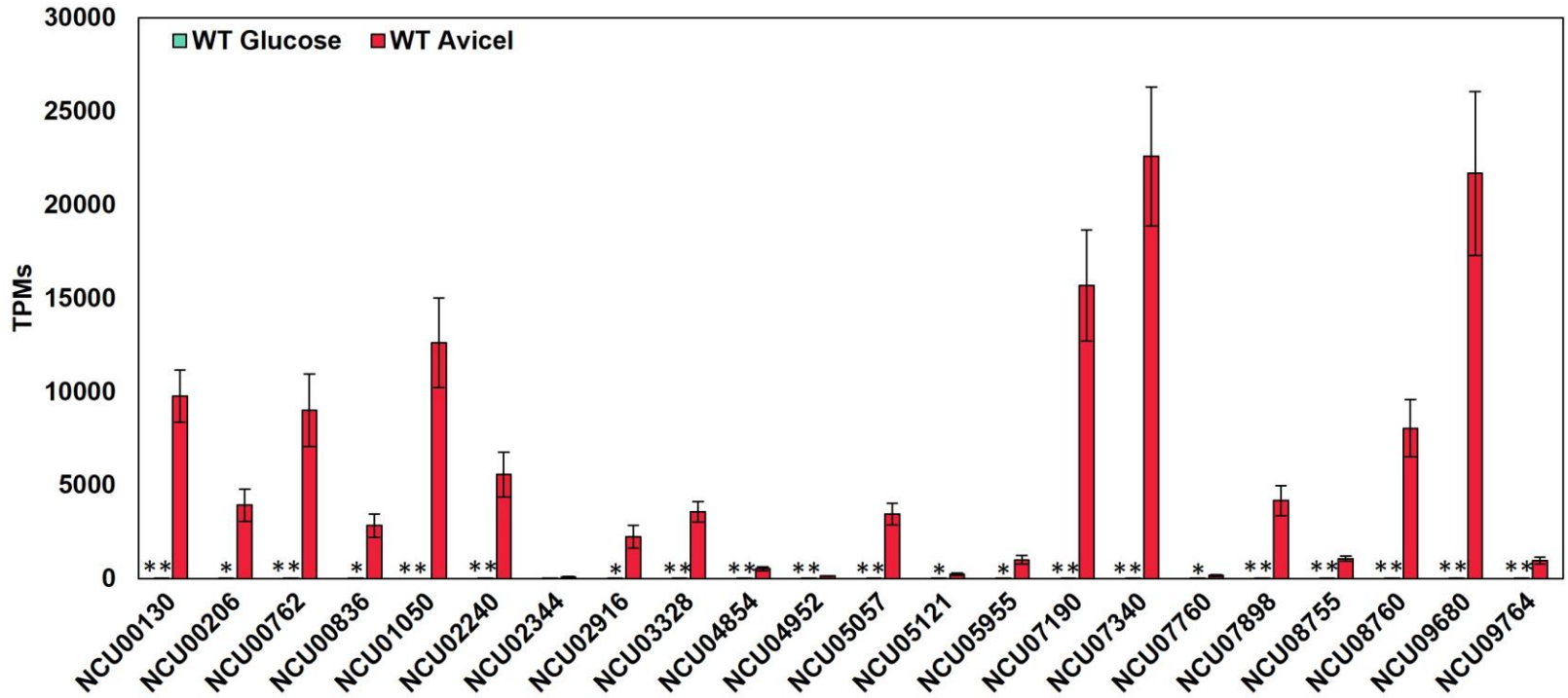

Figure 4.2. Expression of the cellulase enzymes found to be highly expressed in wild type cultured on VM Avicel. Cultures were grown for 12 h on VM-Glucose, then were washed twice in VM without a carbon source. The cultures were transferred to VM-Cellulose or to fresh VM-Glucose for 4 h. Total RNA was isolated and was submitted for PolyA RNAseq analysis. Kallisto was used to map paired reads to known mRNA sequences to generate the counts for each gene. The dataset was then curated to only include genes that had 10 counts or greater. DEseq2 was used to determine differences between VM Glucose cultures and VM Avicel cultures. Genes shown in the heatmap have a log2 fold change that is at least 2 or -2 (4 fold or greater difference), and were limited to 10 or greater TPMs. 22 of the 31 annotated cellulases were found in the 770 genes highly expressed in wild type grown in Avicel conditions Statistical significance relative to wild type on Avicel was determined using a two-tailed Students T-Test and strains with TPMs significantly different than wild type are indicated by an asterisk ($p < 0.05$ = *, $p < 0.01$ = **)

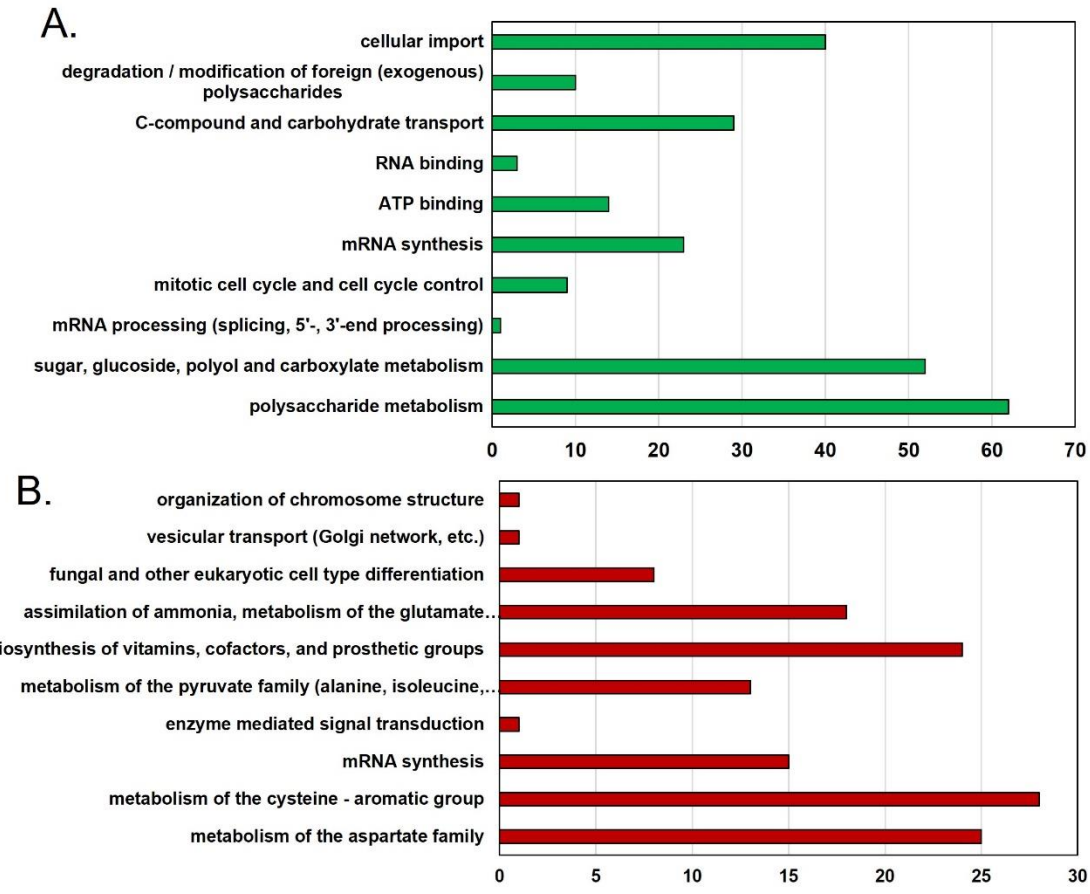

Figure 4.3. Functional Catalogue Analysis of the differentially expressed genes in wild type in glucose vs. Avicel conditions. Cultures were grown as described in the legend for Figure 4.2. Fungifun2 was used to annotate categories for the up-regulated 770 and down-regulated 359 genes in wild type cultures using the Functional Catalogue. Categories were considered significantly enriched if they had a p value less than 0.05, and the third level of the Functional Catalogue was used.

- **A. The top ten categories represented in the 770 highly expressed genes in wild type cultured on VM Avicel.** Functional catalogue were assigned to the 770 genes highly expressed in wild type on VM Avicel.
- **B. The top ten categories represented in the 359 highly expressed genes in wild type cultured on VM Avicel.** Functional catalogue were assigned to the 359 genes poorly expressed in wild type on VM Avicel.

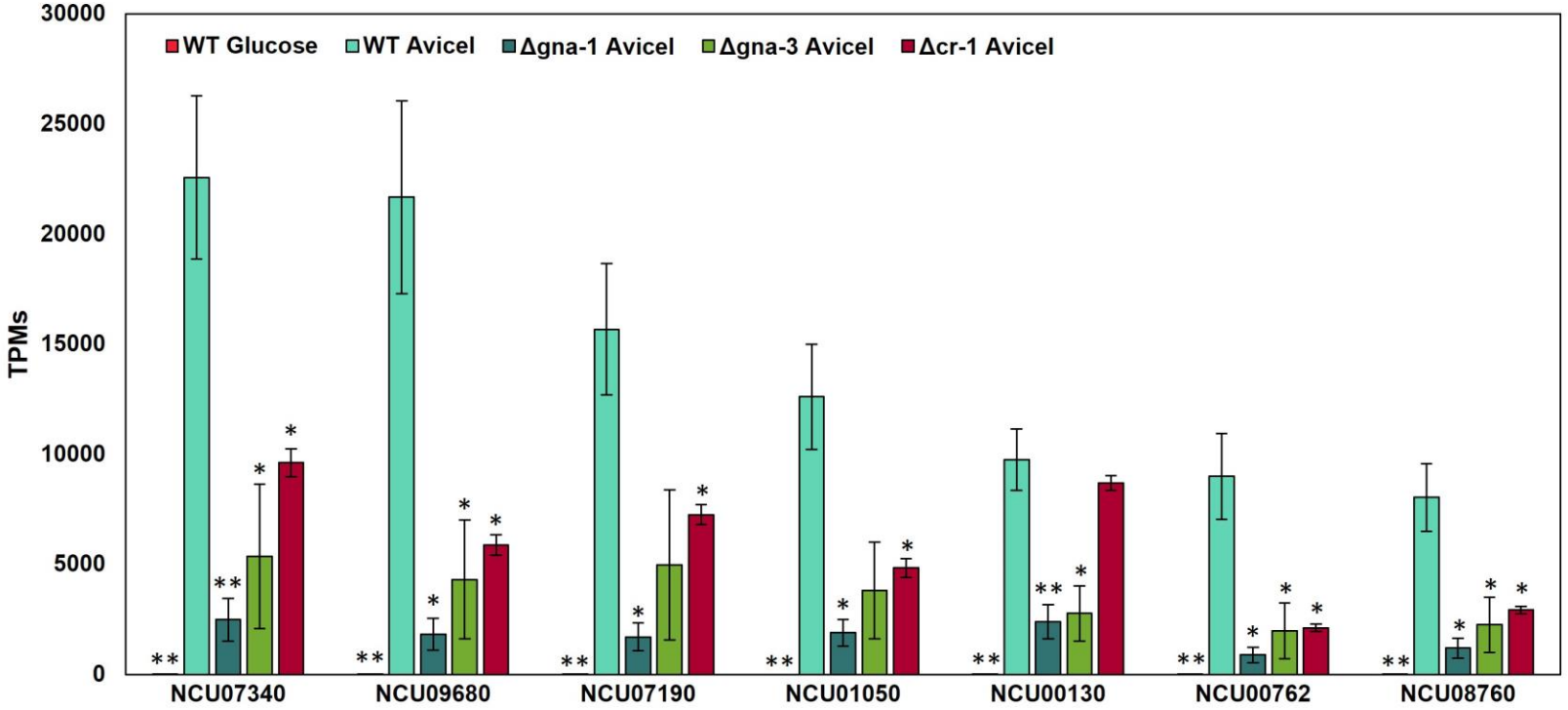

Figure 4.4. Expression of the 7 cellulase enzymes expressed between 25000 and 10000 TPMs in wild type cultured on VM Avicel. The TPMs for the 7 cellulase enzymes were used for each mutant strain as well as wild type. TPMs were generated using Kallisto. Three biological replicates were used and the standard error was used to calculate the error bars. Statistical significance relative to wild type on Avicel was determined using a two-tailed Students T-Test and strains with TPMs significantly different than wild type are indicated by an asterisk ($p < 0.05$ = *, $p < 0.01$ = **)

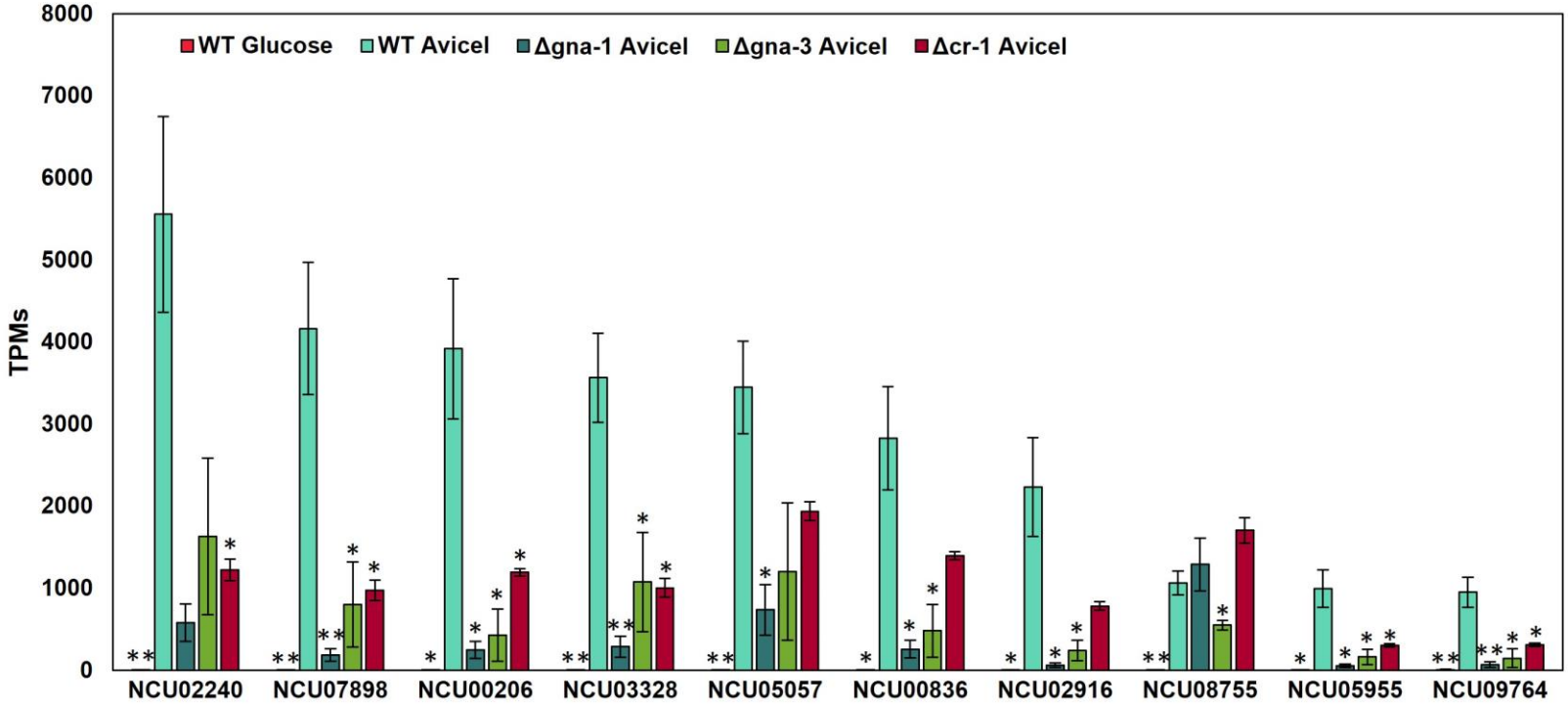

Figure 4.5. Expression of the 10 cellulase enzymes expressed between 6000 and 1000 TPMs in wild type cultured on VM Avicel. The TPMs for the 10 cellulase enzymes were used for each mutant strain as well as wild type. TPMs were generated using Kallisto. Three biological replicates were used and the standard error was used to calculate the error bars. Statistical significance relative to wild type on Avicel was determined using a two-tailed Students T-Test and strains with TPMs significantly different than wild type are indicated by an asterisk ($p < 0.05$ = *, $p < 0.01$ = **)

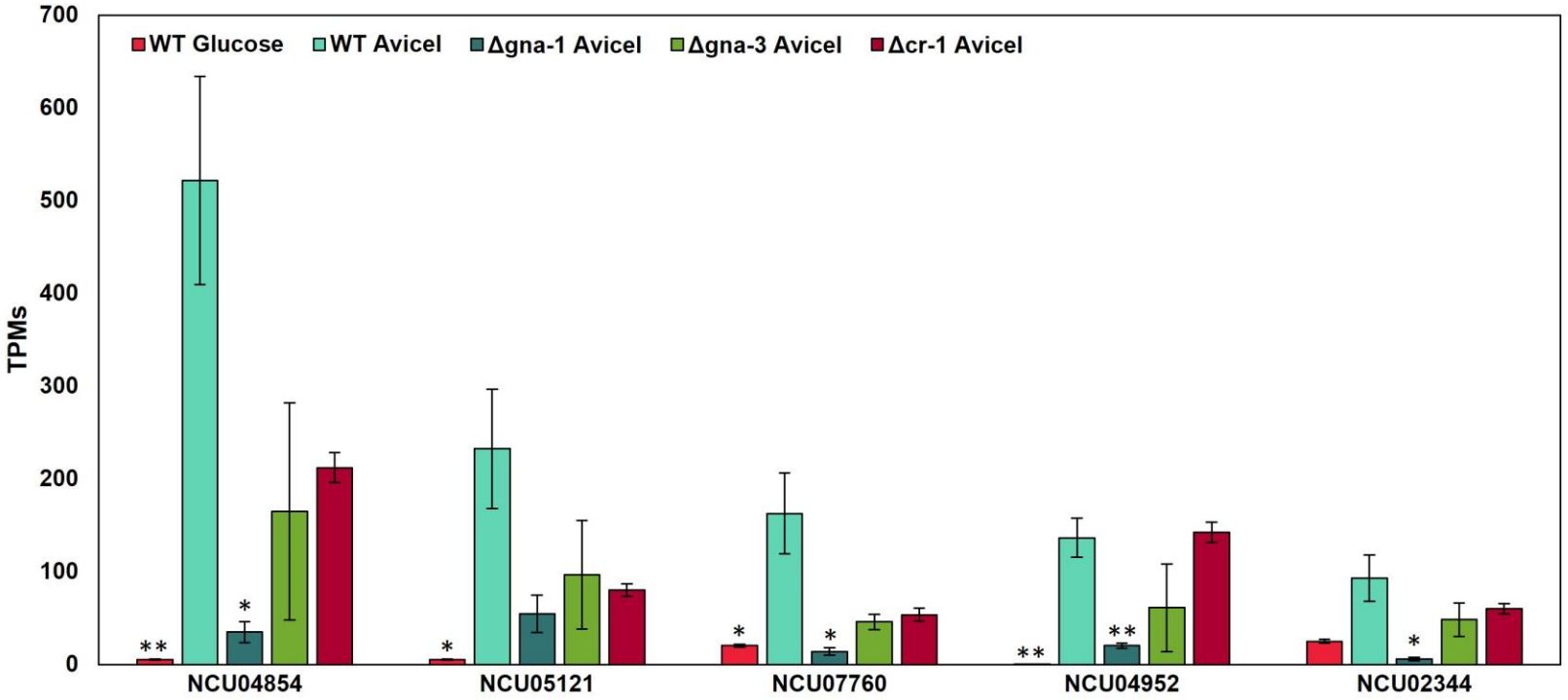

Figure 4.6. Expression of the 5 cellulase enzymes expressed between 600 and 100 TPMs in wild type cultured on VM Avicel. The TPMs for the 5 cellulase enzymes were used for each mutant strain as well as wild type. TPMs were generated using Kallisto. Three biological replicates were used and the standard error was used to calculate the error bars. Statistical significance relative to wild type on Avicel was determined using a two-tailed Students T-Test and strains with TPMs significantly different than wild type are indicated by an asterisk ($p < 0.05$ = *, $p < 0.01$ = **)

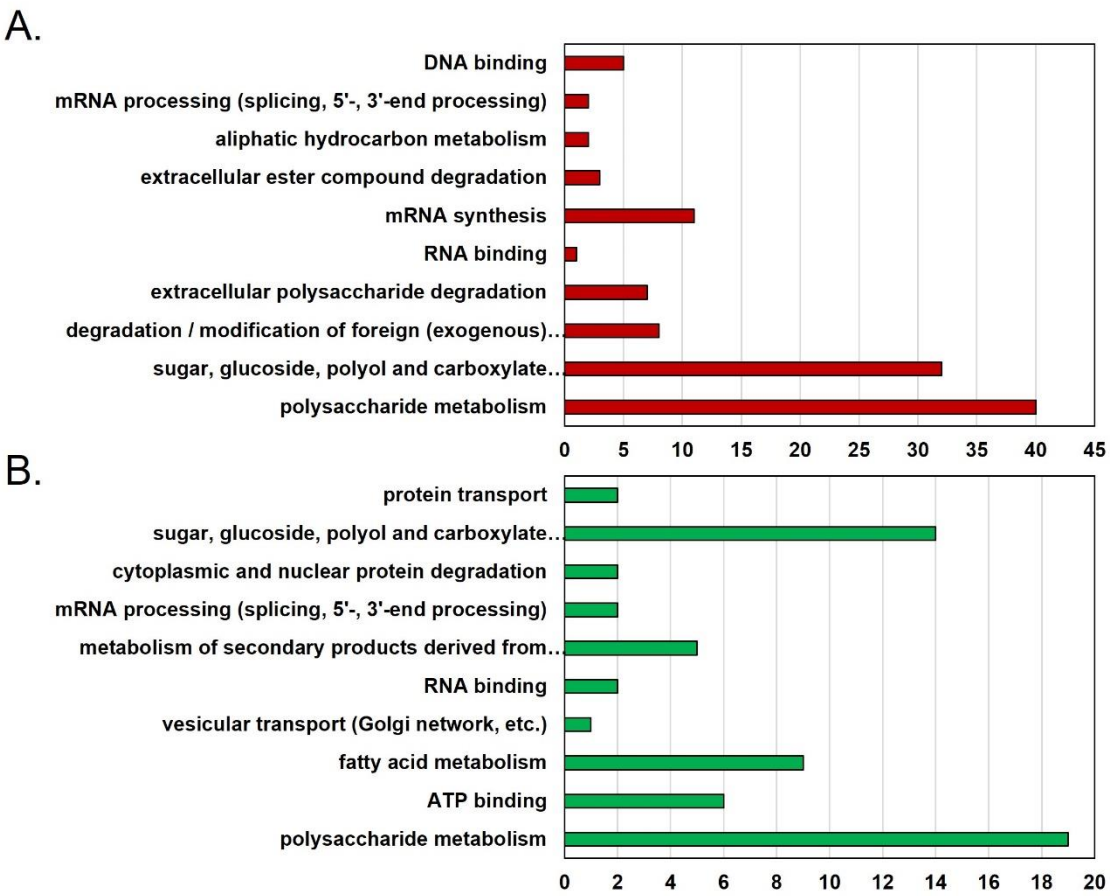

Figure 4.7. Functional Category analysis for the differentially expressed genes in Δ*gna-1* mutants. Cultures were grown and RNAseq data was analyzed as described in the legend for Figure 4.2. DEseq2 was used to determine differences between wild type cultures and Δ*gna-1* mutant cultures grown on VM Avicel. Genes shown in the heatmap have a log2 fold change that is at least 2 or -2 (4 fold or greater difference), and were limited to 10 or greater TPMs.

A. The top ten Functional catalogue represented in the 348 poorly expressed genes in Δ*gna-1* mutants relative to wild type on VM avicel. Functional catalogue were assigned to the highly expressed genes in Δ*gna-1* mutants and were sorted by their significance with a P value cutoff of 0.05. The top 10 Functional catalogue are displayed in this panel. The third level of Functional catalogue were used

B. The top ten Functional catalogue represented in the 351 highly expressed genes in Δ*gna-1* mutants relative to wild type on VM avicel. Functional catalogue were assigned to the highly expressed genes in Δ*gna-1* mutants and were sorted by their significance with a P value cutoff of 0.05. The top 10 Functional catalogue are displayed in this panel. The third level of Functional catalogue were used..

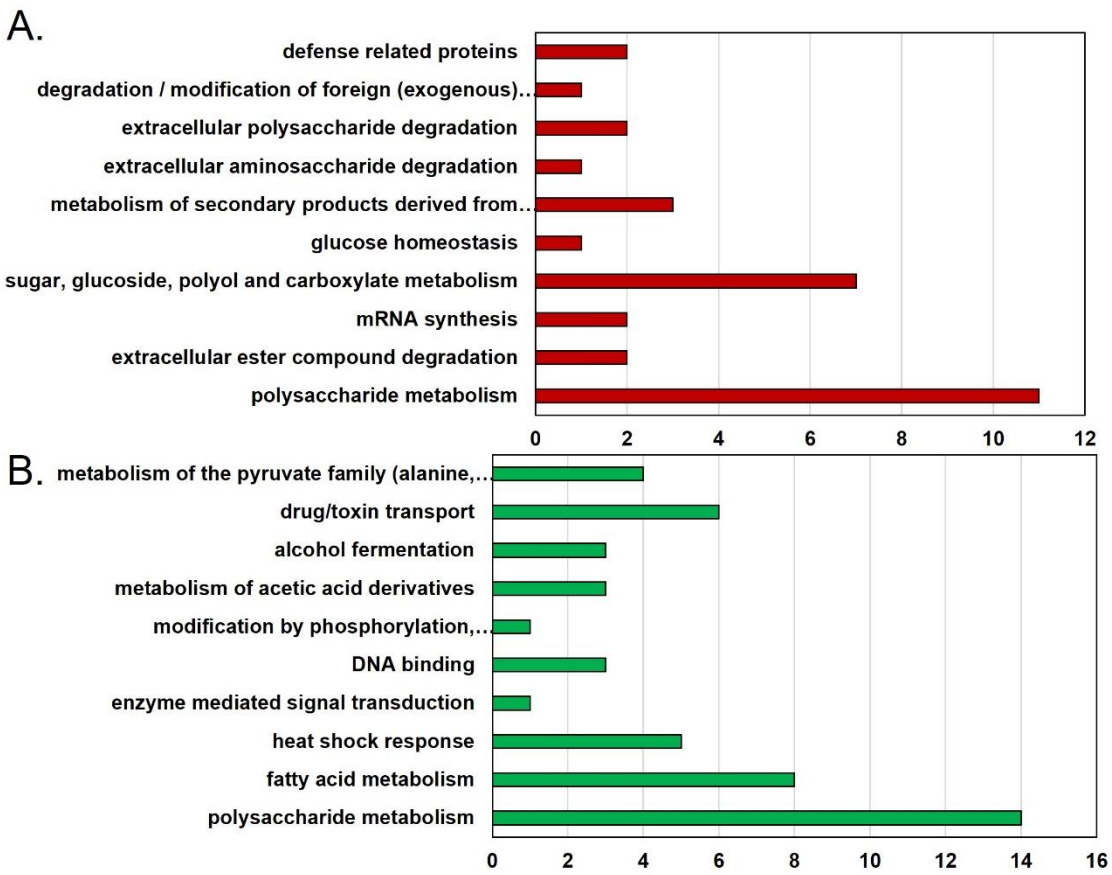

Figure 4.8. Functional Category analysis for the differentially expressed genes in Δ*gna-3* mutants. Cultures were grown and RNAseq data was analyzed as described in the legend for Figure 4.2. DEseq2 was used to determine differences between wild type cultures and Δ*gna-1* mutant cultures grown on VM Avicel. Genes shown in the heatmap have a log2 fold change that is at least 2 or -2 (4 fold or greater difference), and were limited to 10 or greater TPMs.

A. The top ten Functional catalogue represented in the 107 poorly expressed genes in Δ*gna-3* mutants relative to wild type on VM avicel. Functional catalogue were assigned to the highly expressed genes in Δ*gna-1* mutants and were sorted by their significance with a P value cutoff of 0.05. The top 10 Functional catalogue are displayed in this panel. The third level of Functional catalogue were used.

B. The top ten Functional catalogue represented in the 202 highly expressed genes in Δ*gna-3* mutants relative to wild type on VM avicel. Functional catalogue were assigned to the highly expressed genes in Δ*gna-1* mutants and were sorted by their significance with a P value cutoff of 0.05. The top 10 functional categories are displayed in this panel. The third level of Functional Catalogue was used.

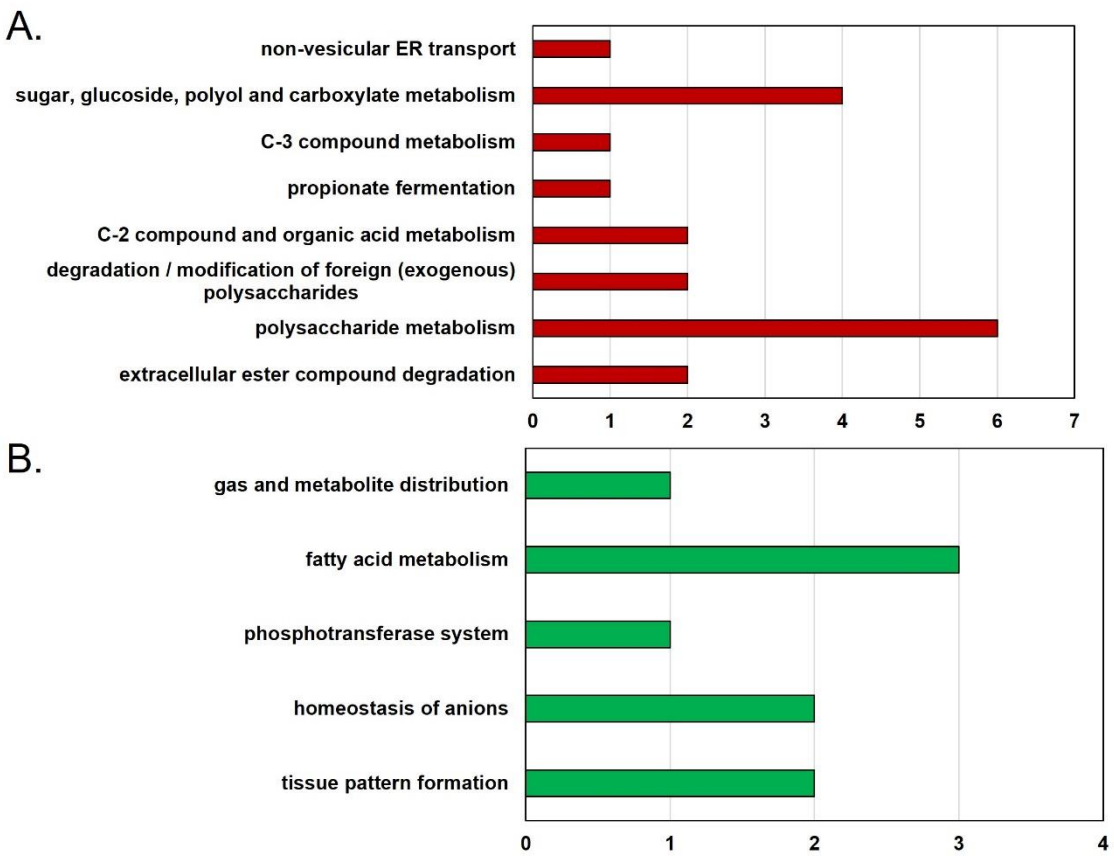

Figure 4.9. Functional Category analysis for the differentially expressed genes in Δ*cr-1* mutants. Cultures were grown and RNAseq data was analyzed as described in the legend for Figure 4.2. DEseq2 was used to determine differences between wild type cultures and Δ*gna-1* mutant cultures grown on VM Avicel. Genes shown in the heatmap have a log2 fold change that is at least 2 or -2 (4 fold or greater difference), and were limited to 10 or greater TPMs.

- **A. The top eight Functional catalogue represented in the 38 poorly expressed genes in Δ*cr-1* mutants relative to wild type on VM avicel.** Functional catalogue were assigned to the highly expressed genes in Δ*gna-1* mutants and were sorted by their significance with a P value cutoff of 0.05. The top 10 Functional catalogue are displayed in this panel. The third level of Functional catalogue were used.
- **B. The top five Functional catalogue represented in the 95 highly expressed genes in Δ*cr-1* mutants relative to wild type on VM avicel.** Functional catalogue were assigned to the highly expressed genes in Δ*gna-1* mutants and were sorted by their significance with a P value cutoff of 0.05. The top 10 Functional catalogue are displayed in this panel. The third level of Functional catalogue were used.

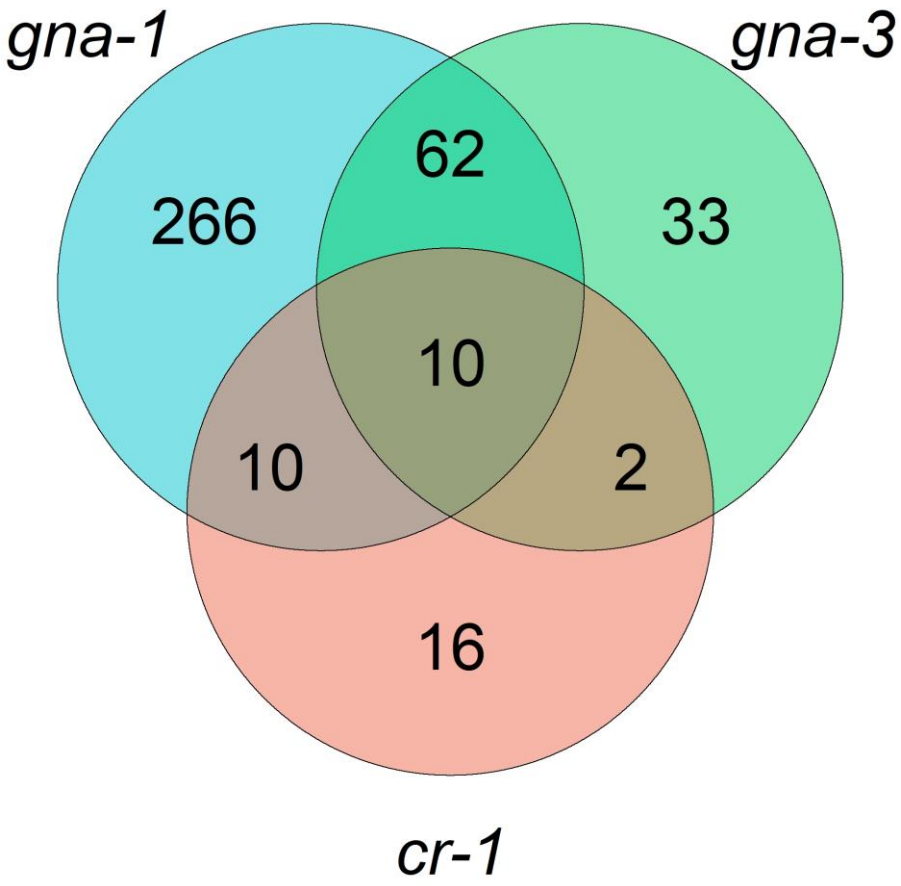

Figure 4.10. Comparisons of the down-regulated transcriptomes of the Gα and adenylate cyclase mutants. The differentially expressed genes that were down-regulated for each mutant strain were compared to each other. Δ*gna-1* and Δ*gna-3* mutants were the most similar, with 62 genes down-regulated in common. Δ*gna-1* and Δ*cr-1* shared 10 genes in common that were down-regulated, and Δ*gna-3* and Δ*cr-1* shared 2 genes in common. All three mutants shared 10 genes in common with each other.

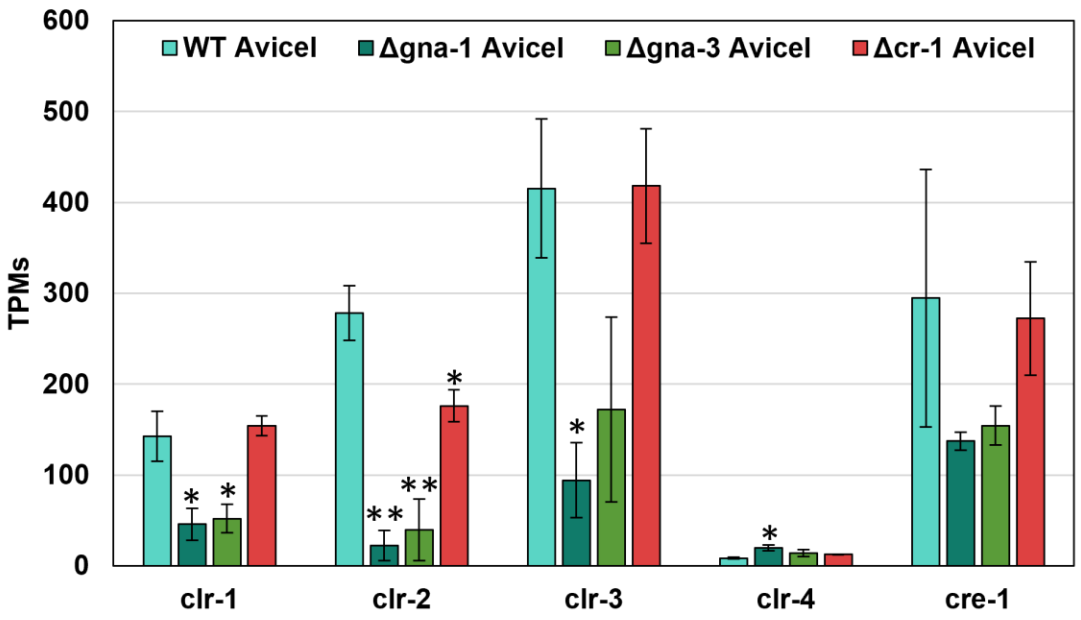

Figure 4.11. Comparisons of the levels of the cellulose related transcriptional regulators between wild type and the Gα and adenylate cyclase mutants. The TPMs for *clr-1, clr-2, clr-3, clr-4,* and *cre-1* for wild type grown on cellulose were compared to Δ*gna-1*, Δ*gna-3,* and Δc*r-1* mutants. Δ*gna-1* mutants had low levels for *clr-1, clr-3,* and *clr-4* mRNA, while Δ*gna-3* mutants only had low levels for *clr-1.* Δc*r-1* mutants had normal levels of the five transcriptional regulators. Statistical significance relative to wild type on Avicel was determined using a two-tailed Students T-Test, and strains with TPMs significantly different than wild type are indicated by an asterisk ($p < 0.05$ = *, $p < 0.01$ = **)

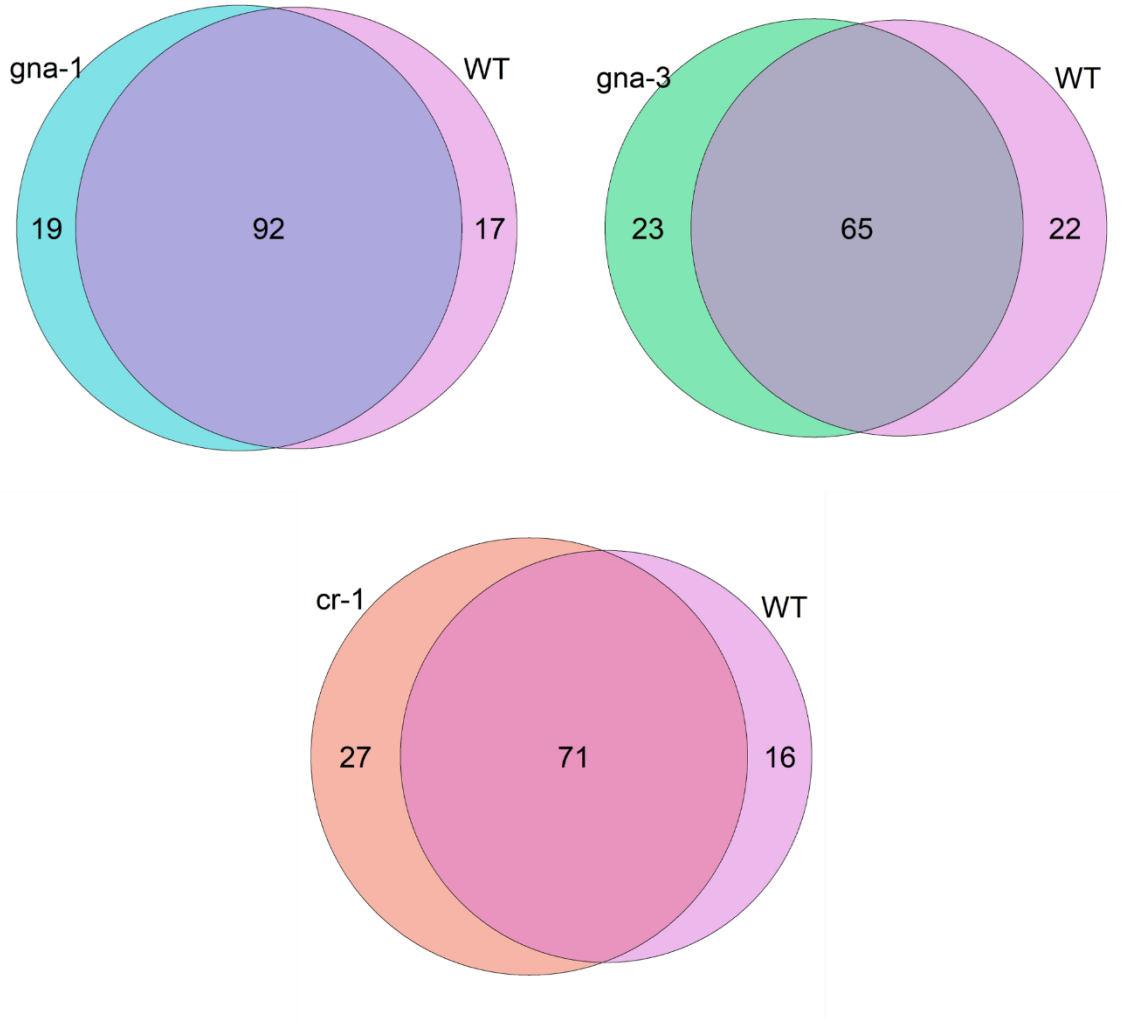

Figure 4.12. Overlap in the exoproteomes of the mutant strains with wild type. peptides from the supernatants of cellulose grown cultures were subjected to LC-MS/MS. 8609 unique peptides were identified and were used to assemble 774 proteins. Venn Diagrams include proteins with at least 10 exclusive spectra in one of the two biological replicates for each mutant that also possess a secretion signal.

Tables

Table 4.1. Strains used in this study.

Strain	Relevant Genotype	Source/Reference #
74-OR23-1A	Wild type, *mat A*	FGSC[1]
OR8-1a	Wild type, *mat a*	FGSC
3b10	Δ*gna-1*::*hph, mat a*	(39)
12378	Δ*gna-2*::*hph, mat A*	FGSC
31c2	Δ*gna-3*::*hph, mat A*	(26)
Δcr-1	Δ*cr-1*::*hph, mat a*	FGSC

1. FGSC = Fungal Genetics Stock Center (47)

Table 4.2. Down-regulated genes in common between Δ*gna-1* and Δ*gna-3* mutants.

Gene ID	Product Description	Name	Gene ID	Product Description	Name
NCU00206	cellobiose dehydrogenase	cdh-1	NCU06326	pectate lyase 1	ply-1
NCU00229	hypothetical protein	N/A	NCU06364	lipase-8	lip-8
NCU00558	hypothetical protein	N/A	NCU06583	serine/threonine protein kinase-44	stk-44
NCU00787	hypothetical protein	N/A	NCU06650	secretory phospholipase A2	spp-3
NCU00911	polysaccharide synthase Cps1p	cps-1	NCU07121	modin	N/A
NCU01045	Ribonuclease T1	grn	NCU07200	metalloprotease-8	mpr-8
NCU01629	hypothetical protein	N/A	NCU07207	hypothetical protein	N/A
NCU02092	hypothetical protein	N/A	NCU07255	hypothetical protein, variant 1	N/A
NCU02096	Flavohemoglobin	fhb-1	NCU07897	hypothetical protein	N/A
NCU02625	hypothetical protein	N/A	NCU08624	hypothetical protein	gpr-34
NCU02850	alcohol dehydrogenase-4	adh-4	NCU08746	starch binding domain-containing protein	N/A
NCU02915	hypothetical protein	N/A	NCU08764	hypothetical protein	N/A
NCU02916	endoglucanase II	gh61-3	NCU08805	hypothetical protein	N/A
NCU03181	carbohydrate esterase family 5-4	ce5-4	NCU08867	hypothetical protein, variant 1	N/A
NCU03383	hypothetical protein	N/A	NCU09024	hypothetical protein	N/A
NCU03433	Septal pore-associated protein 17	spa-17	NCU09214	hypothetical protein	tah-13
NCU04006	hypothetical protein	N/A	NCU09244	Patatin-like phospholipase 1	plp-1
NCU04533	DUF1881 domain-containing protein	app	NCU09245	patatin-like phospholipase domain-containing protein	plp-2
NCU04621	lipoxygenase	N/A	NCU09265	calreticulin	cnx-1
NCU04721	neutral ceramidase	N/A	NCU09356	hypothetical protein	N/A
NCU04774	hypothetical protein, variant 1	N/A	NCU09426	hypothetical protein	N/A
NCU04904	hypothetical protein	N/A	NCU09524	hypothetical protein	N/A
NCU05078	protein-beta-aspartate methyltransferase	N/A	NCU09575	sterol esterase	cea-2
NCU05079	MFS peptide transporter	mfs-9	NCU09712	hypothetical protein, variant 1	N/A
NCU05156	hypothetical protein	N/A	NCU09856	hypothetical protein	N/A
NCU05159	acetylxylan esterase	ce5-2	NCU09992	serine protease-9	spr-9
NCU05161	alpha/beta hydrolase fold-3 domain-containing protein	N/A	NCU10039	hypothetical protein	N/A
NCU05585	MFS quinate transporter	mfs-12	NCU12084	hypothetical protein	N/A
NCU05693	interferon-induced GTP-binding protein Mx2	N/A			
NCU05723	kinetochore protein-11	kpr-11			
NCU05955	Cel74a	gh74-1			
NCU06140	hypothetical protein	vsd-8			
NCU06155	hypothetical protein	N/A			
NCU06250	F-box/LRR repeat containing protein 2	N/A			

Table 4.3. Down-regulated genes in common between Δ*gna-1* and Δ*cr-1* mutants.

Gene ID	Product Description	Name
NCU01195	Glu/Leu/Phe/Val dehydrogenase	am
NCU01886	hypothetical protein	N/A
NCU03756	phenylalanine-9	phe-9
NCU04997	xylanase	gh10-3
NCU04998	hypothetical protein	N/A
NCU06719	MSF1 domain-containing protein	N/A
NCU06815	hypothetical protein	N/A
NCU08507	zinc finger transcription factor-19	znf-19
NCU08790	hypothetical protein	N/A
NCU09364	Hsp30-like protein	hsp30

Table 4.4. Down-regulated genes in common between all three mutant strains.

Gene ID	Product Description	Name
NCU00710	Acetyl xylan esterase	ce1-4
NCU00890	Beta-mannosidase	gh2-1
NCU01298	hypothetical protein, variant 1	N/A
NCU02855	endo-1,4-beta-xylanase A	gh11-1
NCU04494	Acetyl xylan esterase	ce1-3
NCU05598	rhamnogalacturonase B	asd-1
NCU05694	hypothetical protein	N/A
NCU08176	pectate lyase A	ply-2
NCU10045	pectinesterase	ce8-1
NCU11415	inositol-7	inl-7

Table 4.5. Differences in the exoproteomes of wild type and Δ*gna-1*.

	Gene ID	Product Description	Name
Detected in WT only	NCU01123	hypothetical protein	N/A
	NCU02855	endo-1,4-beta-xylanase A	gh11-1
	NCU03000	glycosylhydrolase family 61-8 protein	gh61-8
	NCU03639	lipase	tgl-1
	NCU03646	hypothetical protein	N/A
	NCU04471	hypothetical protein	N/A
	NCU04850	exo-beta-1,3-glucanase	gh55-1
	NCU05358	hypothetical protein	mlh3-1
	NCU05751	cellulose-binding protein	ce3-2
	NCU07776	anchored cell wall protein 5	acw-5
	NCU08720	hypothetical protein	N/A
	NCU09193	hypothetical protein	N/A
	NCU09575	sterol esterase	cea-2
	NCU09582	Chitin deacetylase	ce4-1
	NCU09664	acetylxylan esterase	ce5-3
	NCU09702	endo-beta-1,6-galactanase	gh5-6
	NCU09775	alpha-N-arabinofuranosidase	gh54-1
Detected in Δgna-1 only	NCU00716	non-anchored cell wall protein 5	ncw-5
	NCU00798	hypothetical protein	N/A
	NCU00985	hydrolase	gh2-4
	NCU01353	mixed-linked glucanase	gh16-1
	NCU01720	hypothetical protein	N/A
	NCU02668	glycosyl hydrolase unclassified family-3	ghx-3
	NCU04170	hypothetical protein, variant 1	N/A
	NCU04430	leupeptin-inactivating enzyme 1	N/A
	NCU04479	leucine aminopeptidase-1	lap-1
	NCU04526	hypothetical protein	ce3-1
	NCU04674	Alpha-glucosidase	gh31-3
	NCU04854	endoglucanase EG-1	gh7-2
	NCU05042	bilirubin oxidase-1	bro-1
	NCU05404	glycosyl hydrolase unclassified family-2	ghx-2
	NCU07569	hypothetical protein	pir-1
	NCU07760	endoglucanase IV	gh61-2
	NCU08087	hypothetical protein	gh26-1
	NCU09199	tyrosinase-6	ty-6
	NCU09281	Alpha-glucosidase	gh31-1

Table 4.6. Differences in the exoproteomes of wild type and Δ*gna-3*.

	Gene ID	Product Description	Name
Detected in WT only	NCU00449	hypothetical protein	N/A
	NCU00972	arabinogalactan endo-1,4-beta-galactosidase	gh53-1
	NCU01045	Ribonuclease T1	grn
	NCU02041	anchored cell wall protein 11	acw-11
	NCU03530	anchored cell wall protein 6	acw-6
	NCU04471	hypothetical protein	N/A
	NCU04493	hypothetical protein	N/A
	NCU04623	Beta-galactosidase	gh35-2
	NCU05159	acetylxylan esterase	ce5-2
	NCU05667	anchored cell wall protein 3	acw-3
	NCU05852	glucuronan lyase-1	gll-1
	NCU07029	hypothetical protein	N/A
	NCU07159	proteinase T	spr-7
	NCU07225	endo-1,4-beta-xylanase 2	gh11-2
	NCU07776	anchored cell wall protein 5	acw-5
	NCU08179	hypothetical protein	gh79-2
	NCU09133	ACW-7	acw-7
	NCU09664	acetylxylan esterase	ce5-3
	NCU09691	hypothetical protein	N/A
	NCU09976	rhamnogalacturonan acetylesterase	ce12-1
	NCU09992	serine protease-9	spr-9
	NCU10507	hypothetical protein	N/A
Detected in Δgna-3 only	NCU00292	cholinesterase	cea-3
	NCU00309	WSC domain-containing protein	wsc2-1
	NCU00355	catalase-3	cat-3
	NCU00943	Trehalase	tre-1
	NCU01720	hypothetical protein	N/A
	NCU03290	dipeptidyl peptidase, variant 1	dpp-3
	NCU03996	exoglucanase 3	gh6-1
	NCU04108	isoamyl alcohol oxidase-3	iao-3
	NCU04482	hypothetical protein	N/A
	NCU04674	Alpha-glucosidase	gh31-3
	NCU04850	exo-beta-1,3-glucanase	gh55-1
	NCU05789	secreted glucosidase	gh16-6
	NCU06143	hypothetical protein	gh115-1
	NCU06720	serine protease-11	spr-11
	NCU07269	alpha-1,2-mannosidase	gh92-2
	NCU07520	endo-1,4-beta-glucanase	gh61-11
	NCU07569	hypothetical protein	pir-1
	NCU09046	hypothetical protein	N/A
	NCU09659	nucleotidase-1	nut-1
	NCU09775	alpha-N-arabinofuranosidase	gh54-1
	NCU09791	Beta-1,3-exoglucanase	gh55-4
	NCU09859	metalloprotease-9	mpr-9
	NCU10416	WSC domain-containing protein	N/A

Table 4.7. Differences in the exoproteomes of wild type and Δ*cr-1.*

	Gene ID	Product Description	Name
Detected in WT only	NCU00972	arabinogalactan endo-1,4-beta-galactosidase	gh53-1
	NCU00985	hydrolase	gh2-4
	NCU01045	Ribonuclease T1	grn
	NCU02041	anchored cell wall protein 11	acw-11
	NCU03530	anchored cell wall protein 6	acw-6
	NCU04194	hypothetical protein	N/A
	NCU04493	hypothetical protein	N/A
	NCU05104	exoglucanase 1	gh7-4
	NCU05852	glucuronan lyase-1	gll-1
	NCU07029	hypothetical protein	N/A
	NCU07159	proteinase T	spr-7
	NCU07776	anchored cell wall protein 5	acw-5
	NCU08179	hypothetical protein	gh79-2
	NCU08720	hypothetical protein	N/A
	NCU09664	acetylxylan esterase	ce5-3
	NCU10507	hypothetical protein	N/A
Detected in Δcr-1 only	NCU00309	WSC domain-containing protein	wsc2-1
	NCU00355	catalase-3	cat-3
	NCU00701	N,O-diacetylmuramidase	lyz
	NCU00811	hypothetical protein	N/A
	NCU01298	hypothetical protein, variant 1	N/A
	NCU01720	hypothetical protein	N/A
	NCU02668	glycosyl hydrolase unclassified family-3	ghx-3
	NCU02926	hypothetical protein	srdI
	NCU04108	isoamyl alcohol oxidase-3	iao-3
	NCU04169	hypothetical protein	N/A
	NCU04482	hypothetical protein	N/A
	NCU04674	Alpha-glucosidase	gh31-3
	NCU04882	hypothetical protein	N/A
	NCU04932	hypothetical protein	N/A
	NCU05788	hypothetical protein	N/A
	NCU05789	secreted glucosidase	gh16-6
	NCU06364	lipase-8	lip-8
	NCU07102	hypothetical protein	N/A
	NCU07462	hypothetical protein	N/A
	NCU07569	hypothetical protein	pir-1
	NCU08516	aldose epimerase-1	aep-1
	NCU09046	hypothetical protein	N/A
	NCU09263	anchored cell wall protein 4	acw-4
	NCU09620	hypothetical protein	N/A
	NCU09659	nucleotidase-1	nut-1
	NCU09806	hypothetical protein	N/A
	NCU09848	hypothetical protein	N/A
	NCU09046	hypothetical protein	N/A
	NCU09263	anchored cell wall protein 4	acw-4
	NCU09620	hypothetical protein	N/A
	NCU09659	nucleotidase-1	nut-1
	NCU09806	hypothetical protein	N/A
	NCU09848	hypothetical protein	N/A

References

1. Kubicek CP, Mikus M, Schuster A, Schmoll M, Seiboth B. 2009. Metabolic engineering strategies for the improvement of cellulase production by Hypocrea jecorina. Biotechnol Biofuels 2:19.

2. Sun J, Glass NL. 2011. Identification of the CRE-1 cellulolytic regulon in *Neurospora crassa*. PLoS One 6:e25654.

3. Xiong Y, Sun J, Glass NL. 2014. VIB1, a link between glucose signaling and carbon catabolite repression, is essential for plant cell wall degradation in *Neurospora crassa*. PLoS Genetics 10:e1004500.

4. Huberman LB, Coradetti ST, Glass NL. 2017. Network of nutrient-sensing pathways and a conserved kinase cascade integrate osmolarity and carbon sensing in *Neurospora crassa*. Proc Natl Acad Sci U S A 114:E8665-E8674.

5. Coradetti ST, Craig JP, Xiong Y, Shock T, Tian C, Glass NL. 2012. Conserved and essential transcription factors for cellulase gene expression in ascomycete fungi. Proc Natl Acad Sci U S A 109:7397-402.

6. Huberman LB, Liu J, Qin L, Glass NL. 2016. Regulation of the lignocellulolytic response in filamentous fungi. Fungal Biol Rev 30:101-111.

7. Cupertino FB, Virgilio S, Freitas FZ, Candido Tde S, Bertolini MC. 2015. Regulation of glycogen metabolism by the CRE-1, RCO-1 and RCM-1 proteins in Neurospora crassa. The role of CRE-1 as the central transcriptional regulator. Fungal Genet Biol 77:82-94.

8. de Assis LJ, Ries LN, Savoldi M, Dos Reis TF, Brown NA, Goldman GH. 2015. Aspergillus nidulans protein kinase A plays an important role in cellulase production. Biotechnol Biofuels 8:213.

9. Lichius A, Seidl-Seiboth V, Seiboth B, Kubicek CP. 2014. Nucleo-cytoplasmic shuttling dynamics of the transcriptional regulators XYR1 and CRE1 under conditions of cellulase and xylanase gene expression in Trichoderma reesei. Mol Microbiol doi:10.1111/mmi.12824.

10. Rauscher R, Wurleitner E, Wacenovsky C, Aro N, Stricker AR, Zeilinger S, Kubicek CP, Penttila M, Mach RL. 2006. Transcriptional regulation of xyn1, encoding xylanase I, in Hypocrea jecorina. Eukaryot Cell 5:447-56.

11. van Peij NN, Gielkens MM, de Vries RP, Visser J, de Graaff LH. 1998. The transcriptional activator XlnR regulates both xylanolytic and endoglucanase gene expression in Aspergillus niger. Appl Environ Microbiol 64:3615-9.

12. Coradetti ST, Xiong Y, Glass NL. 2013. Analysis of a conserved cellulase transcriptional regulator reveals inducer-independent production of cellulolytic enzymes in Neurospora crassa. Microbiologyopen 2:595-609.

13. Samal A, Craig JP, Coradetti ST, Benz JP, Eddy JA, Price ND, Glass NL. 2017. Network reconstruction and systems analysis of plant cell wall deconstruction by Neurospora crassa. Biotechnol Biofuels 10:225.

14. Liu Q, Li J, Gao R, Li J, Ma G, Tian C. 2019. CLR-4, a novel conserved transcription factor for cellulase gene expression in ascomycete fungi. Mol Microbiol 111:373-394.

15. Znameroski EA, Li X, Tsai JC, Galazka JM, Glass NL, Cate JH. 2014. Evidence for transceptor function of cellodextrin transporters in Neurospora crassa. J Biol Chem 289:2610-9.

16. Brown NA, Schrevens S, van Dijck P, Goldman GH. 2018. Fungal G-protein-coupled receptors: mediators of pathogenesis and targets for disease control. Nat Microbiol 3:402-414.

17. Li L, Wright SJ, Krystofova S, Park G, Borkovich KA. 2007. Heterotrimeric G protein signaling in filamentous fungi. Annu Rev Microbiol 61:423-52.

18. Mende U, Zagrovic B, Cohen A, Li Y, Valenzuela D, Fishman MC, Neer EJ. 1998. Effect of deletion of the major brain G-protein alpha subunit (alpha(o)) on coordination of G-protein subunits and on adenylyl cyclase activity. J Neurosci Res 54:263-72.

19. Chini B, Parenti M, Poyner DR, Wheatley M. 2013. G-protein-coupled receptors: from structural insights to functional mechanisms. Biochem Soc Trans 41:135-6.

20. Li L, Borkovich KA. 2006. GPR-4 is a predicted G-protein-coupled receptor required for carbon source-dependent asexual growth and development in Neurospora crassa. Eukaryot Cell 5:1287-300.

21. Kim JD, Kaiser K, Larive CK, Borkovich KA. 2011. Use of 1H nuclear magnetic resonance to measure intracellular metabolite levels during growth and asexual sporulation in Neurospora crassa. Eukaryot Cell 10:820-31.

22. Schmoll M, Schuster A, Silva Rdo N, Kubicek CP. 2009. The G-alpha protein GNA3 of Hypocrea jecorina (Anamorph Trichoderma reesei) regulates cellulase gene expression in the presence of light. Eukaryot Cell 8:410-20.

23. Seibel C, Gremel G, do Nascimento Silva R, Schuster A, Kubicek CP, Schmoll M. 2009. Light-dependent roles of the G-protein alpha subunit GNA1 of Hypocrea jecorina (anamorph Trichoderma reesei). BMC Biol 7:58.

24. Collier LA, Ghosh A, Borkovich KA. 2020. Heterotrimeric G-Protein Signaling Is Required for Cellulose Degradation in Neurospora crassa. mBio 11.

25. Kays AM, Borkovich KA. 2004. Severe impairment of growth and differentiation in a *Neurospora crassa* mutant lacking all heterotrimeric Galpha proteins. Genetics 166:1229-40.

26. Kays AM, Rowley PS, Baasiri RA, Borkovich KA. 2000. Regulation of conidiation and adenylyl cyclase levels by the Galpha protein GNA-3 in Neurospora crassa. Mol Cell Biol 20:7693-705.

27. Vogel HJ. 1964. Distribution of lysine pathways among fungi: Evolutionary implications. Am Nat 98:435-446.

28. Garud A, Carrillo AJ, Collier LA, Ghosh A, Kim JD, Lopez-Lopez B, Ouyang S, Borkovich KA. 2019. Genetic relationships between the RACK1 homolog *cpc-2* and heterotrimeric G protein subunit genes in *Neurospora crassa*. PLoS One 14:e0223334.

29. Bray NL, Pimentel H, Melsted P, Pachter L. 2016. Near-optimal probabilistic RNA-seq quantification. Nat Biotechnol 34:525-7.

30. Love MI, Huber W, Anders S. 2014. Moderated estimation of fold change and dispersion for RNA-seq data with DESeq2. Genome Biol 15:550.

31. Priebe S, Kreisel C, Horn F, Guthke R, Linde J. 2015. FungiFun2: a comprehensive online resource for systematic analysis of gene lists from fungal species. Bioinformatics 31:445-6.

32. Basenko EY, Pulman JA, Shanmugasundram A, Harb OS, Crouch K, Starns D, Warrenfeltz S, Aurrecoechea C, Stoeckert CJ, Jr., Kissinger JC, Roos DS, Hertz-Fowler C. 2018. FungiDB: An Integrated Bioinformatic Resource for Fungi and Oomycetes. J Fungi (Basel) 4.

33. Wu VW. 2017. Lessons in plant cell wall degradation by the ascomycete model fungus, *Neurospora crassa*. Ph.D. University of California-Berkeley, University of California.

34. Ruepp A, Zollner A, Maier D, Albermann K, Hani J, Mokrejs M, Tetko I, Guldener U, Mannhaupt G, Munsterkotter M, Mewes HW. 2004. The FunCat, a functional annotation scheme for systematic classification of proteins from whole genomes. Nucleic Acids Res 32:5539-45.

35. Znameroski EA, Coradetti ST, Roche CM, Tsai JC, Iavarone AT, Cate JH, Glass NL. 2012. Induction of lignocellulose-degrading enzymes in *Neurospora crassa* by cellodextrins. Proc Nat Acad Sci USA 109:6012-7.

36. Tian C, Beeson WT, Iavarone AT, Sun J, Marletta MA, Cate JH, Glass NL. 2009. Systems analysis of plant cell wall degradation by the model filamentous fungus Neurospora crassa. Proc Natl Acad Sci U S A 106:22157-62.

37. Phillips CM, Beeson WT, Cate JH, Marletta MA. 2011. Cellobiose dehydrogenase and a copper-dependent polysaccharide monooxygenase potentiate cellulose degradation by Neurospora crassa. ACS Chem Biol 6:1399-406.

38. Lopes DCB, Carraro CB, Silva RN, de Paula RG. 2021. Molecular Characterization of Xyloglucanase cel74a from Trichoderma reesei. Int J Mol Sci 22.

39. Ivey FD, Yang Q, Borkovich KA. 1999. Positive regulation of adenylyl cyclase activity by a Galphai homolog in *Neurospora crassa*. Fungal Genet Biol 26:48-61.

40. Kim H, Borkovich KA. 2004. A pheromone receptor gene, *pre-1*, is essential for mating type-specific directional growth and fusion of trichogynes and female fertility in *Neurospora crassa*. Mol Microbiol 52:1781-98.

41. Wang B, Li J, Gao J, Cai P, Han X, Tian C. 2017. Identification and characterization of the glucose dual-affinity transport system in Neurospora crassa: pleiotropic roles in nutrient transport, signaling, and carbon catabolite repression. Biotechnol Biofuels 10:17.

42. Starr TL, Goncalves AP, Meshgin N, Glass NL. 2018. The major cellulases CBH-1 and CBH-2 of *Neurospora crassa* rely on distinct ER cargo adaptors for efficient ER-exit. Mol Microbiol 107:229-248.

43. Sun J, Phillips CM, Anderson CT, Beeson WT, Marletta MA, Glass NL. 2011. Expression and characterization of the Neurospora crassa endoglucanase GH5-1. Protein Expr Purif 75:147-54.

44. Tang SL, Bubner P, Bauer S, Somerville CR. 2016. O-Glycan analysis of cellobiohydrolase I from Neurospora crassa. Glycobiology 26:670-7.

45. Phillips CM, Iavarone AT, Marletta MA. 2011. Quantitative proteomic approach for cellulose degradation by Neurospora crassa. J Proteome Res 10:4177-85.

46. Hu Y, Liu Y, Hao X, Wang D, Akhberdi O, Xiang B, Zhu X. 2018. Regulation of the Galpha-cAMP/PKA signaling pathway in cellulose utilization of tomium globosum. Microb Cell Fact 17:160.

47. McCluskey K, Wiest A, Plamann M. 2010. The Fungal Genetics Stock Center: a repository for 50 years of fungal genetics research. J Biosci 35:119-26.

Chapter 5: Conclusions and Future Directions

The main objective of this dissertation was to determine the roles of the subunits of the heterotrimeric G protein in detecting extracellular cellulose and directing the cellular response for metabolism of this carbohydrate. In this work, I determined that GNA-1, GNB-1, and GNA-3 act as transcriptional regulators for cellulase enzymes via cAMP signaling, and that CPC-2 and CR-1 affect cellulase enzyme activity in a post-transcriptional process. I also showed the interplay between the subunits of the heterotrimeric G protein on sucrose and cellulose containing medium by demonstrating that GNB-1 regulates levels of GNA-1 and to an extent GNA-3, and that GNB-1 has a tethering relationship with GNA-3, modulating its activity on activating cellulose transcription.

In Chapter 2, we characterized the relationships between the potential Gβ subunit CPC-2 and the other known G protein subunits present in *N. crassa* on minimal medium using sucrose as the carbon source. We investigated a variety of phenotypes in this work; it would be worthwhile to revisit these in cellulose medium to determine if the relationships we discovered were established on complex carbon sources. Since CPC-2 is an alternative Gβ subunit, it would be interesting to determine whether it has a tethering relationship on cellulose similar to that of GNB-1 and GNA-3. In Chapter 3, we show that Δ*cpc-2* mutants had wild-type levels of the cellulase transcripts assayed but have no cellulase activity. While the mRNAs for the cellulases assayed were detectable, it is

possible that these mRNAs are not being properly loaded onto the ribosome, keeping them from being translated. RACK-1 homologs are known to act as chaperones for ribosomal proteins and to regulate translation (1). Assaying the ribosomes for the presence of cellulase mRNAs would determine if CPC-2 is controlling cellulase activity at the level of mRNA loading into the ribosome.

In Chapter 3, we determined that GNA-1, GNA-3, and GNB-1 regulate cellulase transcription. This was reinforced especially for GNA-1, but was also demonstrated for GNA-3, in Chapter 4. Additionally, in Chapter 3 we provided evidence that GNA-1 and GNB-1 may act at least partially independently of cAMP signaling to accomplish cellulose sensing. In Chapter 4, this is reinforced by the striking transcriptional defects in Δ*gna-1* mutants.

Filamentous fungi possess three mitogen activated protein kinase (MAPK) cascades, which are involved in responses to heat and osmotic stress (2, 3). In *T. reesei,* there is evidence that all three MAPK pathways are involved in cellulose metabolism (4). Additionally, the *N. crassa* OS pathway suppresses cellulase expression during growth in glucose medium. This possibly is a result of the increased osmolarity caused by a high concentration of soluble sugars (5). I have already begun to investigate the connection between MAPK signaling and cellulose metabolism, and my preliminary work is compiled in Appendix A.

Another potential downstream pathway that may regulate cellulose metabolism is calcium signaling. In *T. reesei,* addition of extracellular calcium to Avicel medium led to higher levels of cellulase activity in the Rut-C30 strain, and

loss of the calcium-related transcription factor *crz1* resulted in reduced transcription of the homolog of the cellobiohydrolase *cbh-1* and the transcription factor *xyr1,* which activate cellulase transcription in this system. The binding affinity of CRZ-1 for the *cbh1* promoter increased 14-fold in response to 5 mM Ca^{2+} added to the medium (6). The Ca^{2+}/calmodulin pathway in *N. crassa* has been previously characterized and gene deletion mutants for the various components are present in our lab (7, 8). Epistatic effects with regards to cellulase expression and activity between these components and the G protein subunits could be determined in the future.

References

1. Adams DR, Ron D, Kiely PA. 2011. RACK1, A multifaceted scaffolding protein: Structure and function. Cell Commun Signal 9:22.

2. Ghosh A, Servin JA, Park G, Borkovich KA. 2014. Global analysis of serine/threonine and tyrosine protein phosphatase catalytic subunit genes in Neurospora crassa reveals interplay between phosphatases and the p38 mitogen-activated protein kinase. G3 (Bethesda) 4:349-65.

3. Park G, Pan S, Borkovich KA. 2008. Mitogen-activated protein kinase cascade required for regulation of development and secondary metabolism in Neurospora crassa. Eukaryot Cell 7:2113-22.

4. de Paula RG, Antonieto ACC, Carraro CB, Lopes DCB, Persinoti GF, Peres NTA, Martinez-Rossi NM, Silva-Rocha R, Silva RN. 2018. The Duality of the MAPK Signaling Pathway in the Control of Metabolic Processes and Cellulase Production in *Trichoderma reesei*. Sci Rep 8:14931.

5. Huberman LB, Coradetti ST, Glass NL. 2017. Network of nutrient-sensing pathways and a conserved kinase cascade integrate osmolarity and carbon sensing in *Neurospora crassa*. Proc Natl Acad Sci U S A 114:E8665-E8674.

6. Chen L, Zou G, Wang J, Wang J, Liu R, Jiang Y, Zhao G, Zhou Z. 2016. Characterization of the Ca(2+) -responsive signaling pathway in regulating the expression and secretion of cellulases in *Trichoderma reesei* Rut-C30. Mol Microbiol 100:560-75.

7. Gohain D, Tamuli R. 2019. Calcineurin responsive zinc-finger-1 binds to a unique promoter sequence to upregulate neuronal calcium sensor-1, whose interaction with MID-1 increases tolerance to calcium stress in *Neurospora crassa*. Mol Microbiol 111:1510-1528.

8. Tamuli R, Deka R, Borkovich KA. 2016. Calcineurin subunits A and B interact to regulate growth and asexual and sexual development in *Neurospora crassa*. PLoS One 11:e0151867.

Appendix A: Mitogen Activated Protein Kinase (MAPK) involvement in cellulose detection

Overview

Mitogen activated protein kinases (MAPKs) are key signal transduction components in numerous fungal species (1, 2). Each MAPK module consists of three kinases that act in a linear pathway to phosphorylate the next kinase, and typically, the terminal MAPK then activates the downstream targets. There are three major MAPK pathways in *N. crassa*, with terminal MAPKs OS-2, MAK-1 and MAK-2 (3).

Homologous members of the three *N. crassa* pathways are implicated in the response to cellulose in *T. reesei* (4, 5). Gene deletion mutants of the p38 terminal MAPK homolog *tmk-3* produce lower levels of cellulase enzymes following direct inoculation to cellulose medium (4). Additionally, the *N. crassa* OS pathway, containing the p38 MAPK OS-2, has been shown to suppress cellulase expression during growth in glucose. It has been hypothesized that this results from the increased osmolarity caused by a high concentration of free soluble carbohydrates (6). This pathway also regulates the response to other environmental pressure such as oxidative stress in *N. crassa* (7).

Mutants lacking the terminal MAPK *tmk-2* in *T. reesei* (homologous to *N. crassa mak-1*) have β-glucosidase activity 4 times that of the wild type strain (5). By contrast, Δ*tmk-1* mutants (homologous to *N. crassa mak-2*) had half the β-

glucosidase activity of wild type strains in 48-hour old cultures. RNAseq analysis of Δ*tmk-2* strains showed differential expression of the transcripts for the *gna-1* homolog, 3 Pth11-like GPCRs and an RGS protein (5).

The results reported in Chapter 3 and Chapter 4 suggest that GNA-1 is likely targeting another pathway in addition to cAMP signaling to affect cellulase transcription, which could possibly be one or more of the MAPK pathways. These findings, along with the observed effects of MAPK signaling on cellulose metabolism observed in *T. reesei*, prompted us to investigate the three terminal MAPK mutants in *N. crassa* for defects in biomass after direct inoculation to Avicel medium and in cellulase activity. We also performed western blotting analysis for phosphorylated versions of the terminal MAPKs in wild type *N. crassa* to determine if these pathways are activated after the transfer from glucose to Avicel-containing medium.

Materials and Methods

Media and strains.

The strains used in this study are listed in Table A.1. Strains were cultured on Vogel's Minimal Medium (VM, (8)), with the exception that the indicated carbon source replaced sucrose. All carbon sources were used at a final concentration of 2% (weight/volume). Alternative carbon sources were crystalline cellulose (Avicel-PH101, 50 µm particle; Sigma-Aldrich, St. Louis, MO), glucose (MP Biomedicals, Santa Ana, CA) or no carbon source. Macroconidia (conidia) used for inoculation of cultures were obtained as described (9).

Isolation of culture supernatants, cellulase and protein assays and western analysis.

Cultures for direct inoculation to cellulose medium and the cellulase activity assays were grown as described in the Materials and Methods section of Chapter 3. The cellulase enzyme assay used to detect glucose produced from degradation of Avicel and the BCA assay used to determine protein concentration are also described in that chapter.

For western blotting of the phosphorylated MAPKs, wild type cultures were grown in 25 mL of VM-Glucose at 25°C with shaking at 200 rpm in constant light for 12 hours. These were harvested using a funnel lined with Miracloth (Millipore Sigma, Burlington, MA) to minimize cellular stress. A volume containing 25 mL of

1xVM without a carbon source was poured through the funnel containing the hyphae to wash away residual glucose. The hyphae were collected from the mira cloth and transferred to 25 mL of fresh VM-Glucose or VM-Avicel medium, with continued incubation under the conditions outlined above. Samples were then collected in a Miracloth-lined funnel again 0, 30, 60, or 120 minutes after transfer and flash frozen in liquid nitrogen. Cell pads were pulverized in liquid nitrogen using a mortar and pestle. The same volume (200 µL to 1 mL) of MAPK Extraction buffer containing phosphatase inhibitors (50 mM Tris pH 7.5, 10% glycerol, 2 mM EDTA, 1% SDS, 2 mM EGTA, 100 mM NaCl, 1 mM Na_3VO_4, 1 mM NaF) was added to the pulverized tissue. Samples were then heated at 85°C for 10 minutes. After heating, Fungal Protease Inhibitor Cocktail (Research Products International, Mt Prospect, IL, product number P51000-1) was added to a concentration of 0.1%, and PMSF dissolved in 100% isopropanol was added to a concentration of 1 mM. Unbroken cells were pelleted by centrifugation at 4000 x g for 15 minutes at room temperature to keep the SDS from precipitating (Microfuge 16, Beckman Coulter, Brea, CA). Extracted protein was quantified using the BCA assay (Thermo Fisher, Waltham, MA, product number 23225)

Equal amounts of protein were electrophoresed using 10% SDS-PAGE gels and blotted to nitrocellulose as previously described (10). Primary antibodies used to detect phospho-p38 (OS-2) and phospho- (MAK-1 and MAK-2) were used at a 1:1000 dilution (Cell Signaling Technologies, Danvers, MA; product numbers 9101S and 9211S, respectively). Incubation with secondary antibody and chemiluminescent detection were carried out as previously described (10).

Results

All three terminal MAPKs are required for biomass accumulation on Avicel medium

We tested the three terminal MAPK mutants for growth in glucose or Avicel in the same manner as described for other mutants in Chapter 3. We first inoculated conidia to either glucose or Avicel medium directly. We harvested the glucose cultures after overnight growth (16 hours), but allowed the Avicel cultures to grow for three days, as wild type *N. crassa* takes 3 days to clear the media of Avicel particles. We harvested the cell pads and extracted total protein to quantify the biomass as described in Chapter 3. We found that during growth on glucose, Δ*mak-1* and Δ*mak-2* mutants did not grow as well as wild type cultures (Figure A.1). In contrast, Δ*os-2* strains had normal levels of total biomass relative to wild type.

On Avicel medium, all three terminal MAPK mutants had defects in biomass production compared to wild type. The biomass of Δ*mak-1* and Δ*mak-2* mutants was 33% and 38% of wild type, respectively (Figure A.1). Δ*os-2* mutants were the most reduced, producing only 19% of the biomass of wild type cultures (Figure A.1). While wild type cultures exhibited a 27% reduction in the biomass produced in glucose vs. Avicel medium, the mutant strains were diminished by 69%, 62%, and 86% of the amounts produced in glucose medium (Δ*mak-1,* Δ*mak-2,* and Δ*os-2* respectively). The biomass defects in all three MAPK

mutants cultured on Avicel are not proportional to what is observed in wild type Avicel cultures. Therefore, all three MAPK pathways are essential for effective biomass accumulation on cellulose medium in *N. crassa.*

Cellulase activity is greater than wild type in Δ*mak-1* mutants, but lower in Δ*mak-2* and Δ*os-2* mutants

Next, we assayed cell-free supernatants from obtained from the MAPK mutants for their ability to degrade cellulose. We grew cultures on glucose medium overnight (16 hours), and then transferred the cell pads to Avicel medium for three days. After this time, we isolated the supernatant and assayed protein concentration and cellulase activity as described in Chapter 3. We also isolated and measured total biomass protein in the cell pads as described in Chapter 3. We used these total biomass protein measurements to normalize the cellulase activity and supernatant protein levels in order to account for possible biomass accumulation defects in the mutants under these conditions (Figure A.1).

Upon assaying the protein levels, we found that Δ*mak-1* mutants had normal levels of protein in the supernatant, while both Δ*mak-2* and Δ*os-2* had roughly half of the protein present in wild type (Figure A.2). From the cellulase activity assays, we also observed that Δ*mak-1* mutants have higher cellulase activity than wild type, while Δ*mak-2* and Δ*os-2* mutants both have lower activity than wild type (Figure A.2). Δ*mak-1* mutants exhibited reduced protein

accumulation after direct inoculation into Avicel medium (Figure A.1). Allowing the mutant to germinate overnight on glucose medium revealed a role for MAK-1 as a possible repressor of cellulase activity. Additionally, these results suggest that MAK-2 and OS-2 are positive regulators of cellulose metabolism and cellulase activity, since the mutants produce less biomass during direct inoculation experiments and produce lower levels of secreted protein and cellulase activity. These results are consistent with the observations made in *T. reesei* and thus suggest a similar function for MAPK pathways in cellulose metabolism in *N. crassa* (4, 5). It is important to note that in Δ*mak-2* and Δ*os-2* mutants, there is not a complete loss of cellulase activity as observed in Δ*gna-1,* Δ*gna-3,* Δ*gnb-1,* Δ*cpc-2,* Δ*gng-1,* and Δ*cr-1* mutants (Chapter 3). However, analysis of Δ*mak-1* Δ*os-2* double mutants might reveal a complete loss of cellulase activity, suggesting that these terminal MAPKs act synergistically to regulate cellulase activity. It is also possible that there is cross talk between the two MAPK pathways, and gene deletion of both may determine which MAPK is epistatic to the other, if this hypothesis is correct.

MAK-1 and OS-2 are phosphorylated in wild type after transfer from glucose to Avicel medium

We next tested whether any of the three terminal MAPKs were phosphorylated in wild type in response to a transfer from glucose to Avicel medium. Previous studies in *N. crassa* have detected phosphorylation of both MAK-1 and MAK-2 in response to circadian rhythms using the same ERK antibody and our laboratory has also used this antibody to show MAK-1 phosphorylation (11, 12). The MAK-1 and MAK-2 MAPKs are structurally similar, but have a molecular mass difference of approximately 6 kDa and can be distinguished on western blots. Finally, we have used an antibody to detect phosphorylated OS-2 in response to 0.8 M NaCl or the fungicide fludioxonil in our own laboratory (13).

We observed that MAK-1 is not phosphorylated in wild type in glucose conditions. However, phospho-MAK-1 was detected 30 minutes after the transfer to Avicel, and levels were sustained for the full 2 hours of the experiment. This suggests that there is an Avicel-specific response by the MAK-1 MAPK cascade. Since Δ*mak-1* mutants show increased cellulase activity compared to wild type, the MAK-1 cascade may serve as a negative feedback loop, modulating carbon catabolite repression following sufficient breakdown of cellulose. MAK-2 was phosphorylated under all conditions and time points, similar to previous findings involving circadian rhythms (11). While phospho-OS-2 was similarly detected in all conditions, it was in higher abundance after 30 minutes in Avicel. These

higher levels were sustained over the two hours of the experiment. This result, combined with the activity assay data, suggests that OS-2 contributes positively to the response to extracellular cellulose. It is also possible that the MAPK pathways are regulating each other. Further experiments are needed to determine possible epistatic relationships between them.

It is of interest that two background bands were detected in Avicel conditions that cross-reacted with the phospho-OS-2 antiserum. One of these is a lower molecular weight than predicted for phospho-OS-2. This species could potentially be a degradation product, as it is also present under glucose conditions. It is possible that the larger band is a covalently modified version of OS-2 that only exists in cellulose conditions. Due to the intensity of all three bands in Avicel culture conditions, it seems reasonable to suggest that all three are forms of OS-2.

Figures

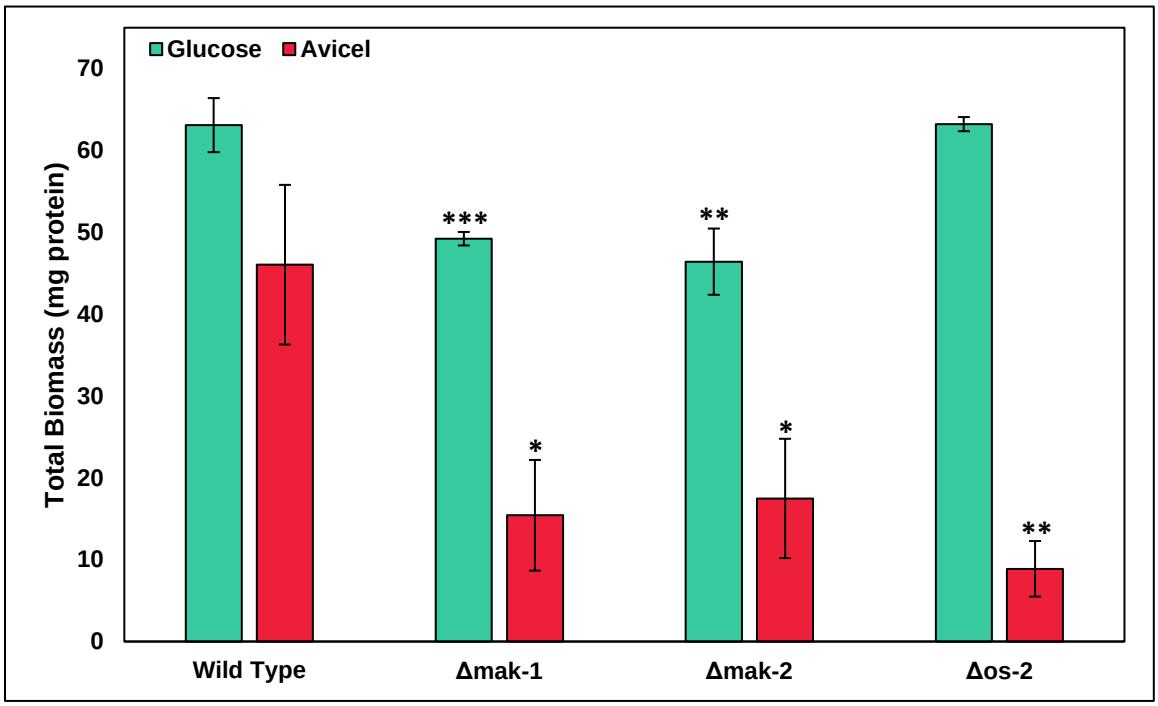

Figure A.1 Total biomass from MAPK gene deletion strains grown on Avicel medium. *N. crassa* strains were inoculated at a density of 1 x10^6 conidia/mL in 25 mL of VM containing 2% Avicel (crystalline cellulose) as the carbon source and grown with shaking in constant light at 25°C for 4 days. Cultures were then centrifuged at 5000xg for 10 min and the supernatant was removed. Cell pads were mixed with 10 ml Protein Extraction Buffer (1% SDS, 50 mM Tris pH 7.5, 5 mM EDTA) and 5 ml glass beads in a 50 ml conical tube and then heated at 60°C with intermittent vortexing over 12 h. The tubes were centrifuged and the supernatant retained and frozen at -20C. This process was repeated 3 times to yield four extract fractions. The total extract volume was recorded and the protein concentration of the pooled extracts was determined via BCA. A minimum of three replicates were used and errors are expressed as the standard error. Statistical significance from Wild Type *mat a* was determined using a two tailed Students T-Test and strains with protein levels or cellulase activity significantly different than wild type are indicated by an asterisk ($p < 0.05$ = *, $p < 0.01$ = **, $p < 0.001$ = ***).

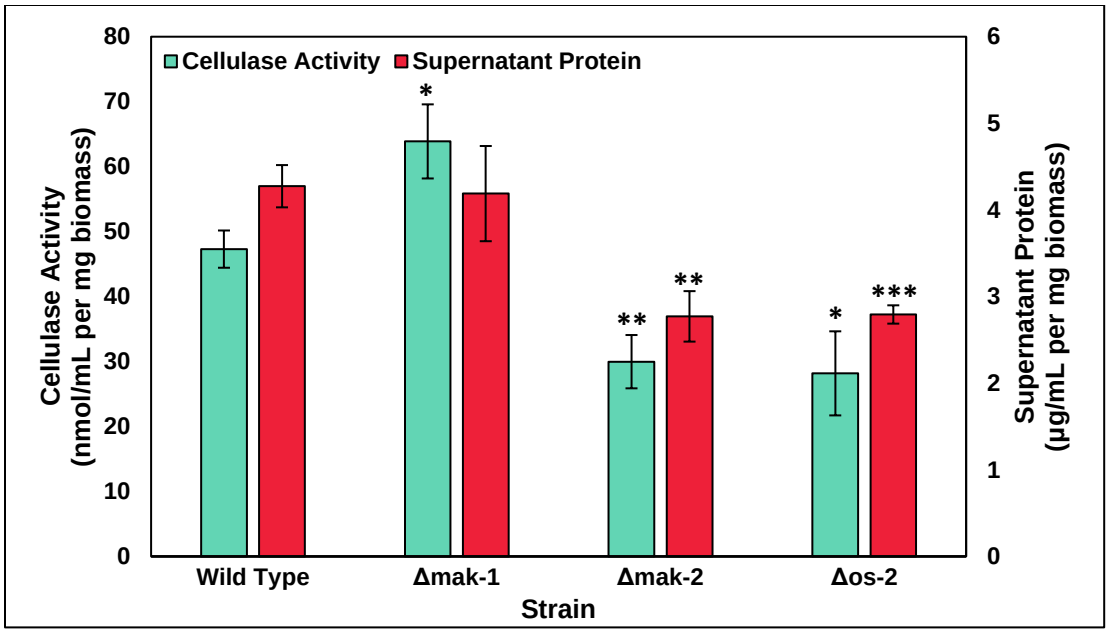

Figure A.2 Cellulase Activity and Secreted Protein levels from MAPK gene deletion strains grown on Avicel medium. Cultures were grown as described in Chapter 3. Cellulase activity was determined by incubating supernatant aliquots in a solution containing 0.5% Avicel for 16 hours. Glucose release activity was assayed as described in Chapter 3, and activity is defined as nmol glucose / mL supernatant / mg biomass produced. A minimum of three replicates were used and errors are expressed as the standard error. Statistical significance from Wild Type *mat a* was determined using a two tailed Students T-Test and strains with protein levels or cellulase activity significantly different than wild type are indicated by an asterisk ($p < 0.05$ = *, $p < 0.01$ = **, $p < 0.001$ = ***).

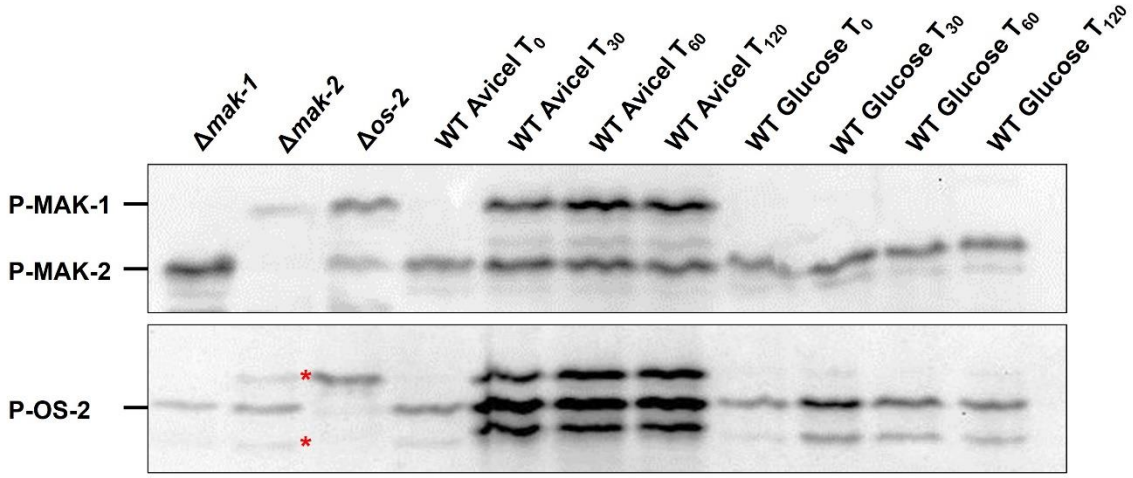

Figure A.3 Time course of the terminal Phospho-MAPK levels in wild type cultures grown under various conditions. Wild type cultures were grown for 12 hours on glucose medium and were transferred as described in Chapter 3 to Avicel or glucose containing medium. T_0, T_{30}, T_{60}, and T_{120} suffixes indicate how long the culture was grown in the new medium prior to flash freezing the culture in liquid nitrogen (Δ*mak-1,* Δ*mak-2,* and Δ*os-2* mutant controls are all at T_0 in glucose medium). Protein was extracted as described in Chapter 2 for western blotting of cytoplasmic proteins (CPC-2). P-MAK-1 was detected at 46.8 kDa and P-MAK-2 was detected at 40.8 kDa using an antibody to P-p42/44 MAPKs. P-OS-2 was detected at 41.2 kDa using an antibody to P-p38 MAPKs. Asterisks indicate background bands that cross react with the P-OS-2 antiserum. These blots are representative of three biological replicates.

Tables

Table A.1 Strains used in this study.

Strain	Relevant Genotype	Source/Reference #
OR8-1a	Wild type, *mat a*	FGSC[1]
11320	Δ*mak-1*::*hph, mat A*	FGSC
Δmak-2	Δ*mak-2*::*hph, mat A*	
d7024-20	Δ*os-2*::*hph, mat A*	

1. FGSC = Fungal Genetics Stock Center (14)

References

1. Saito H, Tatebayashi K. 2004. Regulation of the osmoregulatory HOG MAPK cascade in yeast. J Biochem 136:267-72.

2. Buck V, Quinn J, Soto Pino T, Martin H, Saldanha J, Makino K, Morgan BA, Millar JB. 2001. Peroxide sensors for the fission yeast stress-activated mitogen-activated protein kinase pathway. Mol Biol Cell 12:407-19.

3. Borkovich KA, Alex LA, Yarden O, Freitag M, Turner GE, Read ND, Seiler S, Bell-Pedersen D, Paietta J, Plesofsky N, Plamann M, Goodrich-Tanrikulu M, Schulte U, Mannhaupt G, Nargang FE, Radford A, Selitrennikoff C, Galagan JE, Dunlap JC, Loros JJ, Catcheside D, Inoue H, Aramayo R, Polymenis M, Selker EU, Sachs MS, Marzluf GA, Paulsen I, Davis R, Ebbole DJ, Zelter A, Kalkman ER, O'Rourke R, Bowring F, Yeadon J, Ishii C, Suzuki K, Sakai W, Pratt R. 2004. Lessons from the genome sequence of Neurospora crassa: tracing the path from genomic blueprint to multicellular organism. Microbiol Mol Biol Rev 68:1-108.

4. Wang M, Zhao Q, Yang J, Jiang B, Wang F, Liu K, Fang X. 2013. A mitogen-activated protein kinase Tmk3 participates in high osmolarity resistance, cell wall integrity maintenance and cellulase production regulation in Trichoderma reesei. PLoS One 8:e72189.

5. de Paula RG, Antonieto ACC, Carraro CB, Lopes DCB, Persinoti GF, Peres NTA, Martinez-Rossi NM, Silva-Rocha R, Silva RN. 2018. The Duality of the MAPK Signaling Pathway in the Control of Metabolic Processes and Cellulase Production in *Trichoderma reesei*. Sci Rep 8:14931.

6. Huberman LB, Coradetti ST, Glass NL. 2017. Network of nutrient-sensing pathways and a conserved kinase cascade integrate osmolarity and carbon sensing in *Neurospora crassa*. Proc Natl Acad Sci U S A 114:E8665-E8674.

7. Jones CA, Greer-Phillips SE, Borkovich KA. 2007. The response regulator RRG-1 functions upstream of a mitogen-activated protein kinase pathway impacting asexual development, female fertility, osmotic stress, and fungicide resistance in Neurospora crassa. Mol Biol Cell 18:2123-36.

8. Vogel HJ. 1964. Distribution of lysine pathways among fungi: Evolutionary implications. Am Nat 98:435-446.

9. Garud A, Carrillo AJ, Collier LA, Ghosh A, Kim JD, Lopez-Lopez B, Ouyang S, Borkovich KA. 2019. Genetic relationships between the RACK1 homolog *cpc-2* and heterotrimeric G protein subunit genes in *Neurospora crassa*. PLoS One 14:e0223334.

10. Krystofova S, Borkovich KA. 2005. The heterotrimeric G-protein subunits GNG-1 and GNB-1 form a Gbetagamma dimer required for normal female fertility, asexual development, and Galpha protein levels in *Neurospora crassa*. Eukaryot Cell 4:365-78.
11. Bennett LD, Beremand P, Thomas TL, Bell-Pedersen D. 2013. Circadian activation of the mitogen-activated protein kinase MAK-1 facilitates rhythms in clock-controlled genes in Neurospora crassa. Eukaryot Cell 12:59-69.
12. Park G, Pan S, Borkovich KA. 2008. Mitogen-activated protein kinase cascade required for regulation of development and secondary metabolism in Neurospora crassa. Eukaryot Cell 7:2113-22.
13. Ghosh A, Servin JA, Park G, Borkovich KA. 2014. Global analysis of serine/threonine and tyrosine protein phosphatase catalytic subunit genes in Neurospora crassa reveals interplay between phosphatases and the p38 mitogen-activated protein kinase. G3 (Bethesda) 4:349-65.
14. McCluskey K, Wiest A, Plamann M. 2010. The Fungal Genetics Stock Center: a repository for 50 years of fungal genetics research. J Biosci 35:119-26.